Spine: 5 mm

Volume 74 • Issue 3 • July-September 2025

Journal of The Anatomical Society of India • Volume 74 • Issue 3 • July-September 2025 • Pages 197-288

ISSN : 0003-2778

Scopus Indexed

JOURNAL OF THE ANATOMICAL SOCIETY OF INDIA

An International Journal

An Official Publication of Anatomical Society of India

Full text online at **https://journals.lww.com/joai**
Submit articles online at **https://review.jow.medknow.com/jasi**

Editor-in-Chief
Dr. Vishram Singh

Wolters Kluwer

Medknow

Journal of the Anatomical Society of India

Print ISSN: 0003-2778

GENERAL INFORMATION

About the Journal

Journal of the Anatomical Society of India (ISSN: Print 0003-2778) is peer-reviewed journal. The journal is owned and run by Anatomical Society of India. The journal publishes research articles related to all aspects of Anatomy and allied medical/surgical sciences. Pre-Publication Peer Review and Post-Publication Peer Review Online Manuscript Submission System Selection of articles on the basis of MRS system Eminent academicians across the globe as the Editorial board members Electronic Table of Contents alerts Available in both online and print form. The journal is published quarterly in the months of January, April, July and October.

Scope of the Journal

The aim of the *Journal of the Anatomical Society of India* is to enhance and upgrade the research work in the field of anatomy and allied clinical subjects. It provides an integrative forum for anatomists across the globe to exchange their knowledge and views. It also helps to promote communication among fellow academicians and researchers worldwide. The Journal is devoted to publish recent original research work and recent advances in the field of Anatomical Sciences and allied clinical subjects. It provides an opportunity to academicians to disseminate their knowledge that is directly relevant to all domains of health sciences.

The Editorial Board comprises of academicians across the globe.

JASI is indexed in Scopus, available in Science Direct.

Abstracting and Indexing Information

The journal is registered with the following abstracting partners:

Baidu Scholar, CNKI (China National Knowledge Infrastructure), EBSCO Publishing's Electronic Databases, Ex Libris – Primo Central, Google Scholar, Hinari, Infotrieve, Netherlands ISSN center, ProQuest, TdNet, Wanfang Data

The journal is indexed with, or included in, the following:

SCOPUS, Science Citation Index Expanded, IndMed, MedInd, Scimago Journal Ranking, Emerging Sources Citation Index.

Impact Factor® as reported in the 2024 Journal Citation Reports® (Clarivate Analytics, 2025): 0.2

Information for Authors

Article processing and publication charges will be communicated by the editorial office. All manuscripts must be submitted online at https://review.jow.medknow.com/jasi.

Subscription Information

A subscription to JASI comprises 4 issues. Prices include postage. Annual Subscription Rate for non-members-		
Annual Subscription Rate for non-members		
	India	**Outside India**
Institutional	INR 15000	USD 1200
Individual	INR 7,500	USD 800
The Journal of Anatomical Society of India (ISSN: 0003-2778) is published quarterly **Subscriptions** are accepted on a prepaid basis only and are entered on a calendar year basis. Issues are sent by standard mail Priority rates are available upon request.		

Information to Members/Subscribers

All members and existing subscribers of the Anatomical Society of India are requested to send their membership/existing subscription fee for the current year to the Treasurer of the Society on the following address: Prof (Dr.) Punit Manik, Treasurer, ASI, Department of Anatomy, KGMU, Lucknow - 226003. Email: punitamanik@yahoo.co.in. All payments should be made through an account payee bank draft drawn in favor of the **Treasurer, Anatomical Society of India,** payable at **Lucknow** only, preferably for **Allahabad Bank, Medical College Branch, Lucknow.** Outstation cheques/drafts must include INR 70 extra as bank collection charges.

All complaints regarding non-receipt of journal issues should be addressed to the Editor-in-Chief, JASI at editorjasi@gmail.com. The new subscribers may, please contact wkhlrpmedknow_subscriptions@wolterskluwer.com.

Requests of any general information like travel concession forms, venue of next annual conference, etc. should be addressed to the General Secretary of the Anatomical Society of India.

For mode of payment and other details, please visit www.medknow.com/subscribe.asp

Claims for missing issues will be serviced at no charge if received within 60 days of the cover date for domestic subscribers, and 3 months for subscribers outside India. Duplicate copies cannot be sent to replace issues not delivered because of failure to notify publisher of change of address. The journal is published and distributed by Wolters Kluwer India Pvt. Ltd. Copies are sent to subscribers directly from the publisher's address. It is illegal to acquire copies from any other source. If a copy is received for personal use as a member of the association/society, one cannot resale or give-away the copy for commercial or library use.

The copies of the journal to the subscribers are sent by ordinary post. The editorial board, association or publisher will not be responsible for non receipt of copies. If any subscriber wishes to receive the copies by registered post or courier, kindly contact the publisher's office. If a copy returns due to incomplete, incorrect or changed address of a subscriber on two consecutive occasions, the names of such subscribers will be deleted from the mailing list of the journal. Providing complete, correct and up-to-date address is the responsibility of the subscriber.

Nonmembers: Please send change of address information to subscriptions@medknow.com.

Advertising Policies

The journal accepts display and classified advertising. Frequency discounts and special positions are available. Inquiries about advertising should be sent to Wolters Kluwer India Pvt. Ltd, advertise@medknow. com.

The journal reserves the right to reject any advertisement considered unsuitable according to the set policies of the journal.

The appearance of advertising or product information in the various sections in the journal does not constitute an endorsement or approval by the journal and/or its publisher of the quality or value of the said product or of claims made for it by its manufacturer.

Addresses

Editorial Office

Dr. Vishram Singh, Editor-in-Chief, JASI
B5/3 Hahnemann Enclave, Plot No. 40, Sector 6, Dwarka Phase – 2,
New Delhi - 110 075, India.
Email: editorjasi@gmail.com

Published by

Wolters Kluwer India Pvt. Ltd.,
Fourth Floor, East Wing, Marisoft III, Marisoft Premises,
Part of Software Technology Park, S. No. 15, Vadgaon Sheri,
Kalyani Nagar, Pune – 411 014, Maharashtra, India.
Website: www.medknow.com

Printed at

Nikeda Art Printers Pvt. Ltd.,
Building No. C/3 - 14,15,16, Shree Balaji Complex, Vehele Road,
Village Bhatale, Taluka Bhiwandi, District Thane - 421302, India.

Journal of the Anatomical Society of India

Print ISSN: 0003-2778

EDITORIAL BOARD

Journal of the Anatomical Society of India

Volume 74 | Issue 3 | July-September 2025

CONTENTS

REVIEW ARTICLE

CASE REPORT

The Neuroanatomical Basis of Love, Affection, and Attachment among Human Beings

Introduction

Love, affection, and attachment are central to human relationships and survival. They are not solely cultural or psychological but have deep-rooted neuroanatomical basis. Advances in neuroscience reveal overlapping but distinct neural networks, modulated by neuropeptides and neurotransmitters. The neuropeptides also act as neurotransmitters. The neuropeptides are derived from larger precursor protein molecules and synthesized in nerve cell bodies. Neuropeptides include serotonin, oxytocin, vasopressin, substance P, and endorphins, etc., The classical neurotransmitters on the hand are derived from smaller precursor protein molecules and synthesized in the nerve terminals. Further they are not recycled after release. They include dopamine and serotonin.

Areas of Brain

These include limbic system, ventral tegment area, nucleus accumbens, orbitofrontal and medio frontal cortices, anterior cingulate cortex (ACC), and anterior insula

The *limbic system*, particularly the amygdala, processes emotional salience and contributes to attachment by modulating fear and trust.[1] Functional imaging shows reduced amygdala activity during close bonding.[2] The hippocampus, essential for memory formation, integrates affectionate experiences into autobiographical memory.[3]

The *ventral tegmental area (VTA) and nucleus accumbens*, central to the reward system, show heightened activity in romantic love.[4] Dopaminergic projections from these areas reinforce motivation and the addictive-like qualities of love.[5]

The *orbitofrontal and medial prefrontal cortices* integrate social and emotional signals, supporting trust and long-term relationship maintenance.[6]

The *ACC and insula*, involved in empathy and social pain, explain why loss or separation leads to genuine distress.[7]

Neurotransmitters

The following five neurotransmitters are called as main happy neurotransmitters: Oxytocin, vasopressin, endorphin, dopamine, and serotonin.

Oxytocin, synthesized by neurons in the hypothalamus, especially within supraoptic nucleus and paraventricular nucleus (PVN). It is pivotal in maternal bonding, sexual intimacy, and trust. Released during touch at childbirth, and breastfeeding, it acts on the amygdala and nucleus accumbens to strengthen social attachment.[8]

Vasopressin synthesized in the hypothalamus from the supraoptic and paraventricular nuclei. It contributes to pair bonding, particularly in males. Studies in prairie voles show vasopressin receptor density in the ventral pallidum predicts monogamous behavior.[9]

Endorphins are the body's natural pain relievers and feel-good chemicals. They are synthesized in the neurohypophysis and hypothalamus in the brain. It promotes comfort and satisfaction in long-term stable bonds, supporting transition from passionate to companionate love (non-passionate form of love).[10] It is released by the brain in response to pain, stress, and pleasure activities such as exercise, eating, and sex.

Dopamine is derived from the amino acid "tyrosine." It is synthesized in the VTA and substantia nigara. It is a "feel-good or reward neurotransmitter" and helps the brain learn to seek out rewards. It is responsible for doing self-care activities and celebrating little wins. Further, it influences the mood and social behavior of a person. It is also responsible for romantic love, explaining focused attention and increased energy toward partners.[4,5,11]

Serotonin also known as 5-hydroxytryptamine is derived from the amino acid *tryptaphan* synthesized mainly by enterochromaffin cells of gut (90%) but also by raphe nucleus of brain stem (10%). It is mood stabilizer. It is reduced in early romantic love, correlating with intrusive and obsessive thinking about partners.[12]

Developmental Basis of Attachment

Systems associated with love and affection are activated right from infancy, with maternal bonding relying on oxytocin and dopamine pathways. The hypothalamus, especially the PVN, orchestrates the neurotransmitter signals. It is responsible for early attachment and forms a template for adult romantic relationships.[13,14]

Conclusion

The neuroanatomical basis of love lies in interconnected cortical, limbic, and brain stem circuits, regulated by dopamine, oxytocin, vasopressin, serotonin, and endorphins. These insights explain both the euphoric highs of intimacy and the pains of loss, while providing a basis to understand love, affection, and attachment-related disorders. One can naturally increase these neurochemicals through activities such as exercise, proper nutrition, sufficient sleep, social connections, and meditation.

Vishram Singh, Rashi Singh[1], Gaurav Singh[2]

Department of Anatomy, Kasturba Medical College, Mangalore, Manipal Academy of Higher Education, Manipal, Karnataka, [1]Department of Pediatric and Preventive Dentistry, Santosh Dental College and Hospital, NCR Delhi, Ghaziabad, [2]Clinical Editor, British Medical Journal, NCR Delhi, Noida, Uttar Pradesh, India

Address for correspondence: *Prof. Vishram Singh, B5/3 Hahnemann Enclave, Plot No. 40, Sector 6, Dwarka Phase - 2, New Delhi - 110 075, India.*
E-mail: drvishramsingh@gmail.com

References

1. LeDoux JE. Emotion circuits in the brain. Annu Rev Neurosci 2000;23:155-84.
2. Bartels A, Zeki S. The neural correlates of maternal and romantic love. Neuroimage 2004;21:1155-66.
3. Eichenbaum H. On the integration of space, time, and memory. Neuron 2017;95:1007-18.
4. Fisher H, Aron A, Brown LL. Romantic love: An fMRI study of a neural mechanism for mate choice. J Comp Neurol 2005;493:58-62.
5. Aron A, Fisher H, Mashek DJ, Strong G, Li H, Brown LL. Reward, motivation, and emotion systems associated with early-stage intense romantic love. J Neurophysiol 2005;94:327-37.
6. Rilling JK, Sanfey AG. The neuroscience of social decision-making. Annu Rev Psychol 2011;62:23-48.
7. Eisenberger NI, Lieberman MD. Why rejection hurts: A common neural alarm system for physical and social pain. Trends Cogn Sci 2004;8:294-300.
8. Carter CS. Oxytocin pathways and the evolution of human behavior. Annu Rev Psychol 2014;65:17-39.
9. Young LJ, Wang Z. The neurobiology of pair bonding. Nat Neurosci 2004;7:1048-54.
11. Fisher HE, Xu X, Aron A, Brown LL. Intense, passionate, romantic love: A natural addiction? Soc Cogn Affect Neurosci 2016;11:1832-44.
12. Marazziti D, Akiskal HS, Rossi A, Cassano GB. Alteration of the platelet serotonin transporter in romantic love. Psychol Med 1999;29:741-5.
10. Panksepp J. Affective Neuroscience: The Foundations of Human and Animal Emotions. New York: Oxford University Press; 1998.
13. Bowlby J. Attachment and Loss: Attachment. 2nd ed., Vol. 1. New York: Basic Books; 1982.
14. Feldman R. The neurobiology of human attachments. Trends Cogn Sci 2017;21:80-99.

Article Info

Received: 11 August 2025
Accepted: 19 August 2025
Available online: 30 September 2025

Access this article online	
Quick Response Code:	**Website:** https://journals.lww.com/joai
	DOI: 10.4103/jasi.jasi_137_25

How to cite this article: Singh V, Singh R, Singh G. The neuroanatomical basis of love, affection, and attachment among human beings. J Anat Soc India 2025;74:197-8.

Original Article

Neuroprotective Effects of Taurine May Be Altered by Post-Injury Conditions Following Spinal Cord Injury: Implications for Therapeutic Applications

Sreelakshmi Kokkatt Balachandran, Krithika Iyer[1], Devisree Dhanachezhiyan, Ahamed Siyam Hussain M, Anamika Manoj, Sankar Venkatachalam

Department of Anatomy, Dr. Arcot Lakshmanasamy Mudaliar Postgraduate Institute of Basic Medical Sciences, University of Madras, Taramani Campus, Chennai, Tamil Nadu, India, [1]Spinal Cord and Brain Injury Research Center, College of Medicine, University of Kentucky, Lexington, KY, USA

Abstract

Introduction: Traumatic spinal cord injury (SCI) leads to progressive, multifaceted complications, making treatment challenging. Taurine, a nonessential amino acid, has gained attention for its therapeutic potential due to its reported benefits in various pathologies. However, its antiapoptotic effects remain unexplored in SCI. This study evaluated taurine's efficacy using molecular, histological, and behavioral assessments in a rodent SCI model. **Materials and Methods:** A moderate contusion SCI was induced in Wistar rats. Taurine (200 mg/kg/day) was administered for 2 weeks, and the outcomes were compared to lesion and sham groups. Cell death markers (p53, Bax, caspase-3, AIF, and PARP1) were quantified through western blot 3 days postinjury. In the long term, i.e., up to 4 weeks, motor function deficit/recovery was quantified using behavioral assessments, including gross and fine motor tests. Histological analyses to quantify neuronal apoptosis and spared tissue area were performed in euthanized animals. **Results:** Taurine treatment did not reduce cell death protein levels, nor did it improve motor performance compared to the lesion group. Histological analyses revealed slightly increased cytoarchitectural damage and apoptosis in the taurine-treated group. **Conclusion:** Taurine failed to prevent cell death or improve outcomes after SCI. The reasons for its inefficacy, potentially linked to unaddressed limitations in taurine therapy, are explored based on existing literature. These findings underscore the need for a critical evaluation of taurine's therapeutic viability in SCI and highlight the importance of addressing its limitations before considering it as a treatment option.

Keywords: *Apoptosis, cytoarchitecture, spinal cord injury, taurine*

Introduction

Traumatic spinal cord injury (SCI) disrupts normal life for millions of its victims worldwide due to irreversible functional deficits. The secondary injury processes following SCI, such as inflammation, oxidative stress, excitotoxicity, and demyelination, contribute to cell death both at the injury site and in the surrounding tissue. This delayed cell death/apoptosis significantly impairs the prognosis for recovery. The persistence of apoptosis even during chronic stages[1] underscores the severity of the issue. Experimental studies are ongoing to identify effective treatment strategies to mitigate apoptosis following SCI.

Taurine, or 2-aminoethanesulfonic acid, is a nonproteogenic amino acid ubiquitously present in the human body and involved in various physiological processes, including the development of the central nervous system (CNS).[2] Being a semi-essential amino acid, taurine has been incorporated into dietary supplements and is naturally found in many food products. Numerous studies have reported many potential health benefits due to taurine administration.

Taurine is claimed to function like a neurotransmitter similar to gamma-aminobutyric acid (GABA) and therefore offers protection from excitotoxicity.[3,4] Antioxidant[5,6] and anti-inflammatory[5,7-9] properties of taurine were reported in many studies. Taurine reduces cytosolic Ca^{2+} by both preventing the Ca^{2+} channels from opening as well as inhibiting the release of Ca^{2+} from the endoplasmic reticulum.[3] Through these, it can prevent Ca^{2+}-induced cell death. Taurine is considered to play a vital role in CNS development.[10] There were studies about the neuroprotective[11] and antiapoptotic[12,13] roles of taurine.

How to cite this article: Balachandran SK, Iyer K, Dhanachezhiyan D, Hussain MA, Manoj A, Venkatachalam S. Neuroprotective effects of taurine may be altered by post-injury conditions following spinal cord injury: Implications for therapeutic applications. J Anat Soc India 2025;74:199-208.

Article Info

Received: 10 February 2025
Revised: 15 July 2025
Accepted: 14 August 2025
Available online: 30 September 2025

Address for correspondence:
Prof. Sankar Venkatachalam, Department of Anatomy, Dr. Arcot Lakshmanasamy Mudaliar Postgraduate Institute of Basic Medical Sciences, University of Madras, Taramani Campus, Chennai - 600 113, Tamil Nadu, India.
E-mail: venkatsankar@yahoo.com

Access this article online

Website: https://journals.lww.com/joai

DOI: 10.4103/jasi.jasi_29_25

Quick Response Code:

In addition to these beneficial effects in various pathological conditions, in SCI, taurine levels have been observed to increase near the injury site following steroid therapy, similar to the observations made in brain injuries. It was suggested that the potentiation of taurine levels may contribute to the therapeutic effects of methylprednisolone in SCI.[14] Taurine has been reported to reduce pro-inflammatory cytokines and enhance recovery after SCI. In addition, in lampreys with spinal cord transection, taurine was shown to promote axonal regeneration.[7,15]

Given its ability to mitigate excitotoxicity, inflammation, and oxidative stress, taurine has the potential to reduce injury-induced apoptosis. However, its direct effect on cellular apoptosis after SCI has not been previously reported. The present study aims to investigate the influence of taurine treatment on tissue protection, apoptosis, and functional recovery following SCI using an experimental model.

Materials and Methods

Animals

Female Wistar rats aged 77–90 days were procured from the Central Animal House Facility of the institution. Animals had access to food and water *ad libitum*. Animal maintenance was as per the specifications prescribed by national and international guidelines. All the animal experiments were approved by the Institutional Animal Ethics Committee.

Animal surgeries

The animals were anesthetized using an induction dose of 5% isoflurane and a maintenance dose of 2%. The spinal cord was exposed at the T9–T10 spinal segment level following the standard laminectomy procedure.[16] To induce the contusion SCI, a MASCIS III impactor was used through which a 10 g weight was dropped from 12.5 mm height.[17] After confirming the lesion, the wound was closed in layers, and antiseptics were applied. Prophylactic antibiotics (ampicillin 20 mg/kg/day and gentamicin 2 mg/kg/day) were given intramuscularly for 3 days following surgery. The control group animals underwent sham surgery, i.e., all the surgical procedures except the spinal cord contusion procedure. The animals were divided into different groups, as given in Table 1.

Drug administration and animal maintenance

The postoperative period in the animals was generally uneventful. Urine retention in the acute stage was relieved by the manual expression of the bladder. Starting with the day of injury, taurine (SRL, India), freshly dissolved in sterile physiological saline, was injected intraperitoneally at a dose of 200 mg/kg/day for 3 days and 2 weeks in the animals for western blot and long-term analyses, respectively. On the day of injury, taurine injection was given 2 h before the commencement of surgery and continued for the rest of the days at the same time.

Motor behavior tests

To check the effect of taurine on motor recovery, behavior tests were done for 4 weeks. Gross and fine motor skills were assessed by the tests given below.

Basso–Beattie–Bresnahan scoring

For evaluating the gross motor recovery, Basso–Beattie–Bresnahan (BBB) scoring was done once a week for the long-term animals. The animals were allowed to walk in an open field, and the limb movements were scored on a standard scale of 1–21. The normal animals have a score of 21, whereas complete paraplegic animals which cannot move their hind limbs will get a score of 0.[18]

Narrow beam walking

The integrity of the corticospinal tracts was assessed through narrow beam walking where the animals were allowed to walk through three different wooden beams of varying width. Based on the length and precision of walking through different beams, the scores were given.[19] Normal animals score 6 points, whereas a paraplegic animal, unable to cross the beam(s) would receive a zero score.

Inclined plane

The animals' ability to maintain balance for 5 s in inclined planes ranging from 50° to 90° of inclination was assessed. Scoring was carried out as the maximum angle of inclination managed by the animal. The ability of the animal to hold on to the surface is indicative of the functioning of extrapyramidal tracts, especially the rubrospinal tract.[20]

Horizontal ladder walking

The animals were made to cross a horizontally kept ladder with 20 rungs. The dips or failure to place hind limbs on the ladder rungs was taken as an error.[21] More number of

Table 1: Details of animal distribution among various groups

Group	Description	Animals used for	
		Western blot (3 days)	Motor function assessment and histology (4 weeks)
Control	Animals subjected to sham surgery	3	5
SCI	Contusion SCI (12.5 mm)	3	5
Taurine	SCI + taurine	3	5
Total		24 animals	

SCI: Spinal cord injury

errors is indicative of a higher deficit. This test assesses fine motor skills and coordination.

Tissue isolation and processing for western blotting

After sacrificing the animals with an overdose of anesthesia, a 1 cm piece of the spinal cord with the injury site at its center was isolated and homogenized in radioimmunoprecipitation assay buffer. After centrifuging at 12,000 rpm for 15 min, the supernatant was transferred into a fresh tube, and a protease inhibitor cocktail was added. Protein estimation was done using the Bradford assay using Bio-Rad reagent (Bio-Rad, USA).

Western blotting analysis

For protein expression studies, SDS PAGE with Tris-glycine was done using 10% gel for PARP1 and 16% gel for other proteins. Briefly, protein samples were loaded at appropriate concentrations and electrophoresed at 65 V for 3 h. The immunoblotting was done with Immobilon®-P PVDF Membrane (IPVH00010-Merck, Germany) at 100 V for 75 min. The membranes were then blocked with 5% blocking buffer and incubated overnight at 4°C with the primary antibodies at recommended dilutions. Caspase-3 (1:2000, Bio-vision, USA), AIF (1:1000, Novus Biologicals, USA), PARP1 (1:5000, Abcam, UK), p53 (1:1000, RandD systems, USA), and Bax (1:1000, Cell Signaling Technology, USA) were the antibodies used. On the following day, membranes were washed and incubated in appropriate secondary antibody, i.e., goat antirabbit with HRP (1:5000, GeNei). After washing off unbound secondary antibodies, the membranes were developed using Clarity Western ECL (cat. no. 1705061-BioRad, USA) and imaged using Geldoc (Syngene). The membranes were then stripped and incubated with rat α-tubulin antibody (1:5000, RandD Biosystems, USA) and Goat antimouse secondary antibody (1:5000, Genei, India) for housekeeping protein normalization. The bands were quantified using ImageJ (Ver. 1.47v, Oper Source Software from National Institutes of Health (NIH), USA - Source: https://imagej.net/ij/) and statistical analyses were done using graphpad prism software.

Histology

For histological analysis, the animals were sacrificed with an overdose of anesthesia at the end of 4 weeks. Tissues were fixed through transcardial perfusion with phosphate-buffered saline followed by 4% paraformaldehyde (PFA). After dissecting the vertebral column, a 1 cm piece of the spinal cord with the injury site at its center was isolated and kept in 4% PFA until processing. For tissue processing, standard protocols[22] were followed, and wax-embedded tissue blocks were sectioned using a rotary microtome (Leica, Germany) at 5 μ thickness.

Lesion volume quantification

To evaluate the cytoprotective effects of taurine, lesion volume estimation was done using serial sections stained with hematoxylin and eosin (HE). Using a microscope with a photographic attachment (ECLIPSE Ti2, Nikon, Japan), sections were photographed at ×4. Individual tile images were stitched using proprietary software of the microscope used for panoramic viewing. Using ImageJ software, the total area and cavity/sparred area in the ×4 serial sections were quantified, and graphs were obtained as described in the literature.[23]

Normal and apoptotic cell count

The number of apoptotic cells was counted using modified trichrome staining,[24] which is equivalent to the TUNEL staining for detecting apoptotic cells. After hydrating, the sections were incubated in acid fuschin and acridine orange solution, followed by mordanting in 5% phosphotungstic acid and staining with light green solution. The normal cells were stained as green, and apoptotic cells were in purple/blue shade. Cresyl fast violet as a Nissl stain was used to identify and count the neurons present in the sections using appropriate magnification. The number of total cells as well as apoptotic cells were counted. Results were presented as total neurons present per section and as a percentage of apoptotic cells per section. Representative images were photomicrographed in ×20.

Unbiased quantifications and statistical analyses

All scorers of the quantification data were blinded to the experimental protocol and animal grouping. Quantifications were carried out simultaneously by two independent observers. The quantitative data are presented as line/bar graphs, showing group means ± standard error of the mean. Statistical analysis was performed using Graphpad Prism Version 10 (Dotmatics, Boston, Massachusetts, USA). A one-way analysis of variance, followed by Tukey's *post hoc* test was applied to determine statistical significance, with a threshold of $P < 0.05$.

Results

Motor recovery

BBB which is the test for gross motor behavior did not show any progress after taurine treatment [Figure 1a]. Narrow beam walking test score which is indicative of corticospinal tract connectivity showed numerical differences in the SCI + taurine group when compared with the SCI group; however, the differences were not significant [Figure 1b]. The horizontal ladder walking test for quantifying fine motor control along with coordination also presented data similar to the narrow beam walking test that taurine when causing some numerical difference was not causing significant improvement [Figure 1c]. Inclined plane balancing test results were similar to

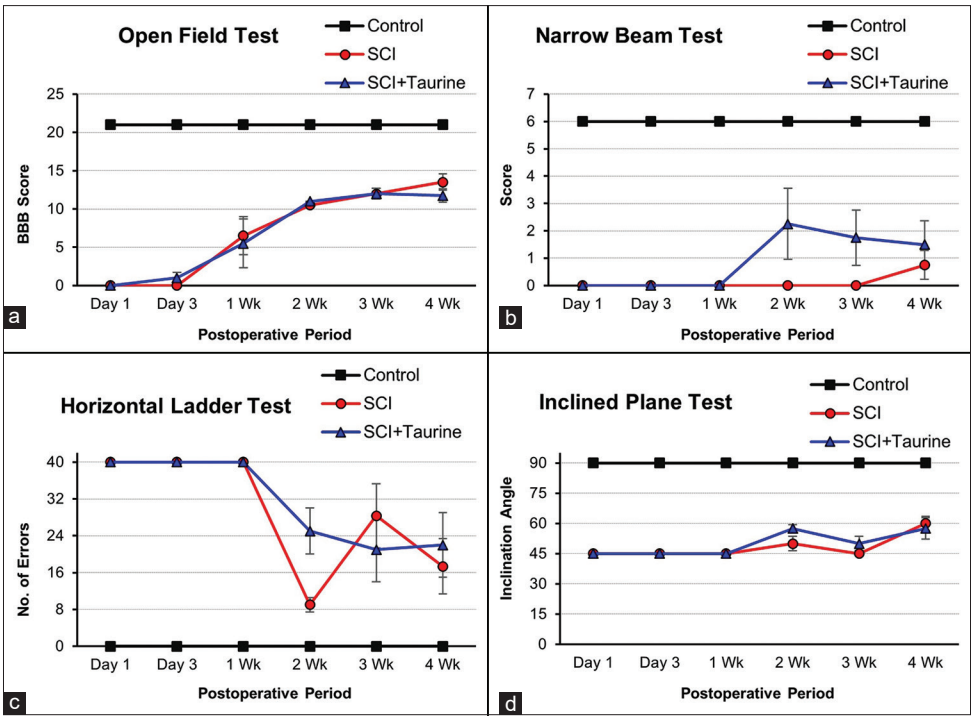

Figure 1: Analysis of functional recovery by motor behavior tests. (a) Gross motor recovery assessed by Basso–Beattie–Bresnahan scoring system. Control group/sham-operated animals showed no deficit with a full score of 21. There was no difference between spinal cord injury (SCI) and SCI + taurine groups. (b) Fine motor recovery indicated by narrow beam walking test scores. With a full score of 6 exhibited by sham-operated animals, no difference was observed between SCI and SCI + Taurine groups. (c) Fine motor recovery with coordination assessment through errors committed in the horizontal ladder walking test. Higher scores indicate a deficit. Sham group animals made no errors, and no difference was observed between the SCI and SCI + taurine groups. (d) Extrapyramidal tracts, especially the rubrospinal tract's connectivity are being tested using the inclined plane test. Sham group animals could maintain balance at a maximum inclination of 90°. The SCI and SCI + taurine group animals barely maintain beyond the basal level of 45°. Taurine treatment did not help in achieving better scores than the SCI group. Please note: At $P < 0.5$ level, the differences between control/sham-operated animals and the rest of the groups were statistically significant. However, the differences between the SCI and SCI + TAURINE groups were not statistically significant. SCI: Spinal cord injury

the other tests that taurine here also failed to show any improvements [Figure 1d].

The function deficits caused by SCI were statistically significant when the control/sham-operated group was compared with SCI and SCI + taurine group. With no statistical significance existing for the differences observed between SCI and SCI + taurine groups, it may be concluded that taurine did not aid toward any improvement in motor function in the spinal cord-injured animals.

Quantification of proteins indicative of apoptosis

The protein p53 is considered a molecular switch between apoptosis and necrosis. Its upregulation pushes a cell toward apoptosis. While there was no significant difference between the control and SCI groups, its levels were significantly upregulated in the SCI + taurine group, indicating a higher push toward apoptosis in taurine-treated group [Figure 2a]. Another proapoptotic protein, Bax, which is involved in mitochondrial pore gating in the intrinsic pathway of apoptosis, was not increased in the SCI group and instead showed a downregulation. Interestingly, taurine treatment increased it to the control group levels which is a significant upregulation when compared with the SCI group [Figure 2b].

The spinal injury was found to have upregulated proteins executing cell death through apoptosis. Both procaspase-3 and active caspase-3 levels were significantly upregulated in the SCI group. In the SCI + taurine group, the levels were slightly higher when compared with the SCI group but not significantly [Figure 3a]. Another apoptotic protein, namely AIF, was highly activated by SCI, and therefore, its uncleaved inactive portion became less in the SCI group. In the SCI + taurine group, the AIF levels were increased significantly when compared with the SCI group, and its active form levels were increased beyond the SCI group but not to the statistical significance [Figure 3b].

PARP1 is a pronecrosis protein, and its overactivation is considered the cause of necrosis. When apoptosis is active, various enzymes involved in apoptosis, like caspase-3, cleave the PARP1 into fragments, thus preventing necrosis and ensuring the progression of apoptosis. The overall increase of PARP1 in both SCI and SCI + taurine groups could be due to the necrosis which is also parallelly executed along with apoptosis after SCI. Interestingly, significantly increased cleaved PARP1 in taurine-treated group over the SCI and control groups is a strong indication of upregulated apoptosis in the SCI + taurine group [Figure 3c].

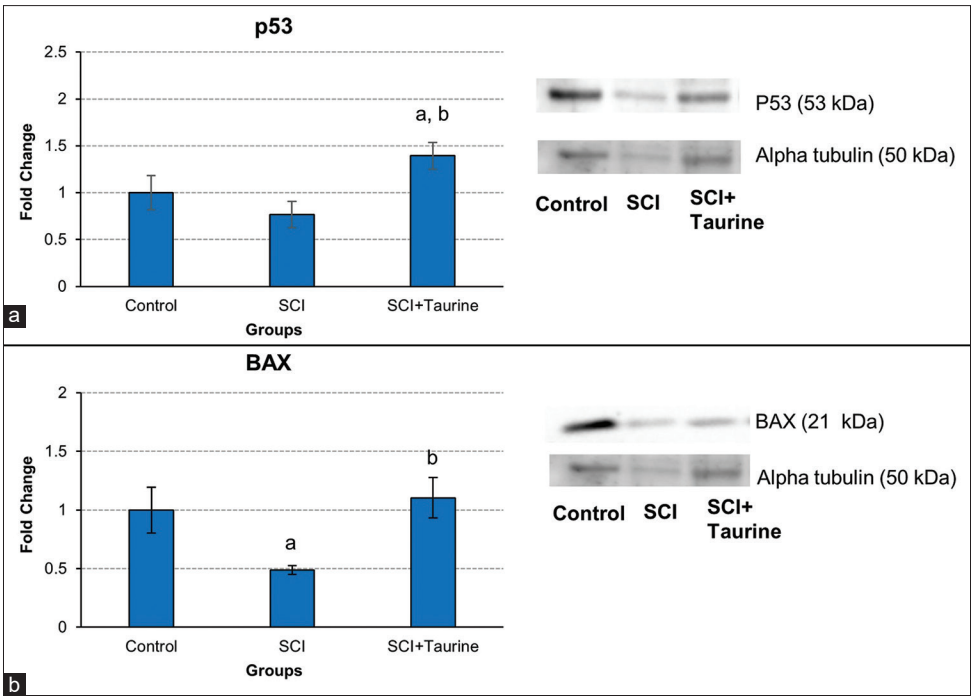

Figure 2: Expression levels of proapoptotic proteins. The bar graphs represent group mean values ± standard error of the mean of proapoptotic proteins p53 (a) and Bax (b). The side panel shows representative western blot band images. At $P < 0.05$ level, "a" represents statistical significance when compared with the control/sham-operated group, and "b" indicates significance when compared with the spinal cord injury group. SCI: Spinal cord injury

The results of the western blot-based protein expression analyses are strongly indicative of both caspase-3-dependent and caspase-3-independent (AIF-based) apoptosis after SCI, and there could be an increase in apoptosis due to taurine administration, although the differences between the SCI group and SCI + taurine groups were not statistically significant.

Spared area

Quantification of spared tissue area (from cavitation) using HE-stained serial sections showed significantly increased damage in the taurine-treated animals [Figure 4]. The extent of tissue damage is visible after injury as well as increased damage in SCI + taurine group animals [top panels in Figure 4]. The decrease in the spared area is due to increased cavitation arising out of cell death [bar graph in Figure 4].

Status of neurons in the spinal segments adjacent to the lesion epicenter

In the spinal segments immediately adjacent to the lesion site, active apoptotic cells could be identified at the end of 4 weeks after the lesion using modified trichrome staining, and there was increased occurrence in the SCI + taurine group [Figure 5a-c]. Nissl staining revealed an appreciable loss in the neurons due to SCI, especially more in the SCI + taurine group [Figure 5d-f].

Neuronal count using Nissl-stained sections presented a significant loss of neurons (more than 50%) due to SCI in the segments adjacent to the lesion site, more so in the SCI + taurine group [Figure 6a]. Alarmingly, even after 4 weeks of injury, progressive apoptosis was evident in those segments, as there were significantly increased apoptosis-positive neurons (from modified trichrome staining) seen in the SCI and SCI + taurine group. Taurine, like in other parameters, here too causes significantly more active apoptosis when compared with other groups [Figure 6b].

The protein expression data, behavior test-based assessment of motor function, and histology-oriented parameters of the present study present a comprehensive picture that taurine when given after SCI in rats did not improve the outcome. Despite the lack of statistical significance for all, the worsened effects due to taurine administration as observed in certain parameters are a worrisome finding.

Discussion

In traumatic brain injury, a 200 mg/kg dose of taurine has been shown to reduce inflammation and prevent tissue damage.[8] Even lower doses have demonstrated antioxidant, anti-inflammatory, and neuroprotective effects in CNS injury models.[7,25,26] Taurine has been reported to reduce myeloperoxidase levels and neutrophil accumulation at the site of injury.[9] In addition, taurine blocks calcium-activated excitotoxicity and calpain-mediated cell death.[2,27]

Despite these promising findings, research on the potential benefits of taurine following SCI remains limited. Taurine has been shown to reduce oxidative stress after SCI[26] and exert anti-inflammatory effects.[7] Acute taurine treatment at

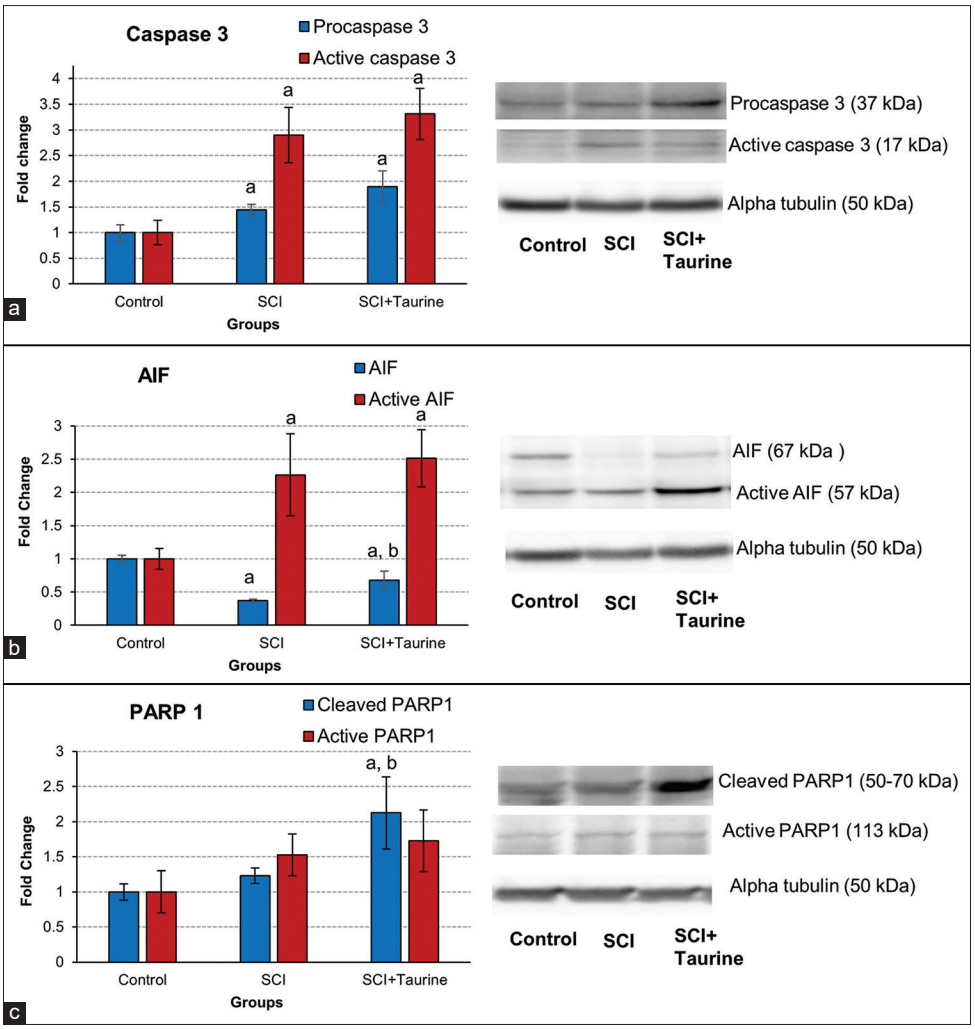

Figure 3: Levels of proteins involved in cell death. The bar graphs show protein levels of procaspase versus active caspase (a), AIF versus active AIF (b), and full-length PARP1 versus cleaved PARP1 (c). Values represent group means ± standard error of the mean. The side panel shows representative western blot band images. At $P < 0.05$ level, "a" represents statistical significance when compared with the control/sham-operated group, and "b" indicates significance when compared with the spinal cord injury group. SCI: Spinal cord injury

the injury site promotes axonal regeneration following spinal cord transection in lampreys.[28] In mice, taurine at a dose of 250 mg/kg was reported to have reduced inflammation and improved locomotor function 4 weeks post-SCI.[7]

Although these studies highlight taurine as a potential therapeutic agent for SCI, most outcomes were assessed based on reductions in inflammation, oxidative stress, and functional recovery. No direct correlation between rescue from cell death and functional recovery was established, necessitating further investigation through the present study to bridge this knowledge gap.

Surprisingly, the present study, which assessed molecular, histological, and functional parameters, found no benefit from taurine treatment. On the contrary, an insignificant increase in apoptosis was observed following taurine administration in a rat contusion SCI model.

Some previous studies have also reported unexpected effects of taurine on neurological functions. For instance, taurine impaired motor performance in the rotarod test. In C57Bl/6J mice, it improved performance in the Morris water maze test but led to severe deficits in the novel object recognition test. In male mice, taurine additionally decreased sociality. Furthermore, while it did not affect passive avoidance behavior in 2-month-old rats, it did affect 16-month-old animals.[3] When administered postweaning, taurine improved visual discrimination tasks; however, when given from birth, it impaired performance compared to controls. Acute taurine treatment reduced fear, while chronic administration increased fear levels compared to controls. These observations suggest that the effects of taurine may depend on factors such as gender, developmental stage, and duration of administration. Notably, taurine appears to be neuroprotective in older animals but raises concerns when used in younger populations.[29]

The present study's findings of increased apoptosis following taurine treatment align with some previous

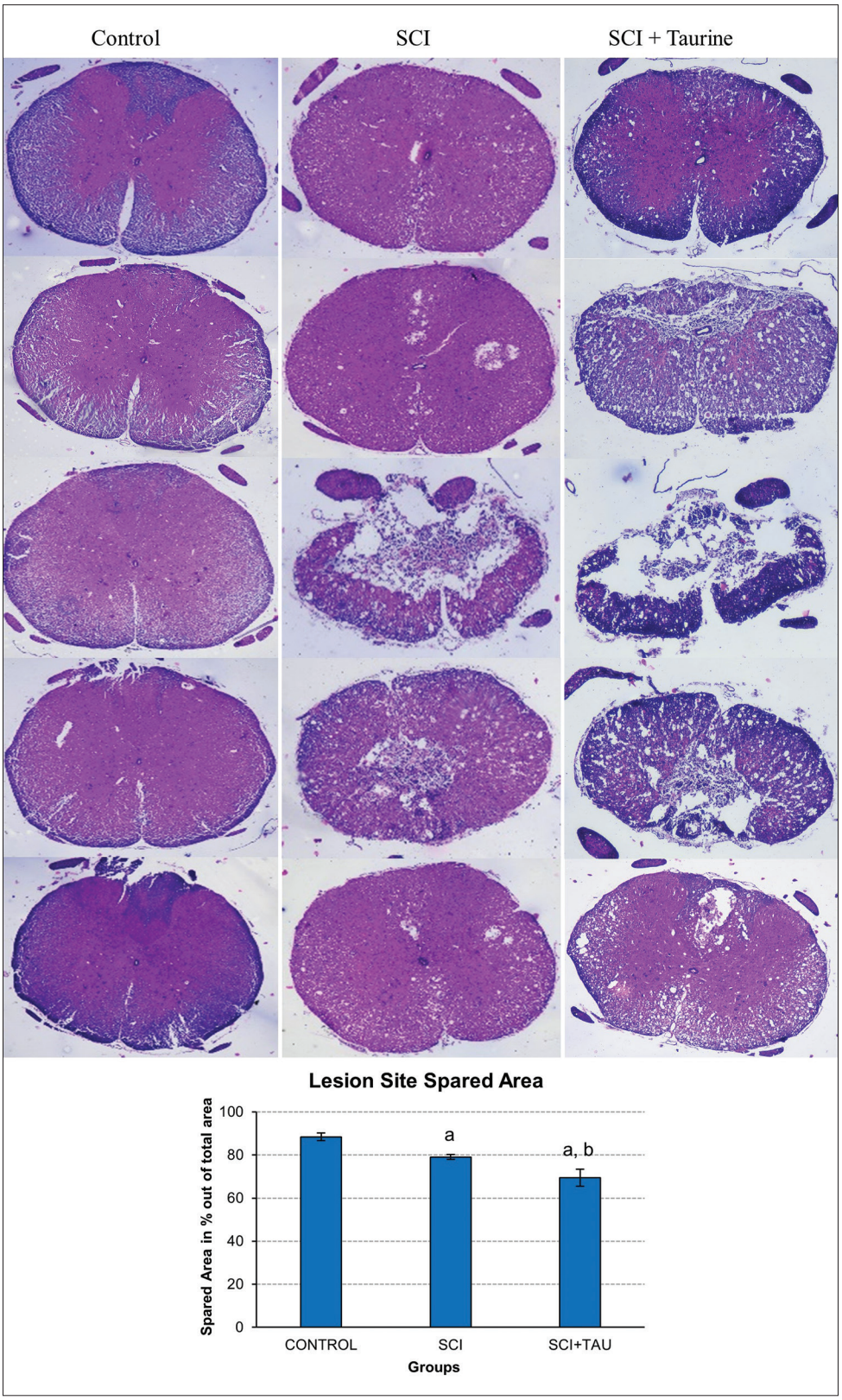

Figure 4: Spared tissue area quantification. The bar graph shows the percentage of tissue area spared in control, lesion, and taurine-treated groups. Values represent group means + standard error of the mean. The side panel shows representative western blot band images. At $P < 0.05$ level, "a" represents statistical significance when compared with the control/sham-operated group, and "b" indicates significance when compared with the spinal cord injury group. The top panel presents representative serial sections stained with hematoxylin and eosin (×4) used for cavity measurement. SCI: Spinal cord injury, TAU: Taurine

reports. Taurine has been shown to induce apoptosis in various cancer cell lines.[30-33] Upregulation of proapoptotic proteins, including p53, Bax, and active caspase-3, observed in this study, has also been reported in cancer cell

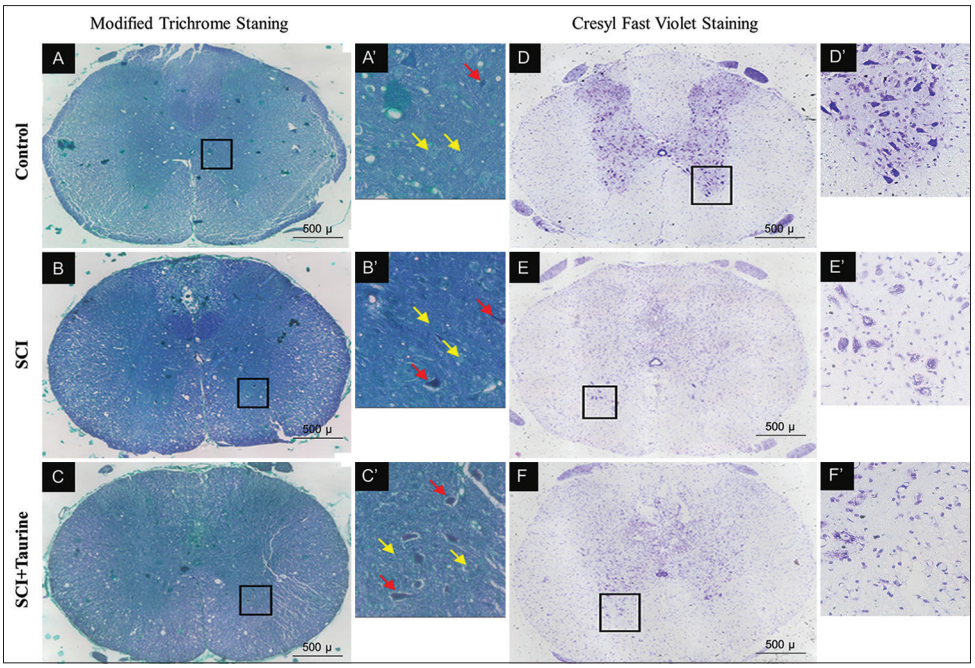

Figure 5: Status of neurons in spinal segments adjacent to the lesion site. Representative images of modified trichrome-stained sections (left) showing apoptotic neurons (a-c) and overall status of neurons using cresyl fast violet (right) as the Nissl stain (d-f). Boxed areas in the sections were shown enlarged in the respective insets (a'-f'). Yellow and red arrows indicate live neurons and dead neurons, respectively. SCI: Spinal cord injury

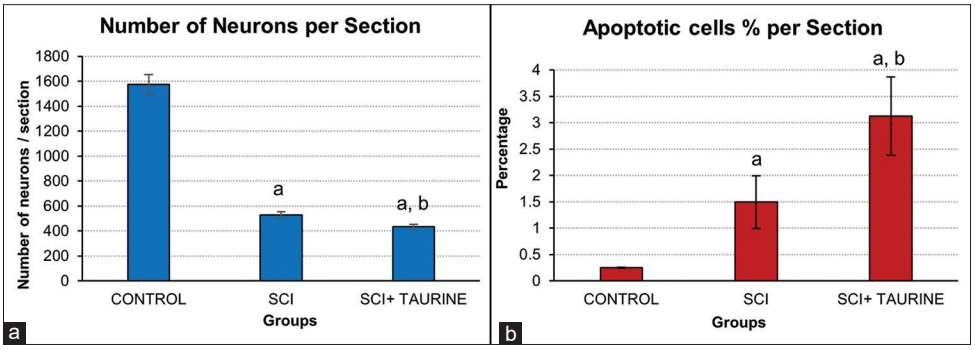

Figure 6: Quantification of apoptotic cells in the spinal segments adjacent to the lesion site. Spinal cord injury (SCI) reduced the number of neurons to more than 50% in the spinal segments immediately adjacent to the lesion epicenter and compared to the SCI group, there was even more reduced number in the SCI + taurine group (a). Percentage of apoptotic neurons calculated by (no. of apoptotic neurons per section/total neurons seen) ×100 presented significantly increased apoptosis in the SCI + taurine group when compared with the SCI and control groups (b). At $P < 0.05$ level, "a" represents statistical significance when compared with the control/sham-operated group, and "b" indicates significance when compared with the spinal cord injury group. SCI: Spinal cord injury

studies involving taurine exposure.[30,31,33] The activation of the p53-mediated pathway is a proposed mechanism for taurine-induced apoptosis in cells.[34] Taurine reduces cytoplasmic calcium levels, which in turn inhibits calcium-triggered calpain activation. In the absence of calpain-mediated apoptosis, DNA damage may trigger p53-mediated apoptotic pathways.

Calpains, regulated by the small subunit CAPNS1 (also known as CAPN4), have been implicated in both proapoptotic and antiapoptotic roles, depending on the context. In mouse embryonic fibroblasts, calpains are proapoptotic in cell death induced by agents such as puromycin, camptothecin, etoposide, hydrogen peroxide, ultraviolet light, and serum starvation. Conversely, they may be antiapoptotic in cell death induced by staurosporine and tumor necrosis factor-α.[35] Calpain-10 is required for mitochondrial function and cell viability, and its decrease during aging is linked to renal function decline.[36] Calpains are also essential for plasma membrane repair following injury by remodeling the cortical cytoskeleton in injured cells.[37]

Taurine's antioxidant effects appear to stem from its ability to restore normal glutathione levels. However, Ozan *et al.* (2012)[38] reported a paradoxical "antioxidative stress" in guinea pigs treated with 300 mg/kg (i.p.) taurine, resulting in increased DNA damage and elevated 3-nitrotyrosine levels in the brain.[39]

Interestingly, from the abovementioned facts, it is obvious that taurine's purported benefits, such as reducing

cytoplasmic calcium, mitigating calpain activation, reducing oxidative stress, and counteracting Ca^{2+}-mediated excitotoxicity, may be counterproductive depending on the tissue and cellular context at the injury site. Moreover, as highlighted earlier, several factors seem to modulate taurine's therapeutic effects.

Concerns have already been raised regarding the validity of claims about taurine's benefits. McClellan and Lieberman argued that many human studies on taurine were poorly conducted, and the combined evidence from human and animal studies did not support claims of enhanced mental or physical performance.[40]

In light of these findings, the present study's observation of increased cell death and lack of functional recovery following taurine treatment raises concerns about its therapeutic potential. These results suggest that the benefits of taurine may depend on yet unidentified conditions. Therefore, further research is required to clarify these uncertainties to consider taurine as a reliable therapeutic agent for neurological disorders.

Conclusion

Despite prior reports of neuroprotection and anti-inflammatory effects in various models, our findings show that taurine treatment after spinal cord injury does not confer functional benefits and is associated with increased apoptosis. These findings, together with contradictory reports in the literature, highlight that taurine's effects are highly context-dependent and sometimes can lead to adverse effects. Further systematic studies are needed before taurine can be considered a reliable therapeutic option

Acknowledgment

The study was supported by the RUSA 2.0 program of the Government of India, awarded to the University of Madras, and SKB received a project fellowship from the program.

Financial support and sponsorship

Nil.

Conflicts of interest

There are no conflicts of interest.

References

1. Wang S, Cheng L. The role of apoptosis in spinal cord injury: a bibliometric analysis from 1994 to 2023. Front Cell Neurosci 2023;17:1-19.
2. Jakaria M, Azam S, Haque ME, Jo SH, Uddin MS, Kim IS, *et al.* Taurine and its analogs in neurological disorders: Focus on therapeutic potential and molecular mechanisms. Redox Biol 2019;24:101223.
3. El Idrissi A. Taurine increases mitochondrial buffering of calcium: Role in neuroprotection. Amino Acids 2008;34:321-8.
4. Wu JY, Prentice H. Role of taurine in the central nervous system. 2010;17 Suppl 1:2-7.
5. Gupta RC, Seki Y, Yosida J. Role of taurine in spinal cord injury. Curr Neurovasc Res 2006;3:225-35.
6. Surai PF, Earle-Payne K, Kidd MT. Taurine as a natural antioxidant: From direct antioxidant effects to protective action in various toxicological models. Antioxidants (Basel) 2021;10:1876.
7. Nakajima Y, Osuka K, Seki Y, Gupta RC, Hara M, Takayasu M, *et al.* Taurine reduces inflammatory responses after spinal cord injury. J Neurotrauma 2010;27:403-10.
8. Su Y, Fan W, Ma Z, Wen X, Wang W, Wu Q, *et al.* Taurine improves functional and histological outcomes and reduces inflammation in traumatic brain injury. Neuroscience 2014;266:56-65.
9. Marcinkiewicz J, Kontny E. Taurine and inflammatory diseases. Amino Acids 2014;46:7-20.
10. Hayes KC, Sturman JA. Taurine in metabolism. Annu Rev Nutr 1981;1:401-25.
11. Wu JY, Prentice H. Role of taurine in the central nervous system. J Biomed Sci 2010;17:(Suppl 1):S1.doi: 10.1186/1423-0127-17-S1-S1.
12. Das J, Sil PC. Taurine ameliorates alloxan-induced diabetic renal injury, oxidative stress-related signaling pathways and apoptosis in rats. Amino Acids 2012;43:1509-23.
13. Zhang F, Tong L, Qiao H, Dong X, Qiao G, Jiang H, *et al.* Taurine attenuates multiple organ injury induced by intestinal ischemia reperfusion in rats. J Surg Res 2008;149:101-9.
14. Benton RL, Ross CD, Miller KE. Spinal taurine levels are increased 7 and 30 days following methylprednisolone treatment of spinal cord injury in rats. Brain Res 2001;893:292-300.
15. Sun M, Xu C. Neuroprotective mechanism of taurine due to up-regulating calpastatin and down-regulating calpain and caspase-3 during focal cerebral ischemia. Cell Mol Neurobiol 2008;28:593-611.
16. Michael FM, Chandran P, Chandramohan K, Iyer K, Jayaraj K, Sundaramoorthy R, *et al.* Prospects of siRNA cocktails as tools for modifying multiple gene targets in the injured spinal cord. Exp Biol Med (Maywood) 2019;244:1096-110.
17. Chandran P, Chandramohan K, Iyer K, Michael FM, Seppan P, Venkatachalam S. Beneficial effects of ethanolic extract of the medicinal herb mucuna pruriens against oxidative stress and inflammation might be limited in contusive spinal cord injury. Biomed Pharmacol J 2022;15:235-48.
18. Basso DM, Beattie MS, Bresnahan JC. A sensitive and reliable locomotor rating scale for open field testing in rats. J Neurotrauma 1995;12:1-21.
19. Luong TN, Carlisle HJ, Southwell A, Patterson PH. Assessment of motor balance and coordination in mice using the balance beam. J Vis Exp 2011;49:5-7. doi:10.3791/2376 .
20. Zhou KL, Chen DH, Jin HM, Wu K, Wang XY, Xu HZ, *et al.* Effects of calcitriol on experimental spinal cord injury in rats. Spinal Cord 2016;54:510-6.
21. Metz GA, Whishaw IQ. The ladder rung walking task: a scoring system and its practical application. J Vis Exp 2009;28:1204. doi:10.3791/1204.
22. Culling CFA. Handbook of Histopathological and Histochemical Techniques. Butterworth-Heinemann, London; 1974.
23. Jakeman LB. Assessment of lesion and tissue sparing volumes following spinal cord injury. In: Animal models of acute neurological injuries II, J. Chen XM, Xu ZC, Xu JH, Zhang (eds.).Springer Protocols Handbooks, Humana Totowa, NJ, USA. 2012, p. 417-442.
24. Anton E. Detection of apoptosis by a modified trichrome technique. J Histotechnol 1999;22:301-4.

25. Gupte R, Christian S, Keselman P, Habiger J, Brooks WM, Harris JL. Evaluation of taurine neuroprotection in aged rats with traumatic brain injury. Brain Imaging Behav 2019;13:461-71.
26. Chen C, Yang Q, Ma X. Synergistic effect of ascorbic acid and taurine in the treatment of a spinal cord injury-induced model in rats. 3 Biotech 2020;10:50.
27. Li Y, Arnold JM, Pampillo M, Babwah AV, Peng T. Taurine prevents cardiomyocyte death by inhibiting NADPH oxidase-mediated calpain activation. Free Radic Biol Med 2009;46:51-61.
28. Sobrido-Cameán D, Fernández-López B, Pereiro N, Lafuente A, Rodicio MC, Barreiro-Iglesias A. Taurine promotes axonal regeneration after a complete spinal cord injury in lampreys. J Neurotrauma 2020;37:899-903.
29. Curran CP, Marczinski CA. Taurine, caffeine, and energy drinks: Reviewing the risks to the adolescent brain. Birth Defects Res 2017;109:1640-8.
30. Zhang X, Tu S, Wang Y, Xu B, Wan F. Mechanism of taurine-induced apoptosis in human colon cancer cells. Acta Biochim Biophys Sin (Shanghai) 2014;46:261-72.
31. Zhang X, Lu H, Wang Y, Liu C, Zhu W, Zheng S, *et al.* Taurine induces the apoptosis of breast cancer cells by regulating apoptosis-related proteins of mitochondria. Int J Mol Med 2015;35:218-26.
32. Okano M, He F, Ma N, Kobayashi H, Oikawa S, Nishimura K, *et al.* Taurine induces upregulation of p53 and Beclin1 and has antitumor effect in human nasopharyngeal carcinoma cells *in vitro* and *in vivo*. Acta Histochem 2023;125:151978.
33. He F, Ma N, Midorikawa K, Hiraku Y, Oikawa S, Zhang Z, *et al.* Taurine exhibits an apoptosis-inducing effect on human nasopharyngeal carcinoma cells through PTEN/Akt pathways *in vitro*. Amino Acids 2018;50:1749-58.
34. Atencio IA, Ramachandra M, Shabram P, Demers GW. Calpain inhibitor 1 activates p53-dependent apoptosis in tumor cell lines. Cell Growth Differ 2000;11:247-53.
35. Tan Y, Wu C, De Veyra T, Greer PA. Ubiquitous calpains promote both apoptosis and survival signals in response to different cell death stimuli. J Biol Chem 2006;281:17689-98.
36. Covington MD, Arrington DD, Schnellmann RG. Calpain 10 is required for cell viability and is decreased in the aging kidney. Am J Physiol Renal Physiol 2009;296:F478-86.
37. Mellgren RL, Zhang W, Miyake K, McNeil PL. Calpain is required for the rapid, calcium-dependent repair of wounded plasma membrane. J Biol Chem 2007;282:2567-75.
38. Ozan G, Turkozkan N, Bircan FS, Balabanli B. Effect of taurine on brain 8-hydroxydeoxyguanosine and 3-nitrotyrosine levels in endotoxemia. Inflammation 2012;35:665–670.
39. Taranukhin AG, Taranukhina EY, Saransaari P, Djatchkova IM, Pelto-Huikko M, Oja SS. Taurine reduces caspase-8 and caspase-9 expression induced by ischemia in the mouse hypothalamic nuclei. Amino Acids 2008;34:169-74.
40. McLellan TM, Lieberman HR. Do energy drinks contain active components other than caffeine? Nutr Rev 2012;70:730-44.

Original Article

On Ameliorating Liver Function through Bee Sting Therapy – Take Nonalcoholic Fatty Liver Disease Rats as an Example

Yanru Sun, Linbing Cheng[1], Xiaoqing Miao[1]

College of Life Sciences, Anhui Normal University, Wuhu, [1]Department of Acupuncture, Fujian Apitherapy Hospital, Fuzhou, China

Abstract

Purpose: Nonalcoholic fatty liver disease (NAFLD) is characterized by lipid accumulation in its early stage and liver fibrosis with time. Bee venom is beneficial against obesity, while there are limited reports on bee sting therapy (BST), a common and traditional type of bee venom therapy, on liver function in NAFLD. Therefore, the effect of BST on liver damage and lipid accumulation in rats with NAFLD caused by a high-fat diet was studied in this study. **Materials and Methods:** We treated high-fat-diet-fed rats with direct bee stings to the epigastric region with different treatment frequency for 28 days. Thereafter, the serum lipid indexes, serum liver function indexes, and liver fibrosis indexes were detected, as well as the histomorphology examination. To find the underlying mechanism, we also tested the expression of proliferator-activated receptor gamma (PPARγ) and TIMP1 through quantitative real-time polymerase chain reaction. **Results:** BST effectively ameliorated liver function with a decrease in serum lipid indexes (triglyceride, total cholesterol, and low-density lipoprotein), serum liver function indexes (aspartate aminotransferase, alanine aminotransferase, and alkaline phosphatase), and liver fibrosis indexes (hyaluronic acid, Type IV collagen, and Type III procollagen). Meanwhile, histomorphology examination showed that the liver was mitigated by BST administration. Subsequently, BST decreased lipid accumulation and liver fibrosis through downregulation of the expression of PPARγ and TIMP1. **Conclusion:** The results indicated that BST can attenuate the progression of liver steatosis and fibrosis by regulating the PPARγ and TIMP1.

Keywords: *Bee venom, lipid accumulation, liver fibrosis, proliferator-activated receptor gamma, TIMP1*

Introduction

Nonalcoholic fatty liver disease (NAFLD) is a chronic metabolic disease caused by nonalcoholic factors, including dietary habit changes.[1,2] With a staggering global frequency of 25.24%, it has emerged as the most commonplace liver disease worldwide.[3] Aspartate aminotransferase (AST) and alanine aminotransferase (ALT) are frequently employed as plasma indicators of liver damage, and NAFLD is characterized by lipid accumulation and insulin resistance, which damage liver cells and elevate aminotransferase levels.[4] The initial stage of NAFLD is characterized by increased triglyceride (TG) synthesis, and the accumulation of TG in the liver and blood further aggravates NAFLD.[5] TG is related to peroxisome proliferator-activated receptor gamma (PPARγ), i.e., the overexpression of PPARγ increased TG synthesis.[6] Besides PPARγ, TIMP1 is another transcriptional regulator key to the formation of hepatic fibrosis.[7] TIMP1 is a crucial member of the TIMP family and is involved in a number of pathophysiologic processes.[8] The rapid reduction in TIMP1 expression is intimately related to the process of lowering liver fibrosis.[9] Liver fibrosis, developed from the initial accumulation of lipids in NAFLD, can increase the clinical risk of liver cirrhosis and hepatocellular carcinoma. Therefore, it is particularly important to achieve early control by interventional treatment from the early NAFLD stage.[10,11] Unfortunately, there is no authorized treatment for patients with NAFLD,[12] so lifestyle changes, like food intervention and increased exercise, are the most frequently recommended treatments.[13,14] However, the weight loss outcomes of NAFLD patients are not always satisfactory due to the patients' willingness and personal condition,[15] a multidisciplinary approach is in need.[16]

Apitherapy is an alternative therapy that uses bee products, especially bee venom, to prevent or treat diseases including liver

How to cite this article: Sun Y, Cheng L, Miao X. On ameliorating liver function through bee sting therapy – Take nonalcoholic fatty liver disease rats as an example. J Anat Soc India 2025;74:209-16.

Article Info

Received: 22 January 2025
Revised: 22 March 2025
Accepted: 24 May 2025
Available online: 30 September 2025

Address for correspondence:
Dr. Yanru Sun,
College of Life Sciences,
Anhui Normal University,
Wuhu 241000, China.
E-mail: sunyanru@ahnu.edu.cn

Access this article online

Website: https://journals.lww.com/joai

DOI: 10.4103/jasi.jasi_18_25

Quick Response Code:

damage.[17] Bee venom therapy is the application of bee venom for therapeutic purposes.[18] The active compounds of bee venom are peptides such as melittin and apamin, and enzymes such as phospholipase A2.[19] Previous studies have revealed that bee venom and its active compounds were effective against human diseases, including rheumatoid arthritis,[20] Parkinson's disease,[21] cardiac dysfunction,[22] and inflammation-induced fibrosis.[23] Besides, bee venom was effective against metabolic diseases caused by diet habits such as obesity and insulin resistance in clinical and *in vivo*.[24-26] The mechanism was involved in the inhibition of adipocyte hypertrophy by suppressing the PPARγ gene and the subsequent phosphorylation of AMP-activated kinase and acetyl-CoA carboxylase in 3T3-L1 cell lines and mice.[27,28] There are several ways of bee venom therapy, i.e., live bee sting, bee venom injection, and bee venom acupuncture.[29] In bee sting therapy (BST), the honeybees inject bee venom directly into the target point via a stinger. Numerous reports focused on bee venom injection and bee venom at special acupuncture points,[27,28] while the bee sting method is traditional and more commonly used in clinical practice despite some disputes on side effects such as local swelling and pain.[18,29,30] However, due to the patients' motivation and individual conditions, the weight loss results of NAFLD patients are not always adequate; therefore, a multidisciplinary approach is required.

This study aimed to investigate whether the BST could ameliorate liver function in NAFLD rats. For this purpose, a daily high-fat diet (HFD) was applied to obtain NAFLD rats. Thereafter, the effect of live bee stings on hepatic fibrosis parameters, including hepatic functional parameters, serum lipid parameters, and morphological changes in histopathology, was observed. A further investigation of the hepatic PPARγ and TIMP1 gene expression in NAFLD rats was assessed.

Materials and Methods

Collection of bees

Honey Bees *(Apis mellifera* L.) fed at Fujian Agriculture and Forestry University were captured in a special plastic box with a long movable cover. On sunny days, a collection box slathered with honey as bait was placed at the entrance of the beehive to attract worker bees. When there were enough bees in the box, the lid was closed and ready for the animal treatment [Figure 1a].

Bee sting treatment

BST does not involve injecting bee venom into the enterocoelia, but rather allowing the stinger to penetrate a specific spot-like acupuncture, and to release the bee venom in a certain area. For each individual bee sting puncture, this study first held the bee with a nail to allow the stinger to touch the central abdomen, then 30 s were given for the bee venom to be delivered into the punctured area [Figure 1b]. Considering that the clinical frequency of BST is normally three times a week,[29] of the researchers in this study managed and administered BST one time per 3 days. Besides, in clinical use, the stinger can usually be stabbed directly to the site of onset,[30] hence the epigastric region, which contains the liver, was chosen as the target area.

Animals and feeds

Forty-eight male rats (weighing 180–220 g) were purchased from Shanghai SLAC Laboratory Animal Co., Ltd. According to the Guidelines of the International Committee on Laboratory Animals, rats were kept in an environmentally controlled room on a 12 h light/dark cycle with a relatively stable ambient temperature of 23°C–27°C and a humidity of 52%–58%. All the rats had unlimited access to food and water. Before the formal testing, the rats were habituated to the food schedule for 1 week. Rats were then separated into six groups, as shown in Table 1. In addition to the BST groups, a positive control (PC) group was established. Animals were fed with compound methionine and choline bitartrate tablets (Sanofi-Aventis Pharmaceutical Co., Ltd., Beijing, China) at 0.32 g/kg body weight per day. Rats in the NC group were fed with a normal diet, while other were fed with HFD, which is composed of 10% fat, 10% yolk, 4%, 1% cholic acid, and 75% normal forage. The animal protocol was approved and recognized by the Animal Care Committee of Fujian Agriculture and Forestry University.

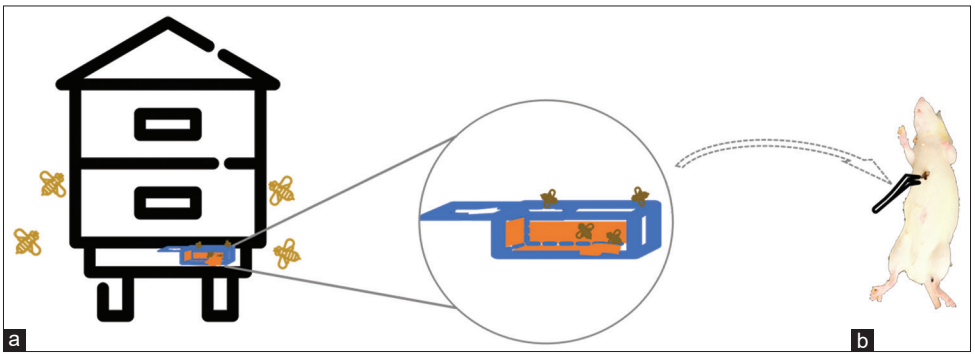

Figure 1: Bee collection and bee sting treatment. (a) A box smeared with honey was placed at the door of the bee hive to attract enough bees for the animal treatment. (b) The bee stinger was punctured to the central abdomen for 30 s to let the bee venom release to the punctured area

Preparation of blood and hepatic samples

After 28 days of treatment, rats were slaughtered. Blood was drawn from the aorta abdominals and kept in centrifuge tubes at room temperature for 2 h. The blood samples were then centrifuged at 3500 rpm for 15 min at 4°C to extract supernatants. The inspection section of Fuzhou 467 Air Force Hospital was entrusted with serum lipid parameters and serum hepatic function indicators. Total glyceride (TG), total cholesterol (TC), and low-density lipoprotein (LDL) were among the serum lipid markers measured. AST, alanine transaminase (ALT), and alkaline phosphatase (AKP) were serum liver function indexes. Parameters, including hyaluronic acid (HA), collage type IV (CIV), and procollagen III (PCIII) were evaluated by enzyme-linked immunosorbent assays (ELISAs) according to the instructions of the ELISA kits (Shanghai Enzyme-linked Biotechnology Co., Ltd.). The whole livers were removed and cleaned as soon as the blood was collected. The equation for calculating the relative liver indexes was (liver/body weight) ×100. The whole livers were then weighed and a piece of liver tissue (0.1 g) was obtained and stored in liquid nitrogen for further use. The remaining liver tissue was fixed in a 4% paraformaldehyde solution.

Histopathology

A series of ethanol concentrations (50%, 70%, 80%, 90%, 95%, and 100%) were used to dehydrate fixed tissues for 1 h. After that, samples were embedded in paraffin blocks after being transparentized with dimethylbenzene. Hematoxylin and eosin staining was used to decorate slices of paraffin-embedded tissue that were cut to a thickness of 5 μm.

Real-time polymerase chain reaction

Following the manufacturer's instructions, total RNA from hepatic tissue was extracted using TransZol UP (Beijing TransGen Biotech Biotechnology Co., Ltd.), and after RNA quality was determined, reverse transcription was carried out. Real-time polymerase chain reaction (PCR) was carried out for the kit (Takara Biotechnology Co., Ltd.) on a CFX384 Touch Real-Time PCR Detection System (Bio-Rad Laboratories, Inc., Hercules, CA, USA) is instructed. Primers were designed and synthesized by Sangon Biotech (Shanghai) Co., Ltd. [Table 2]. The relative value of mRNA expression was measured using the $2^{-\Delta\Delta ct}$ method.

Statistic analysis

All data were expressed as means ± standard deviations. Normally distributed data were analyzed using one-way analysis of variance (ANOVA) followed by least significant difference tests. Data that were not of normal distribution were analyzed by one-way ANOVA followed by Dunnetts' T3 test.

Results

Bee sting therapy improved the relative liver index of nonalcoholic fatty liver disease rats

The liver index for the normal group was 2.57 ± 0.17, as shown in Table 3, and this value differed considerably from that of all other groups. The comparison of the normal control group and the model group suggested that the NAFLD rat model had been successfully established. In addition, each dose of BST treatment considerably reduced

Table 1: Animal groups and treatment

Group name	Drugs	Mode of administration
NC	Saline solution	Ig, per day
MC	Saline solution	Ig, per day
PC	Compound methionine and choline bitartrate tablets at 0.32 g/kg body weight	Ig, per day
BA-1	Bee venom from alive bees	Sting with 1 bee at central abdomen, each 3 days
BA-2	Bee venom from alive bees	Sting with 2 bees at central abdomen, each 3 days
BA-4	Bee venom from alive bees	Sting with 4 bees at central abdomen, each 3 days

NC: Normal control, MC: Model control, PC: Positive control, Ig: Oral gavage, BA: Bee acupuncture

Table 2: Primers used in real-time polymerase chain reaction

Gene name	Accession number	Primers
PPARγ	NM_001145367	Forward: 5'-TGTGGACCTCTCTGTGATGG-3'
		Reverse: 5'-AGCTCTTGTGAACGGGATGT-3'
TIMP1	NM_053819	Forward: 5'-TCTGGCATCCTCTTGTTG-3'
		Reverse: 5'-GCTGGTATAAGGTGGTCTC-3'
β-Actin	NM_031144	Forward: 5'-GGAGATTACTGCCCTGGCTCCTA-3'
		Reverse: 5'-GACTCATCGTACTCCTGCTTGCTG-3'

the liver index as compared to the scenario in the MC group. The BST also showed a dosage-independent effect on the reduction of liver index, meaning that the greater dose worked better.

Bee sting therapy suppressed serum lipid indexes and improved liver function indexes in nonalcoholic fatty liver disease rats

After 4 weeks of HFD feeding, the TG, TC, and LDL levels increased and there was an additional lipid accumulation. Even at the lowest dose (BST-1), BST was effective to alleviate such lipid accumulation in NAFLD rats. Indeed, a dose responsibility was seen in TC and LDL [Figure 2a]. In addition, AST, ALT, and AKP were chosen to identify liver function [Figure 2b]. Each session of bee acupuncture dramatically increased the rats' AST and ALT values, but the AKP level showed no significant changes. Each dose of bee acupuncture significantly improved the AST and ALT values in rats, but no significant changes were detected in AKP. Besides, increased serum indexes including HA, CIV, and PCIII showed liver fibrosis happened after 4-week HFD feeding [Figure 3]. BST at each dose decreased the serum levels of the above indexes, while no dose-dependence effect was observed.

Table 3: Effects of bee sting therapy on relative liver index in nonalcoholic fatty liver disease rats

Group	Liver index (%)
NC	2.57±0.17**
MC	3.85±0.30$^{\#\#}$
PC	3.16±0.17**,$^{\#\#}$
BST-1	3.40±0.11**,$^{\#\#}$
BST-2	3.20±0.63**,$^{\#\#}$
BST-4	3.02±0.11**,$^{\#\#}$

**P<0.01 versus NC group, $^{\#\#}P$<0.01 versus MC group. Values are mean±SD (n=8). SD: Standard deviation, BST: Bee sting therapy, NC: Normal control, MC: Model control, PC: Positive control

Effects of bee sting therapy on hepatic histology

Liver cells from the normal group were unaltered and transparent [Figure 4a]. For MC group rats, hepatic cells have developed steatosis on a large scale, primarily vesicular steatosis, and the cytoplasm of hepatic cells was filled with tiny, dense spherical lipid droplets [Figure 4b]. The nucleus of certain lipid droplets was enormous and filled the whole liver cell [Figure 4b]. As a result, it proved that our experiment's high-fat meals caused the fatty liver of NAFLD. The liver cells in the PC group displayed mild vesicular steatosis, numerous tiny spherical lipid droplets in the cytoplasm [Figure 4c], and expanded liver

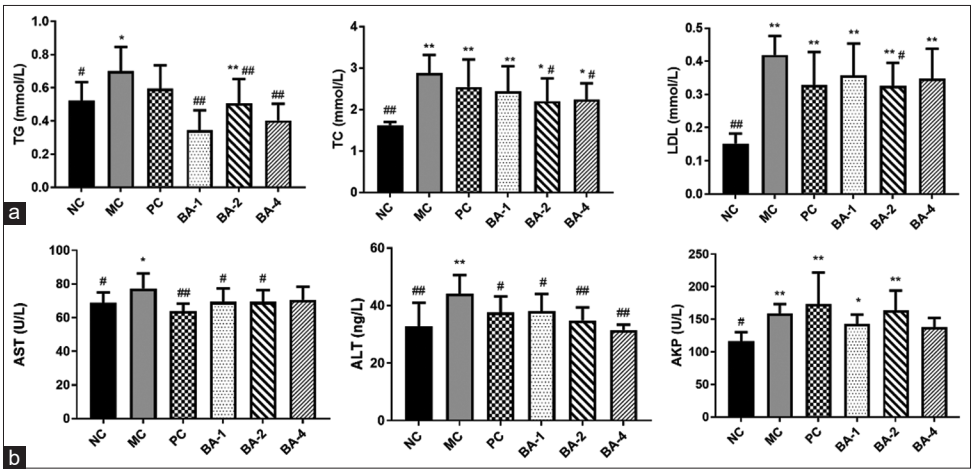

Figure 2: Effect of bee acupuncture on (a) serum lipid indexes and (b) serum liver function indexes in nonalcoholic fatty liver disease rats. Values are mean ± standard deviation (n = 8). *P < 0.05 and **P < 0.01 versus Normal control group; $^{\#}P$ < 0.05 and $^{\#\#}P$ < 0.01 versus model control group. NC: Normal control, MC: Model control, PC: Positive control

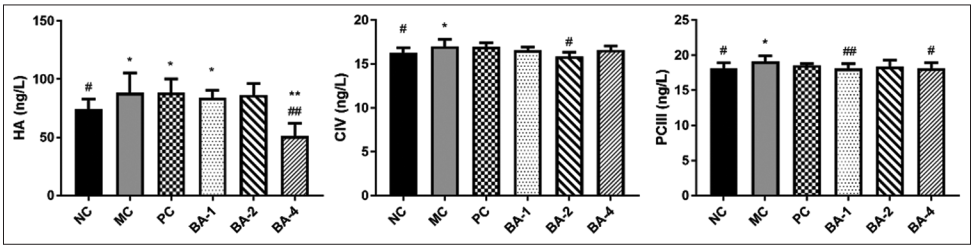

Figure 3: Effect of bee sting therapy on liver fibrosis indexes in nonalcoholic fatty liver disease rats. Values are the mean ± standard error of the mean (n = 8). *P < 0.05 and **P < 0.01 versus Normal control group; $^{\#}P$ < 0.05 and $^{\#\#}P$ < 0.01 versus model control group. NC: Normal control, MC: Model control, PC: Positive control

sinuses [Figure 4c]. BST therapy significantly reduced the symptoms seen in liver cells in rats as compared to those in the MC group. The cytoplasm of liver cells in the BST-1 group was filled with tiny and dense round lipid droplets [Figure 4d]. Lipid droplets in some hepatic cells were slightly larger, and the hepatic sinuses were mildly congested [Figure 4d]. The BST-2 and BST-4 groups performed better than those of the BST-1 group. There were several round lipid droplets of different sizes in the BST-2 group [Figure 4e]. For the BST-4 group, the lipid droplets in a few hepatocytes were slightly larger and the liver sinuses were slightly dilated [Figure 4f].

Effects of bee sting therapy on proliferator-activated receptor gamma and TIMP1 mRNA expression in hepatic tissue

According to real-time PCR, the MC group had considerably higher upregulated levels of PPARγ expression in hepatic tissue than the NC group [$P < 0.01$, Figure 5]. Although bee acupuncture did not bring PPARγ levels back to normal compared to the NC group ($P < 0.05$), they did reduce mRNA expression when compared to the MC group ($P < 0.05$). One of the fibrosis markers is TIMP1. According to Figure 4 ($P = 0.05$), a high-fat meal caused a substantial increase in TIMP1 mRNA expression in the liver. Only CMCB and the medium dose of BST (BA-2 group) significantly reduced TIMP1 mRNA expression in comparison to the MC group (P 0.05) despite the fact that both CMCB and BST decreased TIMP1 mRNA expression.

Discussion

NAFLD is the most prevalent liver disease characterized by excessive lipid accumulation in hepatocytes and activated myofibroblasts.[31] Long-term HFD feeding is widely used to induce obesity and NAFLD in animal models.[32] In this study, we induced NAFLD by feeding HFD to rats for 4 weeks, along with BST every 3 days. Indeed, HFD feeding resulted in a number of NAFLD characteristics of rats according to our study, i.e. increased levels of liver weight index, serum lipid indexes (TG, TC, and LDL), and serum liver function indexes (AST, ALT, and AKP), as well as a clear liver obesity as shown in the hepatic morphology results.

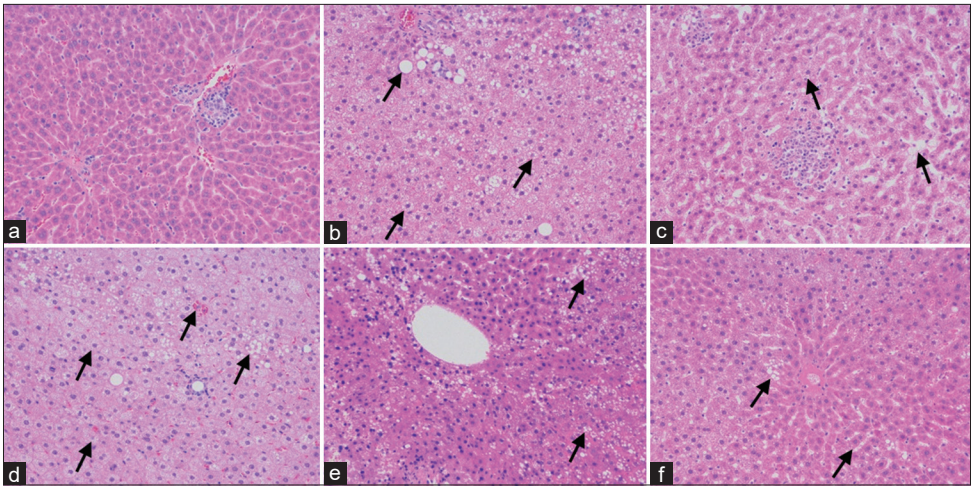

Figure 4: Effect of bee acupuncture on hepatic morphology. (a) Normal control group, (b) MC group, (c) positive control group, (d) BA-1 group, (e) BA-2 group, (f) BA-4 group. Liver sections were stained with hematoxylin and eosin staining (×40). Arrows mark the lesion.

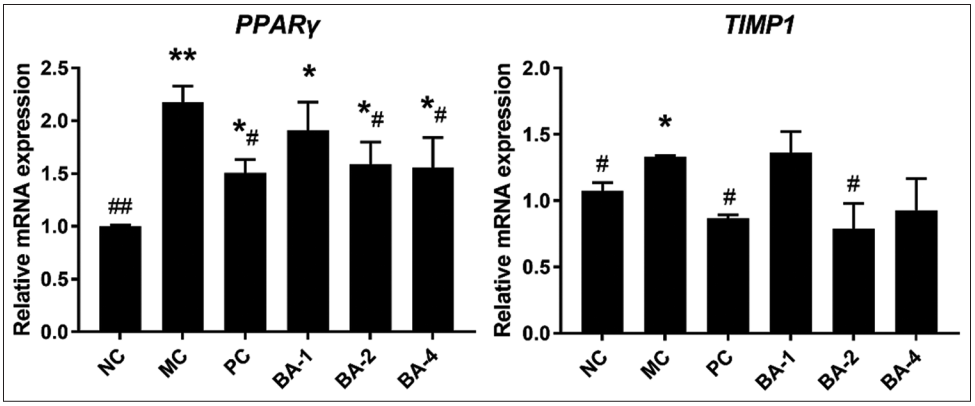

Figure 5: Effect of bee acupuncture on relative mRNA expression of proliferator-activated receptor gamma and TIMP1 in nonalcoholic fatty liver disease rats. Values are mean ± standard error of the mean **P* < 0.05 and ***P* < 0.01 versus the normal control group; #*P* < 0.05 and ##*P* < 0.01 versus MC group. NC: Normal control, MC: Model control, PC: Positive control

Acupuncture and bee venom have both been used to treat many disorders, including obesity.[28] The therapeutic effects of acupuncture and even the bee sting's heating reaction were different from those of a single injection of bee venom.[24] In light of this potential impact and the conventional, historical approach, this study directly concentrated on BST therapy.[33] The inhibitory of BST on obesity accumulation was studied by determining the effect of BST on liver/body index and serum lipid indexes. The rise in liver/body index brought on by HFD feeding in rats was suppressed by BST groups. Aside from that, BST dramatically decreased lipid buildup in NAFLD as evidenced by decreased levels of common blood lipid indexes such as TG, TC, and LDL.

PPARγ is a key factor in glucose and lipid homeostasis.[34] It is mainly expressed in adipose tissue, while the expression is relatively low in the liver.[35,36] As a feature of the steatosis liver, the increased expression of PPARγ is a positive indicator of lipid accumulation in the early pathogenesis of NAFLD.[37] Some studies revealed that the deficiency of hepatic PPARγ greatly inhibited the hepatic *in vitro* and *in vivo*.[6,36] Bee venom was found to inhibit adipogenesis by suppressing adipogenic markers including PPARγ in both cell lines and obese mice.[27,28] In this investigation, bee acupuncture treatment decreased the mRNA expression level of PPARγ in the liver of NAFLD rats, showing that bee acupuncture may minimize the accumulation of lipids and thereby improve the liver status of NAFLD rats. This finding was consistent with previous research that found some natural supplemental medicine to be advantageous to NAFLD models.[38,39] In addition, PPARγ is a vital indicator of TG, and the overexpression of PPARγ increased TG synthesis.[6] Bee acupuncture reduced the amount of TG, which could be due to the reduced expression of PPRAγ. As an upstream regulator of mTOR pathway, PPARγ regulates the TG metabolism.[40,41] Therefore, specific changes of indicators in mTOR pathway by BST should be studied in further studies.

Aside from the evident accumulation of fat in the liver, another feature of NAFLD cell composition alterations is the development of hepatic fibrosis.[31,37] TIMP1 is the most prominent endogenous inhibitor of interstitial collagenase, and it is a well-known biomarker of fibrosis.[42,43] It plays a key role in the NAFLD-related hepatic fibrosis.[7] TIMP1 mRNA expression decreased rapidly throughout the recovery period of hepatic fibrosis.[9] Acupuncture effectively suppressed TIMP1 expression in inflammatory damaged tissues, according to numerous researches,[44,45] and regulated extra TIMP1 expression to alleviate the fibrotic process.[46] Bee venom and its main components effectively inhibited the expression of TIMP1 *in vitro*.[47,48] In this study, BST effectively reduced the serum levels of HA, CIV, and PCIII. The mRNA expression of TIMP1 was also studied after BST in NAFLD rats. According to these findings, liver fibrosis might be another target for BST treatment. There is potential that the BST treatment could relieve the initial experiment stage of liver fibrosis in NAFLD rats.

Conclusion

This study has demonstrated that BST suppressed lipid accumulation by regulating the PPARγ mRNA expression, implying that energy metabolism could be an intriguing target for future research. Moreover, BST ameliorated liver function and liver fibrosis by regulating TIMP1 mRNA expression; however, this was not dose-dependent, which could be due to individual differences. Thus, it can be concluded that BST, a very traditional application of bee venom, might be effective when treating obesity and improving liver function.

Acknowledgments

This study was financially supported by Anhui Normal University Doctoral Research Start-up Project (No. 751916), Natural Science Foundation of Anhui Higher Education (No. KJ2019A0493), and Anhui Natural Science Foundation (No. 2108085QC134).

Financial support and sponsorship

Nil.

Conflicts of interest

There are no conflicts of interest.

References

1. Heindel JJ, Blumberg B, Cave M, Machtinger R, Mantovani A, Mendez MA, *et al.* Metabolism disrupting chemicals and metabolic disorders. Reprod Toxicol 2017;68:3-33.
2. Younossi Z, Tacke F, Arrese M, Chander Sharma B, Mostafa I, Bugianesi E, *et al.* Global perspectives on nonalcoholic fatty liver disease and nonalcoholic steatohepatitis. Hepatology 2019;69:2672-82.
3. Younossi ZM, Koenig AB, Abdelatif D, Fazel Y, Henry L, Wymer M. Global epidemiology of nonalcoholic fatty liver disease-meta-analytic assessment of prevalence, incidence, and outcomes. Hepatology 2016;64:73-84.
4. Sanyal AJ, Friedman SL, McCullough AJ, Dimick-Santos L, American Association for the Study of Liver Diseases, United States Food and Drug Administration. Challenges and opportunities in drug and biomarker development for nonalcoholic steatohepatitis: Findings and recommendations from an American Association for the study of liver diseases-U.S. Food and Drug Administration Joint Workshop. Hepatology 2015;61:1392-405.
5. Nassir F, Rector RS, Hammoud GM, Ibdah JA. Pathogenesis and Prevention of Hepatic Steatosis. Gastroenterol Hepatol (N Y) 2015;11:167-75.
6. Li Z, Xu G, Qin Y, Zhang C, Tang H, Yin Y, *et al.* Ghrelin promotes hepatic lipogenesis by activation of mTOR-PPARγ signaling pathway. Proc Natl Acad Sci U S A 2014;111:13163-8.
7. Tang M, Jia H, Chen S, Yang B, Patpur BK, Song W, *et al.* Significance of MR/OPN/HMGB1 axis in NAFLD-associated hepatic fibrogenesis. Life Sci 2021;264:118619.
8. Wang K, Lin B, Brems JJ, Gamelli RL. Hepatic apoptosis can modulate liver fibrosis through TIMP1 pathway. Apoptosis 2013;18:566-77.

9. Iredale JP, Benyon RC, Pickering J, McCullen M, Northrop M, Pawley S, *et al.* Mechanisms of spontaneous resolution of rat liver fibrosis. Hepatic stellate cell apoptosis and reduced hepatic expression of metalloproteinase inhibitors. J Clin Invest 1998;102:538-49.
10. Chalasani N, Younossi Z, Lavine JE, Diehl AM, Brunt EM, Cusi K, *et al.* The diagnosis and management of non-alcoholic fatty liver disease: Practice guideline by the American Gastroenterological Association, American Association for the study of liver diseases, and American College of Gastroenterology. Gastroenterology 2012;142:1592-609.
11. Maciejewska-Markiewicz D, Stachowska E, Hawryłkowicz V, Stachowska L, Prowans P. The role of resolvins, protectins and marensins in non-alcoholic fatty liver disease (NAFLD). Biomolecules 2021;11:937.
12. Negi CK, Babica P, Bajard L, Bienertova-Vasku J, Tarantino G. Insights into the molecular targets and emerging pharmacotherapeutic interventions for nonalcoholic fatty liver disease. Metabolism 2022;126:154925.
13. Charytoniuk T, Drygalski K, Konstantynowicz-Nowicka K, Berk K, Chabowski A. Alternative treatment methods attenuate the development of NAFLD: A review of resveratrol molecular mechanisms and clinical trials. Nutrition 2017;34:108-17.
14. Chalasani N, Younossi Z, Lavine JE, Charlton M, Cusi K, Rinella M, *et al.* The diagnosis and management of nonalcoholic fatty liver disease: Practice guidance from the American Association for the study of liver diseases. Hepatology 2018;67:328-57.
15. Stewart KE, Haller DL, Sargeant C, Levenson JL, Puri P, Sanyal AJ. Readiness for behaviour change in non-alcoholic fatty liver disease: Implications for multidisciplinary care models. Liver Int 2015;35:936-43.
16. Shetty A, Syn WK. Current treatment options for nonalcoholic fatty liver disease. Curr Opin Gastroenterol 2019;35:168-76.
17. Hellner M, Winter D, von Georgi R, Münstedt K. Apitherapy: Usage and experience in German beekeepers. Evid Based Complement Alternat Med 2008;5:475-9.
18. Zhang S, Liu Y, Ye Y, Wang XR, Lin LT, Xiao LY, *et al.* Bee venom therapy: Potential mechanisms and therapeutic applications. Toxicon 2018;148:64-73.
19. Hossen MS, Gan SH, Khalil MI. Melittin, a potential natural toxin of crude bee venom: Probable future arsenal in the treatment of diabetes mellitus. J Chem 2017;2017:1-7.
20. Lee JA, Son MJ, Choi J, Yun KJ, Jun JH, Lee MS. Bee venom acupuncture for rheumatoid arthritis: A systematic review protocol. BMJ Open 2014;4:e004602.
21. Kim JI, Yang EJ, Lee MS, Kim YS, Huh Y, Cho IH, *et al.* Bee venom reduces neuroinflammation in the MPTP-induced model of Parkinson's disease. Int J Neurosci 2011;121:209-17.
22. Zahran F, Mohamad A, Zein N. Bee venom ameliorates cardiac dysfunction in diabetic hyperlipidemic rats. Exp Biol Med (Maywood) 2021;246:2630-44.
23. Lee WR, Pak SC, Park KK. The protective effect of bee venom on fibrosis causing inflammatory diseases. Toxins (Basel) 2015;7:4758-72.
24. Hanafi MY, Zaher EL, El-Adely SE, Sakr A, Ghobashi AH, Hemly MH, *et al.* The therapeutic effects of bee venom on some metabolic and antioxidant parameters associated with HFD-induced non-alcoholic fatty liver in rats. Exp Ther Med 2018;15:5091-9.
25. Mousavi SM, Imani S, Haghighi S, Mousavi SE, Karimi A. Effect of Iranian honey bee (*Apis mellifera*) venom on blood glucose and insulin in diabetic rats. J Arthropod Borne Dis 2012;6:136-43.
26. Prakash S, Bhargava HR. *Apis cerana* bee venom: It's anti-diabetic and anti-dandruff activity against Malassezia furfur. World Appl Sci J 2014;32:343-8.
27. Kim H, Jo MJ, Nam SY, Kim KM, Choi MB, Lee YH. Evaluating the effects of honey bee (*Apis mellifera* L.) venom on the expression of insulin sensitivity and inflammation-related genes in co-culture of adipocytes and macrophages. Entomol Res 2020;50:236-44.
28. Cheon SY, Chung KS, Roh SS, Cha YY, An HJ. Bee venom suppresses the differentiation of preadipocytes and high fat diet-induced obesity by inhibiting adipogenesis. Toxins (Basel) 2017;10:9.
29. Wesselius T, Heersema DJ, Mostert JP, Heerings M, Admiraal-Behloul F, Talebian A, *et al*. A randomized crossover study of bee sting therapy for multiple sclerosis. Neurology 2005;65:1764-8.
30. Chen J, Lariviere WR. The nociceptive and anti-nociceptive effects of bee venom injection and therapy: A double-edged sword. Prog Neurobiol 2010;92:151-83.
31. Johnson ND, Wu X, Still CD, Chu X, Petrick AT, Gerhard GS, *et al.* Differential DNA methylation and changing cell-type proportions as fibrotic stage progresses in NAFLD. Clin Epigenetics 2021;13:152.
32. Liu J, Han L, Zhu L, Yu Y. Free fatty acids, not triglycerides, are associated with non-alcoholic liver injury progression in high fat diet induced obese rats. Lipids Health Dis 2016;15:27.
33. Cho EJ, Yu SJ, Jung GC, Kwak MS, Yang JI, Yim JY, *et al.* Body weight gain rather than body weight variability associated with increased risk of nonalcoholic fatty liver disease. Sci Rep 2021;11:14428.
34. Wang L, Waltenberger B, Pferschy-Wenzig EM, Blunder M, Liu X, Malainer C, *et al.* Natural product agonists of peroxisome proliferator-activated receptor gamma (PPARγ): A review. Biochem Pharmacol 2014;92:73-89.
35. Ferré P. The biology of peroxisome proliferator-activated receptors: Relationship with lipid metabolism and insulin sensitivity. Diabetes 2004;53 Suppl 1:S43-50.
36. Matsusue K, Haluzik M, Lambert G, Yim SH, Gavrilova O, Ward JM, *et al.* Liver-specific disruption of PPARgamma in leptin-deficient mice improves fatty liver but aggravates diabetic phenotypes. J Clin Invest 2003;111:737-47.
37. Tailleux A, Wouters K, Staels B. Roles of PPARs in NAFLD: Potential therapeutic targets. Biochim Biophys Acta 2012;1821:809-18.
38. Liu B, Zhang J, Sun P, Yi R, Han X, Zhao X. Raw bowl tea (Tuocha) polyphenol prevention of nonalcoholic fatty liver disease by regulating intestinal function in mice. Biomolecules 2019;9:435.
39. Park HJ, Jung UJ, Lee MK, Cho SJ, Jung HK, Hong JH, *et al.* Modulation of lipid metabolism by polyphenol-rich grape skin extract improves liver steatosis and adiposity in high fat fed mice. Mol Nutr Food Res 2013;57:360-4.
40. Grabacka M, Pierzchalska M, Dean M, Reiss K. Regulation of ketone body metabolism and the role of PPARα. Int J Mol Sci 2016;17:2093.
41. Qiao X, Li Y, Mai J, Ji X, Li Q. Effect of dibutyltin dilaurate on triglyceride metabolism through the inhibition of the mTOR pathway in human HL7702 liver cells. Molecules 2018;23:1654.
42. Iredale JP, Pellicoro A, Fallowfield JA. Liver fibrosis: Understanding the dynamics of bidirectional wound repair to inform the design of markers and therapies. Dig Dis 2017;35:310-3.
43. Stetler-Stevenson WG, Liotta LA, Kleiner DE Jr. Extracellular matrix 6: Role of matrix metalloproteinases in tumor invasion

and metastasis. FASEB J 1993;7:1434-41.

44. Chae Y, Hong MS, Kim GH, Hahm DH, Park HJ, Ha E, *et al.* Protein array analysis of cytokine levels on the action of acupuncture in carrageenan-induced inflammation. Neurol Res 2007;29 Suppl 1:S55-8.
45. Zhang S, Ouyang L, Wang X, Xing J, Chen G, Li T. Effect of acupuncture plus thunder-fire moxibustion on MMP-3, TIMP-1 and TGF-β1 in rats with knee osteoarthritis. J Acupunct Tuina Sci 2017;15:322-7. doi: 10.1007/s11726-017-1022-y.
46. Zhao N, Liu B, Liu SW, Zhang W, Li HN, Pang G, *et al.* The combination of electroacupuncture and massage therapy alleviates myofibroblast transdifferentiation and extracellular matrix production in blunt trauma-induced skeletal muscle fibrosis. Evid Based Complement Alternat Med 2021;2021:5543468.
47. Yin CS, Lee HJ, Hong SJ, Chung JH, Koh HG. Microarray analysis of gene expression in chondrosarcoma cells treated with bee venom. Toxicon 2005;45:81-91.
48. Shin SH, Ye MK, Choi SY, Park KK. The effects of melittin and apamin on airborne fungi-induced chemical mediator and extracellular matrix production from nasal polyp fibroblasts. Toxins (Basel) 2017;9:348.

Original Article

Sciatic Nerve Ligation in Rodents: A Morphological and Behavioral Study to Evaluate the Efficacy of Morphine and Ketoprofen

Kajol, Amit Kumar, Subrata Basu Ray

Department of Anatomy, Pain Research Laboratory, All India Institute of Medical Sciences, New Delhi, India

Abstract

Background: Traumatic nerve injuries are associated with neuropathic pain, which is resistant to conventional analgesics. Often, opioids do not have a beneficial effect. Hence, the aim was to evaluate its effect in an animal model and compare it to a nonsteroidal anti-inflammatory drug. Among the different preclinical models for nerve damage, partial sciatic nerve ligation (PSNL) shows persistent levels of nociception without autotomy. In the present study, the ligated sciatic nerve was assessed for damage. Morphine and ketoprofen from two distinct classes of analgesics were evaluated for antinociception in these rats. **Materials and Methods:** Sprague-Dawley rats were divided into the sham surgery (n = 6) and PSNL group (n = 30) where about 1/3–1/2 of the sciatic nerve was ligated. Histological analysis was performed at the end of the study by light and electron microscopy. Nociception was assessed once every week for 3 weeks by von Frey filaments. Nociception was noted to be present throughout the study in the neuropathic group with maximum nociception at the end of the 2nd week when morphine or ketoprofen or both morphine and ketoprofen were administered in separate groups of animals. **Results:** Considerable degeneration was observed in nerve fibers and surrounding myelin within the sciatic nerve in rats with PSNL. Furthermore, these showed decreased withdrawal threshold, which persisted till the end of the study. Morphine and morphine + ketoprofen produced significant antinociceptive effect, but not ketoprofen. **Conclusion:** Morphine likely produced antinociception by binding to μ-opioid receptors. Inhibition of prostaglandin synthesis is not enough to relieve neuropathic pain. The results may have clinical relevance.

Keywords: *Analgesia, neuropathy, nonsteroidal anti-inflammatory drugs, opioids, pain, sciatic nerve*

Introduction

Pain from traumatic damage to peripheral nerves was first reported by Silas Mitchell in 1864 during the American Civil War. It was referred to as causalgia by combining the Greek words for heat and pain. Nerve damage is followed by Wallerian degeneration involving both the axon and myelin sheath.[1] Altered sensory perception like pain to innocuous stimuli (allodynia), excessive pain to a mildly painful stimulus (hyperalgesia), and burning or stabbing pain at rest are common in this condition. Opioids such as oxycodone and morphine are recommended for patients with moderate-to-severe neuropathic pain.[2] However, beneficial effect of morphine remains controversial.[3,4]

Among the different rodent models of neuropathic pain, partial sciatic nerve ligation (PSNL) has been widely used and shows consistent levels of mechanical hypersensitivity (allodynia).[5,6] Although autotomy is observed in some of the models, the rats undergoing PSNL did not show this behavior. In the present study, rats with nerve damage were evaluated for allodynia over a period of 3 weeks [Figure 1]. At the end, animals were euthanized, and the ligated part of the nerve was removed for histological and ultrastructural examination after perfusion–fixation with 4% paraformaldehyde. Apart from this, during the period of maximum nociception, morphine, a gold standard opioid, was administered subcutaneously to detect its antinociceptive effect. Similarly, in a separate set of animals, ketoprofen, a nonselective cyclooxygenase inhibitor, was injected. Finally, both the drugs were coadministered together to observe any synergistic effect, if any.

How to cite this article: Kajol, Kumar A, Ray SB. Sciatic nerve ligation in rodents: A morphological and behavioral study to evaluate the efficacy of morphine and ketoprofen. J Anat Soc India 2025;74:217-20.

Article Info

Received: 26 April 2025
Revised: 04 August 2025
Accepted: 14 August 2025
Available online: 30 September 2025

Address for correspondence:
Dr. Subrata Basu Ray, Department of Anatomy, Pain Research Laboratory, All India Institute of Medical Sciences, New Delhi, India.
E-mail: sbr@aiims.edu

Access this article online

Website: https://journals.lww.com/joai
DOI: 10.4103/jasi.jasi_81_25
Quick Response Code:

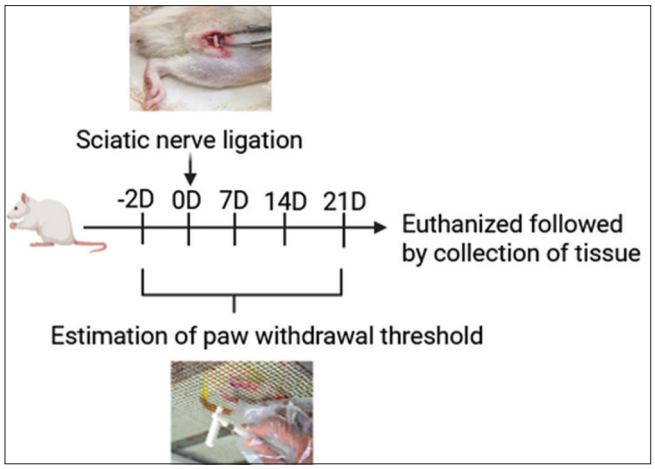

Figure 1: Timeline of experimental work. The rats underwent sciatic nerve ligation on day 0 after determining baseline latency 2 days before ligation. Thereafter, paw thresholds were measured every week at days 7–21 (7 day, 14 day, and 21 day). Finally, the rats were euthanized and sciatic nerve tissue collected for histological examination. Figures in inset show sciatic nerve exposure during partial sciatic nerve ligation (above) and testing for allodynia using von Frey filaments (below)

Materials and Methods

Experimental animals and drug administration

Permission was obtained from the Institutional Ethics Committee (406/IAEC-1/2022). Sprague-Dawley rats (male; 170–200 g) were randomly divided into two main groups: sham (Group I; n = 6) and PSNL (Group II; n = 30). Depending on further procedure, the Group II rats were divided into five subgroups: (a) histological evaluation of the ligated nerve (hematoxylin and eosin [H and E] staining, Osmium tetroxide staining for myelin, and also ultrastructural changes) after day 21; (b) behavioral assessment of mechanical allodynia on days 0, 7, 14, and 21 post-PSNL where day 0 is baseline value; (c) administration of morphine sulfate I.P. (10 mg/kg subcutaneous; Verve Pharmacy, Delhi) on day 14 after PSNL, which coincided with maximum nociception followed by behavioral assessment; (d) administration of ketoprofen I.P. (Neoprofen®; 10 mg/kg s.c.) on day 14 as in Group IIc; and (e) morphine + ketoprofen administration on day 14 as before in Group IIc. Ketoprofen was administered 1 h before morphine. The drugs were given once for determining their acute effect over 24 h.

Procedure of nerve ligation

The rats were anesthetized with isoflurane (2%) inhalation (Orchid Scientific, Pune), and the incision site was shaved and disinfected with 10% povidone-iodine and then isopropyl alcohol. Sciatic nerve was exposed at upper thigh level on the right side and about 1/3–1/2 of the thickness of the nerve ligated with 7-0 Prolene suture as per the earlier protocol.[7] The wound was closed in layers by 4-0 Vicryl for muscle and Ethilon for skin respectively. Rats were injected with analgesic (meloxicam 2 mg/kg subcutaneous once) to relieve postoperative pain from soft tissue injury. Thereafter, these were housed in cages with clean cellulose bedding (Alpha dri®, Shephard Specialty Papers, USA). The procedure for the sham group was the same except that nerve ligation was omitted.

Evaluation of mechanical allodynia

Nociception was evaluated by testing for allodynia by von Frey filaments (Stoelting, USA) using Chaplan's method.[8] Briefly, the rats are allowed to acclimatize on a wire mesh platform for 15 min covered with large transparent Perspex boxes. Thereafter, sufficient pressure was applied by nylon filaments of different sizes in the midplantar aspect of the paw to produce bending of the filament. While healthy rats are oblivious of the pressure, the animals with allodynia abruptly withdrew their paw, often accompanied by flinching or licking, when they feel pain. Allodynia was estimated as 50% withdrawal threshold (g) by an algorithm.[9] The range of pressure exerted on the paw was between 0.4 and 15 g. Paw withdrawal threshold had an inverse relationship with nociception.

Histology of ligated nerve

The rats were euthanized on day 22 by CO_2 inhalation, followed later by thoracotomy, as per the international guidelines. Then, these were perfused with cold 4% paraformaldehyde in 0.1 M phosphate-buffered saline solution by transcardiac route. It was followed up with the collection of the postligated part of the sciatic nerve in the sham and PSNL Group IIa rats. The specimen was processed for H and E staining. Similarly, for myelin staining, fresh tissue (Group IIb) was fixed in Karnovsky's fixative followed by staining with 2% osmium tetroxide solution. The contralateral sciatic nerve was collected for comparison. For transmission electron microscopy, nerve tissue was collected from Group IIb after fixation in Karnovsky's fixative and processing for ultrathin sectioning.

Statistical analysis

The data were analyzed by the statistical analysis program GraphPad Prism software (Ver 10; Boston, MA, USA) using two-way repeated measures ANOVA followed by Tukey's multiple comparison test. $P < 0.05$ was considered statistically significant. Each group of rats had six animals. The values were expressed as mean ± standard error of mean.

Results

The sciatic nerve showed definite evidence of damage on histological evaluation following the ligation [Figure 2]. H and E staining revealed areas, where there was a degeneration of nerve fibers compared to the sham group. This was associated with extensive demyelination as seen by osmium staining. Furthermore, myelin breakdown products were evident as dark granules. It was more clearly observed in the ultrastructural study where extensive damage of the myelin was combined with damage to the nerve fibers.

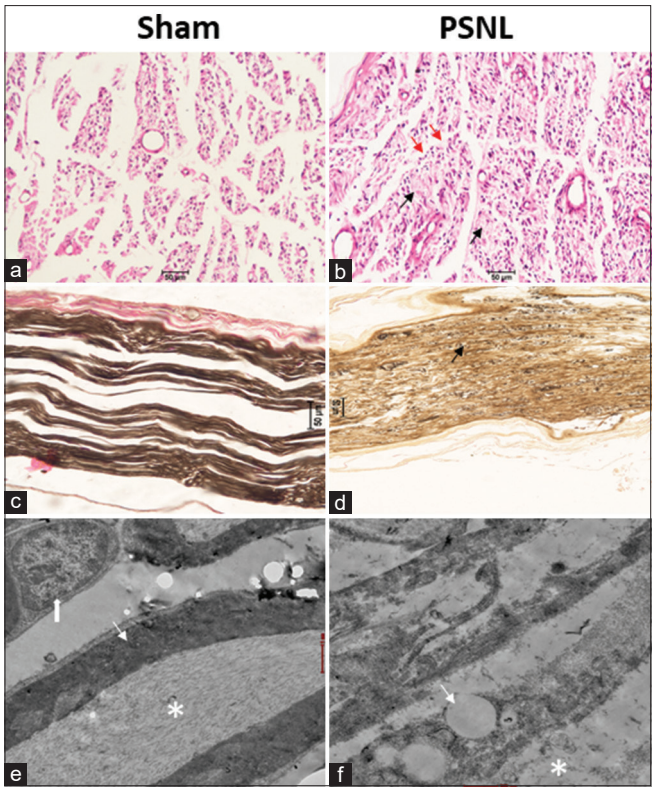

Figure 2: Evaluation of postligated part of the sciatic nerve: (a and b) hematoxylin and eosin; (c and d) osmium staining; (e and f) electron microscopic appearance. (a and b) Compared to the sham group, the rats with partial sciatic nerve ligation (PSNL) showed distinct areas (black arrows) where there was a degeneration of both nerve and myelin. Purple dots represent nuclei of Schwann cell and other connective tissue cells like fibroblasts. Perineurium is shown by red arrows. (c and d) PSNL group showed decreased osmium staining compared to the sham group, and lipid granules, likely breakdown products of myelin (arrow), were observed. (e and f) A nerve fiber is seen in the lower part of the figure in the sham group with distinct axoplasm (*) covered with myelin sheath (line arrow) and Schwann cell cytoplasm. Schwann cell nucleus is also observed (block arrow) in adjacent nerve fiber. In the PSNL group, there is axoplasmic degeneration (*) and myelin breakdown products (arrow). Scale bars in (a-d) 50 μm while that in (e and f) 1 μm (*n* = 6/group)

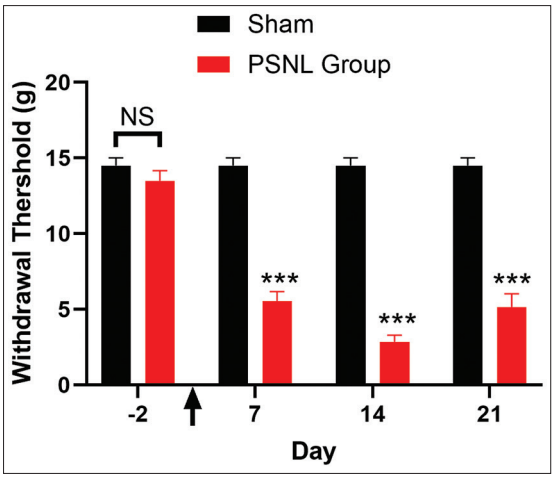

Figure 3: Time of nerve ligation day 0 indicated with arrow on X-axis. Pronounced decrease of paw withdrawal threshold (g) was observed thereafter, indicating allodynia. Minimum values which corresponded with neuropathy-induced allodynia were noted on day 14. The sham group did not show any nociception. The values are represented as mean ± standard error of mean. Difference in baseline thresholds among sham and partial sciatic nerve ligation groups was nonsignificant. *n* = 6/group; ***$P < 0.001$

Compared to the sham group, the rats with PSNL showed a significant decrease of paw withdrawal threshold over a 3-week period. The lowest values were observed on day 14 after sciatic nerve ligation [Figure 3]. Thus, day 14 was chosen for the evaluation. Morphine completely reversed the allodynia as observed by the increase in paw withdrawal threshold at 1 and 3 h, although this effect had disappeared by 24 h [Figure 4]. Compared to morphine, ketoprofen did not show significant antinociceptive effect. Coadministration of both the drugs showed values similar to morphine. That at 1 h was higher than the morphine-alone group, but it was not statistically significant. Similarly, the antinociceptive effect disappeared by 24 h.

Discussion

The current study on rodents showed that opioids like morphine were effective in the treatment of neuropathic pain. On the contrary, ketoprofen, a nonselective cyclooxygenase inhibitor, was ineffective. Neuropathic pain was evaluated as the mechanical threshold for paw withdrawal (g) following innocuous pressure by nylon von Frey filaments. Among the different behavioral tests for estimating neuropathic pain like the cold plate test, pin prick, and acetone spray test, the von Frey method has been noted to be most consistent.[10] The difference between the two drugs is likely related to their different mechanisms of action: activation of G-protein-coupled receptors like the μ-opioid receptor in the nervous system by morphine versus inhibition of prostaglandin synthesis by ketoprofen. Moreover, repeated administration of morphine in these rats over 10 days did not show any tolerance to the antinociceptive effect (data not shown). However, synergistic effect following coadministration, noted at 1 h after administration of morphine + ketoprofen, was absent as the values were not statistically significant [Figure 4]. In chronic constriction injury model, subanalgesic doses of morphine in combination with either nefopam or nimesulide proved synergistic.[11] Apart from this, the earlier study noted that chronic morphine treatment had persistent antinociceptive effect. In the present study, antinociceptive effect of morphine remained the same for 10 days. The difference of result may be due to the fact that nefopam has a different mechanism of action (nonopioid, non-COX inhibitor), while nimesulide is a selective COX-2 inhibitor with different pharmacokinetics compared to ketoprofen.[12] The doses of morphine and ketoprofen chosen for the study were based on earlier reports and fixed at 10 mg/kg.[13,14] The side effects of morphine are sedation, nausea and vomiting, constipation, and, in rare cases, respiratory depression. Ketoprofen can produce abdominal pain, dyspepsia, and worsening of kidney dysfunction.

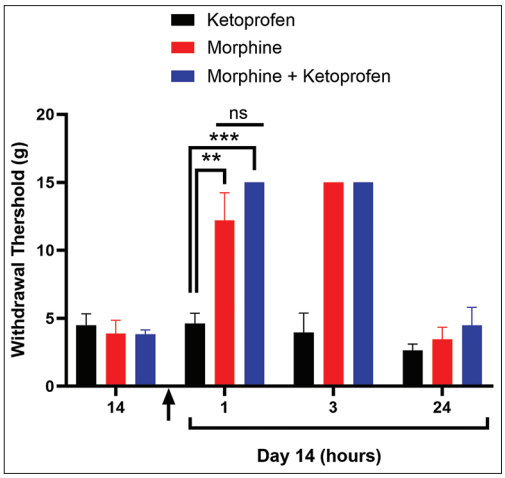

Figure 4: Effect of ketoprofen, morphine, and morphine + ketoprofen on partial sciatic nerve ligation-induced allodynia on day 14. All the three groups showed nociception on day 14 as evident from low paw withdrawal thresholds. Following drug administration, both morphine and morphine + ketoprofen groups showed the reversal of nociception at both 1 and 3 h after treatment, whereas ketoprofen alone-treated group did not show any difference. Arrow indicates time of morphine administration at the beginning of day 14. *n* = 6/group; ***P* < 0.01; ****P* < 0.001

The prevalence of neuropathic pain varies between 7% and 10% in the general population.[15,16] However, due to its complex pathophysiology, treatment with drugs like gabapentin and antidepressants produces mixed results.[17] One of the important factors is cytokines like interleukin (IL)-1β, IL-18, and IL-35, which promote neuroinflammation and indirectly facilitate nociceptive transmission.[18] According to the Cochrane database, moderate improvement was noted with morphine treatment for different types of neuropathy.[4] This was based on five instances of randomized double-blind trials of 2 weeks or longer with morphine, through any route of administration.

The neurohistological findings show evidence of nerve and myelin degeneration, which correlate with the allodynia observed during the study. No evidence of regeneration was observed because the time span was limited.

Conclusion

Morphine was shown to produce robust effect in a rat model of neuropathic pain. Facilitation of pharmacological response by coadministration of different drugs is known as synergism. Morphine + ketoprofen did not show a significant synergic effect at the doses examined. A potential synergistic effect could assist in reducing the dose of morphine with its attendant side effects. Further studies need to investigate novel drug combinations with morphine, which, when coadministered, will potentiate the antinociceptive effect of morphine.

Financial support and sponsorship

Department of Anatomy.

Conflicts of interest

There are no conflicts of interest.

References

1. Ross MH, Pawlina W. Histology – A Text and Atlas. 6th ed. Baltimore, USA: Wolters Kluwer; 2011. p. 386-9.
2. Finnerup NB, Attal N, Haroutounian S, McNicol E, Baron R, Dworkin RH, *et al*. Pharmacotherapy for neuropathic pain in adults: A systematic review and meta-analysis. Lancet Neurol 2015;14:162-73.
3. Arnér S, Meyerson BA. Lack of analgesic effect of opioids on neuropathic and idiopathic forms of pain. Pain 1988;33:11-23.
4. Cooper TE, Chen J, Wiffen PJ, Derry S, Carr DB, Aldington D, *et al.* Morphine for chronic neuropathic pain in adults. Cochrane Database Syst Rev 2017;5:CD011669.
5. Seltzer Z, Dubner R, Shir Y. A novel behavioral model of neuropathic pain disorders produced in rats by partial sciatic nerve injury. Pain 1990;43:205-18.
6. Dowdall T, Robinson I, Meert TF. Comparison of five different rat models of peripheral nerve injury. Pharmacol Biochem Behav 2005;80:93-108.
7. Seltzer Z, Dubner R, Shir Y. A novel behavioral model of neuropathic pain disorders produced in rats by partial sciatic nerve injury. Pain 1990;43:205-18.
8. Chaplan SR, Bach FW, Pogrel JW, Chung JM, Yaksh TL. Quantitative assessment of tactile allodynia in the rat paw. J Neurosci Methods 1994;53:55-63.
9. Dixon WJ. Efficient analysis of experimental observations. Annu Rev Pharmacol Toxicol 1980;20:441-62.
10. Dowdall T, Robinson I, Meert TF. Comparison of five different rat models of peripheral nerve injury. Pharmacol Biochem Behav 2005;80:93-108.
11. Saghaei E, Moini Zanjani T, Sabetkasaei M, Naseri K. Enhancement of antinociception by Co-administrations of nefopam, morphine, and nimesulide in a rat model of neuropathic pain. Korean J Pain 2012;25:7-15.
12. Satoskar RS, Rege NN, Bhandarkar SD. Pharmacology and Pharmacotherapeutics. 23rd ed. Popular Prakashan Pvt Ltd, Mumbai. p. 181-2.
13. Ray SB, Gupta H, Gupta YK. Up-regulation of mu-opioid receptors in the spinal cord of morphine-tolerant rats. J Biosci 2004;29:51-6.
14. Borkowski LF, Keilholz AN, Smith CL, Canda KA, Nichols NL. Nonsteroidal anti-inflammatory drug (ketoprofen) delivery differentially impacts phrenic long-term facilitation in rats with motor neuron death induced by intrapleural CTB-SAP injections. Exp Neurol 2022;347:113892.
15. Baskozos G, Hébert HL, Pascal MM, Themistocleous AC, Macfarlane GJ, Wynick D, *et al.* Epidemiology of neuropathic pain: An analysis of prevalence and associated factors in UK Biobank. Pain Rep 2023;8:e1066.
16. Miclescu A, Straatmann A, Gkatziani P, Butler S, Karlsten R, Gordh T. Chronic neuropathic pain after traumatic peripheral nerve injuries in the upper extremity: Prevalence, demographic and surgical determinants, impact on health and on pain medication. Scand J Pain 2019;20:95-108.
17. Finnerup NB, Kuner R, Jensen TS. Neuropathic pain: From mechanisms to treatment. Physiol Rev 2021;101:259-301.
18. Gonçalves Dos Santos G, Delay L, Yaksh TL, Corr M. Neuraxial cytokines in pain states. Front Immunol 2019;10:3061.

Original Article

Does Internal Carotid Artery Stenosis Affect Vertebrobasilar Arterial Morphometry? Computed Tomography Angiography Analysis

Gizem Nur Bakir, Mennan Ece Pirzirenli, Fatih Uzunkaya[1]

Departments of Anatomy and [1]Radiology, Faculty of Medicine, Ondokuz Mayıs University, Kurupelit, Samsun, Turkey

Abstract

Background: The internal carotid artery (ICA) and the vertebral artery (VA) are responsible for ensuring cerebral perfusion. When the ICA is insufficient in cerebral flow, a collateral rescue system takes place by the circle of Willis. This situation causes increased posterior circulation blood flow and hemodynamic pressure. Therefore, to investigate possible changes in the vertebrobasilar arterial system (VBAS) morphometry. **Materials and Methods:** Brain–neck computed tomography angiography (CTA) images of a total of male (50) and female (46) 96 patients were examined retrospectively. ICA stenosis was measured by the North American Symptomatic Carotid Endarterectomy Trial method and was grouped according to the degree of stenosis in each stenosis group with tandem stenosis (wTS) and without tandem stenosis (woTS). Morphometric evaluation of the VBAS structures of the groups was measured and compared. **Results:** When those wTS and woTS are compared within their own groups, significant differences were detected in VA diameters. When the cases in the group woTS were compared with each other, significant differences were detected in VA diameter values. **Conclusion:** We found that the presence of ICA stenosis and tandem lesions affected the VBAS morphometry.

Keywords: *Angiography, internal carotid artery, stenosis, vertebral artery*

Introduction

The circle of Willis, the fundamental structure of cerebral perfusion, is formed by the collateral connections between the internal carotid artery (ICA), which provides anterior circulation, and the vertebral arteries (VAs), which provide posterior circulation. These collateral connections assume a compensatory rescue role in maintaining cerebral blood flow in cases of severe stenosis or occlusion in either the anterior or posterior circulation.[1,2]

According to this compensatory mechanism, stenosis of the ICA results in alterations in the vertebrobasilar arterial system (VBAS) morphology due to increased posterior blood flow and hemodynamic pressure.[3]

Rather than stenosis occurring at a single localization on the carotid artery, the occurrence of stenosis at multiple localizations is referred to as tandem stenosis. Tandem stenosis is frequently reported at the ICA and middle cerebral artery and less commonly at the ICA and common carotid artery (CCA)[4] [Figure 1].

The North American Symptomatic Carotid Endarterectomy Trial (NASCET) formulation is often used for the evaluation and grading of ICA stenosis in clinical practice.[5-7]

The aim of our study is to investigate the effects of ICA stenosis degrees and the presence of Tandem stenosis on VBAS morphometry in the collateral compensation system in the circle of Willis using computed tomography angiography (CTA) imaging.

Materials and Methods

Our study was conducted in accordance with the principles of the Helsinki Declaration after obtaining approval from the ethics committee of our institution, and ethical rules were adhered to throughout the study period.

Study design

CTA images and clinical data of a total of 200 patients who applied to our university hospital between 2020 and 2023 were examined. Forty-seven patients had undergone brain surgery, 10 patients

How to cite this article: Bakir GN, Pirzirenli ME, Uzunkaya F. Does internal carotid artery stenosis affect vertebrobasilar arterial morphometry? Computed tomography angiography analysis. J Anat Soc India 2025;74:221-7.

Article Info

Received: 17 January 2025
Accepted: 18 August 2025
Available online: 30 September 2025

Address for correspondence:
Dr. Gizem Nur Bakir, Department of Anatomy, Faculty of Medicine, Ondokuz Mayıs University, 55200, Kurupelit, Samsun, Turkey.
E-mail: dr.karakoyun@gmail.com

Access this article online

Website: https://journals.lww.com/joai

DOI: 10.4103/jasi.jasi_12_25

Quick Response Code:

Figure 1: Tandem stenosis on computed tomography scan. Stenotic lesions: (1) at the bifurcation of the common carotid artery and (2) at the proximal internal carotid artery. CCA: Common carotid artery, ICA: Internal carotid artery

were under the age of 18, 31 patients had undergone carotid endarterectomy, seven patients had vertebrobasilar dolichoectasia, and nine patients had cancer. According to the determined inclusion and exclusion criteria, a total of 96 patients, aged between 45 and 92, were included in the study.

Inclusion criteria

Control group: Patients presenting to the clinic with complaints of headache, in whom clinical examinations reveal no evidence of cerebrovascular pathology, and with intact extracranial vascular structures.

Moderate and severe stenosis group: Patients diagnosed with carotid artery stenosis who have not undergone revascularization procedures.

Exclusion criteria

- Being under the age of 18 years
- The presence of pathologies such as hypoplasia, aneurysm, ectasia, arteriovenous malformation, dissection, and vasculitis affecting the lumen diameter in intracranial vascular structures, including the ICA and CCA
- The presence of past brain surgery, tumor, trauma, cerebral hemorrhage, and genetic diseases.

CTA images of the patients were reviewed retrospectively. The levels of ICA stenosis and tandem lesions were determined, and morphometric measurements were conducted on the VBAS.

Using the NASCET measurement method, ICA stenoses were measured on CTA images. The residual lumen (A) at the stenotic region and the distal normal ICA diameter (B) were measured. These measurements were then used in the NASCET formula to calculate the percentage of ICA stenosis[6] [Figure 2].

Consistent with the cutoff values referenced in Barnett *et al*.'s study, we classified the patients into three groups: those without stenosis in either the right or left ICA were categorized as the control group, those with stenosis ranging from 50% to 69% in the right, left, or both ICAs were categorized as the moderate stenosis group, and those with 70%–99% stenosis were categorized as the severe stenosis group.[8-10] In cases where ICA stenosis was observed on both sides, the stenosis percentages for both the right and left sides were calculated and recorded. Regardless of the right or left side, patients were categorized into the moderate or severe group based on the highest degree of stenosis. Each group consisted of 32 patients, resulting in a total of 96 patients.

Tandem stenosis was detected in 14 of 96 patients. The initial stenosis localization in these patients was at the CCA bifurcation, and the second stenosis localization was in the proximal ICA. Stenosis values at the lesion sites of these patients were measured. To assess the impact of tandem lesions on VBAS morphometrics, seven patients were included in the moderate stenosis group and seven patients were included in the severe stenosis group based on the highest stenosis value. Within the moderate and severe stenosis groups, subgroups were formed with tandem stenosis (wTS) consisting of seven patients and without tandem stenosis (woTS) consisting of 25 patients.

The morphometric measurement values of the groups were compared initially by comparing the control, moderate, and severe groups (n = 32). To evaluate the impact of tandem lesions, within the moderate group, a comparison was made between the wTS (7) and woTS (25) subgroups, and the same intragroup comparison was conducted for the severe group. Subsequently, during the comparison between the moderate and severe groups, the wTS and the woTS of both groups were compared.

Computed tomography angiography images

CTA images were acquired using a 64-channel multidetector CT scanner (GE Light Speed VCT; GE Healthcare, Milwaukee, Wisconsin, USA).

In the CTA scans, 60–100 ml of nonionic contrast agent (iohexol) was administered to the patient intravenously. Imaging parameters obtained during the arterial phase were as follows: Slice thickness of 0.625 mm, rotation time of 0.4 s, spiral pitch value of 0.984, tube voltage of 120 kV, and tube amperage of 400–500 mA.

Multiplanar reconstruction and maximum intensity projections options were utilized on the three-dimensional images of the multislice CTA using the OsiriX 64-bit (Lite Digital Imaging and Communications in Medicine Viewer version 5.6, Geneva, Switzerland) software.

Morphometric values for ICA and VBAS were measured separately by a research group consisting of

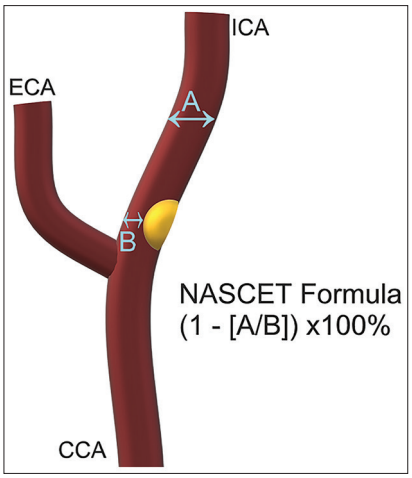

Figure 2: An illustration of the North American Symptomatic Carotid Endarterectomy Trial measurement method. (a) Distal normal internal carotid artery diameter, (b) residual lumen diameter, ICA: Internal carotid artery, ECA: External carotid artery, CCA: Common carotid artery

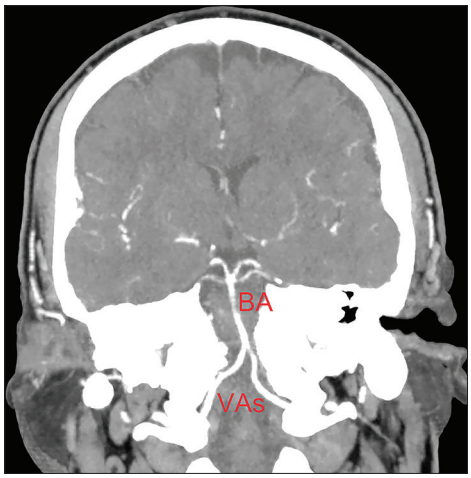

Figure 3: Vertebrobasilar arterial system on computed tomography scan. VAs: Vertebral arteries, BA: Basilar artery

three individuals: two anatomists and one radiologist. The measurements were recorded in centimeters on a measurement scale by taking the average of the values obtained.

On the patients' CTA images, 11 morphometric measurement points were identified for the VA intracranial segment (V4) and basilar artery (BA) in terms of diameter and length parameters of VBAS. These points were measured and recorded.

Vertebrobasilar arterial system morphometric measurement parameters

Different points of vessel diameters of VA and BA and their lengths were measured [Figure 3], including the following:

- Diameter of VA at the intradural entrance (right side VAD1 and left side VAD4)
- Diameter of VA at the level of the posterior inferior cerebellar artery (PICA) origin (right side VAD2 and left side VAD5)
- Diameter of VA at terminal, i.e., just before joining the contralateral VA to form the BA (right side VAD3 and left side VAD6)
- Diameter of BA from two points as the beginning (BAD 1) and terminal (BAD 2)
- Length of VA from the intradural entrance to the vertebrobasilar junction (VBJ) (right side VAL1 and left side VAL2)
- The length of BA from VBJ to terminal (BAL).

A total of 11 morphological parameters were measured across all groups to investigate the presence of statistical relationships among these values and their correlations between groups.

Statistical analysis

The IBM, NY, USA SPSS Statistics V25 package program was utilized for the statistical analysis. Basic characteristics were reported using standard descriptive statistics. Parametric Student's *t*-test was used for independent group comparisons for data conforming to normal distribution, whereas the nonparametric Mann–Whitney *U*-test was used for data not conforming to normal distribution. Kruskal–Wallis tests were used for comparisons involving more than two groups. A significance level of $P < 0.05$ was considered statistically significant for all statistical analyses.

Results

Among the 96 patients included in the study, 46 (47.91%) were female, and 50 (52.08%) were male, with a mean age of 70.54 for all patients. The mean age according to groups was 70.62 in the control group, 70.72 in the moderate group, and 70.28 in the severe group. In both the moderate and severe groups, right ICA stenosis was more prevalent than left ICA stenosis and bilateral stenosis. This difference was more pronounced in the woTS subgroups.

In the group comparison made without separating patients wTS ($n = 32$), there was no statistically significant difference in morphometric measurements related to VBAS among the control group, moderate stenosis, and severe stenosis groups ($P > 0.05$). However, we found that tandem stenosis affected some morphometric parameters. Comparison within the moderate and severe stenosis groups based on the presence or absence of tandem stenosis yielded statistically significant results. The morphometric measurement results for patients wTS and woTS in the moderate and severe groups are presented in Tables 1 and 2.

According to the measurement results, there was a significant difference in the right VA diameter at the PICA origin level (VAD2) between patients woTS and wTS in the moderate stenosis group ($P = 0.028$). The mean VAD2 value was measured as 0.195 cm in woTS cases and 0.243 cm in wTS cases in the moderate group. Thus, wTS cases in the moderate group had a wider diameter. In the severe stenosis group, there was a significant difference

Table 1: Morphometric measurement values of patients without tandem stenosis and patients with tandem stenosis in the moderate group

Parameters (cm)	Moderate group woTS (*n*=25)				Moderate group wTS (*n*=7)				
	Mean	Maximum	Minimum	SD	Mean	Maximum	Minimum	SD	*P*
VAD1 (right)	0.277	0.742	0.131	0.117	0.268	0.397	0.162	0.089	0.553
VAD2 (right)	**0.195**	0.284	0.096	0.050	**0.243**	0.342	0.146	0.088	**0.028**
VAD3 (right)	0.178	0.272	0.116	0.047	0.214	0.322	0.128	0.066	0.640
VAD4 (left)	0.307	0.436	0.149	0.074	0.302	0.352	0.211	0.051	0.600
VAD5 (left)	0.247	0.382	0.141	0.065	0.229	0.291	0.167	0.042	0.220
VAD6 (left)	0.203	0.291	0.103	0.053	0.208	0.281	0.176	0.040	0.891
VAL1 (Right)	3.477	5.022	2.149	0.603	3.458	3.886	2.858	0.424	0.423
VAL2 (left)	3.588	4.808	2.627	0.573	3.260	4.086	2.656	0.615	0.187
BAD1	0.294	0.412	0.161	0.058	0.317	0.366	0.241	0.045	0.325
BAD2	0.257	0.371	0.116	0.071	0.277	0.363	0.186	0.078	0.570
BAL	2.895	3.814	2.207	0.425	2.763	3.759	2.149	0.642	0.083

Significant *P*<0.05 is emphasized in bold text. woTS: Without tandem stenosis, wTS: With tandem stenosis, VAD1: Right VA diameter at the intradural entrance, VAD2: Right VA diameter at PICA origin level, VAD3: Right VA diameter at terminal, VAD4: Left V4 diameter at the intradural entrance, VAD5: Left VA diameter at PICA origin level, VAD6: Left VA diameter at terminal, VAL1: Right VA length, VAL2: Left VA length, BAD1: BA diameter at the beginning, BAD2: BA diameter at terminal, BAL: BA length, SD: Standard deviation, PICA: Posterior inferior cerebellar artery, VA: Vertebral artery

Table 2: Morphometric measurement values of patients without tandem stenosis and patients with tandem stenosis in the severe group

Parameters (cm)	Severe group woTS (*n*=25)				Severe group wTS (*n*=7)				
	Mean	Maximum	Minimum	SD	Mean	Maximum	Minimum	SD	*P*
VAD1 (right)	**0.278**	0.422	0.156	0.065	**0.193**	0.348	0.108	0.093	**0.026**
VAD2 (right)	0.241	0.353	0.147	0.050	0.202	0.272	0.121	0.063	0.178
VAD3 (right)	0.204	0.291	0.102	0.040	0.168	0.265	0.089	0.062	0.078
VAD4 (left)	0.263	0.431	0.103	0.088	0.317	0.378	0.188	0.062	0.148
VAD5 (left)	0.217	0.391	0.106	0.074	0.261	0.377	0.145	0.068	0.373
VAD6 (left)	0.176	0.335	0.089	0.051	0.216	0.273	0.141	0.054	0.061
VAL1 (right)	3.506	4.911	2.128	0.682	3.368	4.631	2.786	0.725	0.669
VAL2 (left)	3.178	1.669	3.106	0.666	3.344	4.451	2.597	0.593	0.845
BAD1	0.308	0.441	0.191	0.060	0.310	0.356	0.211	0.048	0.382
BAD2	0.288	0.412	0.165	0.068	0.276	0.404	0.105	0.089	0.893
BAL	2.929	3.805	2.152	0.441	2.642	3.288	1.896	0.444	0.747

Significant *P*<0.05 is emphasized in bold text. woTS: Without tandem stenosis, wTS: With tandem stenosis, VAD1: Right VA diameter at the intradural entrance, VAD2: Right VA diameter at PICA origin level, VAD3: Right VA diameter at terminal, VAD4: Left V4 diameter at the intradural entrance, VAD5: Left VA diameter at PICA origin level, VAD6: Left VA diameter at terminal, VAL1: Right VA length, VAL2: Left VA length, BAD1: BA diameter at the beginning, BAD2: BA diameter at terminal, BAL: BA length, SD: Standard deviation, PICA: Posterior inferior cerebellar artery, VA: Vertebral artery

in the right VA diameter at the origin (VAD1) between patients woTS and wTS (P = 0.026). The mean VAD1 value in woTS cases in the severe group was 0.278 cm, whereas it was 0.193 cm in wTS cases. When comparing VA diameter, wTS patients in the moderate group had a wider VAD2 diameter, while in the severe group, woTS cases had a wider VAD1 diameter [Table 3]. There was no statistically significant difference in other morphometric measurement parameters between wTS and woTS patients in both the moderate and severe groups (P > 0.05).

No significant difference was found when comparing the morphometric measurement values of wTS cases in the moderate and severe stenosis groups. However, when comparing woTS cases in the moderate and severe stenosis groups, statistically significant differences were observed in the right VA diameter at the PICA origin level (VAD2), right VA diameter at the terminal (VAD3), and left VA length (VAL2) (P < 0.05). In the severe group, the mean VAD2 value was 0.241 cm, which was greater than the VAD2 mean of 0.195 cm measured in the moderate stenosis group. Similarly, in the severe group, the mean VAD3 value was 0.204 cm, which was greater than the VAD3 mean of 0.178 cm measured in the moderate stenosis group (P = 0.05). In the moderate group, the mean VAL2 value was 3.588 cm, which was greater than the VAL2 mean of 3.178 cm measured in the severe stenosis group. It was observed that the VAD2 and VAD3 values were higher

in the severe group, while the VAL2 value was higher in the moderate group [Table 4]. There was no statistically significant difference in the remaining measurement parameters for woTS cases in both the moderate and severe stenosis groups ($P > 0.05$).

Discussion

In our study, in the comparison of the three main groups based solely on the degrees of ICA stenosis, neglecting tandem stenosis, there was no statistically significant difference in morphometric measurements related to VBAS among the control group, moderate stenosis group, and severe stenosis group ($n = 32$, totally = 96) ($P > 0.05$).

In the study by Kizilkilic *et al*., they compared extracranial VA diameter values between the group with ICA stenosis degree above 50% and the group with ICA stenosis degree ≤50%. They reported that there was no correlation between the degree of ICA stenosis and VA diameter values.[11]

Kalayci *et al.* evaluated carotid artery plaques and their effects on and changes in the diameter of the VAs. They found that there was no significant correlation between VA diameters and the degree and/or localizations of carotid artery stenosis.[12]

However, in our study, subgroup comparisons considering tandem stenosis yielded valuable results. We assessed the effects of stenosis in the CCA and ICA on the VAs in patients wTS. When comparing wTS patients between the moderate and severe groups, we did not detect statistically significant morphometric changes. However, we found differences in VA diameter measurement values in woTS patient groups with a single stenosis in the ICA region.

In our study, when evaluating vessel diameters in woTS patients categorized into moderate and severe groups, we found that the parameters – VAD2 and VAD3 were significantly higher in the severe group compared to the moderate group ($P < 0.05$, VAD2 mean: 0.241 cm, VAD3 mean: 0.204 cm). Since VAD2 corresponds to the PICA origin point and VAD3 corresponds to the proximal of the VBJ area. These points may be affected vessel parts by hemodynamic pressure increases due to blood flow dynamics and turbulence at vessel bifurcations.[13,14] Hence, statistically significant differences may have been found as a result.

Zhu *et al*. in their modeling studies showed that the collateral compensatory function of the ipsilateral posterior communicating artery will not be fully activated until a severe stenosis occurs in unilateral ICA stenosis.[1] A stenosis developing in the ICA system might have led to the VA diameter increasing to be compensated by the VBAS. Our study shows that, in line with other studies, there are morphometric changes in vascular structures due to attempts to compensate for the impairment in the anterior circulation by the posterior circulation. In addition, it highlights that during this compensatory phase, morphometric changes become particularly evident at the level of the VAs.[1,6,15]

The most significant feature of tandem stenosis compared to single-location stenosis is its influence on flow dynamics, increasing wall shear stress, damaging the endothelium, and leading to the formation of new plaques.[16] Especially in the carotid bifurcation, tandem stenosis affects flow dynamics more than stenosis at a single location. The increased frequency of ischemic stroke in patients wTS, combined with the proximity of the lesions, poses a greater risk of forming larger stenoses, making tandem stenosis a crucial determinant in long-term prognosis and medical treatment support.[4] Determining the degree of ICA stenosis, which is the most important determinant in managing patients at risk of stroke, along with the patient's clinical presentation and comorbid factors, as well as the presence of tandem stenosis and changes in VBAS morphometrics, guides the evaluation and treatment planning in acute and chronic settings.[12,17,18]

In our study, when comparing woTS patients with wTS patients in the moderate group, we found a statistically significant difference in the VAD2 parameter ($P < 0.05$, VAD2 mean: 0.243 cm). Accordingly, tandem stenosis led to an increase in VA diameter in the moderate group. Similarly, in the severe group, while larger diameters were expected in wTS patients, woTS patients in the severe group had statistically larger VA diameters compared to wTS patients based on VAD1 measurements ($P < 0.05$, VAD1 mean: 0.278 cm). In this case, it can be concluded

Table 3: Morphometric measurement values of patients without tandem stenosis and patients with tandem stenosis in moderate and severe groups

Group	Parameters	woTS (*n*=7)	wTS (*n*=25)	*P*
Moderate	VAD2	0.195	**0.243**	**0.028**
Severe	VAD1	**0.278**	0.193	**0.026**

Significant $P<0.05$ is emphasized in bold text. woTS: Without tandem stenosis, wTS: With tandem stenosis, VAD2: Right VA diameter at PICA origin level, VAD1: Right VA diameter at the intradural entrance, PICA: Posterior inferior cerebellar artery, VA: Vertebral artery

Table 4: Morphometric measurement values of patients without tandem stenosis in severe and moderate groups

Parameters	Severe woTS (*n*=25)	Moderate woTS (*n*=25)	*P*
VAD2	**0.241**	0.195	**0.005**
VAD3	**0.204**	0.178	**0.050**
VAL2	3.178	**3.588**	**0.044**

Significant $P<0.05$ is emphasized in bold text. woTS: Without tandem stenosis, VAD2: Right VA diameter at PICA origin level, VAD3: Right VA diameter at terminal, VAL2: Left VA length, PICA: Posterior inferior cerebellar artery, VA: Vertebral artery

that the hemodynamic effect created by tandem stenosis is most evident in the VAD2 segment, which is the branching point of the VA, and that branching points are more sensitive to hemodynamic changes. The unexpected results in the severe group cannot be explained by any physiological principle and should be evaluated through hemodynamic studies.

When evaluating the VA length parameters, we found that VAL2 values were higher in woTS patients compared to the severe group in the moderate group ($P < 0.05$, VAL2 mean: 3.588 cm). However, we could not find literature information to compare the VAL value with ICA stenosis.

Fang *et al*. in their study stated that unilateral ICA stenosis was attempted to be compensated by the contralateral ICA, and in bilateral ICA stenosis, VBAS assumed the rescuer compensatory role.[17] In the study conducted by Sahan *et al*., unilateral and bilateral ICA stenosis were calculated, and VA dimensions were evaluated according to unilateral and bilateral stenosis. They found an increase in both VA diameters in the unilateral stenosis group, but in the left ICA stenosis group, increasing ipsilateral VA diameter was significant.[15] Unlike these studies, our study did not compare unilateral and bilateral ICA stenosis. However, similarly, our study showed that the VA on the same side as ICA stenosis is affected, and its diameter increases.

Tanaka *et al*.'s study investigated the hemodynamic physiology of the arteries to explain cerebral perfusion after ICA stent placement. They measured the blood flow velocities on bilateral ICA and BA on postoperative day 1, day 7, and at the end of 3 months. They found that the total blood flow velocity in the contralateral ICA and BA decreased at the end of 3 months after carotid artery stent placement.[19] In contrast, our study focused on the impact of ICA occlusion on the VAs rather than on the BA, as observed in Tanaka *et al*.'s study. We highlighted the effects on the VAs and morphometric changes due to the presence of an occlusion in the ICA system, which differs from the focus of the study of Tanaka *et al*.

In our study, we evaluated VBAS morphometry in ICA stenosis groups and tandem subgroups determined by the NASCET method. We could not find any literature information on this specific comparison. Therefore, all the findings we found statistically significant have been shared with their anatomical and morphometric characteristics.

Conclusion

In our study, there was no statistically significant difference in morphometric measurements related to VBAS when comparing the three main groups without distinguishing between patients wTS and woTS. However, subgroup comparisons based on the presence or absence of tandem stenosis yielded significant results. It showed that cerebral perfusion not provided by the anterior circulation creates hemodynamic stress on the posterior circulation, leading to morphometric changes in VBAS. According to the results we obtained, both the hemodynamic burden caused by ICA stenosis and the presence of tandem lesions were attempted to be compensated for by the VA on the same side. This resulted in an increase in diameter, especially at the branching points of the VA. Thus, it demonstrated that vascular branching points are more sensitive to hemodynamic changes.

Limitations of the study: our study should be supported by hemodynamic studies to better understand the relationship between the anterior and posterior circulation.

We believe that our study will serve as a reference for both hemodynamic studies and radiological evaluation, diagnosis, and treatment planning stages of pathologies in the relevant field.

Financial support and sponsorship

Nil.

Conflicts of interest

There are no conflicts of interest.

References

1. Zhu G, Yuan Q, Yang J, Yeo JH. The role of the circle of Willis in internal carotid artery stenosis and anatomical variations: A computational study based on a patient-specific three-dimensional model. Biomed Eng Online 2015;14:107.
2. Oltean-Péter B, Kovács I, Chițu M. Benedek I. The role of carotid ultrasonography in patients with high risk of atherosclerosis. J Interdisc Med 2018;3:229-33.
3. Paşaoğlu L, Vural M, Ziraman I, Uyanık SA. Left internal carotid artery agenesis associated with basilar and left vertebral artery aneurysm. J Clin Imaging Sci 2011;1:60.
4. Wang J, Paritala PK, Mendieta JB, Gu Y, Raffel OC, McGahan T, *et al*. Carotid bifurcation with tandem stenosis-a patient-specific case study combined *in vivo* imaging, *in vitro* histology and *in silico* simulation. Front Bioeng Biotechnol 2019;7:349.
5. Griffiths GD, Razzaq R, Farrell A, Ashleigh R, Charlesworth D. Variability in measurement of internal carotid artery stenosis by arch angiography and duplex ultrasonography – Time for a reappraisal? Eur J Vasc Endovasc Surg 2001;21:130-6.
6. North American Symptomatic Carotid Endarterectomy Trial. Methods, patient characteristics, and progress. Stroke 1991;22:711-20.
7. U-King-Im JM, Trivedi RA, Cross JJ, Higgins NJ, Hollingworth W, Graves M, *et al*. Measuring carotid stenosis on contrast-enhanced magnetic resonance angiography: Diagnostic performance and reproducibility of 3 different methods. Stroke 2004;35:2083-8.
8. Barnett HJ, Taylor DW, Eliasziw M, Fox AJ, Ferguson GG, Haynes RB, *et al.* Benefit of carotid endarterectomy in patients with symptomatic moderate or severe stenosis. North American Symptomatic Carotid Endarterectomy Trial Collaborators. N Engl J Med 1998;339:1415-25.
9. Pisani GP, Calabretto F, Maccario G, Mazzotta G, Bizzarri S, Bonalumi G. Surgery for near occlusion of the internal carotid arteries. A single center experience. Ann Vasc Surg 2021;77:348.e13-8.
10. Rothwell PM, Eliasziw M, Gutnikov SA, Fox AJ, Taylor DW, Mayberg MR, *et al.* Analysis of pooled data from the randomised

controlled trials of endarterectomy for symptomatic carotid stenosis. Lancet 2003;361:107-16.

11. Kizilkilic O, Hurcan C, Mihmanli I, Oguzkurt L, Yildirim T, Tercan F. Color Doppler analysis of vertebral arteries: Correlative study with angiographic data. J Ultrasound Med 2004;23:1483-91.
12. Kalayci T, Sonmezgoz F, Apaydin M, Inci MF, Erdogan H, Oyar O, *et al*. Effects of carotid artery stenosis and plaque localization on the incidence of cerebral infarct and diameter of vertebral artery: A duplex ultrasonography and MRI evaluation. IJCEM 2016;9:22393-7.
13. Givens C, Tzima E. Endothelial mechanosignaling: Does one sensor fit all? Antioxid Redox Signal 2016;25:373-88.
14. Razavi MS, Shirani E, Salimpour MR, Kassab GS. Constructal law of vascular trees for facilitation of flow. PLoS One 2014;9:e116260.
15. Şahan MH, Asal N, Bayar Muluk N, Inal M, Doğan A. Critical stenosis of the internal carotid artery: Variability in vertebral artery diameters and areas of cerebral chronic infarction in computed tomography. J Craniofac Surg 2019;30:e388-92.
16. Li ZY, Taviani V, Tang T, Sutcliffe MP, Gillard JH. The hemodynamic effects of in-tandem carotid artery stenosis: Implications for carotid endarterectomy. J Stroke Cerebrovasc Dis 2010;19:138-45.
17. Fang H, Song B, Cheng B, Wong KS, Xu YM, Ho SS, *et al*. Compensatory patterns of collateral flow in stroke patients with unilateral and bilateral carotid stenosis. BMC Neurol 2016;16:39.
18. Kang T, Mukherjee D, Ryu J. Hemodynamic flow characteristics at stenosed artery: Numerical analysis of three-dimensional patient-specific aortic–cerebral vasculature exposed to progressive carotid stenosis. Physics of Fluids 2022;34.
19. Tanaka H, Watanabe Y, Nakamura H, Takahashi H, Arisawa A, Fujiwara T, *et al*. Multiple blood flow measurements before and after carotid artery stenting via phase-contrast magnetic resonance imaging: An observational study. PLoS One 2018;13:e0195099.

Original Article

Radio-anatomical Study of Critical Shoulder Angle

Nabanita Chakraborty, Sarmistha Chakraborty[1], Pooja Shaw[2]

Department of Anatomy, Jagannath Gupta Institute of Medical Science and Health, North Kolkata, [1]Department of Anatomy, Calcutta National Medical College, [2]Department of Radiodiagnosis, SSKM Hospital, Kolkata, West Bengal, India

Abstract

Introduction: Rotator cuff disease and osteoarthritis are the two most important causes of shoulder pain. In addition to history and physical examination, diagnostic tests for shoulder pain are X-ray and magnetic resonance imaging (MRI). As per previous literature, critical shoulder angle (CSA) evaluation helps to rule out shoulder pathology. Roughly, CSA is the angle between the plane of the glenoid fossa and a line drawn from its lower end to the lateral edge of the acromion. **Aims and Objectives:** To find out the correlation between CSA and shoulder pathology and to assess the clinical and radiological correlation between CSA and shoulder pain. **Materials and Methods:** After getting approval from the institutional ethical committee, the study was conducted within KPC Medical College and Hospital. Detailed history was taken from the patients who came to the orthopedic outpatient department with shoulder pain. The CSA was measured from the X-ray of the shoulder joint, the anteroposterior view of these patients. An MRI was also done for confirmation. **Results:** We studied 100 patients, and among them, patients below the age 50 tend to exhibit rotator cuff tears in X-ray. Whereas, patients above age 50 tend to exhibit osteoarthritis in both X-ray and MRI or computed tomography scan. The chance of developing Osteoarthritis among female patients is generally higher than the male patients. Out of 39 female patients, 25 developed osteoarthritis, whereas out of 61 male patients, 16 developed osteoarthritis. **Conclusion:** We concluded that MRI performed better in detecting partial-thickness tears. If the patient feels continuous pain, that implies the patient could have developed osteoarthritis.

Keywords: *Critical shoulder angle, rotator cuff tear, shoulder osteoarthritis*

Introduction

The shoulder joint is classified as a ball-and-socket joint; however, the joint sacrifices stability for mobility. The rotator cuff consists of four muscles originating on the scapula and inserting on the superior humeral head to improve stability. The subscapularis inserts on the lesser tubercle of the humerus, and it functions as an internal rotator. The supraspinatus muscles insert onto the greater tubercle of the humerus with its function as an abductor for the initial 30° of abduction. The infraspinatus also inserts onto the greater tubercle, but a little inferior to the supraspinatus, and it functions as an external rotator. The teres minor inserts inferior to the infraspinatus on the greater tuberosity, and it functions as an external rotator as well. In addition, they all work as stabilizers of the glenohumeral joint.

Critical shoulder angle (CSA) is the angle between the plane of the glenoid fossa and the imaginary line connecting the lateral border of the acromial process in the X-ray shoulder joint, anteroposterior (AP) view (normal range 30°–35°).[1] Increased CSA is associated with rotator cuff tear, and decreased CSA is associated with osteoarthritis.[2] Patients with complaints of pain during overhead abduction of the shoulder joint need clinical correlation with CSA to prevent progression of shoulder pathology.

Partial tears are at risk for further propagation. These risk factors include: Tear size, symptoms, location, and age. Tear size: A small tear may remain dormant, while larger tears are more likely to undergo structural deterioration. The critical size for sending a small tear towards a larger or complete tear has yet to be defined. Tear propagation correlates with symptom development. Actively enlarging tears have a five times higher likelihood of developing symptoms than those that remain the same size. The location of the tear also influences progression. Anterior tears are more likely to progress to cuff degeneration. Finally, age is a risk factor. Patients over age 60 are more

How to cite this article: Chakraborty N, Chakraborty S, Shaw P. Radio-anatomical study of critical shoulder angle. J Anat Soc India 2025;74:228-30.

Article Info

Received: 21 February 2023
Revised: 23 June 2025
Accepted: 18 August 2025
Available online: 30 September 2025

Address for correspondence:
Dr. Nabanita Chakraborty, Department of Anatomy, ESI-PGIMSR and ESIC Medical College, Joka, Kolkata, West Bengal, India.
E-mail: nabanitargkmc@gmail.com

Access this article online

Website: https://journals.lww.com/joai
DOI: 10.4103/jasi.jasi_16_23
Quick Response Code:

Table 1: Critical shoulder angle based on X-ray

Impression by X-ray	Sample mean	Sample SD	95% CI	
			Lower level	Upper level
Rotator cuff tear	40.79241	3.368037	39.87311	41.7117
Normal	33.41	0.842793	32.36353	34.45647
Osteoarthritis	26.24171	2.518176	25.44687	27.03654

CI: Confidence interval, SD: Standard deviation

Table 2: Critical shoulder angle based on magnetic resonance imaging

MRI or CT scan	Sample mean	Sample SD	95% CI	
			Lower level	Upper level
Infraspinatus tear	41.90583	3.250031	39.84086	43.9708
Subscapularis tear	42.16667	2.145538	38.7526	45.5807
Supraspinatus and infraspinatus tear	43.31	6.319209	33.25473	53.36527
Supraspinatus tear	40.14577	2.721348	39.04659	41.24495
Teres minor tear	42.196	2.649723	38.90593	45.48607
Normal	32.3623	2.806483	30.91939	33.8053
Osteoarthritis	25.4003	2.041795	24.67631	26.12429

CI: Confidence interval, SD: Standard deviation, MRI: Magnetic resonance imaging, CT: Computed tomography

likely to develop tears that progress. Younger patients with full-thickness tears appear more capable of adapting to stress and tear propagation than those 60 years of age and older.[3]

Aims and objectives

1. To find out the correlation between CSA and shoulder pathology
2. To assess the clinical and radiological correlation between CSA and shoulder pain.

Materials and Methods

After getting approval from the institutional ethical committee, the study was conducted within 1 year (June 1, 2021–May 31, 2022) in KPC Medical College and Hospital. Detailed history was taken from the patients who came to the orthopedic outpatient department with shoulder pain. The CSA was measured from the X-ray of the shoulder joint, AP view of these patients. Magnetic resonance imaging (MRI) is also done for confirmation. [Tables 1 and 2] At the end of the study, all data were compiled and tabulated, analysis was done using statistical analysis, and graphical representation was done.

Results

Diagram 1 shows that the correlation coefficient between Age and CSA is −0.751. That is, there is a highly negative linear relationship between age and CSA.

Table 3 shows that:

1. Patients below the age 50 tend to detect rotator cuff tears in X-ray. Whereas, patients above age 50 tend to detect osteoarthritis in both X-ray and MRI or computed tomography (CT) scan
2. The chance of developing Osteoarthritis among female patients is generally higher than the male patients. Out of 39 female patients, 25 developed osteoarthritis, whereas out of 61 male patients, 16 developed osteoarthritis.

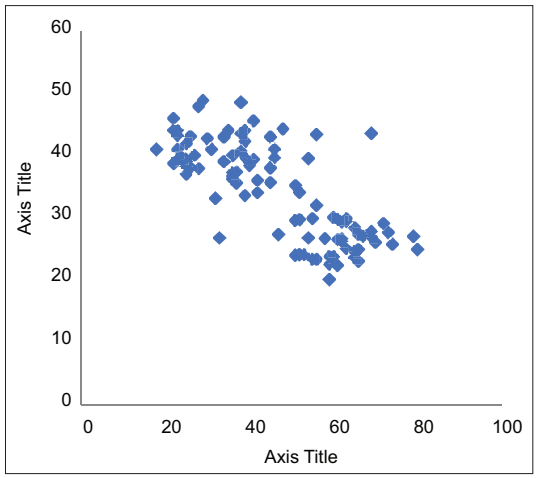

Diagram 1: Correlation coefficient between age and critical shoulder angle is −0.751. That is, there is a highly negative linear relationship between age and critical shoulder angle

Table 4 interprets that if the patient feels continuous pain, that implies the patient could have developed osteoarthritis.

Discussion

In our study, we found that patients below 50 years of age are more prone to rotator cuff tears found in X-ray. Whereas, patients above 50 years tend to develop osteoarthritis, found in both X-ray and MRI or CT scan. Vlychou *et al*.[4] showed that both ultrasound and MRI imaging modalities detected successfully 44 cases of partial tears of the supraspinatus tendon. US imaging yielded a sensitivity of 95.6%, a specificity of 70%, an accuracy of 91%, and a positive predictive accuracy of 93.6%. The corresponding values for MRI were 97.7%, 63.6%, 91%, and 91.7%, respectively. De Jesus *et al*.[5] found that MRI and ultrasound for all tears show the area under the receiver operating characteristic curve is greatest for MR arthrography (0.935), followed by ultrasound (0.889) and then MRI (0.878); however, pairwise comparisons of these curves show no significant differences between MRI and ultrasound ($P > 0.05$). MR arthrography is the most sensitive and specific technique for diagnosing both full-and partial-thickness rotator cuff tears. Ultrasound and MRI are comparable in both sensitivity and specificity. Thakker *et al*.[6] found that the Supraspinatus was the most commonly affected tendon (79%). Partial-thickness tears were the most common rotator cuff pathology.

Teefey *et al*.[7] showed that seventeen measurement errors occurred with full-thickness tears, 15 of those in patients with large or massive tears. Bursal thickening ($n = 4$), nonvisualization of the torn tendon end ($n = 2$), nonretracted

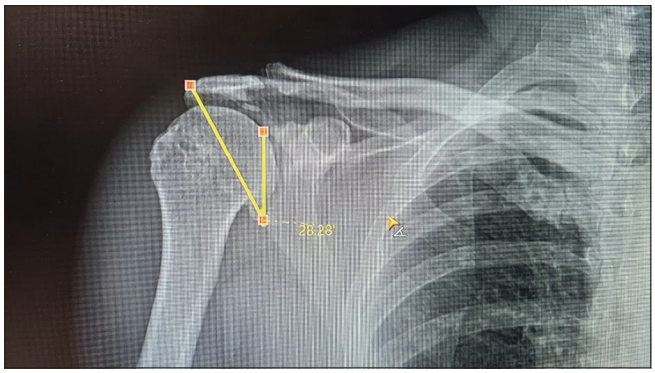

Figure 1: Critical shoulder angle <30°

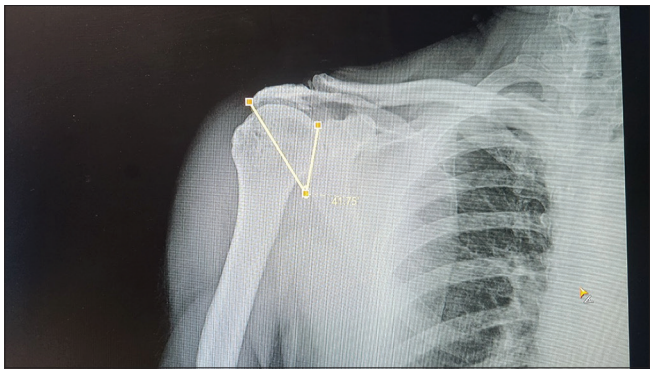

Figure 2: Critical shoulder angle >30°

Table 3: Average critical shoulder angle (°) of different age groups

Age group	Average critical shoulder angle (°)
<20	41.01
20–29	41.4452381
30–39	39.14428571
40–49	38.5575
50–59	28.47
60–69	27.45809524
70–79	27.138
>80	24.9

Table 4: Joint frequency distribution of clinical presentation and X-ray

	Impression by X-Ray		
	Rotator cuff tear	Normal	Osteoarthritis
Clinical presentation			
Continuous pain			16
Pain on movement	54	5	25

tear (n = 2), and complex tear (n = 1) contributed to the errors. Eight measurement errors occurred with partial-thickness tears. Difficulty distinguishing tendinopathy from partial-thickness tears (n = 3) and complex tears (n = 3) accounted for six errors. Aggrawal *et al*.[8] found that full-thickness tear was confirmed in 42 cases, partial-thickness tear in 52 cases.

Bjarnison *et al*.[9] found in their study that osteoarthritis results in a CSA below 30° [Figure 1]. Spiegl *et al*.[10] measured CSA from radiographs demonstrated excellent interobserver agreement with less variability than CSAs from MRI, especially in osteoarthritis patients. Mantell *et al*.[11] found in his study that concurrent glenohumeral osteoarthritis and full-thickness RCT are associated with greater CSA values compared with patients with glenohumeral osteoarthritis alone [Figure 2].

Financial support and sponsorship

Nil.

Conflicts of interest

There are no conflicts of interest.

References

1. Vellingiri K, Ethiraj P, Shanthappa AH. Critical shoulder angle and its clinical correlation in shoulder pain. Cureus 2020;12:e9810.
2. Moor BK, Bouaicha S, Rothenfluh DA, Sukthankar A, Gerber C. Is there an association between the individual anatomy of the scapula and the development of rotator cuff tears or osteoarthritis of the glenohumeral joint? A radiological study of the critical shoulder angle. Bone Joint J 2013;95-B: 935-41.
3. Schmidt CC, Morrey BF. Management of full-thickness rotator cuff tears: Appropriate use criteria. J Shoulder Elbow Surg 2015;24:1860-7.
4. Vlychou M, Dailiana Z, Fotiadou A, Papanagiotou M, Fezoulidis IV, Malizos K. Symptomatic partial rotator cuff tears: Diagnostic performance of ultrasound and magnetic resonance imaging with surgical correlation. Acta Radiol 2009;50:101-5.
5. de Jesus JO, Parker L, Frangos AJ, Nazarian LN. Accuracy of MRI, MR arthrography, and ultrasound in the diagnosis of rotator cuff tears: A meta-analysis. Am J Roentgenol 2009;192:1701-7.
6. Thakker VD, Bhuyan D, Arora M, Bora MI. Rotator cuff injuries: Is ultrasound enough? A correlation with MRI. Int J Anat Radiol Surg 2017;6.
7. Teefey SA, Middleton WD, Payne WT, Yamaguchi K. Detection and measurement of rotator cuff tears with sonography: Analysis of diagnostic errors. Am J Roentgenol 2005;184:1768-73.
8. Aggrawal J, Bansal RP, Shah V. USG and MRI correlation of. Surgery. 2014;41.
9. Bjarnison AO, Sørensen TJ, Kallemose T, Barfod KW. The critical shoulder angle is associated with osteoarthritis in the shoulder but not rotator cuff tears: A retrospective case-control study. J Shoulder Elbow Surg 2017;26:2097-102.
10. Spiegl UJ, Horan MP, Smith SW, Ho CP, Millett PJ. The critical shoulder angle is associated with rotator cuff tears and shoulder osteoarthritis and is better assessed with radiographs over MRI. Knee Surg Sports Traumatol Arthrosc 2016;24:2244-51.
11. Mantell MT, Nelson R, Lowe JT, Endrizzi DP, Jawa A. Critical shoulder angle is associated with full-thickness rotator cuff tears in patients with glenohumeral osteoarthritis. J Shoulder Elbow Surg 2017;26:e376-81.

Original Article

Fissure for Ligamentum Teres Hepatis: A Descriptive Anatomical Study of Variations in Cadaveric Livers

Suma Dnyanesh, Dhanalaxmi Neginhal, Dnyanesh D. K[1], Shilpa Bhimalli

Departments of Anatomy and [1]Paediatrics, J. N. Medical College, KLE Academy of Higher Education and Research Deemed-to-be-University, Belagavi, Karnataka, India

Abstract

Background: There are anatomical variances in the ligamentum teres hepatis (LTH), which is a remnant of the fetal umbilical vein. Individuals exhibit variations in the fissure for the LTH (FLTH) or umbilical fissure, an anatomical feature of the liver. This characteristic is essential for comprehending the architecture of the liver, especially in surgical settings. Being familiar with these variances is essential for precise diagnosis and surgical planning. **Aim:** The aim of this study was to describe anatomical changes in the LTH fissure. **Materials and Methods:** To describe differences in the teres hepatis fissure, we investigated 43 cadaveric livers. The fissures for LTH were observed in all the specimens, and the variations were documented and high-resolution photos were taken. **Results:** Out of the 43 specimens, 22 (52.3%) exhibited Type I, 1 (2.3%) displayed Type II, 4 (9.3%) presented with Type III, and 16 showed Type IV (37.1%) variations. **Conclusion:** This study emphasizes the importance of recognizing and understanding the different anatomical variations in the fissure of the LTH. To prevent misunderstandings during treatments and guarantee the best possible care for patients, radiologists and surgeons must be aware of these variances.

Keywords: *Anatomical variation, cadaveric study, fissure, ligamentum teres hepatis, liver*

Introduction

The liver, the largest organ in the human body, has a unique morphology, including the fissure for the ligamentum teres, a deep cleft extending from the liver's inferior border to the porta hepatis.[1-3] It contains the ligamentum teres hepatis (LTH), a remnant of the left umbilical vein. The liver development process is influenced by growth factors and divided into left and right lobes by the falciform and round ligaments.[4-6] The region's structural complexity is highlighted by four main variations: complete fissures, fibrous tissue-bridged fissures, parenchymal projections, and pons hepatis.[7,8]

This study uses cadaveric livers to describe anatomical changes in the LTH fissure for the ligamentum teres hepatis (LTHF), a fibrous remnant, to enhance surgical planning and diagnostic accuracy. Understanding these variants helps prevent misdiagnosis during imaging studies and influences surgical strategies, emphasizing the need for thorough morphological assessments.[9-11]

Materials and Methods

This descriptive anatomical study examined 43 cadaveric livers obtained from the KAHER's J N Medical College, Belagavi's dissection hall. Ethical approval was obtained from the Institutional Ethical Committee for this research. Livers with normal configuration were included, and livers with any damage or any pathology were excluded from the study. To maintain anatomical correctness, we made sure the livers were well preserved and appropriately hydrated. With the visceral surface facing up, all livers were carefully dissected using conventional dissection instruments. The tissue around the ligamentum teres fissure was carefully removed in order to look for differences in the FLTH.

Detailed observations were made, and high-resolution photographs were taken for each specimen to ensure thorough validity of the findings. To guarantee precision and repeatability, the measurements were made twice by two separate observers. Based on their morphological features, such as the presence and extent of bridging tissue and

How to cite this article: Dnyanesh S, Neginhal D, Dnyanesh DK, Bhimalli S. Fissure for ligamentum teres hepatis: A descriptive anatomical study of variations in cadaveric livers. J Anat Soc India 2025;74:231-5.

Article Info

Received: 03 January 2025
Accepted: 11 August 2025
Available online: 30 September 2025

Address for correspondence:
Dr. Suma Dnyanesh, Department of Anatomy, KAHER's J. N. Medical College, Belagavi - 590010, Karnataka, India.
E-mail: drsuma410@gmail.com

Access this article online

Website: https://journals.lww.com/joai
DOI: 10.4103/jasi.jasi_1_25

Quick Response Code:

parenchymal projections, fissures were classified into four types:

- Type 1: Complete fissures
- Type 2: Fissures bridged by fibrous tissue
- Type 3: Liver parenchyma projecting into the fissure but not covering it
- Type 4: Pons hepatitis.

Dimensions in terms of length and width were measured for Type I and IV (pons hepatis) variants using digital calipers. Pons hepatis was further classified into two types depending on its length.

- Open (Type IV a): Umbilical fissure (UF) is covered by the parenchymal bridge for <2 cm, and most of the UFs are visible as a deep groove
- Closed (Type IV b): The parenchymal bridge is >2 cm, and most of the UFs is covered by the bridge.

Upon completion of the dissection, descriptive statistics were analyzed which help to provide a central tendency (mean, median) and variability (standard deviation [SD]) of the measurements in the specimens analyzed, thus providing a comprehensive overview of the morphological diversity present in the examined livers.

Results

The study identified four distinct variations in the FLTH: complete fissures, fissures bridged by fibrous tissue, liver parenchyma projecting into the fissure, and pons hepatis. Out of the 43 specimens examined,

- 22 exhibited normal fissures
- 1 specimen displayed fibrous tissue bridging [Figure 1]
- 4 specimens showed liver parenchyma projection [Figure 2]
- 16 presented with pons hepatis-5 open type and 11 closed type [Figures 3 and 4].

Dimensions of variants

Out of 43 dissected cadavers, 22 specimens (51.1%) had the Type I variant, considered the "normal" UF, with a mean length of 41.71 mm (median 41.29 mm, SD 8.80 mm) and a mean width of 7.85 mm (median 7.01 mm, SD 3.15 mm), as shown in Tables 1 and 2. Out of 43 dissected cadavers, 5 specimens (11.6%) had the Type IV "a" variant, with a mean length of 11.74 mm (median 11.64 mm, SD 0.48 mm) and a mean width of 4.32 mm (median 3.39 mm, SD 1.8 mm), as shown in Table 3. Eleven (25.5%) specimens had the Type IV "b" variant, with a mean length of 33.9 mm (median 32.8 mm, SD 4.64 mm) and a mean width of 4.98 mm (median 5.12 mm, SD 0.55 mm) as seen in Table 4.

Discussion

The ligamentum teres fissure is a groove in the liver that contains the liver's round ligament. It is sometimes referred to as the hepatic round ligament fissure or the umbilical vein fossa. Significant anatomical differences exist in the FLTH, which have important consequences for surgical and radiological therapy.

The Type I variant, which is "the normal anatomy" of the fissure where it extends from the inferior border of the liver to the left end of the porta hepatis, is found in 22 (51.1%) cases in the current study; other researchers have also reported that the Type I variant is the most common.[7-9,12]

Type II was the least common and was found in only one case (2.3%) in our study where the fissure is bridged by thin fibrous tissue; it appeared to be a membranous structure and could be easily stripped from underlying LTH; this variant was reported to be 1.5% and 10% in two different studies;[9,12] however, Ramanuja *et al*. did not report any such cases out of 40 specimens in their study.[7]

Type III variations were discovered in 4 (9.3%) of the current study's specimens. Cawich *et al*. found in

Figure 1: Type II fissure. Arrow is showing fibrous tissue bridging fissures

Figure 2: Type III fissure. Arrow is showing liver parenchyma projecting into the fissure but not covering it

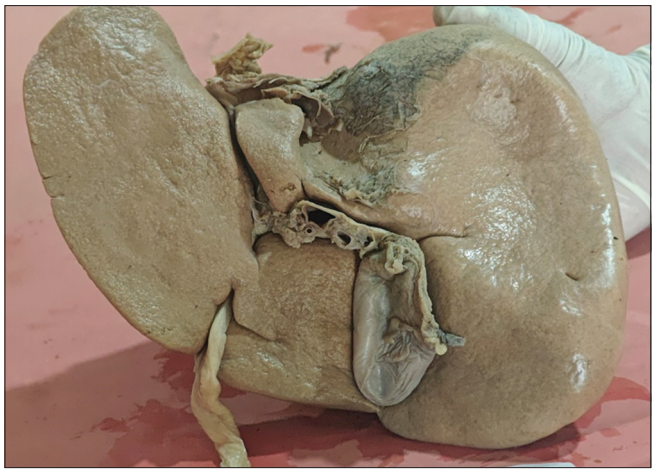

Figure 3: Pons hepatis open (Type IV a) type

Figure 4: Pons hepatis closed (Type IV b) type

Table 1: Results of the study

Types	Specimen	Percentage
I	22	51.1
II	1	2.3
III	4	9.3
IV "a" open	5	11.6
IV "b" closed	11	25.5

Table 2: Measurements of Type I variant

Dimensions	Mean	Median	SD
Length	41.714	41.285	8.800075
Width	7.853	7.01	3.145233

SD: Standard deviation

Table 3: Measurements of Type IV "a" variant

Dimensions	Mean	Median	SD
Length	11.74	11.64	0.48
Width	4.32	3.39	1.8

SD: Standard deviation

Table 4: Measurements of Type IV "b" variant

Dimensions	Mean	Median	SD
Length	33.9	32.8	4.64
Width	4.98	5.12	0.55

SD: Standard deviation

14 (20.3%) cases in their study.[12] Nayak *et al*. labeled them as "lingual process" and reported in 10% cases.[9]

Type IV variations can have incidences ranging from 1.25% to 27.8%; Joshi *et al*. reported a prevalence of 27.8% and Cawich *et al*. observed 33.3%.[12,13]

In the current study, we discovered Type IV variants in 16 (37.1%) cases [Table 5]. Authors have given this variant several names, such as "pons hepatis," "absent fissure for ligamentum teres," or "ligamentum teres tunnel."

After analyzing 125 instances, Onitsuka *et al*. discovered Type IV variants in 31 (25%) of the specimens. It was referred to as "pons hepatis."[14]

"Absent fissure for ligamentum teres" is the term used in another study conducted by Patil *et al*.[15]

In two cases reported by Ebby and Ambike, the ligamentum teres fissure was completely absent; instead, they discovered a tunnel that they called the "ligamentum teres tunnel."[16]

Merkle EM and Gilkeson RC estimated that the ligamentum teres' average length fell between 10 and 20 cm; in our instance, the mean length was determined to be 18.5 cm, which is consistent with this study.[17]

The absence of the left lobe of the liver and the lack of a ligamentum teres fissure were documented by Abdullahi *et al*.[18]

Additionally, Joshi *et al*. showed that 30% of specimens had pons hepatis bridging the ligamentum teres fissure.[13]

In 2020, Anbumani et al. conducted a study on 30 liver specimens and observed the presence of pons hepatis in 5 specimens (16.7%). Among these, 2 specimens (6.7%) exhibited the open type, while 3 specimens (10%) showed the closed type.[8] In a study by Ramanuja *et al*., 12 specimens exhibited Type IV variation, with 3 specimens (7.5%) showing open Type IV and 9 specimens (22.5%) showing closed Type IV, findings that align with the study by Chin *et al*.[7,19]

The UF is used for vascular assessments and liver resections as a landmark.[4] Surgeons use laparoscopic instruments to grab the LTH and use it as a "handle" to move the liver. However, a closed Type IV variant can convert the fissure into a tunnel, increasing navigation difficulties and making it impossible to plan liver resections using the UF. This can lead to severe bleeding from lacerations, as shear force can lacerate the hepatic parenchyma bridging the fissure.[12] 25.5% of the sample had a "closed" variety.

Table 5: Table of comparison

Studies	Number of specimen	Type I	Type II	Type III	Type IV	
					Open	Closed
Cawich *et al*.	69	31 (44.9)	1 (1.5)	14 (20.3)	13 (18.8)	10 (14.5)
Ramanuj *et al*.	40	28	Nil	Nil	3 (6.5)	9 (22.5)
Anbumani *et al*.	30	Not specified	Not specified	Not specified	2 (6.7%)	3 (10%)
Current study	43	22 (51.1)	1 (2.3)	4 (9.3)	5 (11.6)	11 (25.5)

The existence of this tunnel may mislead surgeons during procedures like laparoscopic liver resections and liver transplantations, leading to problems.[20]

When considering surgeries involving the left lobe of the liver, where accurate identification of resection margins is critical, the surgical significance of the LTH becomes even more evident.

When interpreting imaging data in patients with these anatomical variations, radiologists also confront considerable hurdles. If the radiologist is unaware of these possible anatomical irregularities, structures like parenchymal projections (Type III) or the pons hepatis (Type IV) might readily be confused for pathological appearances, like tumors or abscesses, leading to unnecessary diagnostic tests or unsuitable surgical treatments. Understanding these variances is crucial for accurate diagnosis and treatment. Radiologically, these variations can lead to misinterpretations of imaging studies, especially when evaluating liver lesions.[21,22]

The results of this study and previous investigations emphasize the necessity of conducting thorough morphological analyses of the LTH and the structures that surround it. A wide range of variance prevalence has been reported in previous research, with some indicating rates as low as 15%.[23] In a study on Afro-Caribbeans, the pons hepatis is found in 41% of cadavers, which is far greater than the 3.45% global occurrence.[12] On the other hand, our results showing morphological abnormalities in the FLTH in 49.8% of the livers suggest a substantially higher prevalence of these variations in the sample population under study. This disparity highlights the need for population-specific research, as anatomical variations may be more common in certain demographic groups, potentially impacting clinical management.

The LTH is crucial for maintaining liver structural integrity and has been used in surgical procedures like vascular grafting, reinforcing anastomoses, and reconstructive surgery.[24-26] However, the presence of anatomical variations, such as fibrous bridges or pons hepatis, may obscure the surgeon's view and can impact the success of these procedures, emphasizing the need for a comprehensive understanding of the anatomical landscape before and during surgery.

Anatomical variations in the FLTH can present challenges but also give opportunities for surgical innovation.[27] The LTH's strength and flexibility make it ideal for repairing perforations and preventing hemorrhage, leading to better patient outcomes.[25] However, careful management of the LTH and its fissures is crucial during laparoscopic procedures. Identifying these variations preoperatively allows surgeons to adapt their approaches and avoid complications.[10,28] Recent research emphasizes the importance of preoperative evaluation of vasculobiliary anatomy in the UF, especially in perihilar cholangiocarcinoma cases.[29] Studies have demonstrated that approach through the FLTH is a safe, easily operable, and effective method for hepatectomy.[21,30]

These variations can complicate surgical procedures and impact diagnostic accuracy, especially in complex cases. Therefore, clinicians must be aware of these variations.

Conclusion

The clinical implications of the FLTH and its variations are substantial, particularly in the context of surgical and radiological practice. While these variations can complicate procedures and diagnostic evaluations, understanding their prevalence and characteristics is crucial for improving patient care. By expanding their understanding of this anatomically complex region, clinicians can enhance their ability to provide accurate diagnoses, develop appropriate surgical strategies, and ultimately improve patient outcomes. Future research should continue to explore the clinical significance of these variations, particularly in diverse populations, to further refine surgical techniques and enhance diagnostic accuracy.

Acknowledgment

We sincerely acknowledge and extend our heartfelt gratitude to the Head of the Department of Anatomy, JNMC, Belagavi, for her support and encouragement throughout the course of this study.

Financial support and sponsorship

Nil.

Conflicts of interest

There are no conflicts of interest.

References

1. Chauhan HM, Modi HH, Rathod JB, Prajapati HK. Morphological study of human cadaveric livers and its clinical significance. Cureus 2024;16:e53873.

2. Rela M, Rajalingam R, Shanmugam V, O' Sullivan A, Reddy MS, Heaton N. Novel en-bloc resection of locally advanced hilar cholangiocarcinoma: The Rex recess approach. Hepatobiliary Pancreat Dis Int 2014;13:93-7.
3. Sibulesky L. Normal liver anatomy. Clin Liver Dis (Hoboken) 2013;2:S1-3.
4. Cawich SO, Gardner MT, Barrow M, Barrow S, Thomas D, Ragoonanan V, *et al*. Inferior hepatic fissures: Anatomic variants in Trinidad and Tobago. Cureus 2020;12:e8369.
5. Sato S, Watanabe M, Nagasawa S, Niigaki M, Sakai S, Akagi S. Laparoscopic observations of congenital anomalies of the liver. Gastrointest Endosc 1998;47:136-40.
6. Couinaud C. Surgical Anatomy of the Liver Revisited. Paris: Couinaud; 1989.
7. Ramanuja Phanindra ST, Raja A, Yesupadamu K, Sailaja G, Sesi DA. A cadaveric study on the fissure for ligamentum teres hepatis in South Indian population. Eur J Cardiovasc Med 2024;14:92-8.
8. Anbumani L, Pavazhakkurinji TN, Thamaraiselvi A. Morphological study on variation of external surface of liver. Int J Anat Res 2020;8:7481-5.
9. Nayak G, Pradhan S, Nayak L, Sahoo N. Study of variations of umbilical fissure for ligamentum teres hepatis in human cadaveric livers. Ann RSCB 2024;28:1-12.
10. Kumar S, Hare K, Gupta S, Dixit S, Ghatak S. Morphological study of variations of the human cadaveric liver and its clinical implications. Cureus 2023;15:1-15. [doi: 10.7759/cureus. 35507].
11. Singh H, Diwan RK, Rani A, Rani A, Sehgal G, Singh R. Tunnel for ligamentum teres hepatis: A case report. Era J Med Res 2019;6:125-6.
12. Cawich SO, Gardner MT, Shetty R, Lodenquai P, Ramkissoon S, Ho P, *et al.* Clinically oriented classification of anatomic variants of the umbilical fissure for ligamentum teres in the human liver. Cureus 2021;13:e15460.
13. Joshi SD, Joshi SS, Athavale SA. Some interesting observations on the surface features of the liver and their clinical implications. Singapore Med J 2009;50:715-9.
14. Onitsuka A, Katagiri Y, Miyauchi T, Shimamoto T, Mimoto H, Ozeki Y. Metastatic hepatoma originating from the pons hepatis presenting extrahepatic growth – Classification of different patterns covering REX's recessus. Hepatogastroenterology 2003;50:235-7.
15. Patil S, Sethi M, Kakar S. Morphological study of human liver and its surgical importance. Int J Anat Res 2014;2:310-4.
16. Ebby S, Ambike MV. Anatomical variation of ligamentum teres of liver – A case report. Webmed Cent 2012;3:1-7.
17. Merkle EM, Gilkeson RC. Remnants of fetal circulation: Appearance on MDCT in adults. Am J Roentgenol 2005;185:541-9.
18. Zagga AD, Tadros AA, Usman JD, Bello A. Absence of the left lobe of the liver in a cadaver: case report. J Med Trop. 2010;12:45-7.
19. Chin J, O'Toole P, Lin J, Velavan SS. Hepatic morphology: Variations and its clinical importance. Eur J Anat 2018;22:195-201.
20. Gupta A, Kaur J, Loh H, Mehta V. Anomalous peritoneal folds of liver with incomplete fissure for ligamentum teres: A case report. J Anim Sci 2020;28:37-42. [doi: 10.46351/JAS.V28I1PP37 42].
21. Shrestha S, Sharma N, Shah A. Ligamentum teres hepatis tunnel (pons hepatis) in human liver: A case report from Nepal. J Univ Coll Med Sci. 2023;11:67-9. [doi: 10.3126/jucms. v11i03.61617].
22. Simi CP, Uma B, Gopal S, Chaudhary S, Rymbai M, Krishnan M. Pons hepatis of quadrate lobe: A morphological variation of liver. Int J Trend Sci Res Dev 2020;4:107-8.
23. Singh H, Singh R, Singh RK, Sehgal G, Dewan RK. An analysis of the anomalous fissure of the ligamentum teres hepatis: A morphological perspective in the North Indian population. Cureus 2024;16:e58984.
24. Scarpetti L, Bello RJ, Chung SK, Hazeltine MD, Lindberg JM. Utility of ligamentum teres hepatis flap reinforcement to prevent postoperative pancreatic fistulas in robotic distal pancreatectomy. Am J Surg 2024;236:115894.
25. Aini Y, Jiang T, Wen H. Feasibility of surgical application of the ligamentum teres hepatis: a review. iLIVER 2023;2:50-5. [doi: 10.1016/j.iliver. 2023.01.005].
26. Jiang T, Ran B, Guo Q, Zhang R, Duan S, Zhong K, *et al*. Use of the ligamentum teres hepatis for outflow reconstruction during *ex vivo* liver resection and autotransplantation in patients with hepatic alveolar echinococcosis: A case series of 24 patients. Surgery 2021;170:822-30.
27. Mamata S, Singh S, Behera S, Bara DP, Baa J, Mishra S, *et al*. A morphological study of cadaveric liver. J Anat Soc India. 2023;72:131-4.
28. Yang F, Tang C, He F, Chen D, Woraikat S, Luo Y, *et al*. Safety and feasibility of electro-vaporization of ligamentum teres hepatis in totally laparoscopic gastrectomy. J Laparoendosc Adv Surg Tech A 2024;34:721-6.
29. Auh YH, Lim JH, Kim KW, Lee DH, Lee MG, Cho KS. Loculated fluid collections in hepatic fissures and recesses: CT appearance and potential pitfalls. Radiographics 1994;14:529-40.
30. Wu H, Xie K, Huang J, Pan G. Clinical effect of fissure for ligamentum teres hepatic approach in hepatectomy. Chin J Dig Surg 2016;15:53-7.

Original Article

Evaluation of Lamina Papyracea, Jugular Bulb, and Carotid Artery Dehiscence Using Paranasal Computed Tomography

Muhammed Akif Deniz, Ibrahim Akbudak

Department of Radiology, Dicle University Medical Faculty, Diyarbakir, Turkey

Abstract

Background: Determining the presence of lamina papyracea dehiscence (LPD), dominant jugular bulb (DJB), jugular bulb dehiscence (JBD), carotid artery protrusion (CAP), and carotid artery dehiscence (CAD) before endoscopic sinus and middle ear surgeries is of critical importance to avoid intraoperative complications. **Aims:** The aim of the study was to determine the prevalence of LPD, JBD, DJB, CAD, and CAP using paranasal computed tomography (CT), reveal their co-occurrence rates, describe their imaging characteristics on CT, and minimize complications related to anatomical variations during surgery in these regions. We compared our findings with those reported in the literature. **Materials and Methods:** Overall, 1000 patients who underwent paranasal CT for any reason in our outpatient clinic between December 31, 2018, and January 31, 2024, were included in the study. The prevalence of LPD, DJB, JBD, CAP, and CAD in patients and their co-occurrence rates, localization (right/left), and relationships with age and sex was evaluated. **Results:** The mean patient age was 31.6 ± 13.2 (range: 15–79) years. The prevalence of LPD was 2%. The prevalence of JBD was 5.4%, with 55.6% located on the right, 40.7% on the left, and 3.7% bilaterally; that of DJB was 31.8%, with 72.3% on the right and 27.7% on the left; that of CAD was 12.8%, with 26.6% on the right, 10.9% on the left, and 62.5% bilaterally; and that of CAP was 7.8%, with 23.1% on the right, 17.9% on the left, and 59% bilaterally. **Conclusion:** Comprehensive evaluation and identification of LPD, DJB, JBD, CAP, and CAD prior to sinus and middle ear surgeries are important.

Keywords: *Carotid artery, computed tomography, dehiscence, dominant jugular bulb, lamina papyracea, protrusion*

Introduction

The lamina papyracea (LP) is a thin bony structure located between the orbital medial wall and ethmoid sinus. LP dehiscence (LPD) refers to a defect in this bone on the orbital medial wall, with a reported prevalence of 0.76%–10.00%.[1] LP is the weakest area on the medial orbital wall, and iatrogenic, traumatic, congenital, and inflammatory conditions can lead to LPD. Anatomical variations wherein orbital structures herniate into the ethmoid sinus without LPD are considered a potential cause of orbital complications in endoscopic sinus surgery (ESS). Preoperative use of computed tomography (CT), which is highly effective in detecting such anatomical variations, is extremely important to avoid surgical complications.[1]

LPD, which refers to a wall defect at the level of LP, has been classified into three grades: Grade 1 indicates a defect covering less than one-third of the wall, Grade 2 indicates a defect covering between one-third and two-thirds of the wall, and Grade 3 indicates a defect covering greater than two-thirds of the wall.[2]

The jugular bulb (JB) refers to an enlarged segment at the junction of the sigmoid sinus and internal jugular vein. Dominant JB (DJB) refers to the unilateral and asymmetric enlargement of the JB. A large jugular foramen observed on CT represents a large JB.[3] The JB, which is separated from the inner ear and middle ear cavity by compact bone, is located beneath the hypotympanum of the middle ear cavity and the floor of the internal acoustic canal. Although a high-riding JB (HRJB) can lead to hearing impairments, vestibular problems, and tinnitus, it does not cause symptoms. JB dehiscence (JBD) refers to the absence of a bony septum known as the sigmoid plate between the JB and middle ear cavity. Consequently, the JB

How to cite this article: Deniz MA, Akbudak I. Evaluation of lamina papyracea, jugular bulb, and carotid artery dehiscence using paranasal computed tomography. J Anat Soc India 2025;74:236-42.

Article Info

Received: 13 March 2025
Revised: 22 May 2025
Accepted: 18 August 2025
Available online: 30 September 2025

Address for correspondence:
Dr. Muhammed Akif Deniz, Department of Radiology, Dicle University Medical Faculty, Sur, Diyarbakir, Turkey.
E-mail: makifdeniz@yahoo.com

Access this article online

Website: https://journals.lww.com/joai

DOI: 10.4103/jasi.jasi_51_25

Quick Response Code:

may protrude into the middle ear cavity. In cases of JBD variations, the JB becomes easily vulnerable during procedures such as myringotomy and tympanomeatal flap elevation, posing significant risks of morbidity and mortality.[4]

The sphenoid sinuses are divided by a septum and typically comprise two asymmetrical cavities. These cavities, located within the body of the sphenoid bone, are positioned posterior to the upper part of the nasal cavity. The internal carotid artery (ICA), optic nerve, and vidian nerve are in close proximity to the sphenoid sinus. These well-aerated cavities are separated from adjacent structures via thin bony plates. Bony protrusions surrounding the ICA may project into the sinus. Extended pneumatization of the sphenoid bone increases the likelihood of protrusion of neurovascular structures such as the ICA into the sinus. In some individuals, a dehiscence may occur in the thin bony layer surrounding the ICA. This leaves the ICA exposed within the sinus cavity. During ESS, if the surgeon is unaware of the presence of carotid artery protrusion (CAP) into the sinus and/or carotid artery dehiscence (CAD), the surgical process may cause significant injury to the ICA, resulting in uncontrollable and fatal bleeding.[5] Therefore, to avoid intraoperative complications, a detailed CT examination of the anatomical variations in the sphenoid sinus and surrounding structures should be performed before ESS.[6,7]

We aimed to determine the prevalence of LPD, JBD, DJB, CAD, and CAP using paranasal CT, reveal their co-occurrence rates, describe their imaging characteristics on CT, and minimize complications related to anatomical variations during surgery in these regions. Moreover, we compared the study findings with those reported in the literature.

Materials and Methods

This study was designed as a retrospective study and approved by the local ethics committee. A retrospective analysis was conducted on 1000 patients who underwent paranasal CT for any reason in our outpatient clinic between December 31, 2018, and February 31, 2024, and in whom the carotid artery, JB, and LP were completely visualized in the imaging area were included in the study. Patients were evaluated based on sex, age, JBD, CAD, and LPD. In patients with dehiscence, the type of dehiscence, dehiscence levels, dehiscence localization, the relationship between dehiscence and age and sex, and the relationship between different types of dehiscence were evaluated. In patients with LPD, the extent of dehiscence, presence of herniated tissue at the dehiscence level, and type of herniated tissue were examined.

This study also investigated the presence of CAP and DJB and assessed the relationship between CAP and CAD in patients with CAP, as well as the relationship between DJB and JBD in patients with DJB.

Computed tomography and evaluation protocol

All examinations were performed using a 64-detector CT scanner (Philips Brilliance 64 Channel, Philips Healthcare, Eindhoven, Netherlands). All images were transferred to the picture archiving and communication system to create and evaluate multiplanar images. The images were reviewed by two radiologists with at least 5 years of experience in head and neck imaging. Discrepancies were resolved by joint evaluation to reach a consensus. For patients with multiple scans, only those without artifacts and with clearly delineated boundaries of the LP, carotid artery, and JB were included in the study.

Images that did not allow for clear evaluation of these structures or were affected by artifacts, trauma, fractures, masses, or surgical alterations, which distorted the normal anatomy, were excluded from the study.

Statistical analysis

Analyses were conducted using SPSS (Statistical Package for Social Sciences; SPSS Inc., Chicago, IL, USA) version 22. Descriptive data were presented as number (n) and frequency (%) for categorical variables and mean ± standard deviation for continuous variables. Pearson Chi-squared test was used to compare categorical variables between the two groups. The conformity of continuous variables to normal distribution was evaluated via Kolmogorov–Smirnov test. Mann–Whitney *U*-test was used to compare the variables between the two groups. A $P < 0.05$ was considered to indicate statistical significance in all analyses.

Results

In our study, 1000 patients with a mean age of 31.6 ± 13.2 (range: 18–79) years. Of these, 48% were females and 52% were males. The prevalence of LPD was 2% in this population. Among the detected LPD cases, 70% were Grade 1, 20% were Grade 2, and 10% were Grade 3. Among the detected LPDs, 70% were located on the left side and 30% on the right side [Figure 1]. Although 60% of patients with LPD had herniated tissue, herniated tissue was identified as fatty tissue in 83.3% and medial rectus muscle in 16.7% of these cases.

The prevalence of JBD was 5.4%, with 55.6% of the detected JBDs located on the right, 40.7% on the left, and 3.7% bilaterally. The prevalence of DJB was 31.8%, with 72.3% of the detected DJBs located on the right [Figure 2] and 27.7% on the left [Figure 3].

The prevalence of CAD was 12.8%, with 26.6% of the detected CADs located on the right, 10.9% on the left, and 62.5% bilaterally [Figure 4]. The prevalence of CAP was 7.8%, with 23.1% of the detected CAPs located on the right, 17.9% on the left, and 59% bilaterally [Table 1].

The prevalence of LPD was significantly higher in males (3.1%) than in females (0.8%) ($P = 0.011$). The

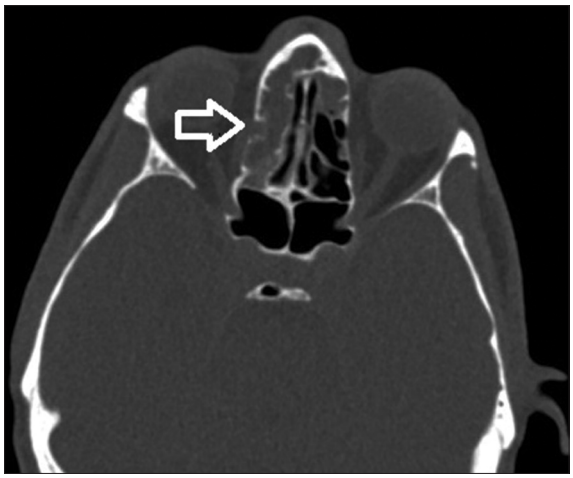

Figure 1: A 56-year-old female patient showing dehiscence in the right lamina papyracea (arrow)

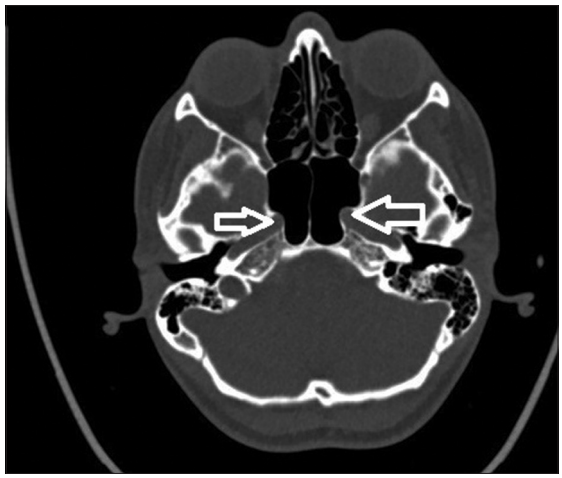

Figure 2: A 45-year-old male patient showing protrusion of the carotid arteries into the sphenoid sinus bilaterally and dehiscence at these levels (arrows)

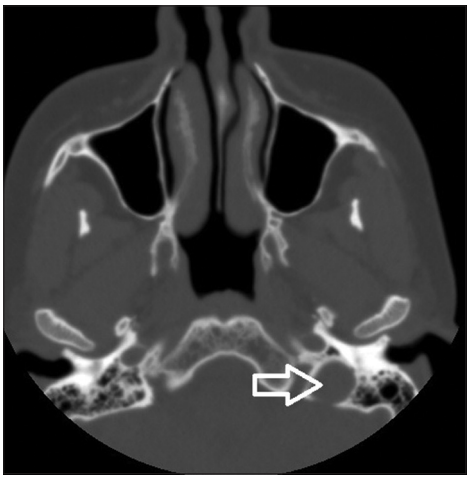

Figure 3: A 39-year-old male patient showing a dominant jugular bulb on the left (arrow)

Figure 4: A 43-year-old female patient showing a dominant jugular bulb on the right side and dehiscence at this level (arrow)

mean age of patients with LPD was significantly higher than that of patients without LPD ($P = 0.004$).

There was no statistically significant difference in the prevalence of JBD and DJB between males and females or across age distributions. The prevalence of CAP was significantly higher in males (9.6%) than in females (5.8%) ($P = 0.026$). No significant difference was noted in the prevalence of CAP and CAD across age distributions. In addition, there was no significant difference in the prevalence of CAD between males and females [Table 2].

Overall, 71.4% of patients with right LPD had Grade 1 and 28.6% had Grade 2 LPD, whereas 66.7% of those with left LPD had Grade 1 and 33.3% had Grade 3 LPD, with no significant difference between the two groups ($P = 0.063$). Furthermore, 66.7% of patients with herniated tissue had Grade 1, 16.7% had Grade 2, and 16.7% had Grade 3 LPD, whereas 75% of those without herniated tissue had Grade 1 and 25% had Grade 2 LPD, with no significant difference between the two groups ($P = 0.619$).

The prevalence of DJB was significantly higher in patients with JBD (70.4%) than in those without jugular dehiscence (29.6%) [$P < 0.001$; Table 3].

The prevalence of CAP was significantly higher in patients with CAD (12.5%) than in those without CAD (7.1%) [$P = 0.034$; Table 4].

The prevalence of JBD was significantly higher in patients with LPD (20%) than in those without LPD (5.1%) ($P = 0.019$). None of the patients with LPD had CAD, whereas 13.1% of patients without dehiscence had CAD. There was no significant difference no significant difference was noted between the two groups [$P = 0.096$; Table 5].

The prevalence of CAD was 7.4% in patients with JBD and 13.1% in those without JBD, with no significant difference between the two groups [$P = 0.223$; Table 6].

Discussion

The LP is the weakest region on the medial orbital wall, and LPD is a bone defect in this weak region. As a

Table 1: Characteristics and imaging findings of the patients included in the study

	n (%)
Age, mean±SD	31.6±13.2
Sex	
Female	480 (48.0)
Male	520 (52.0)
LPD	
Yes	20 (2.0)
No	980 (98.0)
LPD grade	
Grade 1	14 (70.0)
Grade 2	4 (20.0)
Grade 3	2 (10.0)
LPD localization	
Right	14 (70.0)
Left	6 (30.0)
Presence of herniated LPD tissue	
Yes	12 (60.0)
No	8 (40.0)
Type of herniated LPD tissue	
Fatty tissue	10 (83.3)
Superior orbital muscle	2 (16.7)
Presence of JBD	
Yes	54 (5.4)
No	946 (94.6)
JBD localization	
Right	30 (55.6)
Left	22 (40.7)
Bilateral	2 (3.7)
Presence of DJB	
Yes	318 (31.8)
No	682 (68.2)
DJB localization	
Right	230 (72.3)
Left	88 (27.7)
Presence of CAD	
Yes	128 (12.8)
No	872 (87.2)
CAD localization	
Right	34 (26.6)
Left	14 (10.9)
Bilateral	80 (62.5)
Presence of CAP	
Yes	78 (7.8)
No	922 (92.2)
CAP localization	
Right	18 (23.1)
Left	14 (17.9)
Bilateral	46 (59.0)

SD: Standard deviation, CAP: Carotid artery protrusion, CAD: Carotid artery dehiscence, DJB: Dominant jugular bulb, JBD: Jugular bulb dehiscence, LPD: Lamina papyracea dehiscence

paranasal sinus variation, LPD typically does not cause symptoms. It is characterized by protrusion of orbital fat through a defect in the wall between the anterior ethmoid sinus and orbit.[1] It is important to distinguish LPD from a fracture. CT plays a key role in diagnosing this variation and is highly valuable for preoperative and intraoperative planning in functional ESS.[8]

The prevalence of LPD reportedly ranges from 0.76% to 10.00%.[9,10] Kitaguchi *et al*.[11] examined 315 patients using CT and reported an LPD prevalence of 1.9%, whereas Xu *et al*.[1] revealed an LPD prevalence of 2.58% in their study involving 893 patients. In another study involving 1024 patients, the prevalence of LPD was reported as 6.5%.[2] In the present study, the prevalence of LPD was 2%, which is consistent with the literature.

LPD is classified into three grades based on the extent of bone defect. Han *et al*. evaluated 1024 patients and reported that Grade 1 dehiscence was the most common (59%) and Grade 3 dehiscence was the least common (10%).[2] Xu *et al*.[1] found Grade 3 LPD to be the least common (8.7%) and Grade 1 LPD to be the most common (69%). In the present study, Grade 1 LPD was reported most frequently at 70%, whereas Grade 3 LPD was reported least frequently at 10%, consistent with the literature.

Although LPD is usually unilateral, it can rarely be bilateral. Kaya *et al*.[12] and Xu *et al*.[1] found no statistically significant difference between the occurrence of dehiscence on the right and left sides. In contrast, the present study revealed that dehiscence was significantly more frequent on the right side than on the left side. However, no statistically significant difference was noted between the dehiscence grade and its localization in the present study.

Previous studies on LPD have frequently reported herniation of orbital fat tissue into the ethmoid sinus. In contrast, herniation of orbital muscle structures, particularly the medial rectus muscle, into the ethmoid sinus has been reported less frequently.[1-4] In the present study, 60% of LPD cases exhibited herniation of orbital structures into the sinus, with orbital fat tissue showing the majority of herniation (83%), consistent with the literature.

Previous studies have reported a nonstatistical increase in the prevalence of LPD with aging.[2,13] In the present study, the prevalence of LPD significantly increased with aging. We believe that this is secondary to the weakening of the bone structure associated with aging. Açar *et al*.[13] reported that the prevalence of LPD was significantly higher in males than in females. Kaya *et al*.[12] did not report a statistically significant difference in the prevalence of LPD between males and females. In line with Açar *et al*.,[13] the present study found a significantly higher prevalence of LPD in males than in females.

JBD, especially in association with an HRJB, may cause tinnitus. It is extremely important for radiologists to report JBD appropriately to avoid significant complications such as bleeding during middle ear surgeries. Studies have shown that the prevalence of JBD ranges from 2.6% to

Table 2: Comparison between demographic characteristics and features related to variations

	Female, *n* (%)	Male, *n* (%)	*P**	Age, mean±SD	*P***
LPD					
Yes	4 (0.8)	16 (3.1)	0.011	40.7±16.1	0.004
No	476 (99.2)	504 (96.9)		31.4±13.0	
LPD localization					
Right	4 (100.0)	10 (62.5)	0.267	43.7±18.0	0.444
Left	0	6 (37.5)		33.7±8.1	
LPD herniated tissue					
Yes	2 (50.0)	10 (62.5)	0.648	45.3±18.8	0.238
No	2 (50.0)	6 (37.5)		33.8±7.6	
JBD					
Yes	30 (6.3)	24 (4.6)	0.253	31.9±11.5	0.318
No	450 (93.8)	496 (95.4)		31.6±13.3	
DJB					
Yes	148 (30.8)	170 (32.7)	0.528	30.2±11.4	0.144
No	332 (69.2)	350 (67.3)		32.3±13.9	
CAD					
Yes	52 (10.8)	76 (14.6)	0.074	32.9±13.3	0.255
No	428 (89.2)	444 (85.4)		31.4±13.1	
CAP					
Yes	28 (5.8)	50 (9.6)	0.026	34.7±15.0	0.083
No	452 (94.2)	470 (90.4)		31.3±13.0	

*Chi-squared test, **Mann–Whitney *U*-test were performed. SD: Standard deviation, CAP: Carotid artery protrusion, CAD: Carotid artery dehiscence, DJB: Dominant jugular bulb, JBD: Jugular bulb dehiscence, LPD: Lamina papyracea dehiscence

Table 3: Evaluation of the presence of a dominant jugular bulb according to the presence of jugular bulb dehiscence

	DJB is present, *n* (%)	No DJB, *n* (%)	*P**
Presence of JBD			
Yes	38 (70.4)	16 (29.6)	<0.001
No	280 (29.6)	666 (70.4)	

*Chi-squared test was performed. DJB: Dominant jugular bulb, JBD: Jugular bulb dehiscence

Table 4: Evaluation of the presence of carotid artery protrusion according to the presence of carotid artery dehiscence

	CAP is present, *n* (%)	No CAP, *n* (%)	*P**
Presence of CAD			
Yes	16 (12.5)	112 (87.5)	0.034
No	62 (7.1)	810 (92.9)	

*Chi-squared test was performed. CAP: Carotid artery protrusion, CAD: Carotid artery dehiscence

7.5%.[14,15] Atmaca *et al*.[4] revealed a JBD prevalence of 7.5% in their CT study involving 1010 cases in the Turkish population, whereas Park *et al*.[16] reported a JBD prevalence of 3.8% in their CT study involving 276 cases in the German population. In the present study, the prevalence of JBD was 5.4%, which is consistent with the average prevalence of these two studies. However, Irabien–Zuñiga *et al*.[17] reported a lower JBD prevalence of 1.3% in their CT study involving 229 cases in the Mexican population. We believe that the higher prevalence observed in the present study is due to differences in the number of cases and ethnic populations. In the study by Atmaca *et al*.,[4] the prevalence of JBD was higher on the right side and in females, consistent with the present study.

In CT studies, it is well acknowledged that a larger jugular foramen contains a larger JB. In a previous CT study, JB was larger on the right side in 58.8%, larger on the left side in 29.4%, and of equal size in 11.8% of patients.[3] Another study reported that DJB was detected on the right side in 66.6% of patients.[18] Consistently, the present study reported that the prevalence of DJB was significantly higher on the right side (72.3%). In our study, there was no significant difference noted in the prevalence of DJB between sexes. However, the prevalence of DJB in patients with JBD (70.4%) was significantly higher than that in patients without JBD (29.6%).

CAP is defined as the carotid artery surrounded by the sphenoid sinus air in any plane. If the carotid artery is entirely embedded in a bone, it should not be considered a protrusion.[19] The absence of bone separating the ICA from the sphenoid sinus along the canal is defined as CAD.[20] In CT studies, a protrusion of the carotid artery into the sphenoid sinus has been reported in 5%–28% of patients.[21,22] Lakhani *et al*.[5] evaluated 270 cases using CT and reported the prevalence of CAD as 16.6%, with the majority of dehiscence cases being unilateral (62.2%). In

Table 5: Evaluation of the presence of jugular bulb dehiscence and carotid artery dehiscence according to the presence of lamina papyracea dehiscence

	LPD is present, *n* (%)	No LPD, *n* (%)	*P**
Presence of JBD			
Yes	4 (20.0)	50 (5.1)	0.019
No	16 (80.0)	930 (94.9)	
Presence of CAD			
Yes	0	128 (13.1)	0.096
No	20 (100.0)	852 (86.9)	

*Chi-squared test was performed. CAD: Carotid artery dehiscence, JBD: Jugular bulb dehiscence, LPD: Lamina papyracea dehiscence

Table 6: Evaluation of the presence of carotid artery dehiscence according to the presence of jugular bulb dehiscence

	CAD is present, *n* (%)	No CAD, *n* (%)	*P**
Presence of JBD			
Yes	4 (7.4)	50 (92.6)	0.223
No	124 (13.1)	822 (86.9)	

*Chi-squared test was performed. CAD: Carotid artery dehiscence, JBD: Jugular bulb dehiscence

the same study, the prevalence of CAP was 10.3%, with most protrusion cases being unilateral (60.7%). In a study conducted in Turkey by Arslan *et al*.,[23] the prevalence of CAP was 8%. It has been noted that the prevalence of CAD varies between 5% and 48% in different studies.[20-27] In a study conducted by Kajoak *et al*.[25] in Sudan, the prevalence of CAD was 12.4%. Fatihoglu *et al*.[26] conducted a study involving 1003 cases and reported the prevalence of CAP as 31.9%, with the majority of protrusion cases being bilateral (77.5%). In the same study, the prevalence of CAD was reported as 21.9%, with the majority of dehiscence cases being bilateral (68.5%).[26] In the present study, the prevalence of CAD was 12.8%, whereas that of CAP was 7.8%, which are generally consistent with the prevalence ranges reported in the literature. In the studies by Lakhani *et al*.[5] and Arslan *et al*.,[23] the prevalence of CAP was 10.3% and 8%, respectively, consistent with the present study. The prevalence of CAD observed in the present study (12.8%) was similar to that reported by Kajoak *et al*. (12.4%)[25] but lower than that reported by Fatihoglu *et al*.(21.9%).[26] Fatihoglu *et al*.[26] found that CAP and CAD localization were mostly bilateral (77.5% and 68.5%, respectively). In the present study, consistent with the literature, the majority of cases with CAP and CAD were bilateral (CAP: 59%, CAD: 62.5%). In the study by Famurewa *et al*.,[19] the prevalence of CAP was higher in females (67%). In the present study, the prevalence of CAP was higher in males. We believe this is due to differences in societal structure and the varying number of patients.

In our study, the prevalence of JBD in patients with LPD (20%) was significantly higher than that in patients without LPD (5.1%). None of the patients with LPD had CAD, whereas 13.1% of patients without LPD had CAD, with no significant difference between the two groups. The prevalence of CAD was 7.4% in patients with JBD and 13.1% in those without JBD, with no significant difference between the two groups. In the present study, we evaluated the relationship between these three anatomical variations and their co-occurrence. To the best of our knowledge, no studies in the literature have explored the co-occurrence of LPD with CAD and JBD. Likewise, we did not find any study evaluating the relationship between CAD and JBD or their co-occurrence. This is the first study to evaluate variations in LPD, JBD, and CAD using a single imaging method (noncontrast paranasal sinus CT) and reveal their co-occurrence rates, which are extremely important and should be known in advance to avoid surgical complications in relevant regions. We believe this aspect of our study will make a significant contribution to the literature.

Our study had several limitations. These include the retrospective and single-center design, relatively small sample size, and the lack of confirmation of findings through endoscopic intervention and/or surgery.

Conclusion

The prevalence and co-occurrence rates of anatomical variations, such as LPD, JBD, DJB, CAD, and CAP, in the Turkish population were determined using paranasal sinus CT. These anatomical variations can be successfully demonstrated using CT without the need for contrast material. Surgeons should be aware of these anatomical variations in the preoperative period to prevent injuries to orbital structures, JB, and ICA, as well as potentially fatal bleeding during ESSs (for the ethmoid and sphenoid sinuses) and middle ear surgeries. Therefore, radiologists should carefully examine CT images for anatomical variations before surgery and report findings that will serve as navigation aids for the surgeon during operations, thereby minimizing complications.

Declaration of patient consent

The authors certify that they have obtained all appropriate patient consent forms. In the form, the patient has given his consent for his images and other clinical information to be reported in the journal. The patient understands that his name and initials will not be published and due efforts will be made to conceal his identity, but anonymity cannot be guaranteed.

Financial support and sponsorship

Nil.

Conflicts of interest

There are no conflicts of interest.

References

1. Xu J, Qin L, Wang D. Analysis of the lamina papyracea dehiscence based on computed tomography findings. J Craniofac Surg 2022;33:e580-3.
2. Han MH, Chang KH, Min YG, Choi WS, Yeon KM, Han MC. Nontraumatic prolapse of the orbital contents into the ethmoid sinus: Evaluation with screening sinus CT. Am J Otolaryngol 1996;17:184-9.
3. Cormio M, Robertson CS. Ultrasound is a reliable method for determining jugular bulb dominance. J Neurosurg Anesthesiol 2001;13:250-4.
4. Atmaca S, Elmali M, Kucuk H. High and dehiscent jugular bulb: Clear and present danger during middle ear surgery. Surg Radiol Anat 2014;36:369-74.
5. Lakhani M, Mohiuddin M, Khan RN, Raza I, Santosh Kumar Sidhwani SK, Hassan N. Variation in internal carotid artery protrusion and dehiscence in a subset of Karachi population. J Rawalpindi Med Coll 2023;27:74-8.
6. Budu V, Mogoantă CA, Fănuţă B, Bulescu I. The anatomical relations of the sphenoid sinus and their implications in sphenoid endoscopic surgery. Rom J Morphol Embryol 2013;54:13-6.
7. Rahmati A, Ghafari R, AnjomShoa M. Normal variations of sphenoid sinus and the adjacent structures detected in cone beam computed tomography. J Dent (Shiraz) 2016;17:32-7.
8. Papadopoulou AM, Chrysikos D, Samolis A, Tsakotos G, Troupis T. Anatomical variations of the nasal cavities and paranasal sinuses: A systematic review. Cureus 2021;13:e12727.
9. Moulin G, Dessi P, Chagnaud C, Bartoli JM, Vignoli P, Gaubert JY, *et al.* Dehiscence of the lamina papyracea of the ethmoid bone: CT findings. Am J Neuroradiol 1994;15:151-3.
10. Chao TK. Uncommon anatomic variations in patients with chronic paranasal sinusitis. Otolaryngol Head Neck Surg 2005;132:221-5.
11. Kitaguchi Y, Takahashi Y, Mupas-Uy J, Kakizaki H. Characteristics of dehiscence of lamina papyracea found on computed tomography before orbital and endoscopic endonasal surgeries. J Craniofac Surg 2016;27:e662-5.
12. Kaya M, Cankal F, Tekdemir I. Bone dehiscences of medial orbital wall on computed tomography and assessment of terminological errors in literature. Folia Morphol (Warsz) 2022;81:175-82.
13. Açar G, Büyükmumcu M, Güler İ. Computed tomography based analysis of the lamina papyracea variations and morphology of the orbit concerning endoscopic surgical approaches. Braz J Otorhinolaryngol 2019;85:551-9.
14. Sarioglu FC, Pekcevik Y, Guleryuz H, Olgun Y, Guneri EA. Variations of the vascular canals in the cochlear implant candidates. Int J Pediatr Otorhinolaryngol 2019;123:123-7.
15. Brook CD, Buch K, Kaufmann M, Sakai O, Devaiah AK. The prevalence of high-riding jugular bulb in patients with suspected endolymphatic hydrops. J Neurol Surg B Skull Base 2015;76:471-4.
16. Park JJ, Shen A, Keil S, Kuhl C, Westhofen M. Jugular bulb abnormalities in patients with Meniere's disease using high-resolution computed tomography. Eur Arch Otorhinolaryngol 2015;272:1879-84.
17. Irabien-Zuñiga M, Gonzalez-Treviño M, Pinales-Razo R, Quiroga-Garza A, Kohn-Gutierrez AE, Elizondo-Omaña RE, *et al*. Prevalence of high riding jugular bulb and dehiscence: An evaluation using computed tomography. Med Univ 2022;24:19-24.
18. Swartz JD, Harnsberger HR. Imaging of the Temporal Bone. Stuttgart: George Thieme Verlag; 1998.
19. Famurewa OC, Ibitoye BO, Ameye SA, Asaleye CM, Ayoola OO, Onigbinde OS. Sphenoid sinus pneumatization, septation, and the internal carotid artery: A computed tomography study. Niger Med J 2018;59:7-13.
20. Dal Secchi MM, Dolci RL, Teixeira R, Lazarini PR. An analysis of anatomic variations of the sphenoid sinus and its relationship to the internal carotid artery. Int Arch Otorhinolaryngol 2018;22:161-6.
21. Kazkayasi M, Karadeniz Y, Arikan OK. Anatomic variations of the sphenoid sinus on computed tomography. Rhinology 2005;43:109-14.
22. Tomovic S, Esmaeili A, Chan NJ, Shukla PA, Choudhry OJ, Liu JK, *et al.* High-resolution computed tomography analysis of variations of the sphenoid sinus. J Neurol Surg B Skull Base 2013;74:82-90.
23. Arslan H, Aydınlıoğlu A, Bozkurt M, Egeli E. Anatomic variations of the paranasal sinuses: CT examination for endoscopic sinus surgery. Auris, Nasus, Larynx 1999;26:39-48.
24. Tesfaye S, Hamba N, Gerbi A, Negeri Z. Radio-anatomic variability in sphenoid sinus pneumatization with its relationship to adjacent anatomical structures and their impact upon reduction of complications following endonasal transsphenoidal surgeries. Translational Research in Anatomy 2021;24:100126.
25. Kajoak SA, Ayad CE, Najmeldeen M, Abdalla EA. Computerized tomography morphometric analysis of the sphenoid sinus and related structures in Sudanese population. Glob Adv Res J Med Med Sci 2014;3:160-7.
26. Fatihoglu E, Aydin S, Karavas E, Kantarci M. The pneumatization of the sphenoid sinus, its variations and relations with surrounding neurovascular anatomic structures: A computerized tomography study. Am J Otolaryngol 2021;42:102958.
27. Sasagawa Y, Tachibana O, Doai M, Hayashi Y, Tonami H, Iizuka H, *et al.* Carotid artery protrusion and dehiscence in patients with acromegaly. Pituitary 2016;19:482-7.

Original Article

A Cephalometric Study of the Adult Subjects Attending General Outpatient Department in North Bengal Medical College and Hospital in Relation to Sex and Racial Factors

Sudeshna Majumdar, Amitesh Bhowal[1]

Department of Anatomy, Jhargram Medical College, Jhargram, [1]Department of Anatomy, North Bengal Medical College, Darjeeling, West Bengal, India

Abstract

This descriptive cross-sectional study was conducted on a total of 600 subjects (150 males and 450 females) in the age group of 18–50 years who were attending the General Outpatient Department and residing in one of the eight districts of North Bengal. The participants were classified in relation to gender and racial factors. One of the chief objectives of this study was to compare cephalic indices among males and females statistically and to find out the most common skull type in North Bengal population. Other objectives include the comparison of cranial parameters between different linguistic groups. Data collection for this study was carried out in between June 2019 and February 2020. Head measurements were taken with the help of spreading calipers. After calculating the cephalic indices, it was found that the most number of subjects belonged to mesocephalic group (271), followed by brachycephalic group (212). Among males, mean confidence interval (CI) was 78.94 ± 3.72; among females, mean CI was 79.32 ± 3.93. Mean CI of the total population was 79.23 ± 3.88. Mean CI of Bengali, Rajbangsi, and Nepali communities was 79.30, 78.63, and 80.62, respectively.

Keywords: *Calipers, cephalic index, cephalometry, ethnicity, measurement, race, skull type*

Introduction

Objectives of this study were to measure the cephalic index of participants who attended the general outpatient department (OPD) of North Bengal Medical College and Hospital, belonging to 18–50-year age group, coming from different districts of North Bengal and also to compare the cephalic index of males and females of Bengali, Nepalese, and Rajbangsi subjects.

Materials and Methods

It is a descriptive cross-sectional study that has been conducted in North Bengal Medical College under the Department of Anatomy and the general OPD from June 2019 to February 2020. The subjects who fulfilled the inclusion criteria were approached, and head measurements were taken at the General OPD with the help of spreading calipers after obtaining their informed consent [Figures 1 and 2]. The data were tabulated and analyzed with the help of Microsoft Excel.

Results

Out of a total 600 subjects belonging to 18–50-year age group in the study, 150 (25%) were male and 450 (75%) were female. All of them were subgrouped into three categories: 18–30 years, 31–40 years, and 41–50 years.

On the basis of the cephalic index calculated from head length and breadth, the study participants were classified into six skull types.

45.17% of all the subjects belonged to mesocephalic group, followed by brachycephalic (35.33%), dolichocephalic (11.33%), and hyperbrachycephalic (6.83%) groups. Only 0.83% were hyperdolichocephalic and 0.5% were found to be ultrabrachycephalic.

The male subjects presented with confidence interval (CI) ranging from 70 to 90.53, mean CI 78.94, standard deviation 3.7208, and the female subjects presented with CI ranging from 66.30 to 93.96, mean CI was 79.32, and standard deviation was 3.9288. The total population had mean CI of 79.23 and standard deviation of 3.8814.

How to cite this article: Majumdar S, Bhowal A. A cephalometric study of the adult subjects attending general outpatient department in North Bengal Medical College and Hospital in relation to sex and racial factors. J Anat Soc India 2025;74:243-5.

Article Info

Received: 05 June 2023
Revised: 31 May 2025
Accepted: 18 August 2025
Available online: 30 September 2025

Address for correspondence:
Dr. Amitesh Bhowal, 31, Girish Ghosh Sarani, Hakimpara, Siliguri - 734 001, West Bengal, India.
E-mail: dramiteshbhowal87@gmail.com

Access this article online

Website: https://journals.lww.com/joai
DOI: 10.4103/jasi.jasi_54_23
Quick Response Code:

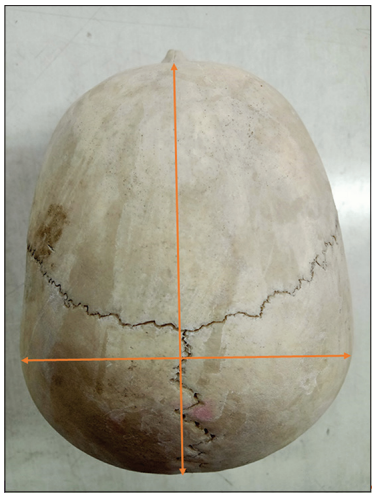

Figure 1: Cephalic index is calculated using the ratio between maximum breadth and length of skull

In the Bengali-speaking group, mean CI was 79.30, standard deviation = 3.8777. Among the Hindi-speaking group originating from Bihar, mean CI was 78.93 and standard deviation = 4.1340. The Nepalese participants showed mean CI of 80.62, standard deviation = 2.8736. Rajbangsi people showed mean CI of 78.63 and standard deviation = 3.7414. Among the Sadri-speaking or the tribal group, mean CI was found to be 78.41 and standard deviation = 3.8422 As seen in [Figure 3a-d].

Difference between CI of male and female participants was not found to be statistically significant ($P > 0.05$) at 95% confidence limit. Difference between CI of Bengali and Rajbangsi castes was statistically insignificant ($P > 0.05$). Difference between CI of Bengali and Nepali communities was observed to be statistically insignificant ($P > 0.05$) as seen in [Figure 3a-d].

Discussion

There are significant variations in cephalic indices of different geographical populations over the world. African crania are mostly mesocephalic, but European crania are considered dolichocephalic, and Asia has a prevalence of brachycephalic crania.[1] In a study undertaken by Golalipour on adult fars males from North Iran, most of the crania (52%) were found to be hyperbrachycephalic.[2] Another study by Heidari *et al*. showed that 41.3% of females from South-East Iran were mesocephalic, 31.5% were brachycephalic and 21.3% were dolichocephalic.[3] Yagain *et al*. studied cephalic index in Indian students, in which dominant head shape types in males were dolichocephaly (33%) and brachycephaly (33%). Mean cephalic index was 77.92 (mesocephalic) in males and 80.85 in females.[4]

In the present study, mean cranial index was 78.94 (male) and 79.32 (female). This finding was higher than those of Bhils (76.98),[5] people from Bayesla state of Nigeria (73.68),[6] but lower than those of Barelas (79.8),[7]

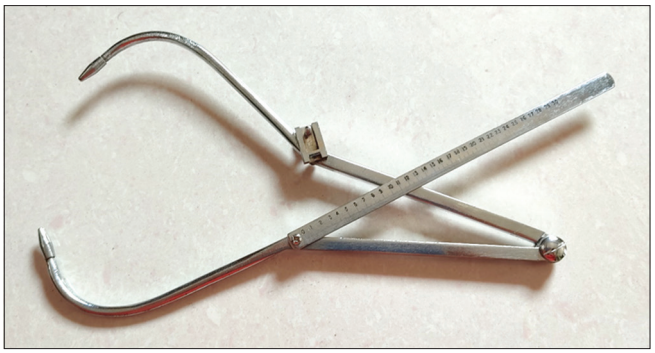

Figure 2: Spreading calipers used in measurement of head parameters

medical students of Nepal (81.24),[8] Igbo (79.04) and Ijaw (80.98) tribes,[9] the South of Iran (82.40),[10] and Mapuche population in Chile (80.42).[11] Priti *et al*. selected 160 males and 160 females from Maharashtra, mean CI was 78.25, male population had mean CI of 77.96, females had mean CI of 78.53.[12]

In a study among 90 males and 50 females from the Mahakaushal region of MP performed by Setiya *et al*., mean CI was estimated to be 77.89, CI in males was 77.65, and in females, CI was 78.13. Out of the 140 candidates, 66.67% of males and 68% of females were found to be mesocephalic, 31.11% of males and 28% of females were dolichocephalic.[13] Bharati *et al*. had compared cephalic indices of different climatic zones in India. People from tropical, monsoon, and cold areas had mean CI of 75.52, 75.99, and 77.09, respectively.[14]

All these data are in favor of brachycephalization – progressive brain growth in the lateral direction. Most common skull type in North Bengal was mesocephaly, brachycephaly being the second-most frequent type.

Conclusion

The result of the study showed that mesocephaly is the commonest skull type, followed by brachycephaly, in both male and female participants from each of the Bengali, Rajbangsi, and Nepalese communities. This finding is consistent with other studies, which indicate that majority of the Indians show mesocephalic features. The study outcome had more similarity with research works based on Indians rather than those on people from outside the Indian subcontinent.

This study was also intended to compare the cephalic index of various ethnic group of North Bengal and to identify intergender variation of the same. While there were some differences in the mean CI, the differences between genders and the ethnic groups compared were found to be statistically insignificant.

Limitations

Since the study was conducted in the General OPD of NBMC hospital located in Darjeeling district, majority of them belonged to Darjeeling and Jalpaiguri districts. The number of participants from other districts were significantly

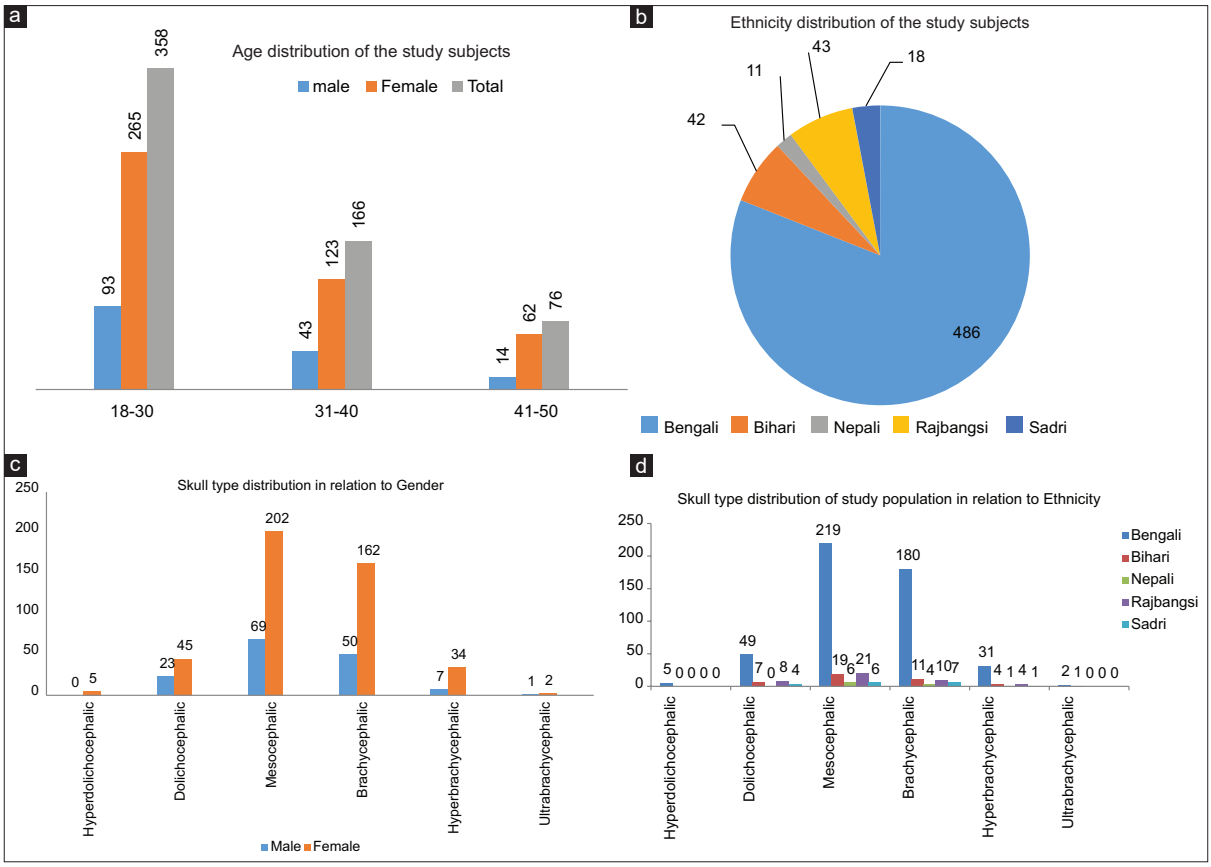

Figure 3: (a) Age distribution of the study subjects, (b) Ethnicity distribution of the study subjects, (c) Skull type distribution in relation to Gender, (d) Skull type distribution of study population in relation to Ethnicity

less. It was intended to compare cephalic indices of several ethnic or linguistic groups. But compared to the Bengali community, very less number of Rajbangsi and Nepali individuals were found to attend this hospital.

There were chances of manual error while taking measurements, because not all the subjects had prominent bony landmarks. There may be subjective variation of age, as the investigator had to completely rely on the statements by the participants.

Being a descriptive cross-sectional study, the statistical significance of the result is comparable with similar studies only.

Financial support and sponsorship

Nil.

Conflicts of interest

There are no conflicts of interest.

References

1. Chaudhury RK, Sah SK, Parajuli SB, Deo SK. Pattern of cephalic index among medical students of a medical college in Eastern Nepal. J Coll Med Sci Nepal 2019;15:256-9.
2. Golalipour MJ. The variation of head shapes in 17-20 years old native Fars male in Gorgan-North of Iran. Int J Morphol 2006;24:187-90.
3. Heidari Z, Sagheb HR, Mugahi MH. Morphological evaluation of head and face in 18-25 years old women in Southeast of Iran. J Med Sci 2006;6:400-4.
4. Yagain VK, Pai SR, Kalthur SG, Chethan P, Hemlatha I. Study of cephalic index in Indian students. Int J Morphol 2012;30:125-9.
5. Bhargava T, Kher GA. Anthropometric study of central India. Bhils of Dhar districts of Madhya Pradesh. J Anatomical Soc India 1960;9:14-9.
6. Eroje MA, Fawehinmi HB, Jaja BN, Yaakor L. Cephalic index of Ogbia tribe of Bayesla State. Int J Morphol 2010;28:389-92.
7. Bhargav T, Kher GA. A comparative anthropometric study of Bhils and Barelas of central India. J Anatomical Soc India 1961;10:23-6.
8. Manandhar B. Cephalic index among Nepalese medical students. Orthod J Nepal 2017;7:20-3.
9. Oladipo GS, Olatu J. Anthropometric comparison of cephalic indices between Ijaw and Igbo tribes. Glob Int J Pure Appl Sci 2006;12:127-38.
10. Vojdani Z, Bahmanpour S, Momeni S, Vasaghi A, Yazdizadeh A, Karamifar A. Cephalometry in 14-18 years old girls and boys of Shiraz- Iran high school. Int J Morphol 2009;27:101-4, 9.
11. Del Sol M. Cephalic index in a group of Mapuche individuals in the IX region of Chile. Int J Morphol 2005;23:241-6.
12. Priti A, Nemade PA, Nemade AS. Study of cephalic index in Maharashtra. Int J Biol Med Res 2014;5:4258-60.
13. Setiya M, Tiwari A, Jehan M. Morphometric estimation of cranial index in Mahakaushal region of Madhya Pradesh: Craniometric study. Int J Sci Study 2018;6:143-6.
14. Bharati S, Som S, Bharati P, Vasulu TS. Climate and head form in India. Am J Hum Biol 2001;13:626-34.

Original Article

Morphometric Study of Hard Palate and Its Clinical Correlation

Syed Mubashir Yousuf, Shah Sumaya Jan, Mohd Saleem Itoo, Javed Ahmad Khan, Ghulam Mohammad Bhat

Department of Anatomy Government Medical College, Srinagar, Jammu and Kashmir, India

Abstract

Background: The hard palate is formed by the joining of two palatal processes of the maxilla and two horizontal processes of the palatine bones which are connected to each other by cruciform suture. The hard palate is very essential for articulation and is different for adults and children. For local nerve block, in daily faciomaxillary procedures, the maxillary nerve which is the second division of the trigeminal nerve is mostly anesthetized. Unilateral maxillary anesthesia is greatly achieved by locally anesthetizing the maxillary nerve. This technique is very effective in maxillary surgical approaches or in the case of quadrant dentistry. **Material and Methods:** Fifty dried human skulls were taken from the Department of Anatomy from Government Medical College, Srinagar. The palatine index was noted according to the method given by hasanali and Mwaniki. The distance of various parameters was measured from various bony landmarks of the hard palate: distance between IF and greater palatine foramen (GPF), lesser palatine foramen (LPF), and premaxillary incisive margin and distance between GPF and IMS, LPF, and PTH. The location of GPF with respect to molar teeth was also noted. **Results:** Leptostaphyline was found <79.9, mesostaphyline: 80–84.9, and brachystaphyline. Similarly, various parameters of IF, GPF, and LPF were recorded with the help of vernier caliper. Observation recorded would be helpful to dentists, anatomists anesthetists, and fasciomaxillary surgeons. **Conclusion:** The results obtained in this study can be utilized for ethnic and racial classification of crania and performing certain surgical procedures in hard palate and soft palate.

Keywords: *Hard palate, palatine foramen, vernier caliper*

Introduction

The hard palate is formed by the joining of two palatal processes of the maxilla and two horizontal processes of the palatine bones which are connected to each other by cruciform suture. The hard palate forms the important part of the skull.[1,2] For local nerve block, in daily faciomaxillary procedures, the maxillary nerve which is the second division of the trigeminal nerve is mostly anesthetized. Unilateral maxillary anesthesia is greatly achieved by locally anesthetizing the maxillary nerve. This technique is very effective in maxillary surgical approaches or in the case of quadrant dentistry.[3] The hard palate is very essential for articulation and is different for adults and children.[4] Accessing the terminal location for anesthetic distribution can be done using one of two methods. The high tuberosity and the greater pterygopalatine canal through greater palatine foramen (GPF).[5] The surgical procedures like maxillary sinus augmentation for dental implants in the posterior maxilla rely on accurate prediction and effective block of the maxillary nerve and its branches with a single dose of anesthesia.[6] The incisive fossa is present in the anterior part of the hard palate, in which the incisive canal acts as a channel between oral and nasal cavities and it transmits the nasopalatine nerve. This canal also contains the anastomosis of greater palatine and sephanopalatine arteries.[6]

Materials and Methods

This study was carried out in the Department of Anatomy, Government Medical College, Srinagar, on 50 dry adult human skulls of unknown sex.

The following parameters were recorded using the vernier caliper.

Length

The length was taken from the anteriormost point of the incisive suture positioned in between the dental alveoli of the two

How to cite this article: Yousuf SM, Jan SS, Itoo MS, Khan JA, Bhat GM. Morphometric study of hard palate and its clinical correlation. J Anat Soc India 2025;74:246-9.

Article Info

Received: 05 January 2024
Revised: 25 January 2025
Accepted: 22 April 2025
Available online: 30 September 2025

Address for correspondence:
Dr. Javed Ahmad Khan, Department of Anatomy Government Medical College Srinagar - 190 010, Jammu and Kashmir, India.
E-mail: drjavedkhan2073@gmail.com

Access this article online

Website: https://journals.lww.com/joai

DOI: 10.4103/jasi.jasi_7_24

Quick Response Code:

medial incisors of the upper jaw to the posteriormost point on the posterior nasal spine the staphylion.

Width

Width was taken from the inner margins of dental alveoli of the 2nd molars of the upper jaw that is the endomolaria.

Palatine index

Classification of the palatine index has been done by the method given by hasanali and Mwaniki[7] and is determined by the formula palatine width by palatine length × 100 that is p-width ÷ p-length × 100.[7] The palatine index is expressed in percentage and is equal to the ratio of width to length of the palate.

Palates were classified according to the palatine index into.

- Type 1: This type of palate has narrow width with p.i 80% and is called leptostaphyline
- Type 2: This type of palate has intermediate width with p.i 80%–85% and is called as mesostaphyline
- Type 3: This type of palate has wide width with index > 85% and is called as brachystaphyline.

Incisive fossa

The position of incisive fossa was determined with respect to premaxillary incisive margin (PIM), lesser palatine foramen (LPF), and GPF.

Greater and lesser palatine foramen

The length in between intermaxillary suture and GPF was also measured bilaterally.

Results

The present study was carried out on 51 adult human skulls of unknown sex taken from Department of Anatomy, Government Medical College, Srinagar, for the morphometric study of hard palate study. All parameters were recorded and have been statistically analyzed. The average and standard deviation of all recorded parameters have been calculated and were penned down in tabulated forms.

Categorization

According to the palatal index, 70.58% of the palate were found with a narrow width that is leptostaphyline, 17.64% were found with intermediate width, and 11.76% with wide width and are called as mesostaphyline and brachystaphyline, respectively. The palatal index was calculated by palatal breadth by palatal length × 100 (P.I = $\frac{p-breadth}{p-length}\times 100$).[7] The observations recorded are given in Table 1/Figure 1.

Incisive fossa

As shown in Figure 1/Table 2, the location of the incisive fossa was determined from PIM, from greater palatine formen, and from the LPF by measuring the length from

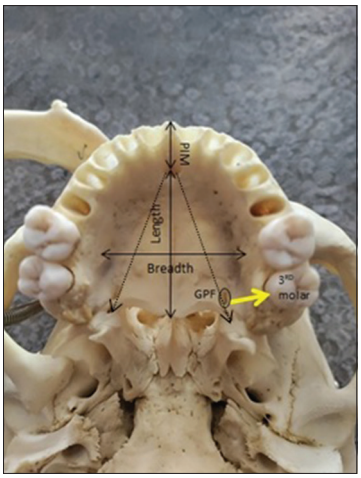

Figure 1: Shows preincisive maxilla, length of palate, breadth of palate, distance between lesser palatine foramen (dotted lines) and location of greater palatine foramen with respect to 3rd molar

Table 1: Distribution of palate as per palatal index

Variant	PI	Quantity (%)
Leptostaphyline	<79.9	36 (70.58)
Mesostaphyline	80–84.9	9 (17.64)
Brachystaphyline	>85	6 (11.76)

PI: Premaxillary incisive

Table 2: The location of incisive fossa with respect to premaxillary incisive margin, greater palatine foramen, and lesser palatine foramen

Parameters measured	Results		
	Range (mm)	Mean±SD (mm)	*P*
Distance from PIM	6–16	10.94±2.52	
Distance from GPF on right side	34–45	40.66±2.88	0.08
Distance from GPF on left side	34–46	39.92±2.77	0.17
Distance from LPF on right side	37–51	43.01±4.37	0.15
Distance from LPF on left side	35–50	42.21±3.83	0.31

PIM: Premaxillary incisive margin, GPF: Greater palatine foramen, LPF: Lesser palatine foramen, SD: Standard deviation

middle of the incisive fossa as follows and is penned down in Figure 2/Table 2.

1. Distance taken from incisive fossa to PIM was noted as "A" mean value of which was found to be 10.94 ± 2.52.
2. Distance taken from right-sided GPF to IF was noted by the letter "B" and by the letter "C."

On left-sided GPF to IF was noted as 40.66 ± 2.88 and 39.92 ± 2.77, respectively. Similarly, "D" and "E" from LPF to IF on the right and left side, respectively, and their values were recorded as 43.01 ± 4.37 and 42.21 ± 3.83, respectively.

Greater palatine foramen

As shown in Figure 2/Table 3, the position of GPF with respect to intermaxillary suture, from the posterior border of the hard palate, from pterygoid hamulus, and from the

posterior nasal spine was determined by measuring the distance between GPF and above said landmarks. Then, the mean distance between the intermaxillary suture to GPF was observed at 17.60 ± 0.93 mm with *P* value of 0.01 on the right side and 17.96 ± 0.79 mm with *P* value of 0.03 on the left side. From the posterior border of the hard palate, the mean distance to GPF on the right and left side was measured as 5.01 ± 1.34 mm with *P* value of 0.47 and 5.03 ± 1.55 with *P* value of 0.94, respectively. 14.37 ± 2.16 mm with *P* value of 0.09 and 14.88 ± 2.51 mm with *P* value of 0.18 were the distances measured from pterygoid hamulus to GPF on the right and left side, respectively. Similarly, distances from the posterior nasal spine on the right and left side to the respective GPF were also determined and were observed as 16.01 ± 2.21 mm with *P* values 0.09 and 16.62 ± 2.30 mm on the respective sides.

In Figure 2/Table 4, the position of GPF has been determined with respect to maxillary molars. It has been found that the 84.31% greater palatine foramina are located in proximity to the 3rd molar, 13.72% lies between the 2nd and 3rd molar whereas only 1.96% lies in proximity to the 2nd molar tooth.

Discussion

According to Williams PL *et al*, The hard palate is an important part of the skull, made up of palatine parts from maxilla and the horizontal plates of the palatine bones. These bones are joined together by a cruciform suture.[8] According to Lammert A *et al*, and Subbaramaiah M *et al,* The most significant changes in the shape of the palate happen in early childhood. Researchers found that the hard palate grows quickly until around 18 months old, by which time it reaches about 80% of its full adult size. After the age of 11, its shape remains mostly unchanged.[9,10] According to Dave *et al*.'s study,[11] 63% of the participants had leptosaphyline, 24% had mesotaphyline, and 13% had brachystaphyline. However, according to Jotania *et al.*'s research,[12] leptosaphyline was the predominant form of palatine index, with mesotaphyline and brachystaphyline having equal values. These studies are in close association with our present study, where we also observed a predominance of leptosaphyline (70.58%), followed by mesotaphyline (17.64%) and brachystaphline (11.76%), respectively. Gujar and Oza[13] found in their study that leptostaphyline, mesostaphyline, and brachystaphyline were 68%, 20%, and 12%, respectively, and these are found to be in close relation to our study, where leptostaphyline was found to be 70.58%, mesostaphyline (17.64%), and brachystaphyline (11.76%). Sarilita and Soames[14] found that small palates (leptostaphyline) accounted for 84% of the skulls, whereas intermediate palates (mesostaphyline) and broad palates (brachystaphyline) made up just 8% of the skulls. Some researchers have found similar results in Indian skulls, with the exception of D'Souza *et al*.,[15] who found that brachystaphyline was somewhat more prevalent than leptostaphyline.

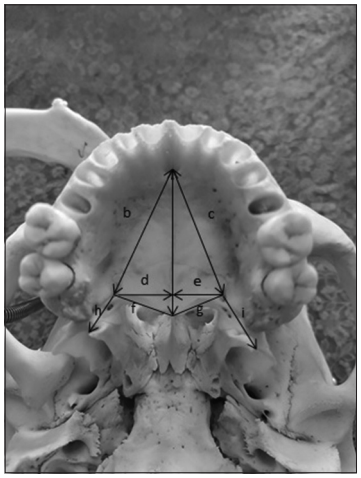

Figure 2: Shows distance between greater palatine foramen and incisive fossa (b and c) on right and left side, mims (mid line intermaxillary suture) on right and left side d and e, gf and posterior nasal spine f and g and h and i distance between pterygoid hammulus and gf

Previous research has demonstrated that the GPF and LPF are located in different places. In their 2019 study, Bahsi *et al*.[16] examined the sites of IF and GPF in a Turkish population and reported statistical variances based on anatomical landmarks: In men, the left IF-GPF measures 32.70 ± 2.99 mm, while in females, it is 31.65 ± 2.5 mm. In females, the right IF-GPF is 31.45 ± 2.26 mm, while in males, it measures 32.43 ± 2.70 mm. There is not really a big difference. Similarly, the location of the IF and GPF in a Korean population was examined by Kang *et al*.,[17] who discovered that the statistical variances from the perpendicular length in the coronal plane between the IF and GPF were 32.04 ± 3.31 mm. Gibelli *et al*.[18] examined into the positions of the incisive IF and GPF in a population from Italy and discovered statistical variances based on a

Table 3: Location of greater palatine foramen from various bony landmarks of hard palate

Location of GPF	Measurements recorded					
	Right side			Left side		
	Range (mm)	Mean±SD (mm)	*P*	Range (mm)	Mean±SD (mm)	*P*
From MMS	16–19	17.60±0.93	0.01	17–19	17.96±0.79	0.03
From posterior border of hard palate	2–9	5.01±1.34	0.47	2–9	5.03±1.55	0.94
From pterygoid hamulus	7–19	14.37±2.16	0.09	6–19	14.88±2.51	0.18
From posterior nasal spine	11–20	16.01±2.21	0.09	12–21	16.62±2.30	0.19

GPF: Greater palatine foramen. SD: Standard deviation, MMS: Middle maxillary suture

Table 4: The location of greater palatine foramen with respect to molars of upper jaw

Position	Right side, *n* (%)	Left side, *n* (%)	Total, *n* (%)
In proximity to 3rd molar	22 (51.16)	21 (48.83)	43 (84.31)
in between 2nd and 3rd molar	4 (7.84)	3 (5.88)	7 (13.72)
In proximity to 2nd molar	1 (1.96)	0	1 (1.96)

variety of anatomical features: the average measurements of the left IF-GPF in males and females are 40.4 ± 2.5 mm, 38.8 ± 2.6 mm, and 40.5 ± 2.6 mm for the right IF-GPF in males and 38.8 ± 2.4 mm for females, respectively. In our study, no significant difference was found in the mean distance from the IF to the right-sided GPF of 40.66 ± 0.08 and the left GPF of 39.92 ± 0.17, respectively, and is almost similar to the findings of Gibelli *et al*.[18] (2017) Sharma *et al*.,[19] in their study, found the locations of IF and GPF in the Indian population and also displayed statistical differences based on some anatomical characteristics. IF-GPF values for the left side are 37.89 ± 2.83 mm, while the right side is 37.74 ± 2.39 mm. Saralaya and Nayak (2007)[20] conducted a study on a population from southern India, examined the IF and GPF locations, and reported statistical variances from several landmarks: in terms of IF-GPF, the left is 37.4 ± 0.301 mm, while the right is 37.2 ± 0.292 mm, and the results of their studies were almost similar.

Financial support and sponsorship

Nil.

Conflicts of interest

There are no conflicts of interest.

References

1. DuBrul EL. Sicher and DuBrul's Oral Anatomy. 8th ed. St Louis: Ishiyaku EuroAmerica; 1988. p. 269-84.
2. Williams PL, Warwick R, Dyson M, Bannster H. Gray's Anatomy. 38th ed. London: Longmans; 1995.
3. Chrcanovic BR, Custódio AL. Anatomical variation in the position of the greater palatine foramen. J Oral Sci 2010;52:109-13.
4. Ahmad Fauzi NQ, Yuvaraj Babu K. Morphometric analysis of the hardpalate. Int J Curr Res 2017;9:57134-5.
5. Malamed SF. Handbook of Local Anesthesia. 4th ed. St Louis: Mosby; 1997. p. 187-91.
6. Lake S, Iwanaga J, Kikuta S, Oskouian RJ, Loukas M, Tubbs RS. The incisive canal: A comprehensive review. Cureus 2018;10:e3069.
7. Kumar P, Lata P, Prasad R. Hard Palate Dimensions in North Indian Adult Skulls: A Morphometric Study. Azerbaijan Pharmaceutical and Pharmacotherapy J 2024;23:1-6.
8. Williams PL, Warwick R, Dyson M, Bannster H. Gray's Anatomy. 37th edition, London, 1989. p. 354.
9. Lammert A, Proctor M, Narayanan S. Morphological variation in the adult hard palate and posterior pharyngeal wall. J Speech Lang Hear Res 2013;56:521-30.
10. Subbaramaiah M, Jagannatha SR, Archana R, Suhas C. Morphometric evaluation of hard palate in Indian male and female skulls. J Human Anatomy 2021;5:1-6.
11. Dave MR, Gupta S, Vyas K, Joshi HG. A study of palatal indices and bony prominences and grooves in the hard palate of adult human skulls. NJIRM 2013;4:7-11.
12. Jotania B, Patel SV, Patel SM, Patel P, Patel S, Patel K. Morphometric analysis of hard palate. Int J Res Med 2013;2:72-5.
13. Gujar SM, Oza SG. Morphometric analysis of hard palate and its clinical importance. Natl J Clin Anat 2018;7:36-40.
14. Sarilita E, Soames R. Morphology of the hard palate: A study of dry skulls and review of the literatur morphology of the hard palate. Rev Argent Anat Clin 2015;7:34-43.
15. D'Souza AS, Mamatha H, Jyothi N. Morphometric analysis of hard palate in South Indian skulls. Biomed Res 2012;23:173-5.
16. Bahsi I, Orhan M, Kervancıoglu P, Yalçın ED. Morphometric evaluation and clinical implications of the greater palatine foramen, greater palatine canal and pterygopalatine fossa on CBCT images and review of literature. Surg Radiol Anat 2019;41:551-67.
17. Kang SH, Byun IY, Kim JH, Park HK, Kim MK. Three-dimensional analysis of maxillary anatomic landmarks for greater palatine nerve block anesthesia. J Craniofac Surg 2012;23:e199-202.
18. Gibelli D, Borlando A, Dolci C, Pucciarelli V, Cattaneo C, Sforza C. Anatomical characteristics of greater palatine foramen: A novel point of view. Surg Radiol Anat 2017;39:1359-68.
19. Sharma N, Varshney R, Ray S. Anatomic and anaesthetic considerations of greater palatine nerve block in Indian population. Saudi J Med Med Sci 2014;2:197-201.
20. Saralaya V, Nayak SR. The relative position of the greater palatine foramen in dry Indian skulls. Singapore Med J 2007;48:1143-6.

Original Article

Morphological Variations of Sacrum and Sacralization of Fifth Lumbar Vertebra with its Clinico-embryological Implications

Pankaj Kumar Rathi, Hem Singh, Shubhi Saini, Pradeep Kumar Gowda, Preeti Goswami, Babita Pangtey, Sabita Mishra

Department of Anatomy, Maulana Azad Medical College, New Delhi, India

Abstract

Aims and Objective: To find the prevalence and incidence of sacralisation and to find any nonfusion of sacral hiatus in the Indian population using a dry bone study. **Introduction:** Sacralization of the fifth lumbar vertebra (L5) is a congenital anatomical variation that can also be acquired due to degenerative changes. It is characterized by the fusion of L5 with the S1 vertebra, resulting in a sacralized L5 or a six-vertebra lumbar spine. Nonfusion of vertebral lamina with the median sacral crest leads to sacral canal defects. **Materials and Methods:** Ninety-six sacra and pelvis dry bones were studied at the Department of Anatomy, Maulana Azad Medical College, New Delhi. **Results:** Six sacra were observed with partial (n = 2) and complete sacralization (n = 4) of L-5 vertebra. An incompletely formed sacral canal was present in 13 sacra, with variable levels of hiatal apex. **Conclusion:** Sacralization of L5 and varied level of hiatal apex clinical significance in certain individuals presenting with low back pain or other related conditions. **Summary:** The prevalence of sacralization of L5 in this study was found to be 6.25%. Sacralization of L5 has been associated with low back pain, altered biomechanics, and increased risk of disc herniation. Knowledge of clinico-embryological aspects of structural variations of the sacrum can help clinicians and surgeons during patient management.

Keywords: *Low back pain, sacral hiatus, sacralization, transitional vertebra*

Introduction

Sacralization of the fifth lumbar vertebra (L5) is a spinal condition where the L5 vertebra fuses with the sacrum.[1] Instead of having five distinct lumbar vertebrae and a separate sacrum, the L5 vertebra is partially or completely fused with the sacrum, resulting in a four-vertebra lumbar spine and a larger sacrum.[2] Sacralization of the L5 vertebra can be identified through imaging tests, and in most cases, it is asymptomatic. However, in some cases, it can cause lower back pain, stiffness, and reduced mobility.[3]

The exact cause of sacralization of the L5 vertebra is unknown, but it is believed to be a developmental anomaly occurring during fetal development.[2] It is more common in males and can occur in both children and adults. While sacralisation of the L5 vertebra may be asymptomatic, it can lead to chronic lower back pain, especially in cases where the fusion of the vertebra is incomplete.[4] In addition, sacralisation of the L5 vertebra can also contribute to other spinal conditions such as spinal stenosis, spondylolisthesis, and disc herniation.[3-5]

The aim of this study was to determine the incidence of sacralisation of dry bones and to observe sacral canal fusion and level and shape of sacral hiatus.

Materials and Methods

This study was conducted after obtaining approval from the Department of Anatomy at MAMC, New Delhi. The study was conducted on a total of 96 dried bones comprising 70 sacra and 26 pelvises, irrespective which were present in the bone bank.

- Inclusion criteria: Un-damaged bones
- Exclusion criteria: Bone with broken/ missing parts.

Bones were manually observed for sacralisation and fusion of sacral canal.

Results

In our study of 96 bones, six sacra were observed with partial (n = 2) and complete sacralization (n = 4) of L-5 vertebra, as shown in Figures 1 and 2 and Table 1.

How to cite this article: Rathi PK, Singh H, Saini S, Gowda PK, Goswami P, Pangtey B, *et al.* Morphological variations of sacrum and sacralization of fifth lumbar vertebra with its clinico-embryological implications. J Anat Soc India 2025;74:250-2.

Article Info

Received: 26 August 2023
Revised: 24 August 2024
Accepted: 18 August 2025
Available online: 30 September 2025

Address for correspondence:
Dr. Preeti Goswami, Department of Anatomy, Maulana Azad Medical College, New Delhi, India. E-mail: drpreetigoswami@gmail.com

Access this article online

Website: https://journals.lww.com/joai

DOI: 10.4103/jasi.jasi_90_23

Quick Response Code:

Incompletely formed sacral canal was present in 13 sacra, with variable levels of hiatal apex [Figure 3 and Table 2].

Discussion

The incidence of sacralisation of the fifth lumbar vertebra (L5) varies depending on the population studied and the diagnostic criteria used.[6-8] In the present study, the incidence of sacralisation was found to be 6.25%. The majority of the explained cases of low back pain, especially in young adults, may be diagnosed and treated, keeping sacralization as one of the etiological factors.[9] The relationship between low back pain and sacralization of lumbar vertebra is very well explained by Bertolotti, 1917. Their reported incidence rate varied widely, ranging from 4% to 30%. This may be due in part to differences in the diagnostic criteria used, as well as variations in the genetic and environmental factors that can influence spinal development.[9]

Figure 1: (a and b) Complete sacralization showing fusion of the transverse processes of L-5 vertebra with alae

Figure 2: Sacralisation-complete in (a and c), partial in (b)

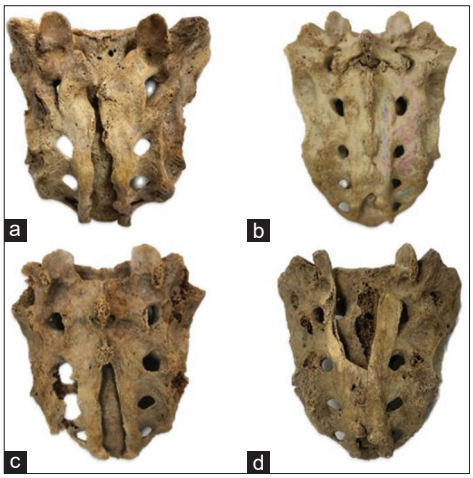

Figure 3: Exposed sacral canal with complete nonunion in (a), partial fusion with v-shaped apex in (b and c), and inverted V-shaped in (d)

The clinical significance of sacralization of the fifth lumbar vertebra (L5) is dependent on the degree of fusion and the presence of any associated spinal conditions. Most common clinical implication of this condition is low back pain, particularly in cases where the fusion is complete. Other conditions like increased risk of developing spondylolisthesis, disc herniation, and spinal stenosis are also reported.[10,11] These conditions can cause pain, numbness, and weakness in the legs and feet, and can significantly impact a person's quality of life.

Development of lumbar vertebrae commences at 3rd week of intrauterine life. All vertebrae originate from somites that form along the cranial-caudal axis, on either side of the notochord, from mesoderm. Somite differentiates into sclerotome and dermatomyotomes. Densely packed cells of sclerotome move cranially opposite the center of myotome, where they form the intervertebral disc.[11,12] The remaining densely packed cells fuse with the loosely arranged cells of immediately caudal sclerotome to form mesenchymal centrum, body of the vertebra. The mesenchymal cells surrounding the neural tube form the neural arch. Ossification of vertebra begins in 8th week and ends by 25th year. The primary cause of sacralization is cranial shift of the last lumbar vertebrae.[11] Shift can be partial or complete, resulting in complete or incomplete sacralisation, respectively.

Hiatal and dorsal wall agenesis of sacrum are not very common findings. Its reported incidence range is 0.98%–4.8%.[12,13] Failure of the lamina of vertebra to

Table 1: Bones with partial and complete sacralization

Type of sacralisation	Total bones
Partial	2
Complete	4

Table 2: Variable degree of hiatal fusion and level of fused hiatal apex are as shown

Shape of hiatus	Total bones
Inverted V-shaped	7
Complete nonfusion	1
Inverted V	3

fuse with the medial sacral crest results in sacral canal anomalies. Defective induction process during notocord development, similar to pathogenesis of spina bifida, possibly due to sonic hedgehog signaling, is cited as an embryological reason for the same.[12,14] Dry human sacral studies have revealed that variations in the shape, length, diameter, and position of the sacral hiatus occur in different races and genders. Normally described as being triangular, the hiatus is stated to consist of an apex and a base. However, a variety of shapes have been documented.[14] These include the inverted "U," inverted "V," M, dumbbell, bifid, and irregular. Total absence of the sacral hiatus has also been reported in cases of congenital malformations of the vertebra, such as spina bifida occulta.[15,16] In this study, the most common shape was inverted V. Out of 96 sacra studied in this study, 14 showed various degrees of nonfusion of the sacral canal. In one sacrum, sacral canal was fully open. Four sacra showed inverted V-shaped sacral hiatus, with apex at S-3.

Conclusion

Overall, the clinical significance of sacralization of the L5 vertebra is dependent on the degree of fusion and the presence of any associated spinal conditions. Treatment options may include pain management, physical therapy, lifestyle modifications, and in some cases, surgical intervention. Nonfusion of sacral canal is although rare, can be implicated in various clinical pathologies.

Financial support and sponsorship

Nil.

Conflicts of interest

There are no conflicts of interest.

References

1. Fischer CR, Ducoffe AR, Errico TJ. Posterior lumbar fusion: Choice of approach and adjunct techniques. J Am Acad Orthop Surg 2014;22:503-11.
2. Athanasakopoulos M, Mavrogenis AF, Triantafyllopoulos G, Koufos S, Pneumaticos SG. Posterior spinal fusion using pedicle screws. Orthopedics 2013;36:e951-7.
3. Lee SM, Lee GW. The impact of generalized joint laxity on the clinical and radiological outcomes of single-level posterior lumbar interbody fusion. Spine J 2015;15:809-16.
4. Cunningham JE, Elling EM, Milton AH, Robertson PA. What is the optimum fusion technique for adult isthmic spondylolisthesis – PLIF or PLF? A long-term prospective cohort comparison study. J Spinal Disord Tech 2013;26:260-7.
5. Takeuchi M, Kamiya M, Wakao N, Hirasawa A, Kawanami K, Osuka K, *et al.* Large volume inside the cage leading incomplete interbody bone fusion and residual back pain after posterior lumbar interbody fusion. Neurosurg Rev 2015;38:573-8.
6. Galimberti F, Lubelski D, Healy AT, Wang T, Abdullah KG, Nowacki AS, *et al*. A systematic review of lumbar fusion rates with and without the use of rhBMP-2. Spine (Phila Pa 1976) 2015;40:1132-9.
7. Liu X, Wang Y, Qiu G, Weng X, Yu B. A systematic review with meta-analysis of posterior interbody fusion versus posterolateral fusion in lumbar spondylolisthesis. Eur Spine J 2014;23:43-56.
8. Park P, Garton HJ, Gala VC, Hoff JT, McGillicuddy JE. Adjacent segment disease after lumbar or lumbosacral fusion: Review of the literature. Spine (Phila Pa 1976) 2004;29:1938-44.
9. Oh HS, Kim JS, Lee SH, Liu WC, Hong SW. Comparison between the accuracy of percutaneous and open pedicle screw fixations in lumbosacral fusion. Spine J 2013;13:1751-7.
10. Makino T, Kaito T, Fujiwara H, Ishii T, Iwasaki M, Yoshikawa H, *et al.* Does fusion status after posterior lumbar interbody fusion affect patient-based QOL outcomes? An evaluation performed using a patient-based outcome measure. J Orthop Sci 2014;19:707-12.
11. Parker SL, Amin AG, Santiago-Dieppa D, Liauw JA, Bydon A, Sciubba DM, *et al.* Incidence and clinical significance of vascular encroachment resulting from freehand placement of pedicle screws in the thoracic and lumbar spine: Analysis of 6816 consecutive screws. Spine (Phila Pa 1976) 2014;39:683-7.
12. Okuda S, Iwasaki M, Miyauchi A, Aono H, Morita M, Yamamoto T. Risk factors for adjacent segment degeneration after PLIF. Spine (Phila Pa 1976) 2004;29:1535-40.
13. Magora A, Schwartz A. Relation between the low back pain syndrome and x-ray findings. 2. Transitional vertebra (mainly sacralization). Scand J Rehabil Med 1978;10:135-45.
14. Liang J, Dong Y, Zhao H. Risk factors for predicting symptomatic adjacent segment degeneration requiring surgery in patients after posterior lumbar fusion. J Orthop Surg Res 2014;9:97.
15. Jones-Quaidoo SM, Djurasovic M, Owens RK 2nd, Carreon LY. Superior articulating facet violation: Percutaneous versus open techniques. J Neurosurg Spine 2013;18:593-7.
16. Oh KW, Lee JH, Lee JH, Lee DY, Shim HJ. The correlation between cage subsidence, bone mineral density, and clinical results in posterior lumbar interbody fusion. Clin Spine Surg 2017;30:E683-9.

Original Article

Unraveling the Mystery of Tensor of Vastus Intermedius: Anatomical Insight and Clinical Implications

Abstract

Introduction: The presence of a small muscle, tensor vastus intermedius (TVI), can sometimes complicate surgical procedures such as knee arthroplasty and quadriceps tendon repair. It is located in the anterior compartment of thigh and assists in extending the knee joint and stabilizing the patella. It has been observed that the description and knowledge regarding the attachments and variability of TVI are lacking in the North Indian population. Hence, the study was planned to identify the presence of TVI muscle in North Indian population, observe its attachments and to classify it into different types. **Materials and Methods:** The dissection was carried out in 34 lower limbs, presence of any additional muscle belly (TVI) was identified, cleared and its attachment traced. Its relation with vastus lateralis (VL) and vastus intermedius (VI) was noted. TVI was classified according to the classification given by Grob *et al*. and was photographed. Findings were recorded and the data were analyzed using the standard statistical techniques. **Results:** TVI was found between VL and VI in 14 lower limbs. Type 1 (Independent type) was seen in 5.88% cases, Type II (VI type) in 23.53%, Type III (VL type) in 8.82% cases, and Type IV (Common type) was seen in 2.94% cases. **Conclusion:** The presence of TVI suggested inter and intraracial variation among various populations in the world. The presence or absence of TVI carries great importance since it has important role in various surgical procedures.

Keywords: *Anterior cruciate ligament graft, quadriceps femoris, tensor vastus intermedius, vastus lateralis*

Seema Gupta, Ajay Kumar, Anshu Soni, Hitant Vohra

Department of Anatomy, Dayanand Medical College and Hospital, Ludhiana, Punjab, India

Introduction

Tensor vastus intermedius (TVI) is a small muscle located in the anterior compartment of the thigh. It originates from the anteroinferior aspect of greater trochanter of femur and inserts into the medial aspect of the base of patella. It assists in extending the knee joint and stabilizes the patella.[1,2] Grob *et al*. studied quadriceps femoris in Swiss population and found the presence of an additional muscle head in between vastus lateralis (VL) and vastus intermedius (VI). This newly discovered muscle was named as tensor vastus intermedius (TVI) according to the nature of muscle fibers, tendon, and aponeurosis. Knowledge of existence of this muscle can help in understanding the common clinical problems. This muscle may go unnoticed in some but in some individuals can cause pain or deformity and hinder in the mechanics of joint movement of lower limb.[2] Patellar instability or patellofemoral pain syndrome can occur due to weakness of VI.[3,4] The presence of this muscle at times can complicate surgical procedures such as knee arthroplasty and quadriceps tendon repair. Orthopedic surgeons should be aware of presence of this muscle to prevent intraoperative complications. In knee injuries such as anterior cruciate ligament (ACL) tear, TVI may be involved. Rehabilitation program targeting strengthening exercises for this muscle may help in stabilizing knee joint and prevent further injury to the joint.[2] It has been observed that the description and knowledge regarding the attachments and variability of TVI are lacking in the North Indian population. Hence, the study was planned to investigate the TVI muscle in the North Indian Population. The purpose of this study was to identify the presence of TVI muscle and to study its attachments. In addition to studying its attachment, an attempt is being made to classify the muscle into different types according to its attachment and relation with VL and VI.

How to cite this article: Gupta S, Kumar A, Soni A, Vohra H. Unraveling the mystery of tensor of vastus intermedius: Anatomical insight and clinical implications. J Anat Soc India 2025;74:253-7.

Article Info

Received: 06 August 2024
Revised: 15 March 2025
Accepted: 04 July 2025
Available online: 30 September 2025

Address for correspondence:
Dr. Seema Gupta, Department of Anatomy, Dayanand Medical College and Hospital, College Campus, Near Dandi Swami Chowk, Ludhiana - 141 001, Punjab, India.
E-mail: seemagarg09@gmail.com

Access this article online

Website: https://journals.lww.com/joai
DOI: 10.4103/jasi.jasi_112_24
Quick Response Code:

Materials and Methods

The present study was conducted after obtaining approval by the Institutional Ethics committee in 2021–2022 (IEC No. 2022-723).17 formalin fixed donated human cadavers were chosen for the study. Out of these 17 cadavers, 15 were male and 2 were female. Cadavers with any previous surgical scar, fatty degeneration, fractures, hematoma, tumors or any other deformity of lower limb were excluded from the study. Lower limbs were studied for the additional muscle tensor vastus intermedius (TVI).

The dissection was carried out in the 34 lower limbs. Cunningham's Manual of Practical Anatomy was followed for the entire dissection procedure.[5] A longitudinal incision was given in front of the thigh from mid inguinal point to the patella. One transverse incision was made in the inguinal region from the anterior superior iliac spine to the pubic tubercle and other was made at the apex of patella. The skin flaps were reflected, superficial fascia was removed and the deep fascia was cleared. The quadriceps muscle was then identified and the components of the muscle were carefully separated by blunt dissection. Sartorius and Rectus femoris (RF) muscle were reflected. VL and VI were cleared [Figure 1]. The presence of any additional muscle belly (TVI) was identified, cleared, and its attachment traced. Its relation with VL and VI was noted. TVI was classified according to the classification given by Grob *et al*. and was photographed.[1] Findings were recorded and the data were analyzed using the standard statistical techniques.

Results

The dissection was carried out in 34 lower limbs (n = 34). TVI was found between VL and VI in 14 lower limbs, 7 on the right side, and 7 on the left side. The attachment of muscle was noted in proximal, middle, and distal parts. Based on its proximal attachment, the muscles were classified into the following four types.

Type 1 (independent type)

In two cases [5.88%, Table 1], muscle took origin from intertrochanteric line and from greater trochanter, but the origin was separable from the VL origin [Figure 1]. One case was typical independent type as the aponeurosis was separable both from VL and VI. In the other case, the mid part could not be separated from VI.

Type II (vastus intermedius type)

In eight cases [23.53%, Table 1], the muscle took origin from VI and the posterior border of TVI was fused with the VI. The anterior border of TVI was free, and posteriorly, the muscle fused with the VI [Figure 2]. The aponeurosis was separable from VL but not from the VI in five cases (Typical VI type). In three cases, in the middle, the aponeurosis was separable from VI and not from VL.

Type III (vastus lateralis type)

In three cases [8.82%, Table 1], the muscle took origin with VL and the origin is inseparable from VL. The aponeurosis was separable from VI but not from VL [Figure 3]. In one case, the aponeurosis was combination of VL and VI type, separable from both VL and VI.

Type IV (common type)

It was seen in one case only [2.94%, Table 1]. The origin of TVI was with VL and VI and the aponeurosis was separable from both the muscles [Figure 4].

In all the 14 limbs distally, the muscle formed a flat aponeurosis and fused with VL, VI, or RF. There was

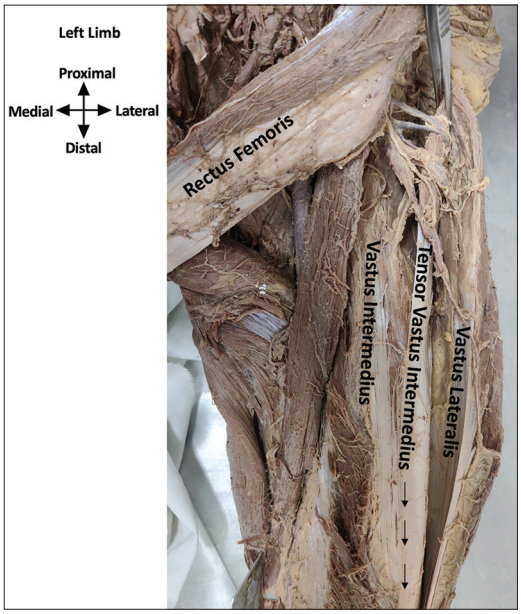

Figure 1: Anterior view of the left thigh showing type I tensor vastus intermedius (TVI). rectus femoris is reflected. TVI is seen to be separate from vastus lateralis

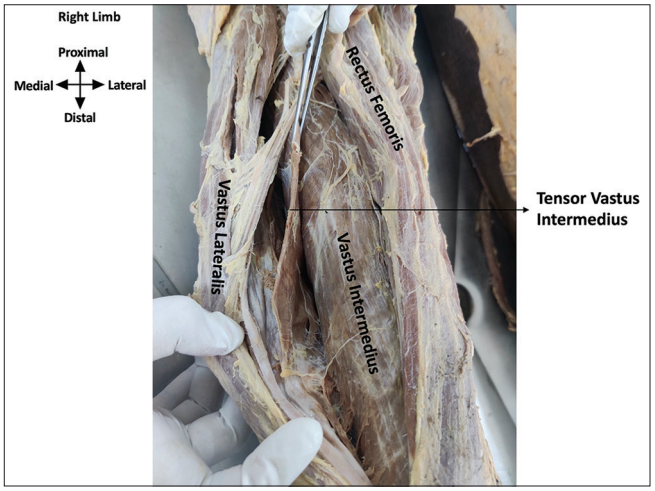

Figure 2: Anterior view of the right thigh. Rectus femoris and vastus lateralis are reflected to show Type II tensor vastus intermedius (TVI). The muscle is held in forceps, the anterior border of TVI is free, and posteriorly, the muscle is fused with the vastus intermedius

a combination of two or all the three muscles and got inserted into the medial part of patella together.

Discussion

The quadriceps femoris is composed of four muscles (VL, VI, RF, and TVI) and functions as the primary extensor of the knee joint. The presence of additional muscle has created interest during research worldwide. The cadaveric study by Willan *et al*. in 1990 on 40 Caucasian cadavers reported an additional muscle lamina between VL and VI in 36% cases but did not name the muscle.[6] The TVI was first described as a new muscle by Grob *et al*. in 2016.[1] Bonnechère *et al*. also in the year 2020 on 20 lower limbs found TVI in 35% cases. The TVI in our study was present in 14 out of 34 limbs (41.18%) [Table 2].[7] A study done by Veeramani and Ganansekaran in 2017 on South Indian population TVI was found in all the 36 sides of the lower extremity.[8] In the present study, the cadavers were all donated bodies from Northern India and the incidence was low (41.18%) [Table 2]. This can be attributed to inter racial variation. In another study by Ogami-Takamura in the year 2021 on Japanese cadavers, TVI was found in all the 35 limbs which were dissected (100%).[9] Olewnik *et al*. in 2020 found additional heads of the Quadratus femoris in 64.1% of the limbs.[4] It means that TVI shows ethnic variation and the morphology of TVI varies from individuals and regions, a fact which has been shown in various studies [Table 2]. Due to the scarcity of voluntarily donated cadavers, we were not able to compare the sex differences between male and females. The human donors in the present study were mainly males (15/17).

Table 1: Results on the basis of classification of tensor vastus intermedius based on its proximal attachment

Type	Number of cases (%)
Type 1 (independent)	2 (5.88)
Type 2 (VI)	8 (23.53)
Type 3 (VL)	3 (8.82)
Type 4 (common)	1 (2.94)
2 muscle bellies	0
Absent TVI	20 (58.8)

VI: Vastus intermedius, TVI: Tensor VI, VL: Vastus lateralis

The classification of muscle according to its attachment and relations to VL and VI also showed variation in ethnicity [Figure 5 and Table 3]. Bonnechère *et al*.[7] found the most common type to be VL (Type 3) in Caucasians, whereas the most common type on South Indian population was independent type in a study by Veeramani and Ganansekaran.[8] The present study on the North Indian population showed type II being the most common type. The inter- and intraracial variation in the presence and attachment of the muscle is thus evident.

During the development of muscles of anterior compartment of thigh, TVI develops from VI. Muscle primordia within different layers of thigh fuse to form single muscle. Some primordia disappear which can explain the different types of TVI. However, the genetic and embryological basis of TVI variations needs further research.[12]

The various researchers suggested that the function of TVI is to stabilize the patella or could help in knee extension.[6,13] Traditionally, quadriceps tendon grafts are used for ACL reconstruction surgery, but in some cases, TVI graft may be used as an alternative.[14-16] The whole muscle can be harvested from the patella and re-implanted as ligament between femur and tibia. TVI being a strong muscle decreases the chances of re-rupture and lowers the risk of graft rejection. Another advantage is that it

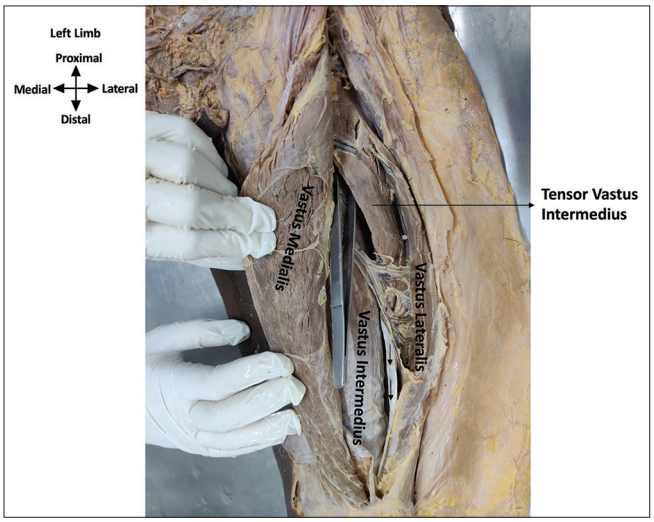

Figure 3: Anterior view of the left thigh showing Type III tensor vastus intermedius (TVI). Vastus medialis is reflected. TVI is inseparable from vastus lateralis but separable from vastus intermedius

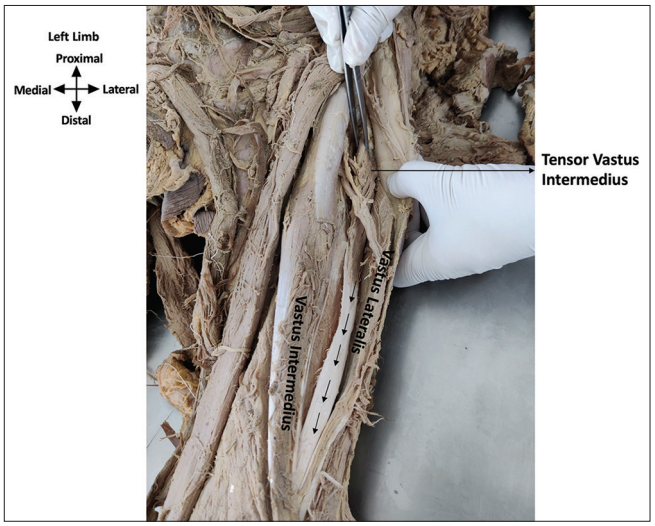

Figure 4: Anterior view of the left thigh showing Type IV tensor vastus intermedius (TVI). The origin of TVI was with vastus lateralis and vastus intermedius

reduces risk of donor site morbidity as TVI harvesting does not require any separate incisions. This results in speedy and less painful postoperative recovery.[17] The major drawback is that the traditional grafts are easy to harvest and have proper shape as compare to TVI which is small and may not be sufficient in patients with severe ACL injuries. TVI grafts can be a good option, but efficacy and safety of the TVI graft are to be explored further.

Limitations of the study

The limitation of the study was that

1. Due to availability of limited number of donated cadavers, the present study on the anatomy of TVI was conducted on 34 lower limbs
2. Out of these 34 lower limbs, only four limbs of female cadavers were there, so the sex differences in the morphology of TVI could not be compared
3. The low incidence could also be attributed to the fact that imaging was not performed due to financial constraints. Further work can combine anatomical studies with advanced imaging techniques.

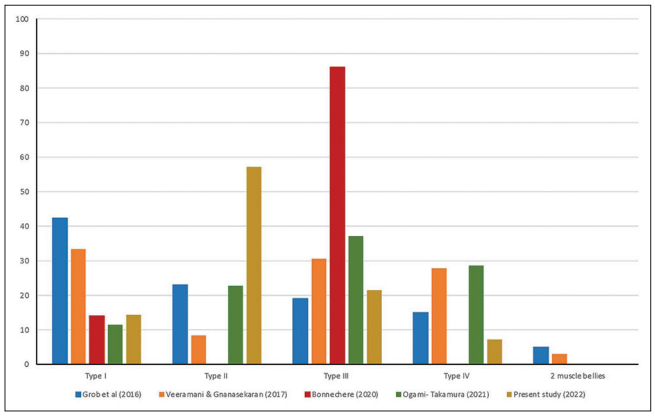

Figure 5: Comparison of classification of TVI based on its proximal attachment between studies

Table 2: Comparison of presence of tensor vastus intermedius in various studies

Author	Population studied	Number of cases studied	Presence of TVI (%)
Grob *et al*., 2016[1]	Swedish	21	100
Rajasekaran and Hall, 2016[10]	American	26	100
Veeramani and Ganansekaran, 2017[8]	South Indian	22	100
Bonnechere *et al*., 2019[7]	Belgian	20	35
Olewnik *et al*., 2020[4]	Polish	23	64.1
Sahinis *et al*., 2020[11]	Greek	24	100
Ogami-Takamura *et al*., 2021[9]	Japanese	25	100
Present study 2022	North Indian	34	41.18

TVI: Tensor vastus intermedius

Conclusion

This study provides valuable insights into the presence, classification, and clinical relevance of the Tensor Vastus Intermedius (TVI) in the North Indian population. The muscle was identified in 41.18% of the dissected lower limbs, with Type II (VI type) being the most common variant. The findings indicate significant inter- and intra-racial variations in the occurrence and morphology of TVI compared to other global populations.

The anatomical presence of TVI is of clinical importance in orthopedic surgeries, particularly in knee arthroplasty, quadriceps tendon repair, and ACL reconstruction. Awareness of TVI can help surgeons to minimize intraoperative complications and optimize rehabilitation strategies for knee stability.

However, due to the limited sample size and lack of imaging-based validation, further studies combining cadaveric dissection with advanced imaging techniques are necessary to better understand the embryological, genetic, and functional significance of TVI. Exploring its potential as a graft alternative in ligament reconstruction could further enhance its clinical relevance.

Acknowledgment

The authors sincerely thank those who donated their bodies to science so that anatomical research could be performed. Results from such research can potentially increase mankind's overall knowledge that can then improve patient care. Therefore, these donors and their families deserve our highest gratitude.

Financial support and sponsorship

Nil.

Conflicts of interest

There are no conflicts of interest.

Table 3: Comparison of Classification of TVI based on its proximal attachment between studies

Type	Grob *et al.* (2016)	Veeramani and Gnanasekaran (2017)	Bonnechere (2020)	Ogami- Takamura (2021)	Present study (2022)
Type I	42.31	33.33	14	11.4	14.29
Type II	23	8.33	0	22.8	57.14
Type III	19	30.56	86	37.1	21.43
Type IV	15	27.78	0	28.6	7.14
2 muscle bellies	5	3	0	0	0

References

1. Grob K, Ackland T, Kuster MS, Manestar M, Filgueira L. A newly discovered muscle: The tensor of the vastus intermedius. Clin Anat 2016;29:256-63.
2. Grob K, Fretz CH, Kuster MS, Gilbey H, Ackland T. Knee pain associated with rupture of tensor vastus intermedius, a newly discovered muscle: A case report. J Clin Case Rep 2016;6:828.
3. Miao P, Xu Y, Pan C, Liu H, Wang C. Vastus medialis oblique and vastus lateralis activity during a double-leg semisquat with or without hip adduction in patients with patellofemoral pain syndrome. BMC Musculoskelet Disord 2015;16:289.
4. Olewnik Ł, Tubbs RS, Ruzik K, Podgórski M, Aragonés P, Waśniewska A, *et al.* Quadriceps or multiceps femoris? Cadaveric study. Clin Anat 2021;34:71-81.
5. Koshi R. Cunningham's Manual of Practical Anatomy. 16th ed., Vol. 1. New York: Oxford; 2016.
6. Willan PL, Mahon M, Golland JA. Morphological variations of the human vastus lateralis muscle. J Anat 1990;168:235-9.
7. Bonnechère B, Louryan S, Feipel V. Triceps, quadriceps or pentaceps femoris? Need for proper muscle definition. Morphologie 2020;104:77-84.
8. Veeramani R, Gnanasekaran D. Morphometric study of tensor of vastus intermedius in South Indian population. Anat Cell Biol 2017;50:7-11.
9. Ogami-Takamura K, Saiki K, Endo D, Murai K, Nishi K, Okamoto K, *et al.* Gross anatomical investigation of the muscular head between the vastus lateralis and intermedius in the Japanese population: A cadaver study. Anat Sci Int 2021;96:231-8.
10. Rajasekaran S, Hall MM. Sonographic appearance of the tensor of the vastus intermedius. PM R 2016;8:1020-3.
11. Sahinis C, Kellis E, Ellinoudis A, Dafkou K. *In vivo* assessment of the tensor vastus intermedius cross-sectional area using ultrasonography. Muscles 2020;10:416.
12. Utsunomiya N, Kodama R, Yamaguchi Y, Tsuge I, Yamada S. The development of the tensor vastus intermedius during the human embryonic period and its clinical implications. J Anat 2021;239:583-8.
13. Franchi T. Tensor vastus intermedius: A review of its discovery, morphology and clinical importance. Folia Morphol (Warsz) 2021;80:792-8.
14. Crall TS, Gilmer BB. Anatomic All-inside anterior cruciate ligament reconstruction using quadriceps tendon autograft. Arthrosc Tech 2015;4:e841-5.
15. Geib TM, Shelton WR, Phelps RA, Clark L. Anterior cruciate ligament reconstruction using quadriceps tendon autograft: Intermediate-term outcome. Arthroscopy 2009;25:1408-14.
16. Lee JK, Lee S, Lee MC. Outcomes of anatomic anterior cruciate ligament reconstruction: Bone-quadriceps tendon graft versus double-bundle hamstring tendon graft. Am J Sports Med 2016;44:2323-9.
17. Lobb R, Tumilty S, Claydon LS. A review of systematic reviews on anterior cruciate ligament reconstruction rehabilitation. Phys Ther Sport 2012;13:270-8.

Original Article

Do we have a Dorsal Venous Arch on the Dorsum of the Hand?

Amjad T. Shatarat[1,2], Islam A. Altarawneh[2], Amneh F. Alnsour[3], Malak S. Alessa[3], Sallam Atallah Jaafreh[3], Haya J. Yanes[3], Ala'a M. Alsukhni[4], Muna A Salameh[5], Sara S. Elmegarhi[6], Darwish H Badran[2,7]

[1]Aqaba Medical Sciences University, Aqaba, Departments of [2]Anatomy and Histology and [3]School of Medicine, University of Jordan, [7]Ibin Sina University for Medical Sciences, Amman, [4]School of Medicine, Jordan University of Science and Technology, Irbid, [5]School of Medicine, Al Balqa Applied University, Al Salt, Jordan, [6]Department of Anatomy and Embryology, University of Tripoli, Tripoli, Libya,

Abstract

Aim: The dorsal venous arch is a well-known used anatomical term, however, looking over many anatomical texts it gives that there is no complete consensus on the naming of the dorsal veins on hand as an arch or a network of veins. Therefore, the aim of the present study was to revisit the superficial veins on the dorsum of the hand to identify the dorsal venous arch of the hand. The presence of a dorsal venous arch on the dorsum of the hand has been a subject of debate among anatomists and clinicians. The aim of the present study is to investigate the existence and anatomical characteristics of a dorsal venous arch in the hand. The study will involve a comprehensive review of existing literature, anatomical dissections, and imaging techniques to examine the venous network on the dorsum of the hand. The primary objective is to determine whether a consistent and well-defined dorsal venous arch can be identified. In addition, the present study aims to explore potential variations in the anatomy of the dorsal venous arch, including its location, and connections to other venous structures. The findings from this research will contribute to a better understanding of hand anatomy, potentially aiding in clinical procedures such as venous access, reconstructive surgeries, and micro vascular procedures. **Materials and Methods:** Using the infrared vein illuminator, 804 hands of students and staff members of the Hashemite University in Jordan were initially examined. Only 540 hands were included in the final analysis. The possible horizontal connections between the superficial veins of the dorsum of the hand were described as anatomical patterns. **Results:** Four different patterns were recognized; 75% of the studied veins were not connected at all, 12% showed a connection between only two veins, and 12% of the hands showed no specified pattern. A connection between all superficial veins of the dorsum of the hand and the digital veins of the thumb and little finger was found in a negligible percentage of < 1%. **Conclusion:** Different anatomical patterns were given away in this study indicating that there is an interruption in the formation of a venous arch on the dorsum of the hand in the majority of the population's hands tested in this study. In conclusion, this study has revealed that there is a lack of a consistent and well-formed dorsal venous arch on the dorsum of the hand in the majority of individuals tested. The findings indicate that there are various anatomical patterns and interruptions in the formation of this venous arch. These results highlight the variability and complexity of hand anatomy, suggesting that clinicians should be aware of these variations when performing procedures such as venous access or reconstructive surgeries. Further research is needed to better understand the underlying factors contributing to these anatomical differences and their potential implications for clinical practice.

Keywords: *Access, arch, dorsal, metacarpal veins, network, venous*

Introduction

The superficial veins on the dorsum of the hand have high clinical importance hence they are used in everyday clinical practice worldwide.[1-3] The dorsal veins on hand are anatomically variant,[4] but there is limited data about the morphological picture of these dorsal veins

Some would simply refer to it as a dorsal venous arch,[5] another one describes the veins in a more complex way as a network formed by the union of three dorsal metacarpal veins (DMVs) in which the dorsal veins drain into a network of veins against the metacarpals.[6] This was in censuses with the description in Standring's book which mentions that there are oblique branches that connect the dorsal and palmar digital veins into three DMVs to form a dorsal venous network over the metacarpal bones.[4]

In a previous study, the course of the DMVs and all possible anatomical patterns formed by these veins were described.[7] It came to our attention that DMVs rarely connect horizontally but rather they were running vertically on both radial and ulnar sides of the dorsum of the hand to give rise to the

How to cite this article: Shatarat AT, Altarawneh IA, Alnsour AF, Alessa MS, Jaafreh SA, Yanes HJ, *et al.* Do we have a dorsal venous arch on the dorsum of the hand? J Anat Soc India 2025;74:258-62.

Article Info

Received: 02 January 2024
Revised: 01 August 2025
Accepted: 11 August 2025
Available online: 30 September 2025

Address for correspondence:
Prof. Amjad T. Shatarat, Aqaba Medical Sciences University, Aqaba, Jordan. Department of Anatomy and Histology, School of Medicine, University of Jordan, Amman, Jordan.
E-mail: a.shatarat@ju.edu.jo

Access this article online

Website: https://journals.lww.com/joai

DOI: 10.4103/jasi.jasi_2_24

Quick Response Code:

cephalic and basilic veins respectively. This observation has also been reported in Gray's anatomy which described the origin of the cephalic and basilic veins as radial and ulnar groups of veins on corresponding sides of the hand.[4] These observations have raised questions about the very existence of the dorsal venous arch DVA of the hand. A thorough literature review about the DVA of the hand was carried out which has shown that the DVA of the hand is an overlooked structure. It has been mentioned only as the origin of both cephalic and basilic veins but there was no proper anatomical description for it.

One cross-sectional (cadaveric) study was conducted about the DVA, however, it was more to assess the length of the DVA of the hand, diameter, and thickness of cephalic and basilic vein, rather than to describe the morphology of the DVA.[8] Another study to describe the DVA in Colombia showed that the DMVs are formed near the metacarpal head, but do not always unite closely to form a closed venous arch.[1]

Clinically, the DMVs are preferentially cannulated with cubital veins and.[9,10] As they are easily palpated against the metacarpal bones they were the first choice for cannulation in pediatric groups.[11] In a study on obstetric patients, the DMVs were associated with a higher first-time cannulation success rate compared to those in the cubital fossa.[10] In addition, DMVs were recommended as the primary cannulation site for patients with chronic kidney disease.[12] The veins of the dorsum of the hand have also received considerable attention in computer science as a putative biometric parameter in recognition of each individual based on his DMVs patterns.[13,14]

Despite its location in an area of clinical value, especially, in venous access, the DVA has not gained considerable attention. Therefore, the present study aimed to revisit the superficial veins on the dorsum of the hand to identify the dorsal venous arch of the hand.

Indeed, infrared (IR) thermography has been extensively utilized in venous visualization, such that the potential of its use in standard medical practice has been investigated. Whether vein imaging is conducive to pediatric venipuncture is the subject of conflicting reports (Hess; Rothbart *et al*.).[19,20] However, a growing body of evidence supports the utility of vein imaging in a clinical setting (Katsogridakis *et al*.; Hess; Chapman *et al*.; Kim *et al*.).[19,21-23]

There are other techniques for identifying the superficial veins on the dorsum of the hand such as transillumination, vein contrast enhancers, handheld Doppler ultrasound, etc., ultrasound guided venepuncture has been described for placement of central venous lines via peripheral veins.[3] However, using IR vein illumination offers several advantages over traditional techniques for identifying veins for instance, less dependency on external lighting, less operator skill required, as well as noninvasive and painless.

Materials And Methods

Participants

Initially, 402 students and staff members of ages ranging 18–35 years were consecutively enrolled in this study from the School of Medicine at the Hashemite University, Jordan. A total of 804 hands were examined. Exclusion criteria included high hair density, injuries, scars, burns, and cutaneous lesions on the dorsum of the hand. Written consent was a prerequisite for participation in the study and the study was approved by the Institutional Review Board (IRB) of the Hashemite University (IRB No. P. 0/222/1704841).

Experimental setup

The IR vein illumination system (Sure vein ZDJM-260-01) (Infrared Venous Displayer belong to class 1 type 2, have CE ISO, china) has been used to identify all the superficial veins on the dorsum of the hand. It utilizes 750–980 nm wavelength of IR light (this wavelength does not reach deeply located arteries) with an effective distance of projection of 29–31 cm.

The methods employed to enhance visualization constituted two independent study arms consisting of unique individuals (i.e. participants were assigned to one study arm only). Participants were asked to clench their fists. Participants were asked to grasp the enhancer component of the near- IR light device. The light was directed to a target area on the dorsum of the hand. The adjustable neck of the bracket was used to manipulate light coverage on the target area. The room was dark.

Study protocol

The procedure was conducted in a dark room with a temperature between 24°C and 26°C. On the day of the experiment, participants were asked to sit and remain in a seated position for a period of 5 min, which was the duration of the experiment. Participants were then instructed to grip the transmitter device while the forearm was in a pronated position. Before exposing the hand to the IR beam, the examined area was carefully identified. The identified area extended distally to the flexed second, third, fourth, and fifth metacarpophalangeal joints (MPJs) while proximally it was identified by the wrist joint. Medially, an imaginary line parallel to the medial side of the fifth MPJ was taken and another imaginary line from the lateral side of the second MPJ was considered the lateral boundary. The adjustable neck of the bracket was used to focus the IR beam on the examined area. The veins appeared dark blue on the dorsum of the hand. These veins were carefully examined for any horizontally running veins. For all participants, images were then captured for the examined area using a digital camera. Images were serially numbered and stored in Joint Photographic Experts Group (JPEG) file format. The

same procedure was conducted for each hand in the same participant.

Evolving classification for collected data

The DMVs on the dorsum of the examined hands were traced from MPJs to the wrist joint. Detected veins were categorized based on the presence or absence of horizontal or curved connection between any of the veins (venovenous anastomoses) on the dorsum of the hand in the examined area. Several patterns were seen and described below. The morphology of each pattern was represented by prominent veins; smaller veins were disregarded.

Statistical analysis

Data analysis was performed using IBM SPSS Statistics version 22 software (IBM Corp., Armonk, NY, USA). $P < 0.05$ was considered to indicate a statistically significant difference.

Results

Three hundred and twenty-four subjects were included in the final study analysis from the initial 402 participants, 171 were males and 153 were females. 540 hands were analyzed; there were 252 female hands and 288 male hands [Table 1]. The participants were all from the same ethnicity (Arab). The analyzed hands were put into four categories: A, B1, B2, and C [Figure 1]. The Categorization [Figure 1] was based on the presence or absence of a direct connection between any of the medial, middle, and lateral metacarpal veins.

Category A: no connection between the medial, middle and lateral DMVs. This was observed in 407 hands, 189 were females and 218 were males [Figure 2a and b]. Category B1: there was a connection only between two metacarpal veins [Figure 2c and d]; this was observed in 62 hands, 30 were females and 32 were males. Category B2: a direct connection exists between the three metacarpal veins and the connection ended up in the basilic and cephalic veins which comprised a venous arch [Figure 2e and f]. This was observed only in six hands. Two of them were females and four were males. The two venous arches observed in the aforementioned females were unilateral and on the left hand. Regarding the male subjects, two of the venous arches found were unilateral and on the left hand in each subject, the other two venous arches were bilateral and observed in the same subject. Category C: no specified pattern of connection or complicated networks of DMVs were put in category C [Figure 2g-i]; this category was comprised of 65 hands, 31 females and 34 males.

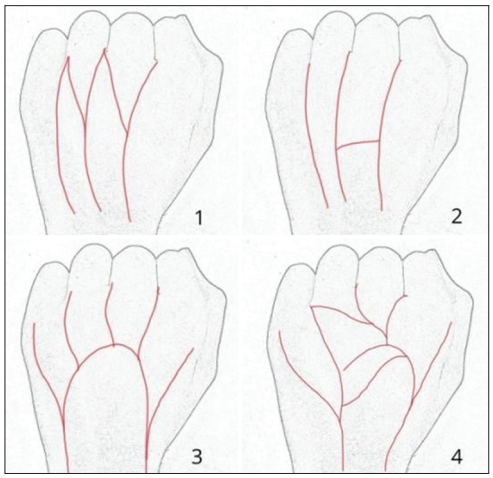

Figure 1: Simplified illustration of categorization of dorsal metacarpal veins (DMVs). (1) no direct horizontal connection between DMVs representing category A. (2) Connection between two DMVs only which represents category B1. (3) Connection between the three DMVs representing category B2. (4) DMVs forming a complicated network or a nonspecified pattern which represents category C

Discussion

It is well established that cephalic and basilic veins originate from the lateral and medial sides of the dorsal venous arch of the hand, respectively.[2,4,15] Though it was noticed, while studying the DMVs on the dorsum of the hand and the origin of the cephalic vein, that the most DMVs on the dorsum of the hand do not seem to form an arch but rather they tend to run in vertical lines from the level of MPJs and run back to the level of the wrist joint. Therefore, this study has been designed to look for the presence of DVA in the hand. The first question come to our minds was at which level to look for the DVA? Does

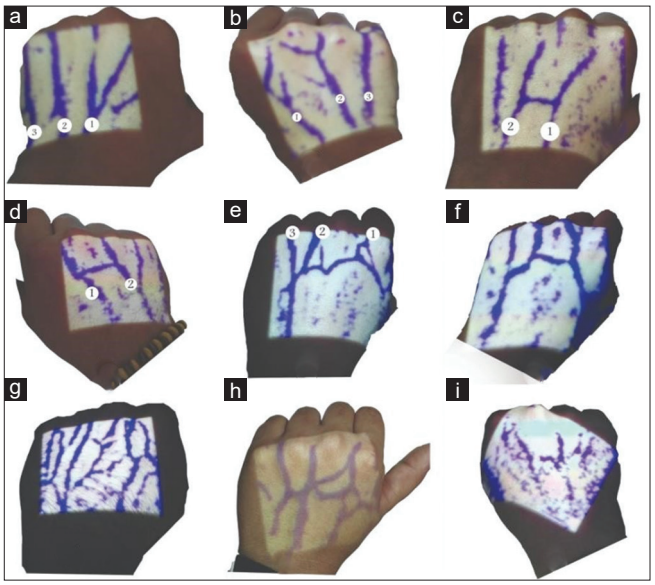

Figure 2: (a and b) Category A; (a) a left hand showing dorsal metacarpal veins (1-3) with no direct horizontal connection, (b) a right hand showing dorsal metacarpal veins (1-3) with no direct horizontal connection. (c) A left-hand representing category B1 showing horizontal connection between two metacarpal veins (1 and 2). (d) A right hand, also represents category B1, showing horizontal connection between two metacarpal veins (1 and 2). (e) The three metacarpal veins (1-3) are connected horizontally and drain into the basilic and cephalic veins forming a venous arch which represents category B2. (f) Another example on category B2 (venous arch). Hands in (g-i) represent category C and show the dorsal metacarpal veins forming a network pattern or a pattern that can't be otherwise specified

Table1: The counts and percentages of venous arch categories in males and females

Category	Female		Male		Total (female and male)	
	Count	Percentage of the same category	Count	Percentage of the same category	Count	Percentage
A. Veins are not connected	189	46	218	54	407	75
B1. Only two veins are connected	30	48	32	52	62	12
B2. Veins are connected in a shape of an arch	2	33	4	67	6	1
C. Veins are connected in a network shape otherwise nonspecified	31	48	34	52	65	12
Subtotal	252	47	288	53	540	

it form an arch at level of the MPJs? Or is it near the level of the wrist joint as it gives origin to both cephalic and basilic veins? Or the arch could be found in the middle of the dorsum of the hand?

The anatomical presentation of the dorsal veins of the hand in textbooks and many previous studies demarcated that the dorsal veins of the hand as a network of veins without concentrating on its clear morphological image as an arch compared to arterial arches of the hand for example.[4,6,16]

Susan Standring described the dorsal veins as a network of veins against the metacarpal bones formed by the union of three DMVs which are joined on the lateral side by a dorsal digital vein from the index finger and dorsal digital veins of the thumb and continue as cephalic vein and on the medial side joined by a dorsal digital vein from little finger, which finally drains into the basilic vein, while in the same book the author describes the arterial blood supply to form a shape of an arch on either the dorsal or palmer surfaces.[4] In addition, Susan Standring mentioned that digital veins bend as they reach the level of MPJs forming diagonal veins which join the next diagonal vein of the following digital vein.[15] Therefore, in the current study, we assumed that the veins over the level of MPJs are not representing the DVA but rather diagonal veins.

This definition was matched with a study by Tanjea *et al*. It was reported that the formation of the DVA of the hand was assembled by fusion of the dorsal digital vein of the fifth finger, three metacarpal veins, and digital vein of the thumb.[16]

The venous arrangement was simply termed as a dorsal venous arch lying proximal to the MPJs;[5] this definition was not in accordance with some articles and textbooks which described it as a network of veins rather than an arch.

We have also carefully reviewed the literature in search of the formation of DVA near the wrist joint. Most articles were already described at this level (at the level of the wrist joint) as the origin of the cephalic and basilic veins but not the DVA. This made us conclude that the DVA has been formed above this area (wrist joint) hence it participates in the formation of the cephalic and basilic veins. Furthermore, in a preliminary study, we noticed that the cephalic vein was formed in the anatomical snuffbox.[17] Therefore, we have adopted that the DVA of the hand should be above the wrist joint since most articles indicate that the level of snuffbox and the wrist joints are the origins of the cephalic and basilic veins.

Our results have shown that DMVs on the dorsum of the hand are rather running vertically with occasional horizontal connections between them. Four anatomical patterns were found based on the horizontal connections between DMVs. The first pattern (A) comprised the majority of the studied hands. There was no connection between the DMVs. This was observed in 407 hands; 189 were females and 218 were males. Three other patterns were recognized but comprised only 25%. In the second group, a connection between only two metacarpal veins was found to form 12% of the studied hands. While in the third group, six hands of all the hands studied were found to have a connection between the three metacarpal veins and that connection ended up in the basilic and cephalic veins accounting for only 1% of the population. The hands in group C showed no specified pattern of connection between DMVs; this group formed 12% of the studied hands.

These results are indicating that the so-called DVA of the hand as anatomical structure seemed to be nonexistent. These results were not surprising for us because the veins of the dorsum of the hand as a whole were overlooked. Our previous works were among the first articles[7,18] to study the DMVs of the hand in detail and it was essential to find the so-called DVA as a reference point, which was confusing due to the contradictory information about it in the literature. To claim that the DVA does not exist, we should declare that the DVA we were looking for is not the one described in the literature as a connection around the MPJs. We did not find any structure that looks like an arch on the dorsum of the hand between the MPJs and the wrist joint.

We do not know why there was this assumption about the presence of DVA on the dorsum of the hand but we can offer an explanation as to why there was confusion about it. Looking at the foot, there is a real dorsal venous arch[16] and it is always tempting to compare the upper and lower limbs, especially, due to the resemblance between the origin of the superficial veins of the lower and upper limbs from the venous arches. However, there is a big difference between

the foot and the hand in terms of their functions. The thumb is an active part of the hand and it has its muscles, nerves, arteries, and veins. Therefore, the veins of the thumb and the index usually run vertically and laterally to form a lateral group of veins which gives rise to the cephalic vein while the other fingers drain medially to form the basilic vein. These two groups do not seem to communicate horizontally, and therefore, there is no DVA on the hand. However, in the foot, the big toe does not function differently from other toes as the whole foot is designed for walking. Thus, veins coming from the toes tend to arch as they drain the toes.

Anatomic variations are immensely consequential in clinical practice; a great many iatrogenic diseases occur as a result of surgical injury to variant anatomic structures (Ogeng'o 2013); for instance, venipuncture-induced causalgia may be precipitated by variant relationships between superficial veins and cutaneous nerves, in concert with venipuncture failure (Horowitz 2000). On that account, investigation of anatomic variations cannot be classified as ''blue-sky'' research; rather, it is germane to surgical and medical outcomes.

Conclusion

The present study has shown that we do not have an anatomical structure called the dorsal venous arch on the dorsum of the hand. Veins on the dorsum of the hand can form four patterns based on their horizontal connections, but they do not form an arch. These findings have an anatomical value as they describe overlooked veins on the dorsum of the hand and a clinical value as it is an area commonly used for venous access.

Financial support and sponsorship

Nil.

Conflicts of interest

There are no conflicts of interest.

References

1. CORZO GEG, GÓMEZ OLD, SERRANO SG, SAAVEDRA MM, DÍAZ JJJ. Anatomical Description of the Dorsal Venous Arch of the Hand in a Population Sample of Bucaramanga, Colombia. Int. J. Morphol., 2020;38:109-113. Available from: http://dx.doi.org/10.4067/S0717-95022020000100109. [Last accessed on 2023 Nov 11].
2. Lee SH, Chun KJ, Lee DS, Lee SY, Hwang J, Chon MK, *et al.* Right cardiac catheterization using the antecubital fossa vein in Korean patients. Korean Circ J 2016;46:207-12.
3. Mbamalu D, Banerjee A. Methods of obtaining peripheral venous access in difficult situations. Postgrad Med J 1999;75:459-62.
4. Standring S. Gray's Anatomy. The Anatomical Basis of Clinical Practice. 41st ed. New York: Elsevier; 2016. p. 890.
5. Wineski LE. Snell's clinical anatomy by regions, 10e. Lippincott Williams & Wilkins, a Wolters Kluwer business. 2019. p. 384.
6. Moore KL, Dalley AF, Agur AM Clinically Oriented Anatomy. 7th ed. Madrid: Médica Panamericana; 2014.
7. Elmegarhi SS, Amarin JZ, Hadidi MT, Badran DH, Massad IM, Bani-Hani AM, *et al*. Dorsal metacarpal veins: Anatomic variation and potential clinical implications. Anat Sci Int 2018;93:238-43.
8. Tiwari N, Budhathoki D, Shrestha I, Timsina R, Shah SK, Malla BK. Morphology of Dorsal Venous Arch of Hand: A Cadaveric Study. J College of Med Sciences-Nepal, 2019;15:139-143. Available from: https://doi.org/10.3126/jcmsn.v15i2.23294. [Last accessed on 2023 Dec 11].
9. Cole TJ. Too many digits: The presentation of numerical data. Arch Dis Child 2015;100:608-9.
10. Tan PC, Mackeen A, Khong SY, Omar SZ, Noor Azmi MA. Peripheral intravenous catheterisation in obstetric patients in the hand or forearm vein: A randomised trial. Sci Rep 2016;6:23223.
11. King C, Henretig FM. Textbook of Pediatric Emergency Procedures. Philadelphia, PA: Lippincott Williams and Wilkins; 2008.
12. Dougherty L. Peripheral cannulation. Nurs Stand 2008;22:49-56.
13. Egan G, Healy D, O'Neill H, Clarke-Moloney M, Grace PA, Walsh SR. Ultrasound guidance for difficult peripheral venous access: Systematic review and meta-analysis. Emerg Med J 2013;30:521-6.
14. Nandini C, Ashwini C, Aparna M, Ramani N, Kini P, Sheeba K. Biometric authentication by dorsal hand vein pattern. Int J Eng Technol 2012;2:837-40.
15. Sadeghi A, Setayesh Mehr M, Esfandiari E, Mohammadi S, Baharmian H. Variation of the cephalic and basilic veins: A case report. J Cardiovasc Thorac Res 2017;9:232-4.
16. Taneja C, Younus M, Howale D. The study of dorsal venous arch of hand in living adult males in Udaipur district of Raasthan. Int J Curr Res Rev 2012;4:89.
17. Salameh MA, Shatarat AT, Badran DH, Abu Abeeleh MA, Kanaan TM, Bani-Hani AM, *et al*. Revisiting the anatomy of the cephalic vein, its origin, course and possible clinical correlations in relation to the anatomical snuffbox among Jordanian. Folia Morphol (Warsz) 2021;80:344-51.
18. Salameh MA, Shatarat AT, Badran DH, Abu-Abeeleh MA, Massad IM, Bani-Hani AM. The best vein to be accessed based on descriptive study of dorsal metacarpal vein. Anat Cell Biol 2019;52:390-6.
19. Hess HA. A biomedical device to improve pediatric vascular access success. Pediatr Nurs 2010;36:259-63.
20. Rothbart A, Yu P, Mu Nachtigall I. Peripheral intravenous cannulation with support of infrared laser vein viewing system in a pre-operation setting in pediatric patients. BMC Res Notes 2015;9:463.
21. Katsogridakis YL, Seshadri R, Sullivan C, Waltzman ML. Veinlite transillumination in the pediatric emergency department: A therapeutic interventional trial. Pediatr Emerg Care 2008;24:83-8.
22. Chapman LL, Sullivan B, Pacheco AL, Draleau CP, Becker BM. VeinViewer-assisted intravenous catheter placement in a pediatric emergency department. Acad Emerg Med 2011;18:966-71.
23. Kim MJ, Park JM, Rhee N, Je SM, Hong SH, Lee YM, *et al.* Efficacy of VeinViewer in pediatric peripheral intravenous access: A randomized controlled trial. Eur J Pediatr 2012;171:1121-5.

Review Article

A Systematic Review of Y Chromosome Conservation Across Vertebrates: Mechanisms and Evolutionary Implications

Sanjeev Kumar Jain, Vishram Singh[1], Sonika Sharma, Piyush Kumar

Department of Anatomy, TMMC and RC, Teerthanker Mahaveer University, Moradabad, Uttar Pradesh, [1]Department of Anatomy, Kasturba Medical College, Mangalore, Manipal Academy of Higher Education, Manipal, Karnataka, India

Abstract

Background: The Y chromosome has a much smaller effective population size—being present at only about one-quarter the frequency of autosomes—and, because selection acts on the chromosome as a whole rather than on individual genes, it is more prone to the accumulation of deleterious mutations and progressive genetic deterioration. While beneficial alleles may be lost if they arise on a degenerated Y chromosome, harmful mutations may be repaired by genetic hitchhiking. **Aim:** Sequence conservation, pseudoautosomal areas, gene duplication, and dosage compensation mechanisms are among the genetic and epigenetic elements that affect Y chromosome conservation in animals. Structural changes, repetitive sequences, and extensive regions of heterochromatin contribute to the instability and gradual degeneration of the Y chromosome. Y chromosome studies should be examined for methodological flaws and research gaps in order to inform future studies on the evolution of vertebrate sex chromosomes. **Methodology:** According to Page *et al*. (2021), this systematic review adheres to the Preferred Reporting Items for Systematic reviews and Meta-analyses 2020 guidelines. Randomized, observational, and laboratory studies, as well as meta-analyses, have investigated Y chromosome conservation across various animal and vertebrate species. Excluded will include review studies, case reports, observational studies, and randomized controlled trials that employ human evaluation. Seven hundred thirty-one records in total were initially acquired, 674 of which were from PubMed databases and the remaining 57 from other sources, such as websites and other databases. After fulfilling the inclusion requirements, 14 studies were ultimately selected for the systematic review. **Results:** Different Y chromosome evolutionary trends among animals are shown by comparative genomic investigations. Fish and amphibians display gradual degeneration, but primates display conservation of Y-linked genes. Studies on reptiles and birds emphasize the structural dynamics of the sex chromosome. Results cast doubt on linear gene degradation models, highlighting the role of evolutionary limitations, functional retention, and selective pressures in the evolution of the Y chromosome in vertebrates. **Conclusion:** Elucidation of sex chromosome evolution demands a comprehensive phylogenomic analysis of Y chromosome in vertebrates, including fish, birds, reptiles, amphibians, and mammals.

Keywords: *Phylogenomic analysis, vertebrates, Y chromosome*

Introduction

Background

Muller's[1] hypothesis that the X and Y chromosomes originated from a homologous pair of autosomes initiated the study of sex chromosome evolution, which has garnered significant interest for over a century. He hypothesized that the chromosomes of the pair created a testis-determining factor, which made sex-specific genes cluster around this newly found area. Recombination suppression was preferred to preserve such sex-linked genes. Failure of selection and genetic drift (Muller's ratchet) leads the Y chromosome to deteriorate if recombination does not occur.[2] Selection acting at the level of the whole chromosome instead of specific genes and smaller effective population size of the Y chromosome – only present at some fraction of autosomal frequency – add to such deterioration. Harmful mutations may become fixed through genetic hitchhiking, while advantageous alleles could be lost if they emerge on a deteriorated Y chromosome.[3] In addition, the Y experiences higher mutation rates due to the increased number of cell divisions in the testis. Consequently, the progressive loss of genes and degeneration of the Y chromosome (or the W chromosome in ZW systems) has occurred over time.[2,4] Comparative genomics, which shows that the sex chromosomes in a single vertebrate

How to cite this article: Jain SK, Singh V, Sharma S, Kumar P. A systematic review of Y chromosome conservation across vertebrates: Mechanisms and evolutionary implications. J Anat Soc India 2025;74:263-77.

Article Info

Received: 03 April 2025
Revised: 25 May 2025
Accepted: 29 August 2025
Available online: 30 September 2025

Address for correspondence:
Dr. Sonika Sharma, Department of Anatomy, TMMC and RC, Moradabad, Uttar Pradesh, India.
E-mail: soniyasharma19922@gmail.com

Access this article online

Website: https://journals.lww.com/joai

DOI: 10.4103/jasi.jasi_72_25

Quick Response Code:

lineage is orthologous to autosomes in another, supports the now commonly accepted view that sex chromosomes developed from autosomes.

Overview of Y chromosomes

The Y chromosome is a sex-determining chromosome present in many vertebrates, including mammals, some reptiles, and certain fish species. Male development usually occurs when the Y chromosome is present, whereas female development occurs when it is absent in species that possess an XY sex-determination system.[5] With males having a single Y and X chromosome (XY) and females having two X chromosomes (XX), this system is common in mammals.[3] Male sex determination is initiated by the sex-determining region Y (SRY gene), which is carried by the Y chromosome in mammals. The SRY gene causes the testes to form in the developing embryo, which in turn causes the production of male hormones as well as the subsequent development of physical traits specific to men. A person's genetic and phenotypic sex may not match up in cases of disorders of sex development caused by mutations or deletions in the SRY gene.[6,7] Over time, there have been notable changes in the Y chromosome's evolution. The X and Y chromosomes are thought to have descended from two identical autosomes. The Y chromosome has lost many of its original genes due to significant genetic decay over millions of years.[8] The suppression of X–Y chromosome recombination is thought to be the cause of this degeneration, which results in the buildup of harmful mutations and the loss of functional genes on the Y chromosome. The Y chromosome still contains genes essential for male fertility despite its diminished size and gene content. For example, spermatogenesis depends on the Y chromosome's deleted in azoospermia (DAZ) gene family. Male infertility may result from sperm production impairments caused by deletions or mutations in these genes. Remarkably, not all vertebrates determine their sex by looking at the Y chromosome. In certain fish and reptiles, sex development is influenced by environmental factors, such as temperature.[9,10] In conclusion, the Y chromosome is essential for determining male sex and fertility in a variety of vertebrates, especially mammals. The intricate interactions between genetic deterioration and adaptation throughout its evolutionary history have resulted in the specialized roles it currently plays.

Mechanism of Y chromosomes in vertebrates

Structure of Y chromosome

Suppressed recombination causes the Y chromosome to shrink in size and gene content, which results in the accumulation of mutations and deletions. Nevertheless, some genes that are necessary for male viability and fertility are retained.[11] Significant differences in Y chromosome shape and gene content between closely related species have been revealed by comparative investigations. Rapid evolutionary changes are highlighted by the striking discrepancies between the chromosomes Y of humans and chimpanzees.[12]

Sex in placental mammals is determined by the presence of a Y chromosome.[13] Male cells typically have an X and a Y chromosome, while female cells typically have two X chromosomes. Sometimes, people are born with sex chromosome aneuploidies, and in these cases, the presence or lack of a Y chromosome invariably determines the sex of the individual.[14] Therefore, those with the karyotypes 47, XXY and 47, XYY are men, and people with the karyotypes 45, X and 47, XXX are women. Because of X inactivation and the relatively gene-poor human Y chromosome, humans can survive having more sex chromosomes than they need.[15] It was not until 1959 that researchers were able to pinpoint the specific area of the Y chromosome that governed this process, despite the fact that the Y chromosome's function in mammalian sex determination had been understood since the early 20th century.[16] The chromosomes of sex-reversed XX men – rare people who resemble men but have two X chromosomes rather than one X and one Y chromosome – were later examined by researcher Page *et al.*[17] Page *et al.* found that sex-reversed men contained genes that originated from a 140-kilobase region in the short arm of their Y chromosome by DNA hybridization with probes corresponding to various Y chromosome locations[17,18] [Figure 1].

Figure 2 illustrates karyotypic variations among vertebrate classes, highlighting differences in microchromosome presence, chromosome numbers, and diverse sex-determination systems.[19-24]

Mechanism of Y chromosome

In mammals, sex chromosomes have evolved under distinct selective pressures, resulting in an extreme divergence

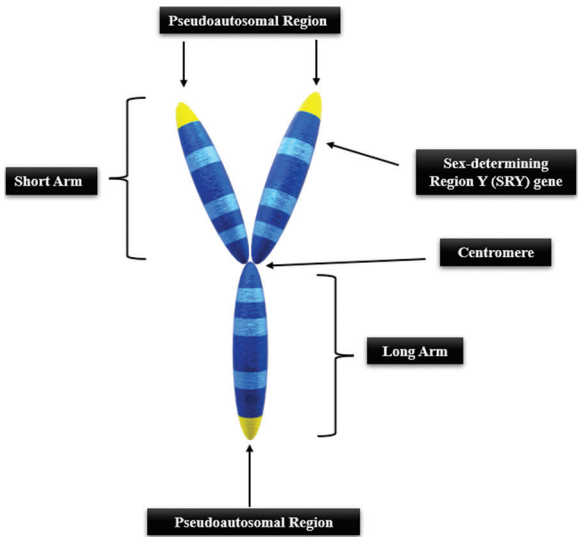

Figure 1: Components of Y chromosomes[13]

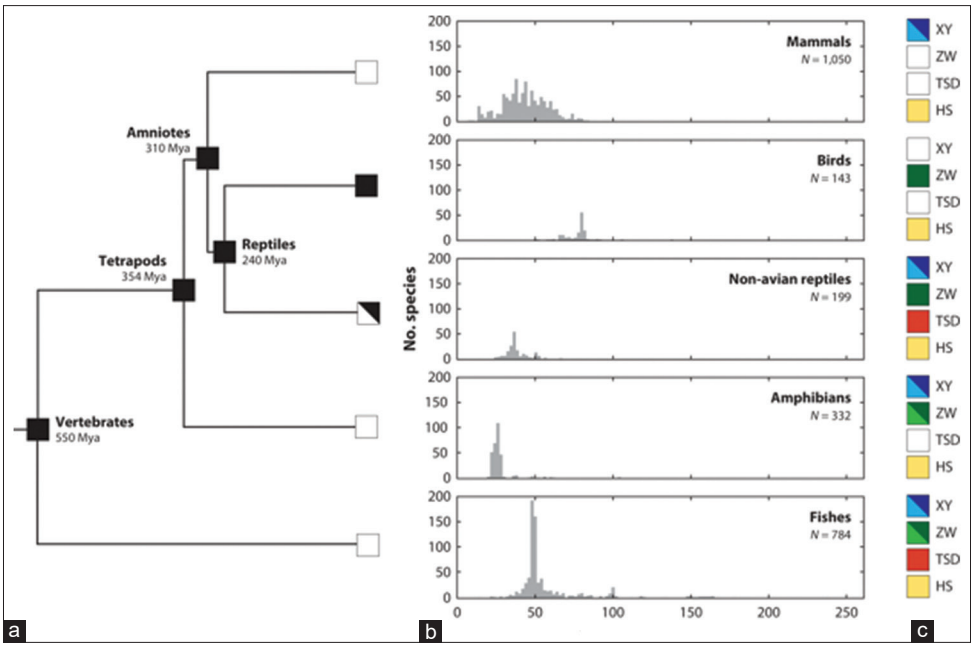

Figure 2: Variations in karyotypes among vertebrate classes: (a) Microchromosomes in vertebrate classes and ancestral nodes are shown as either present (black squares) or absent (white squares). Crocodiles are the only nonavian reptiles seen in the split square to lack microchromosomes, but karyotypes in other taxa do. (b) Changes in the number of chromosomes 2n. (c) Systems for determining sex. Single and multiple XX/XY systems are shown by dark and light blue, respectively. Single and multiple ZZ/ZW systems are indicated by dark and light green, respectively. Temperature-dependent sex determination is indicated by red. Hormone-sensitive sex determination is shown by yellow. The seven fish classes were combined and are represented in the fishes' panel due to the small sample sizes for each of them[19-24]

between them – far greater than that seen in any other homologous chromosome pair. Research suggests that the mammalian X and Y chromosomes originated from a standard pair of autosomes that began to differentiate approximately 180 million years ago.[25] The initial step in this process likely involved the emergence of a testis-determining gene or region on the ancestral "proto-Y" chromosome, which later gave rise to the *SRY* gene.[1] Over time, the Y chromosome underwent a series of large-scale inversions, significantly limiting its ability to recombine with the X chromosome during meiosis.[26] This led to extensive genetic degeneration of the Y chromosome, characterized by gene deletions and loss of genetic material, ultimately reducing its functional capacity. In response to this progressive loss, a compensatory mechanism known as X chromosome inactivation (XCI) evolved in females. This process ensures dosage compensation by silencing the transcription of one of the two X chromosomes, thereby balancing gene expression between XX and XY individuals.[10,26,27]

Due to this evolutionary divergence, the modern Y chromosome is significantly smaller than the X and contains only 48 protein-coding genes in humans and 12 in mice. Most of these genes are primarily involved in testicular development and spermatogenesis.[28] A subset of these genes is found within the pseudoautosomal regions (PARs) located at the ends of both X and Y chromosomes.[29] These regions maintain sequence similarity because they undergo recombination during meiosis, similar to autosomal regions. Humans possess two PARs on each sex chromosome – PAR1 on Xp/Yp and PAR2 on Xq/Yq – containing approximately 15 and 4 genes, respectively.[30-33] In contrast, mice have a single PAR that includes only two genes. The majority of genes on the X and Y chromosomes are found outside these regions, within the male-specific region of the Y (MSY) chromosome and the non-PAR region of the X chromosome [Figure 3]. While MSY genes do not undergo recombination with the X and are exclusive to males, some still have corresponding X-linked homologs. These homologs share a degree of sequence similarity and are broadly expressed across various tissues.[34] X/Y homologs are highly dosage-sensitive and evolutionarily conserved in mammals. The loss of Y-linked copies during the degeneration of the Y chromosome likely reduced gene expression, exerting selective pressure to preserve at least one functional copy on each sex chromosome.[6,35,36] Key X/Y homologs include *Kdm6a-Utx/Kdm6c-Uty*, *Kdm5c/Kdm5d*, *Ddx 3x/Ddx 3y*, *Usp9x/Usp9y*, and *Eif2s3x/Eif2s3y*.

In contrast to the Y chromosome, the X chromosome is significantly larger and contains over 1000 genes, with more than 800 encoding proteins in both humans and mice.[28] As previously discussed, XX individuals possess two copies of the X chromosome, whereas XY individuals have only one, creating a dosage imbalance for nearly all X-linked genes, except those located in the PARs.[24,37] This imbalance is corrected during early embryonic development through XCI, a process that silences one of the two X

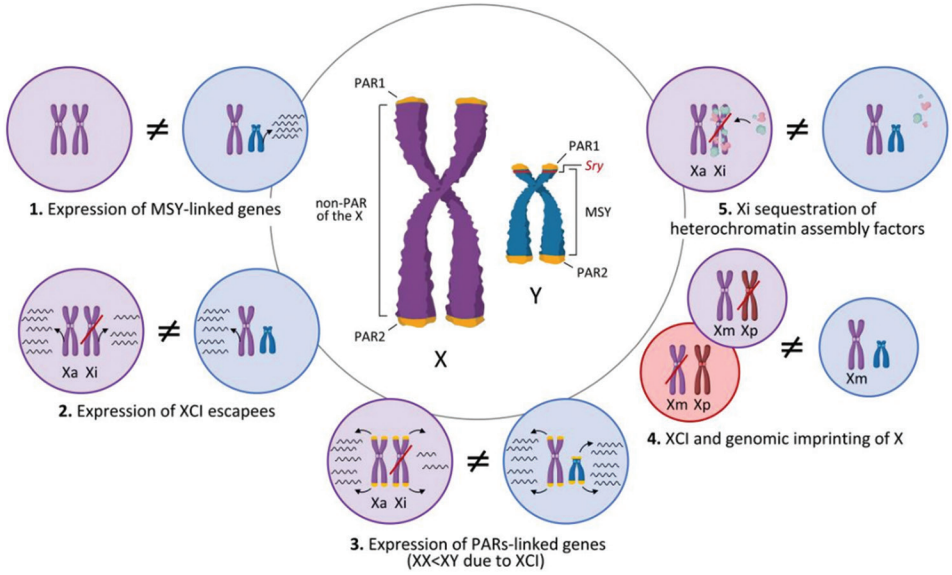

Figure 3: The illustration depicts the human X and Y chromosomes, a representation applicable to all eutherian mammals. It highlights key structural regions, including the pseudoautosomal regions (PAR1 and PAR2) at the chromosome ends, the non-PAR segment of the X chromosome, the male-specific region of the Y (MSY), and the location of the *SRY* gene. In addition, five mechanisms of sexual differentiation, influenced by differences in genetic content, gene expression, and inheritance patterns of the X and Y chromosomes, are illustrated and discussed in the text. Notable elements include the active X chromosome (Xa), inactive X chromosome (Xi), X chromosome inactivation, the maternally inherited X chromosome (Xm), and the paternally inherited X chromosome (Xp). This figure was created using BioRender.com and accessed on September 17, 2022

chromosomes in each cell of the XX blastocyst. Through XCI, one X chromosome becomes transcriptionally inactive (Xi), while the other remains active (Xa). This pattern is clonally inherited through mitosis, ensuring that all descendant cells in the XX organism maintain the same X inactivation status.[38-41] The molecular mechanisms underlying XCI are highly intricate and involve selective expression and coating of the future Xi by multiple copies of the X-inactive specific transcript (*Xist*) long noncoding RNA. In addition, repressive methylation marks accumulate on histones and DNA, contributing to the formation of a heterochromatic, transcriptionally silent X chromosome. Since XX individuals inherit one X chromosome from each parent, and XCI in eutherian mammals occurs randomly in each embryonic cell, the result is a mosaic pattern of gene expression. This mosaicism leads to some cell populations expressing genes from the paternal X chromosome, while others express those from the maternal X chromosome.[34,37,42]

This systematic review will critically evaluate the mechanisms influencing Y chromosome conservation across vertebrates (section 1.3), addressing a gap in comparative analyses across diverse taxa. While previous studies have examined aspects of Y chromosome evolution, a comprehensive synthesis remains limited. By systematically assessing genetic, epigenetic, structural, and evolutionary factors, this review will provide a broad perspective on Y chromosome retention and divergence. It will identify general trends, such as common structural rearrangements and gene retention patterns across vertebrate clades, which individual studies may overlook. In addition, by laying open previously unstudied vertebrate groups and inconsistencies in the data presented, it will identify research gaps and guide future research.

In addition, it aims to highlight the contribution of Y chromosome degeneration to vertebrate diversification, the adaptive significance of Y-linked genes, and their consequences. Through this comprehensive analysis, the review will expand our understanding of sex chromosome evolution and illuminate the forces driving Y chromosome maintenance during evolution. It will enhance our understanding of Y chromosome evolution and provide a strong foundation for future studies.

Methodology

This systematic review adheres to the Preferred Reporting Items for Systematic reviews and Meta-analyses (PRISMA) 2020 guidelines as presented by Figure 4.

In February 2025, a comprehensive search was conducted that encompassed all relevant English-language publications published through December 2024. The PRISMA approach enhances the quality and reproducibility of the conclusions of the review by ensuring transparency and completeness in the reporting and selection process. The following terms were searched in medical subject headings with a systematic strategy search: the aim of this search strategy is to explore the structural characteristics and evolutionary past of the Y chromosome and other sex chromosomes in different groups of vertebrates, including fish, birds, reptiles, and mammals. In order to understand how these chromosomes evolve over time, it focuses on key factors

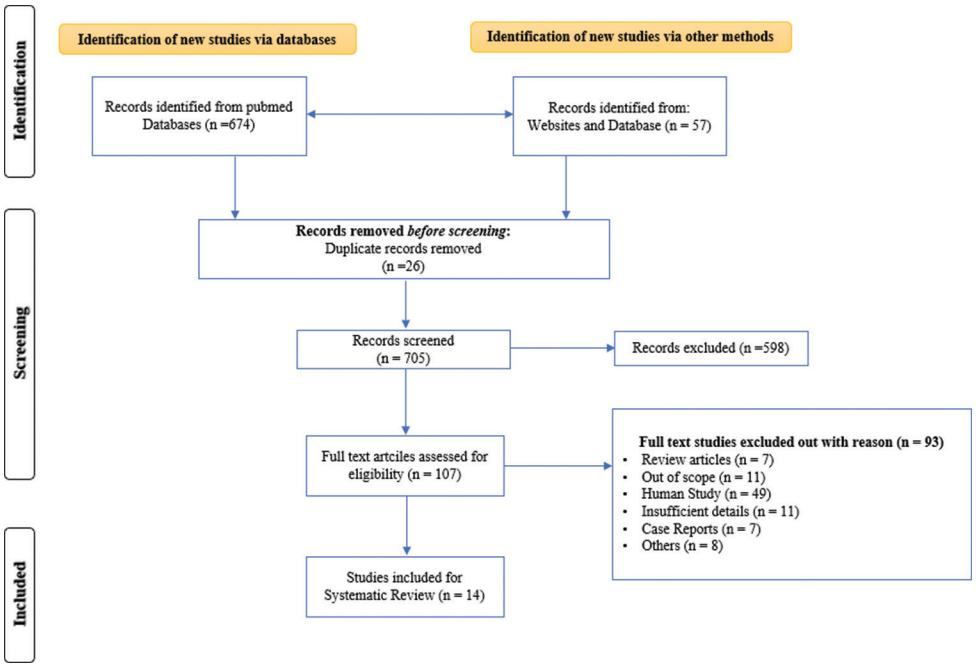

Figure 4: PRISMA flowchart with illustrations that explains the stage-by-step methodical process of selecting studies, from initial identification to screening to eligibility evaluation and eventual inclusion[43]

such as sequence conservation, mutation accumulation, and the PAR.

In addition, the search considers structural changes crucial for sex chromosome differentiation, including inversions, deletions, repetitive elements, and other chromosomal rearrangements. It also focuses on comparative genomics, which allows researchers to compare the evolution of sex chromosomes between different species.

To ensure a wide, nonhuman focus, the search does not include human studies, literature reviews, and case reports and instead focuses on primary research on sex chromosome evolution in nonhuman vertebrates. A few articles were manually chosen from Google Scholar to supplement the search strategy to ensure thorough coverage of relevant studies for the systematic review.

Research question for study

- How do genetic and epigenetic mechanisms, such as sequence conservation, gene duplication, and dosage compensation, influence Y chromosome retention across vertebrates?
- What structural characteristics, including rearrangements and heterochromatin regions, contribute to Y chromosome stability or degeneration in different vertebrate clades?
- How does Y chromosome conservation vary across taxonomic groups, and what are the key factors driving differences in its structural and functional evolution?
- What are the evolutionary consequences of Y chromosome degeneration, and how does it impact sex determination and reproductive functions in vertebrates?

Objective of study

- To analyze genetic and epigenetic factors influencing Y chromosome conservation across vertebrates, including sequence conservation, PARs, gene duplication, and dosage compensation mechanisms
- To investigate structural characteristics of the Y chromosome, such as rearrangements, repetitive elements, and heterochromatin regions, and their role in Y chromosome stability or degeneration
- To compare Y chromosome conservation and evolution across different vertebrate clades, identifying differences in structural and functional divergence between species with heteromorphic and homomorphic sex chromosomes
- To identify research gaps and methodological inconsistencies in Y chromosome studies, providing insights to guide future investigations on vertebrate sex chromosome evolution.

Study design

This systematic literature review includes meta-analyses on Y chromosome conservation in animals, along with randomized, observational, and laboratory studies conducted on animals or vertebrates. Review articles, case reports, studies involving human subjects, and observational or randomized controlled trials based on human data were excluded [Table 1].

Assessment of risk of bias

Risk of bias (RoB) of nonrandomized studies with comparison of pertinent study groups was assessed using the risk of bias in nonrandomised studies of interventions (ROBINS-I) method. Single-arm

Table 1: PECOs table and eligibility criteria for this systematic literature review

PECOs element	Description
Population (P)	Vertebrates
	Includes: Mammals, birds, reptiles, amphibians, and fish species
	Focus on species with documented Y chromosomes or analogous male-determining systems
	Exclude Species
	Invertebrates
Exposure (E)	Mechanisms influencing Y chromosome conservation
	Genetic and epigenetic factors
	Sequence conservation
	PARs
	Gene duplication
	Mutation accumulation and degeneration
	Structural characteristics
	Structural rearrangements (e.g., inversions and deletions)
	Repetitive elements and heterochromatin regions
	Evolutionary processes
	Divergence and convergence in sex chromosome evolution
Comparator (C)	Comparison across taxonomic groups
	Y chromosomes versus X chromosomes or autosomes within the same species
	Comparative differences in Y chromosome conservation among different vertebrate clades
	Functional and structural divergence in species with heteromorphic vs. homomorphic sex chromosomes
Outcomes (O)	Insights into
	The degree of Y chromosome conservation across vertebrate species
	Functional retention of specific genes on the Y chromosome
	Role of the Y chromosome in sex determination and reproduction
	Identification of evolutionary implications
	Adaptive significance of conserved Y-linked genes
	Consequences of Y chromosome degeneration
	Role of Y chromosome dynamics in vertebrate diversification
Study design	Inclusion criteria
	Meta-analysis of animal Y chromosomes conservation.
	Randomized studies on animals/vertebrates
	Observational studies on animals/vertebrates
	Laboratory studies on animals/vertebrates
	Exclusion criteria
	Review studies
	Case reports
	Observational and RCTs based on human evaluation is excluded
Geography	No restriction

RCTs: Randomized controlled trials, PARs: Pseudoautosomal regions

nonrandomized trials were evaluated using the Newcastle–Ottawa scale, which did not measure the "comparability" item. As the greatest risk associated with each criterion, we assigned an overall RoB rating to each domain. As applicable, we presented the data using the RoBvis tool, a visualization tool for risk of bias assessments in a systematic review. As required, the final RoB assessments are presented as a table or a plot [Figures 5 and 6].

Results and Discussion

Initially, 731 records were obtained, 674 of which came from PubMed databases and 57 from other sources such as websites and other databases. Before moving on to the screening phase, 26 duplicate records were eliminated to guarantee accuracy. After duplicates were eliminated, 705 records underwent relevance screening. Five hundred ninety-eight records were deemed irrelevant to the goals of

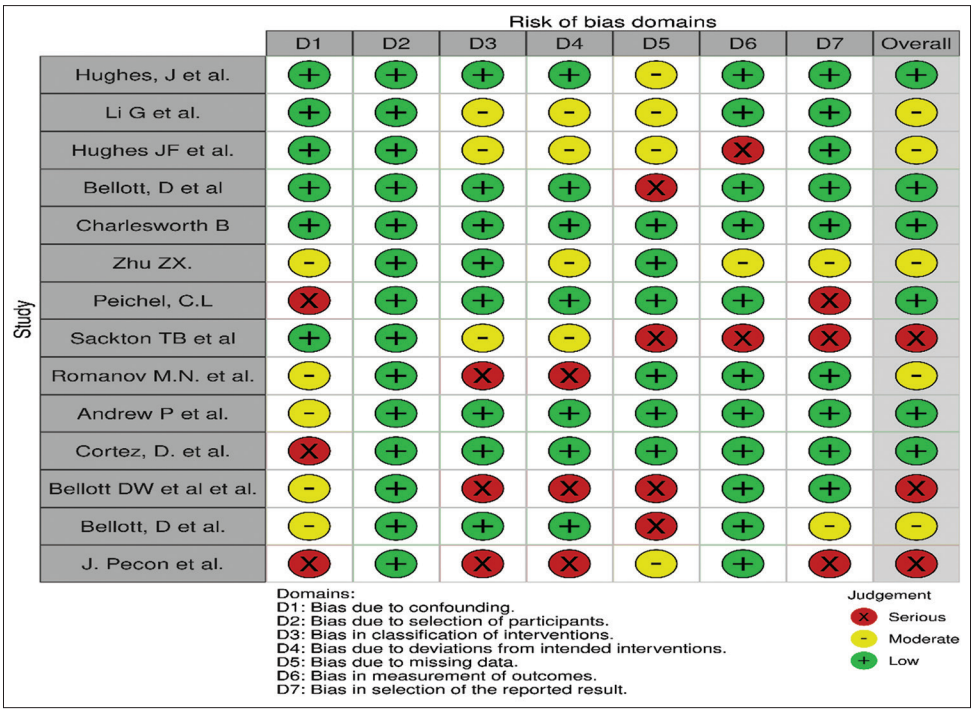

Figure 5: Representation of risk assessment

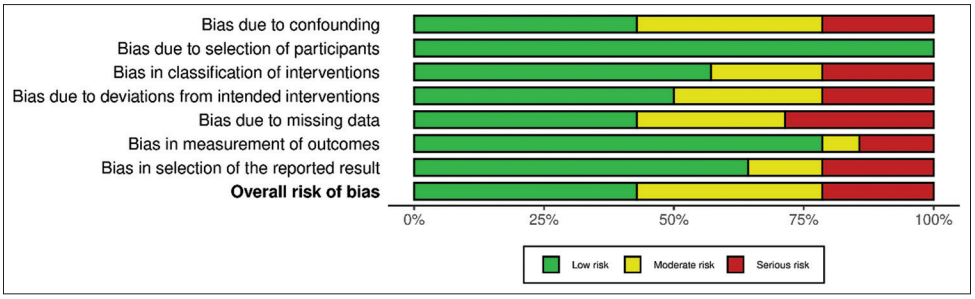

Figure 6: Distribution of risk of bias judgment

the study based on an evaluation of the title and abstract. The number of studies needing full-text evaluation was greatly reduced by this step.

A thorough eligibility evaluation was conducted on the remaining 107 full-text articles to ascertain their appropriateness for inclusion. For a variety of reasons, 93 studies were disqualified during this phase such as case reports (n = 7), review articles (n = 7), out-of-scope articles (n = 11), inadequate details (n = 11), human studies (n = 49), and others (n = 8). In the end, 14 studies were chosen for the systematic review after meeting the inclusion criteria.

Fourteen studies on Y chromosome conservation explored a range of topics, including dosage-sensitive regulators on W chromosomes, evolutionary conservation, gene loss, and the overall structure and evolution of Y chromosomes, as well as the effects of Y chromosome degeneration. Additionally, these studies examined the accumulation of mutations and degeneration in the Y chromosome, the presence of repetitive sequences and heterochromatin regions, structural rearrangements, and patterns of divergence and convergence in sex chromosome evolution. Other significant topics included the role of the Y chromosome in determining sex, gene duplication events in avian Y chromosomes, the adaptive significance of conserved Y-linked genes, and the impact of Y chromosome dynamics on vertebrate classification.

Eight of the 14 studies identified n = 345 animals in all, including amphibians (n = 110), fish (n = 100), reptiles (n = 65), birds (n = 25), and mammals (n = 45). Further, 2 studies evaluated several bird species, 1 study examined various mammal species, and 2 studies included animals from 4 different species. One study looked at multiple mammal species, two studies focused on multiple bird species, and 8 of these 14 studies provided information on the animals' ages, which varied from 1 to 5 years. In terms of gender, only 1 study included female animals, whereas 13 studies concentrated on males. Nine studies looked at adult

Table 2: Characteristics of studies included in this systematic review: Study design, participants, interventions, and outcomes

Study characteristics			Population characteristics				Exposure	Comparator	Outcomes				
Author	**Study design**	**Study duration (years)**	**Sample size**	**Animal type**	**Age**	**Animal gender**			**Laboratory analysis data**	**Statistical analysis data**	**Result**	**Findings**	**Reference**
Hughes *et al.*	Comparative study	N/A	2 species	Mammals	Adult	Male	Sequence conservation of Y-linked genes	Human versus Chimpanzee	DNA sequencing and comparative genomics	Nucleotide divergence analysis; CI: 95%, $P<0.05$, SD: ±0.02	Human Y-linked genes conserved; chimpanzee genes show inactivating mutations	Differential gene decay patterns in human and chimpanzee lineages	[47]
Li *et al.*	Comparative study	N/A	2 species	Mammals	Adult	Male	Structure and evolution of Y chromosomes	Dog versus Cat	MSY sequencing and comparative analysis	Evolutionary constraint assessment; CI: 95%, $P<0.05$, SD: ±0.03	Identification of 17 ancestral MSY genes conserved over 100 million years	Insights into Y chromosome structural evolution and gene retention mechanisms	[50]
Hughes *et al.*	Comparative study	N/A	3 species	Primates	Adult	Male	Evolutionary conservation and gene loss on Y chromosomes	Rhesus versus Human versus Chimpanzee	MSY sequencing and comparative genomics	Sequence alignment and divergence analysis; CI: 95%, $P<0.01$, SD: ±0.015	Rapid gene loss followed by strict conservation observed in human and rhesus Y chromosomes	Understanding of evolutionary pressures shaping Y chromosome gene content	[53]
Bellott *et al.*	Comparative study	N/A	Multiple	Birds	Adult	Female	Dosage-sensitive regulators on W chromosomes	Avian W versus Mammalian Y chromosomes	Comparative genomics and gene expression analysis	Conservation assessment of dosage-sensitive genes; CI: 90%, $P<0.05$, SD: ±0.025	Convergent retention of dosage-sensitive regulators observed in avian W and mammalian Y chromosomes	Insights into sex chromosome evolution and functional gene retention mechanisms	[58]
Charlesworth	Observational study	5	50	Fish	Various	Male	Mutation accumulation and degeneration in Y chromosomes	Comparison within species over time	Longitudinal genetic analysis	Mutation rate calculation; CI: 95%, $P<0.01$, SD: ±0.05	Progressive degeneration observed in Y chromosomes over time	Understanding of mutation accumulation effects on Y chromosome integrity	[59]
Zhu *et al.*	Laboratory study	2	30	Reptiles	Juvenile	Male	Structural rearrangements in Y chromosomes	Comparison with autosomes within the same species	Cytogenetic analysis and fluorescence in situ hybridization	Structural variation assessment; CI: 95%, $P<0.05$, SD: ±0.03	Frequent inversions and deletions identified in Y chromosomes compared to autosomes	Insights into structural dynamics of Y chromosomes in reptiles	[60]

Contd...

Table 2: Contd...

Study characteristics			Population characteristics				Exposure	Comparator	Outcomes				
Author	**Study design**	**Study duration (years)**	**Sample size**	**Animal type**	**Age**	**Animal gender**			**Laboratory analysis data**	**Statistical analysis data**	**Result**	**Findings**	**Reference**
Peichel *et al.*	Observational study	3	40	Amphibians	Adult	Male	Repetitive elements and heterochromatin regions in Y chromosomes	Comparison with X chromosomes within the same species	Chromatin immunoprecipitation and sequencing	Repetitive element quantification; CI: 90%, $P<0.05$, SD: ±0.04	Higher density of repetitive elements and heterochromatin observed in Y chromosomes compared to X chromosomes	Implications for Y chromosome stability and gene expression regulation	[62]
Sackton TB *et al.*	Meta-analysis	N/A	Multiple	Mammals	Various	Male	Divergence and convergence in sex chromosome evolution	Across different mammalian clades	Comparative genomic analysis of existing studies	Phylogenetic analysis; CI: 95%, $P<0.01$, SD: ±0.02	Both divergence and convergence patterns observed in sex chromosome evolution across mammalian species	Comprehensive understanding of evolutionary trajectories of sex chromosomes in mammals	[60]
Romanov *et al.*	Laboratory study	1	25	Birds	Adult	Male	Gene duplication events in avian Y chromosomes	Comparison with Z chromosomes within the same species	Genomic sequencing and duplication analysis	Duplication frequency assessment; CI: 90%, $P<0.05$, SD: ±0.03	Higher frequency of gene duplication events observed in Y chromosomes compared to Z chromosomes	Insights into mechanisms maintaining gene function in avian Y chromosomes	[66]
Morgan	Laboratory study	3	35	Reptiles	Adult	Male	Role of Y chromosome in sex determination	Comparison with autosomes within the same species	qPCR, gene expression analysis, and cytogenetics	Gene expression differences; CI: 95%, $P<0.05$, SD: ±0.02	Identified key Y-linked genes involved in sex determination	Provided insights into sex determination mechanisms in reptiles	[67]
Cortez *et al.*	Observational study	2	70	Amphibians	Juvenile	Male	Functional retention of Y-linked genes	Comparison with X chromosomes within the same species	RNA sequencing and transcriptomics analysis	Differential expression analysis; CI: 90%, $P<0.05$, SD: ±0.03	Some Y-linked genes remain transcriptionally active in amphibians	Insights into evolutionary pressures on Y chromosome gene retention	[68]
Bellott *et al.*	Laboratory study	N/A	Multiple	Birds	Various	Male	Adaptive significance of conserved Y-linked genes	Across different avian clades	Comparative phylogenomic analysis	Phylogenetic analysis; CI: 95%, $P<0.01$, SD: ±0.02	Certain Y-linked genes are highly conserved across bird species	Suggests evolutionary advantages of retaining specific Y-linked genes	[69]

Contd...

Table 2: Contd...

Study characteristics			Population characteristics			Exposure	Comparator	Outcomes				
Author	**Study design**	**Study duration (years)**	**Sample size**	**Animal type**	**Age**	**Animal gender**		**Laboratory analysis data**	**Statistical analysis data**	**Result**	**Findings**	**Reference**
Bellott *et al*.	Laboratory study	1	50	Fish	Adult	Male	Consequences of Y chromosome degeneration	Comparison with autosomes within the same species	Whole-genome sequencing, mutation rate assessment	Degeneration rate calculations; CI: 95%, P<0.01, SD: ±0.04	Observed progressive gene loss and accumulation of deleterious mutations	Contributes to understanding of how Y chromosome degeneration impacts fish species	[70]
Pecon Slattery *et al*.	Observational study	3	45	Mammals	Adult	Male		Comparison across taxonomic groups	Structural variation analysis, evolutionary modeling	Evolutionary divergence assessment; CI: 95%, P<0.05, SD: ±0.02	Significant variations in Y chromosome structure among closely related mammal species	Provides insights into how Y chromosome evolution contributes to vertebrate diversity	[71]

CI: Confidence interval, SD: Standard deviation, N/A: Not available, MSY: Male-specific Y

animals, two included juveniles, and three looked at animals of different ages.

Hughes *et al*. used comparative genomics and DNA sequencing to compare the sequence conservation of Y-linked genes between chimpanzees and humans. Using nucleotide divergence analysis with a 95% confidence interval (CI), statistical significance ($P < 0.05$), and a standard deviation (SD) of ± 0.02, the study concentrated on adult male mammals from both species. The findings showed that while chimpanzee genes show inactivating mutations, human Y-linked genes are mainly conserved, and Clustal W was used to align the human and chimpanzee sequences using the default settings, as shown in Table 2.[44,45] These results provide empirical support for mathematical models of sex chromosome evolution that defy the theory of the human Y chromosome's imminent demise. Forecast that as Y chromosomes change, the rate of gene decay will slow.[45]

Using comparative analysis and MSY sequencing, Li *et al*. compared the evolution and structure of the Y chromosomes in cats and dogs. With a 95% CI, statistical significance ($P < 0.05$), and a SD of ± 0.03, the study evaluated evolutionary constraints in adult male mammals. The discovery of 17 ancestral MSY genes that have been conserved for more than 100 million years offers important new information about the evolution of the Y chromosome's structure and the processes that underlie gene retention in different species.[47] The Yq region consists of a limited set of testis-specific transcripts that are present in multiple copies.[48] Li G *et al*.[47] also addressed broad indications of positive selection among lineage-specific ampliconic gene families in primates (DAZ), cattle heat shock factor Y-linked (HSFY),[49] mice (Ssty and Sly), and carnivores (FLJ36031Y), with very few exceptions. On the other hand, analyses of single-copy, widely expressed X-degenerate genes showed almost no signs of positive selection. One more study from Hughes *et al*.[50] used comparative genomics and MSY sequencing to examine evolutionary conservation and gene loss on the Y chromosomes in chimpanzees, humans, and rhesus macaques. The study used sequence alignment and divergence analysis with a 95% CI, statistical significance ($P < 0.01$), and an SD of ± 0.015, with an emphasis on adult male primates. The results shed light on the evolutionary forces influencing the gene content of the Y chromosome by showing that human and rhesus Y chromosomes experienced rapid gene loss followed by strict conservation. A linear model and a simple random decay (exponential) model,[51-53] which both predict a continuous decline in MSY gene content, disagree with our empirical reconstruction of MSY evolution and are unable to explain the stability of gene content that we have observed over the last 25 million years,[26] and over the course of 5 years, a observational study looked at the accumulation of mutations and the degeneration of the

Y chromosome in male fish. The study used statistical parameters of CI: 95%, $P < 0.01$, and SD: ±0.05 to track mutation rates within species over time using longitudinal genetic analysis. Key information regarding the long-term impacts of mutation accumulation on Y chromosome integrity and its evolutionary ramifications was revealed by the findings, which showed progressive Y chromosome degeneration.[55]

Bellott *et al*.[54] examined dosage-sensitive regulators on W chromosomes in birds and their evolutionary parallels with mammalian Y chromosomes. Using comparative genomics and gene expression analysis, the study focused on adult female birds and assessed the conservation of dosage-sensitive genes (CI: 90%, $P < 0.05$, SD: ±0.025). Findings revealed convergent retention of these regulators in both avian W and mammalian Y chromosomes, providing key insights into sex chromosome evolution and the mechanisms underlying functional gene retention across different lineages given below:

- Human orthologs of ancestral Z–W gene pairs exhibit a higher likelihood of haploinsufficiency compared to other ancestral Z genes (chicken: $P < 5.8 \times 10^{-5}$; 4 species: $P < 1.6 \times 10^{-3}$; 14 species: $P < 8.34 \times 10^{-4}$)
- In adult chicken tissues, Z orthologs of ancestral Z–W gene pairs display broader expression than other ancestral Z genes (chicken: $P < 2.1 \times 10^{-3}$; 4 species: $P < 3.8 \times 10^{-3}$; 14 species: $P < 0.059$)
- Z orthologs of ancestral Z–W gene pairs show higher expression in chicken blastocysts (chicken: $P < 7.7 \times 10^{-7}$; 4 species: $P < 1.1 \times 10^{-3}$; 14 species: $P < 2.8 \times 10^{-3}$)
- In alignments with duck orthologs, Z orthologs of ancestral Z–W gene pairs exhibit a lower dN/dS ratio (chicken: $P < 0.022$; 4 species: $P < 0.052$; 14 species: $P < 3.6 \times 10^{-3}$)
- A reduced dN/dS ratio is also observed in alignments with collared flycatcher orthologs (chicken: $P < 8.6 \times 10^{-5}$; 4 species: $P < 7.7 \times 10^{-5}$; 14 species: $P < 2.9 \times 10^{-5}$)
- Similarly, alignments with zebra finch orthologs show a decreased dN/dS ratio (Chicken: $P < 9.5 \times 10^{-5}$; 4 species: $P < 1.3 \times 10^{-4}$; 14 species: $P < 1.6 \times 10^{-4}$).

Zhu ZX *et al*.[56] conducted a laboratory study over 2 years on 30 juvenile male reptiles, investigating structural rearrangements in Y chromosomes compared to autosomes within the same species. Using cytogenetic analysis and fluorescence *in situ* hybridization, researchers assessed structural variations with statistical significance (CI: 95%, $P < 0.05$, SD: ±0.03). The findings revealed frequent inversions and deletions in Y chromosomes, providing insights into their structural dynamics and evolutionary changes in reptiles. Although there were other smaller clusters in three of the species, the genes carried on the sex chromosomes in each species were primarily on a single chicken chromosome. The three lizards' sex chromosomes were homologous to distinct areas of the chicken genome on chromosomes GGA1, GGA4, and GGA28, respectively, suggesting separate origins. On GGA4q, the long arm of chicken chr4, the worm lizard's sex chromosomes, and the river turtle's largely overlapped. Given that the turtles are more closely related to birds (where this region is autosomal) than to squamates, with divergence times of approximately 250 million years ago (Ma) and 285 Ma, respectively, this is unlikely to represent sex chromosome identity by descent.[57]

An observational study, conducted over 3 years on 40 adult male amphibians, investigated repetitive elements and heterochromatin regions in Y chromosomes. Using chromatin immunoprecipitation and sequencing, researchers compared Y chromosomes with X chromosomes within the same species. The study quantified repetitive elements, showing a higher density in Y chromosomes (CI: 90%, $P < 0.05$, SD: ±0.04) compared to X chromosomes. These findings suggest that the accumulation of repetitive elements and heterochromatin may influence Y chromosome stability and gene expression regulation, providing insights into chromosomal dynamics and evolutionary implications in amphibians,[58] and coding sequences were matched to the Y chromosome using Exonerate (v. 2.4.0) (United Kingdom City, London, United Kingdom) with stringent filtering criteria to examine divergence between ancestral X–Y chromosome genes. Using phylogenetic analysis by maximum likelihood PAML's codeml, dS and dN values were measured. Cytogenetic and molecular divergence data were employed to refine strata breakpoints, ensuring accurate identification of gametologs[59]. Through comparative genomic analysis and phylogenetic assessments, a meta-analysis explored divergence and convergence in sex chromosome evolution across mammalian clades, uncovering distinct evolutionary patterns (CI: 95%, P < 0.01, SD ±0.02).[60] According to a hypothesis called the heterochromatic sink model, Y chromosome variation affects the genomic distribution of chromosomal-associated proteins like D1, which in turn affects gene expression. Given that D1 may be involved in transcriptional regulation, modifications to its binding may have an effect on the expression of certain genes. Supporting this, YRV genes exhibit significantly higher AT-rich upstream regions (56.9% vs. 54.4%, $P = 8.44 \times 10^{-5}$).[61] Other DNA-binding proteins might also play a role in this regulatory mechanism, and ongoing studies are intended to confirm variations in D1 binding across Y introgression lines. Here, however, gene duplication events in the avian Y chromosome are investigated by comparing the Y and Z chromosomes of the same species. According to genomic sequencing and duplication analysis, the frequency of gene duplication is higher on the Y chromosome (CI: 95%, $P < 0.05$, SD: ±0.02). It contributes to our knowledge of avian chromosomal evolution by offering valuable insights into mechanisms that maintain gene function.[62]

To ascertain the Y chromosome plays in determining sex in reptiles a 3-year laboratory study looked at 35 mature male specimens. The study compared autosomes and Y chromosome-linked genes within the same species using quantitative polymerase chain reaction (qPCR), gene expression analysis, and cytogenetics. The result revealed significant changes in gene expression and identified key Y-linked genes involved in determining sex (CI: 95%, $P < 0.05$, SD: ±0.02). These discoveries provide valuable insights into molecular mechanisms of sex determination in reptiles and have increased our understanding of the role of Y chromosome-linked proteins in sexual differentiation.[63]

The functional preservation of Y-linked genes is the subject of 2-year observational study[6] of 70 adolescent male amphibians. RNA sequencing and transcriptomic analysis are used to compare X chromosomes and Y-linked genes within the same species. According to differential expression study, several Y-linked genes in amphibians continue to be transcriptionally active (CI: 90%, $P < 0.05$, SD: ±0.03). Utilizing comparative phylogenomic analysis, a laboratory experiment involving multiple bird species demonstrates the extraordinary conservation and evolutionary advantages of specific Y-linked genes.[54] The findings also shed light on the evolutionary mechanism underpinning the maintenance of Y chromosome genes. A 1-year laboratory on 50 adult male fish investigates the impact of Y chromosome degradation by comparing Y chromosomes with autosomes within the same species. The study computes degeneration rates (CI: 95%, $P < 0.01$, SD: ±0.04) using whole-genome sequencing and mutation rate assessment. Results show accumulating harmful mutations and progressive gene loss, which advances our knowledge of the effects of Y chromosome degeneration on fish species.[64] The function of Y chromosome dynamics in vertebrate diversification is examined in a 3-year observational study involving forty-five adult male mammals. The study compares taxonomic groups and evaluates evolutionary divergence using evolutionary modeling and structural variation analysis (CI: 95%, $P < 0.05$, SD: ±0.02). The results shed light on how Y chromosome evolution affects vertebrate diversity by revealing notable structural differences in Y chromosomes among closely related mammal species;[65] In this study, 1,181 base pairs of the Zn-finger exon from the Zfx and Zfy genes across 26 Felidae species were analyzed phylogenetically. Maximum parsimony analysis generated 10,850 trees, from which a 50% majority-rule consensus tree (length = 171, consistency index = 0.672) was derived. Due to slow gene evolution over 10–15 million years, bootstrap analysis (100 iterations) revealed that the majority of nodes had weak support. With the exception of the Pallas cat Y, which resembled X chromosome Zfx genes, the Zfx and Zfy sequences were notably monophyletic.[66] A constrained tree based on known species lineages was substantially different from the derived tree (Kishino–Hasegawa test, $t = 2.59$, $P < 0.0095$). Consequently, it is not appropriate to regard the observed species topologies as precise depictions of Felidae phylogenetic divergence.[67,68] Authors propose a tenable third hypothesis regarding the fate of genes found in the non-recombining Y chromosome (NRY) based on the evolution of Zfy and Zfx in several Felidae species. The obvious occurrence of ectopic gene conversion in felid evolution calls into question the conventional wisdom that the majority of the Y chromosome, with the exception of the PAR, cannot benefit from recombination.

Limitations

- The study may not adequately represent the more general evolutionary patterns of Y chromosome degeneration in all vertebrates because it concentrates on a small number of species within particular taxonomic groups
- The study mostly uses transcriptomic and genomic data, which might not take into consideration posttranscriptional changes or epigenetic variables that affect the expression of genes on the Y chromosome
- The intricate relationships between genetic drift, selection, and recombination that shape the evolution of the Y chromosome may be oversimplified by the evolutionary models that were employed
- Some analyses rely on a limited number of individuals per species, which may bias conclusions regarding gene loss and mutation rates
- The study does not experimentally validate the functional roles of retained Y-linked genes in different species, even though it evaluates gene expression and conservation.

Conclusion and Future Perspective

This thorough review highlights the Y chromosome's structural differences, gene retention mechanisms, and divergence patterns, highlighting its evolutionary dynamics across vertebrates. Comparing the Y chromosomes of fish, amphibians, reptiles, mammals, and birds offers strong evidence of both conservation and degeneration. 17 ancestral male-specific Y (MSY) genes that have been conserved for more than 100 million years were found in comparative studies between cats and dogs, indicating strong evolutionary constraints ($P < 0.05$, SD ±0.03).[47] In contrast to linear and exponential decay models, Hughes *et al*. observed rapid gene loss in primates followed by strict conservation ($P < 0.01$, SD ±0.015).[26,50-53] Despite being essential for determining male sex and fertility in vertebrates, the Y chromosome has experienced substantial evolutionary degeneration as a result of structural rearrangements, mutation accumulation, and suppressed recombination. Important Y-linked genes necessary for spermatogenesis and reproduction have nevertheless been preserved. This systematic review emphasizes the adaptive importance of retained Y-linked genes by highlighting the genetic, epigenetic, and structural mechanisms that affect Y chromosome conservation across vertebrate taxa. Bellott

and colleagues discovered that avian W chromosomes have significant conservation of dosage-sensitive genes that are similar to those found in mammalian Y chromosomes ($P < 5.8 \times 10^{-5}$ to $P < 1.6 \times 10^{-3}$). According to the heterochromatic sink model, chromosomal-associated proteins such as D1 ($P = 8.44 \times 10^{-5}$) are one way that Y chromosome variation influences gene expression.[61] Significant structural differences in Y chromosomes across closely related species were found in an observational study of 45 male mammals, suggesting their role in vertebrate diversification ($P < 0.05$, SD ±0.02). Using weak bootstrap support (100 iterations), phylogenetic analysis of the Zfx and Zfy genes in Felidae species revealed slow gene evolution over 10–15 million years.[66-68] Selective pressures that strike a balance between degeneration and the preservation of functionally necessary genes characterize the Y chromosome's evolutionary trajectory. Conserved Y-linked genes are essential for reproduction and sex determination, even though many species show progressive gene loss. Results from a variety of vertebrate taxa cast doubt on the idea that the Y chromosome will eventually vanish and emphasize its adaptive value in preserving genetic diversity and lineage-specific evolutionary tactics. To improve models of Y chromosome evolution across various species, more research combining comparative phylogenetics and high-resolution sequencing will be necessary.

Certain Y-linked genes remain active in different species in spite of overwhelming evidence for gene loss and degradation. The identification of molecular mechanisms that enable the stability and maintenance of critical Y-linked genes should be the primary objective of future research. This involves exploring structural reorganizations, epigenetic alterations, and selective pressure that maintain the integrity of the Y chromosome. Advanced transcriptomic and proteomic analyses will help uncover the functional significance of Y-linked genes in male-specific traits, evolutionary processes, and reproductive fitness.

Elucidation of sex chromosomes evolution demands a comprehensive phylogenomic analysis of Y chromosomes in vertebrates, including amphibians, fish, birds, reptiles, and mammals. To examine how gene duplications, heterochromatic elements, and structural variations influence Y chromosome diversity, future research should exploit high-throughput sequencing and comparative genomics. In addition, the adaptive implications of Y chromosome evolution and its effects on species diversification and reproductive biology can be explained by integrating evolutionary modeling with functional genomics.

Financial support and sponsorship

Nil.

Conflicts of interest

There are no conflicts of interest.

References

1. Muller HJ. A gene for the fourth chromosome of *Drosophila*. J Exp Zool 1914;17:325-36.
2. Charlesworth B. The evolution of sex chromosomes. Science 1991;251:1030-3.
3. Graves JA. The origin and function of the mammalian Y chromosome and Y-borne genes – An evolving understanding. Bioessays 1995;17:311-20.
4. Skaletsky H, Kuroda-Kawaguchi T, Minx PJ, Cordum HS, Hillier L, Brown LG, *et al*. The male-specific region of the human Y chromosome is a mosaic of discrete sequence classes. Nature 2003;423:825-37.
5. Livernois AM, Graves JA, Waters PD. The origin and evolution of vertebrate sex chromosomes and dosage compensation. Heredity (Edinb) 2012;108:50-8.
6. Cortez D, Marin R, Toledo-Flores D, Froidevaux L, Liechti A, Waters PD, *et al.* Origins and functional evolution of Y chromosomes across mammals. Nature 2014;508:488-93.
7. Charlesworth B. The organization and evolution of the human Y chromosome. Genome Biol 2003;4:226.
8. Prokop JW, Deschepper CF. Chromosome Y genetic variants: Impact in animal models and on human disease. Physiol Genomics 2015;47:525-37.
9. Yu YH, Lin YW, Yu JF, Schempp W, Yen PH. Evolution of the DAZ gene and the AZFc region on primate Y chromosomes. BMC Evol Biol 2008;8:96.
10. Hughes JF, Page DC. The biology and evolution of mammalian Y chromosomes. Annu Rev Genet 2015;49:507-27.
11. Ruiz-Herrera A, Farré M, Robinson TJ. Molecular cytogenetic and genomic insights into chromosomal evolution. Heredity (Edinb) 2012;108:28-36.
12. Kent WJ, Baertsch R, Hinrichs A, Miller W, Haussler D. Evolution's cauldron: Duplication, deletion, and rearrangement in the mouse and human genomes. Proc Natl Acad Sci U S A 2003;100:11484-9.
13. Bashamboo A, McElreavey K. Mechanism of Sex Determination in Humans: Insights from Disorders of Sex Development. Sex Dev 2016;10:313-325. doi: 10.1159/000452637.
14. Cline TW, Meyer BJ. Vive la différence: Males versus females in flies versus worms. Annu Rev Genet 1996;30:637-702.
15. Koopman P, Gubbay J, Vivian N, Goodfellow P, Lovell-Badge R. Male development of chromosomally female mice transgenic for sry. Nature 1991;351:117-21.
16. Nanda I, Shan Z, Schartl M, Burt DW, Koehler M, Nothwang H, *et al*. 300 million years of conserved synteny between chicken Z and human chromosome 9. Nat Genet 1999;21:258-9.
17. Page DC, de la Chapelle A, Weissenbach J. Chromosome Y-specific DNA in related human XX males. Nature 1985;315:224-6.
18. McLaren A. The making of male mice. Nature 1991;351:96.
19. Hsu TC, Benirschke K. An Atlas of Mammalian Chromosomes. New York: Springer; 1967. p. 1.
20. Benirschke K, Hsu TC. Chromosome Atlas: Fish, Amphibians, Reptiles and Birds. Coordinating Editors: Benirschke K, Hsu TC. New York: Springer-Verlag; 1971.
21. Gregory TR, Nicol JA, Tamm H, Kullman B, Kullman K, Leitch IJ, *et al*. Eukaryotic genome size databases. Nucleic Acids Res 2007;35:D332-8.
22. O'Brien SJ, Menninger JC, Nash WG. Atlas of Mammalian Chromosomes. Hoboken, NJ: John Wiley and Sons; 2006.
23. Uno Y, Nishida C, Tarui H, Ishishita S, Takagi C, Nishimura O, *et al*. Inference of the protokaryotypes of amniotes and tetrapods

and the evolutionary processes of microchromosomes from comparative gene mapping. PLoS One 2012;7:e53027.
24. Capel B. Vertebrate sex determination: Evolutionary plasticity of a fundamental switch. Nat Rev Genet 2017;18:675-89.
25. Muller HJ. Genetic variability, twin hybrids and constant hybrids, in a case of balanced lethal factors. Genetics 1918;3:422-99.
26. Graves JA. Sex chromosome specialization and degeneration in mammals. Cell 2006;124:901-14.
27. Graves JA. Evolution of vertebrate sex chromosomes and dosage compensation. Nat Rev Genet 2016;17:33-46.
28. Wijchers PJ, Festenstein RJ. Epigenetic regulation of autosomal gene expression by sex chromosomes. Trends Genet 2011;27:132-40.
29. Simmler MC, Rouyer F, Vergnaud G, Nyström-Lahti M, Ngo KY, de la Chapelle A, *et al*. Pseudoautosomal DNA sequences in the pairing region of the human sex chromosomes. Nature 1985;317:692-7.
30. Charchar FJ, Svartman M, El-Mogharbel N, Ventura M, Kirby P, Matarazzo MR, *et al*. Complex events in the evolution of the human pseudoautosomal region 2 (PAR2). Genome Res 2003;13:281-6.
31. Monteiro B, Arenas M, Prata MJ, Amorim A. Evolutionary dynamics of the human pseudoautosomal regions. PLoS Genet 2021;17:e1009532.
32. Perry J, Palmer S, Gabriel A, Ashworth A. A short pseudoautosomal region in laboratory mice. Genome Res 2001;11:1826-32.
33. Morgan AP, Bell TA, Crowley JJ, Pardo-Manuel de Villena F. Instability of the pseudoautosomal boundary in house mice. Genetics 2019;212:469-87.
34. Morey C, Avner P. Genetics and epigenetics of the X chromosome. Ann N Y Acad Sci 2010;1214:E18-33.
35. Raznahan A, Parikshak NN, Chandran V, Blumenthal JD, Clasen LS, Alexander-Bloch AF, *et al.* Sex-chromosome dosage effects on gene expression in humans. Proc Natl Acad Sci U S A 2018;115:7398-403.
36. Bellott DW, Hughes JF, Skaletsky H, Brown LG, Pyntikova T, Cho TJ, *et al*. Mammalian Y chromosomes retain widely expressed dosage-sensitive regulators. Nature 2014;508:494-9.
37. Lyon MF. Gene action in the X-chromosome of the mouse (*Mus musculus* L.). Nature 1961;190:372-3.
38. Lee JT, Bartolomei MS. X-inactivation, imprinting, and long noncoding RNAs in health and disease. Cell 2013;152:1308-23.
39. Gayen S, Maclary E, Hinten M, Kalantry S. Sex-specific silencing of X-linked genes by Xist RNA. Proc Natl Acad Sci U S A 2016;113:E309-18.
40. Penny GD, Kay GF, Sheardown SA, Rastan S, Brockdorff N. Requirement for Xist in X chromosome inactivation. Nature 1996;379:131-7.
41. Marahrens Y, Loring J, Jaenisch R. Role of the Xist gene in X chromosome choosing. Cell 1998;92:657-64.
42. Disteche CM, Berletch JB. X-chromosome inactivation and escape. J Genet 2015;94:591-9.
43. Page MJ, Moher D, Bossuyt PM, Boutron I, Hoffmann TC, Mulrow CD, *et al*. PRISMA 2020 explanation and elaboration: updated guidance and exemplars for reporting systematic reviews. BMJ 2021;372:n160.
44. Hughes JF, Skaletsky H, Pyntikova T, Minx PJ, Graves T, Rozen S, *et al.* Conservation of Y-linked genes during human evolution revealed by comparative sequencing in chimpanzee. Nature 2005;437:100-3.
45. Charlesworth B, Charlesworth D. The degeneration of Y chromosomes. Philos Trans R Soc Lond B Biol Sci 2000;355:1563-72.
46. Thompson JD, Higgins DG, Gibson TJ. CLUSTAL W: Improving the sensitivity of progressive multiple sequence alignment through sequence weighting, position-specific gap penalties and weight matrix choice. Nucleic Acids Res 1994;22:4673-80.
47. Li G, Davis BW, Raudsepp T, Pearks Wilkerson AJ, Mason VC, Ferguson-Smith M, *et al*. Comparative analysis of mammalian Y chromosomes illuminates ancestral structure and lineage-specific evolution. Genome Res 2013;23:1486-95.
48. Murphy WJ, Pearks Wilkerson AJ, Raudsepp T, Agarwala R, Schäffer AA, Stanyon R, *et al*. Novel gene acquisition on carnivore Y chromosomes. PLoS Genet 2006;2:e43.
49. Hamilton CK, Revay T, Domander R, Favetta LA, King WA. A large expansion of the HSFY gene family in cattle shows dispersion across Yq and testis-specific expression. PLoS One 2011;6:e17790.
50. Hughes JF, Skaletsky H, Brown LG, Pyntikova T, Graves T, Fulton RS, *et al*. Strict evolutionary conservation followed rapid gene loss on human and rhesus Y chromosomes. Nature 2012;483:82-6.
51. Aitken RJ, Marshall Graves JA. The future of sex. Nature 2002;415:963.
52. Graves JA, Koina E, Sankovic N. How the gene content of human sex chromosomes evolved. Curr Opin Genet Dev 2006;16:219-24.
53. Marshall Graves JA. Weird animal genomes and the evolution of vertebrate sex and sex chromosomes. Annu Rev Genet 2008;42:565-86.
54. Bellott DW, Skaletsky H, Cho TJ, Brown L, Locke D, Chen N, *et al*. Avian W and mammalian Y chromosomes convergently retained dosage-sensitive regulators. Nat Genet 2017;49:387-94.
55. Charlesworth B. Sex determination: Primitive Y chromosomes in fish. Curr Biol 2004;14:R745-7.
56. Zhu ZX, Matsubara K, Shams F, Dobry J, Wapstra E, Gamble T, *et al*. Diversity of reptile sex chromosome evolution revealed by cytogenetic and linked-read sequencing. Zool Res 2022;43:719-33.
57. Wang Z, Pascual-Anaya J, Zadissa A, Li W, Niimura Y, Huang Z, *et al*. The draft genomes of soft-shell turtle and green sea turtle yield insights into the development and evolution of the turtle-specific body plan. Nat Genet 2013;45:701-6.
58. Peichel CL, McCann SR, Ross JA, Naftaly AF, Urton JR, Cech JN, *et al*. Assembly of the threespine stickleback Y chromosome reveals convergent signatures of sex chromosome evolution. Genome Biol 2020;21:177.
59. White MA, Kitano J, Peichel CL. Purifying selection maintains dosage-sensitive genes during degeneration of the threespine stickleback Y chromosome. Mol Biol Evol 2015;32:1981-95.
60. Sackton TB, Hartl DL. Meta-analysis reveals that genes regulated by the Y chromosome in *Drosophila melanogaster* are preferentially localized to repressive chromatin. Genome Biol Evol 2013;5:255-66.
61. Larracuente AM, Clark AG. Surprising differences in the variability of Y chromosomes in African and cosmopolitan populations of *Drosophila melanogaster*. Genetics 2013;193:201-14.
62. Romanov MN, Farré M, Lithgow PE, Fowler KE, Skinner BM, O'Connor R, *et al*. Reconstruction of gross avian genome structure, organization and evolution suggests that the chicken lineage most closely resembles the dinosaur avian ancestor. BMC Genomics 2014;15:1060.

63. Morgan AP, Pardo-Manuel de Villena F. Sequence and structural diversity of mouse Y chromosomes. Mol Biol Evol 2017;34:3186-204.
64. Bellott DW, Skaletsky H, Pyntikova T, Mardis ER, Graves T, Kremitzki C, *et al*. Convergent evolution of chicken Z and human X chromosomes by expansion and gene acquisition. Nature 2010;466:612-6.
65. Pecon Slattery J, Sanner-Wachter L, O'Brien SJ. Novel gene conversion between X-Y homologues located in the nonrecombining region of the Y chromosome in Felidae (*Mammalia*). Proc Natl Acad Sci U S A 2000;97:5307-12.
66. Kumar S, Tamura K, Nei M. MEGA: Molecular Evolutionary Genetics Analysis (Pennsylvania State Univ., University Park), 1993. p. 1.
67. Swofford DL. PAUP*: Phylogenetic Analysis Using Parsimony (*And Other Methods) (Sinauer, Sunderland, MA). Version 4; 2002.
68. Miyata T, Hayashida H, Kuma K, Mitsuyasu K, Yasunaga T. Male-driven molecular evolution: A model and nucleotide sequence analysis. Cold Spring Harb Symp Quant Biol 1987;52:863-7.

Case Report

Renal Artery Originating from the Thoracic Aorta: A Critical Variant for Preoperative Awareness

Fatma Durmaz, Ebru Kurt, Ilyas Dundar

Department of Radiology, Van Yuzuncu Yil University School of Medicine, Van, Turkey

Abstract

This case report highlights a rare variation, in which the right renal artery originates from the thoracic aorta, passing through the diaphragm to reach the renal hilum, identified through contrast-enhanced computed tomography (CT). While renal artery variations are common, this particular variant, with the kidney in its normal position, is exceedingly rare. The origin of renal arteries typically occurs at the L1-L2 vertebral level, with variations often arising from the persistence of mesonephric arteries. This case adds to the literature and underscores the importance of recognizing such anomalies, particularly as these variations can impact surgical procedures, including laparoscopic nephrectomies and renal transplantation. Multidetector CT angiography is recommended as a valuable tool for accurately visualizing renal vascular anatomy, aiding in preprocedural planning, and improving clinical outcomes.

Keywords: *Ectopic renal artery origin, supradiaphragmatic renal artery, surgery, thoracic renal artery, vascular variant*

Introduction

Renal artery variations hold significant relevance in both vascular and interventional radiological procedures, as well as in renal transplantation. Typically, the renal arteries are paired lateral branches of the abdominal aorta, originating at the level of the intervertebral disc between the L1 and L2 vertebrae, just below the origin of the superior mesenteric artery. However, the exact level of origin can vary between the upper border of the L1 and the lower border of the L2 vertebrae.[1]

The renal arteries are among the most variable branches of the abdominal aorta, both in terms of their origin and number. Due to the high frequency of anatomical variants in renal arterial supply, they are often encountered in abdominal computed tomography (CT) scans but frequently go unreported by radiologists.[2] Among the most frequently observed variations are early prehilar divisions and the presence of additional renal arteries, with the latter being more prevalent on the right side.[1]

Although renal artery variations are common, a thoracic origin of a single renal artery, with the kidney remaining in its normal position, is considered a rare anatomical variant. The first documented case was reported by Doppman in 1967, who described a renal artery originating at the T11 vertebral level, beneath the right crus of the diaphragm.[3]

An understanding of renal artery variations is crucial in the management of renal trauma, surgical interventions, transplantation, and aortic surgeries.[4] This knowledge is especially important when performing renal angioplasty or planning vascular reconstruction for remediable vascular lesions.[5]

In this rare case report, we present an incidental finding of a supradiaphragmatic right renal artery originating from the thoracic aorta, as identified in a male patient through contrast-enhanced CT.

Case Report

A 51-year-old male patient presented with abdominal pain. No significant findings were observed on physical examination. Laboratory tests revealed no significant findings except for a positive fecal occult blood test. Due to the positive fecal occult blood, abdominal contrast-enhanced CT was performed in our clinic, which did not show any radiological pathology in the abdominal

How to cite this article: Durmaz F, Kurt E, Dundar I. Renal artery originating from the thoracic aorta: A critical variant for preoperative awareness. J Anat Soc India 2025;74:278-80.

Article Info

Received: 18 February 2025
Accepted: 11 August 2025
Available online: 30 September 2025

Address for correspondence:
Dr. Fatma Durmaz, Department of Radiology, Van Yuzuncu Yil University School of Medicine, Van, Turkey. E-mail: dr.fatmadrmz@gmail.com

Access this article online

Website: https://journals.lww.com/joai

DOI: 10.4103/jasi.jasi_33_25

Quick Response Code:

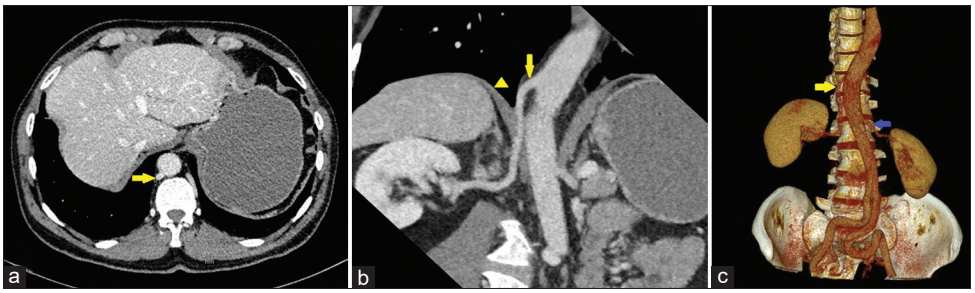

Figure 1: (a) Axial computed tomography (CT) scan showing the right main renal artery (arrow) originating from the descending thoracic aorta. (b) Curved multiplanar reconstruction CT demonstrating the renal artery (arrow) traversing the diaphragm (arrow head) to reach the renal hilum. (c) Volume-rendered CT image depicting the right renal artery (yellow arrow) originating from the level of superior body of the T12 vertebra and the left renal artery (blue arrow) from its normal origin

solid organs or intestinal loops. Incidentally, it was noted that the right main renal artery originated from the right posterolateral aspect of the thoracic aorta [Figure 1a], coursing caudally through a hiatus in the diaphragm crus to reach the renal hilum [Figure 1b]. While the left renal artery had a common origin from abdominal aorta at the level of L1-2 intervertebral disk, the right renal artery, as a rare variant, originated from the thoracic aorta at the level of the superior body of the T12 vertebra [Figure 1c].

Discussion

Renal arteries arise from the lateral mesonephric arteries, which develop from the dorsal aorta. These mesonephric arteries supply the mesonephros, metanephros, suprarenal glands, and gonads and are categorized into three groups: cranial, middle, and caudal. The renal artery usually develops from the lowermost mesonephric artery of the middle group or the uppermost mesonephric artery of the caudal group.[6]

The most common origin of the main renal artery is at the lower margin of the L1 vertebra on the right side (25%) and the upper margin of the L2 vertebra on the left side (24%). Aberrant, accessory, and anomalous renal arteries often result from the persistence of middle group vasculature or failure of kidney migration. The persistence of cranial mesonephric arteries is considered a probable cause of the rare thoracic origin of the renal artery.[7]

Renal arterial variations are common, with accessory renal arteries being the most frequently observed, present in about one-third of the population.[2] However, renal arteries originating from the thoracic aorta are extremely rare. The first case was described by Doppman in 1967, in which the renal artery originated at T11 and passed beneath the right crus of the diaphragm.[3]

Recent literature has documented several cases of ectopic right renal arteries originating from the thoracic aorta. Ichikawa *et al*.[2] identified seven such cases, whereas Matusz *et al*.[5] reported 12 cases, eight of which originated ectopically from the thoracic aorta. In these cases, the kidney was in its normal position despite the vascular variation. Ishida *et al*.[8] reviewed 10 reports, all involving right-sided renal arteries originating from the thoracic aorta.

A comprehensive review of 24 cases of supradiaphragmatic renal artery origins found that 20 were on the right side, with the remaining 4 on the left. In addition, in 5 of these cases, additional renal arteries arising from the abdominal aorta supplied a normally positioned right kidney. The increased detection of such variations in recent years has been attributed to the wider use of contrast-enhanced CT imaging.[9]

Renal artery variants can lead to significant complications, including ischemia, hemorrhage, and postoperative hypertension. These variations have also been associated with higher complication rates, complicated laparoscopic donor nephrectomies, and difficulties in retroperitoneal renal transplantation.[10]

Conclusion

We presented a rare case of a right renal artery originating from the thoracic aorta and passing through the diaphragm, identified on CT. Awareness of such renal arterial anomalies is crucial for surgeons and radiologists, as understanding these variations can improve outcomes in laparoscopic, retroperitoneal surgeries, renal transplantation, and interventional procedures. Multidetector CT angiography offers accurate visualization of renal vascular anatomy and should be used as a preprocedural diagnostic tool.

Declaration of patient consent

The authors certify that they have obtained all appropriate patient consent forms. In the form, the patient has given his consent for his images and other clinical information to be reported in the journal. The patient understands that his name and initials will not be published and due efforts will be made to conceal his identity, but anonymity cannot be guaranteed.

Financial support and sponsorship

Nil.

Conflicts of interest

There are no conflicts of interest.

References

1. Ozkan U, Oğuzkurt L, Tercan F, Kizilkiliç O, Koç Z, Koca N. Renal artery origins and variations: Angiographic evaluation of 855 consecutive patients. Diagn Interv Radiol 2006;12:183-6.
2. Ichikawa T, Iino M, Koizumi J, Hara T, Kazama T, Sekiguchi T, *et al*. A case of right renal artery originating from the thoracic aorta. Jpn J Radiol 2014;32:716-20.
3. Gulas E, Wysiadecki G, Szymański J, Majos A, Stefańczyk L, Topol M, *et al.* Morphological and clinical aspects of the occurrence of accessory (multiple) renal arteries. Arch Med Sci 2018;14:442-53.
4. Sousa PM, Ferreira AC. Thoracıc orıgın of the rıght renal artery: An ıncıdental fındıng. Port J Card Thorac Vasc Surg 2021;28:69-70.
5. Matusz P, Miclăuș GD, Gabriel A, Catereniuc I, Olariu S, Tubbs RS, *et al.* Single ectopic thoracic renal artery associated with a normal kidney position and renal artery stenosis: A case report and review of literature. Rom J Morphol Embryol 2015;56:557-62.
6. Delasotta LA, Olivieri B, Malik A, Nguyen C, Bhatia V, Burke W. Thoracic renal artery: A rare variant. A case study and literature review. Surg Radiol Anat 2015;37:561-4.
7. Arazińska A, Polguj M, Topol M, Wojciechowski A, Trębiński Ł, Stefańczyk L. Renal artery entrapment – Anatomical risk factors rating. Folia Morphol (Warsz) 2016;75:486-92.
8. Ishida M, Namiki Y, Watanabe M. Thoracic renal artery: A rare case of the renal artery originating from the thoracic aorta and literature review. Anat Sci Int 2016;91:211-4.
9. Rameshbabu CS, Kumar A, Gupta OP, Sharma Y. Supradiaphragmatic origin of right renal artery from thoracic aorta: case report and literature review. Int J Anat Res 2020;8:7829-34.
10. Al-Smair A, Aloqaily M, Alqudah M, Saadeh A, Al-Ali A. Supradiaphragmatic origin of the right renal artery: A case report. Radiol Case Rep 2022;17:3903-6.

The Editorial Process

A manuscript will be reviewed for possible publication with the understanding that it is being submitted to Journal of the Anatomical Society of India alone at that point in time and has not been published anywhere, simultaneously submitted, or already accepted for publication elsewhere. The journal expects that authors would authorize one of them to correspond with the Journal for all matters related to the manuscript. All manuscripts received are duly acknowledged. On submission, editors review all submitted manuscripts initially for suitability for formal review. Manuscripts with insufficient originality, serious scientific or technical flaws, or lack of a significant message are rejected before proceeding for formal peer-review. Manuscripts that are unlikely to be of interest to the Journal of the Anatomical Society of India readers are also liable to be rejected at this stage itself.

Manuscripts that are found suitable for publication in Journal of the Anatomical Society of India are sent to two or more expert reviewers. During submission, the contributor is requested to provide names of two or three qualified reviewers who have had experience in the subject of the submitted manuscript, but this is not mandatory. The reviewers should not be affiliated with the same institutes as the contributor/s. However, the selection of these reviewers is at the sole discretion of the editor. The journal follows a double-blind review process, wherein the reviewers and authors are unaware of each other's identity. Every manuscript is also assigned to a member of the editorial team, who based on the comments from the reviewers takes a final decision on the manuscript. The comments and suggestions (acceptance/ rejection/ amendments in manuscript) received from reviewers are conveyed to the corresponding author. If required, the author is requested to provide a point by point response to reviewers' comments and submit a revised version of the manuscript. This process is repeated till reviewers and editors are satisfied with the manuscript.

Manuscripts accepted for publication are copy edited for grammar, punctuation, print style, and format. Page proofs are sent to the corresponding author. The corresponding author is expected to return the corrected proofs within three days. It may not be possible to incorporate corrections received after that period. The whole process of submission of the manuscript to final decision and sending and receiving proofs is completed online. To achieve faster and greater dissemination of knowledge and information, the journal publishes articles online as 'Ahead of Print' immediately on acceptance.

Clinical trial registry

Journal of the Anatomical Society of India favors registration of clinical trials and is a signatory to the Statement on publishing clinical trials in Indian biomedical journals. Journal of the Anatomical Society of India would publish clinical trials that have been registered with a clinical trial registry that allows free online access to public. Registration in the following trial registers is acceptable: http://www.ctri.in/; http://www.actr.org.au/; http://www.clinicaltrials.gov/; http://isrctn.org/; http://www.trialregister.nl/trialreg/index.asp; and http://www.umin.ac.jp/ctr. This is applicable to clinical trials that have begun enrollment of subjects in or after June 2008. Clinical trials that have commenced enrollment of subjects prior to June 2008 would be considered for publication in Journal of the Anatomical Society of India only if they have been registered retrospectively with clinical trial registry that allows unhindered online access to public without charging any fees.

Authorship Criteria

Authorship credit should be based only on substantial contributions to each of the three components mentioned below:

1. Concept and design of study or acquisition of data or analysis and interpretation of data;
2. Drafting the article or revising it critically for important intellectual content; and
3. Final approval of the version to be published.

Participation solely in the acquisition of funding or the collection of data does not justify authorship. General supervision of the research group is not sufficient for authorship. Each contributor should have participated sufficiently in the work to take public responsibility for appropriate portions of the content of the manuscript. The order of naming the contributors should be based on the relative contribution of the contributor towards the study and writing the manuscript. Once submitted the order cannot be changed without written consent of all the contributors. The journal prescribes a maximum number of authors for manuscripts depending upon the type of manuscript, its scope and number of institutions involved (vide infra). The authors should provide a justification, if the number of authors exceeds these limits.

Contribution Details

Contributors should provide a description of contributions made by each of them towards the manuscript. Description should be divided in following categories, as applicable: concept, design, definition of intellectual content, literature search, clinical studies, experimental studies, data acquisition, data analysis, statistical analysis, manuscript preparation, manuscript editing and manuscript review. Authors' contributions will be printed along with the article. One or more author should take responsibility for the integrity of the work as a whole from inception to published article and should be designated as 'guarantor'.

Conflicts of Interest/ Competing Interests

All authors of must disclose any and all conflicts of interest they may have with publication of the manuscript or an institution or product that is mentioned in the manuscript and/or is important to the outcome of the study presented. Authors should also disclose conflict of interest with products that compete with those mentioned in their manuscript.

Submission of Manuscripts

All manuscripts must be submitted on-line through the website https://review.jow.medknow.com/jasi. First time users will have to register at this site. Registration is free but mandatory. Registered authors can keep track of their articles after logging into the site using their user name and password.

- If you experience any problems, please contact the editorial office by e-mail at editor@jasi.org.in

The submitted manuscripts that are not as per the "Instructions to Authors" would be returned to the authors for technical correction, before they undergo editorial/ peer-review. Generally, the manuscript should be submitted in the form of two separate files:

[1] Title Page/First Page File/covering letter:

This file should provide

1. The type of manuscript (original article, case report, review article, Letter to editor, Images, etc.) title of the manuscript, running title, names of all authors/ contributors (with their highest academic degrees, designation and affiliations) and name(s) of department(s) and/ or institution(s) to which the work should be credited, . All information which can reveal your identity should be here. Use text/rtf/doc files. Do not zip the files.
2. The total number of pages, total number of photographs and word counts separately for abstract and for the text (excluding the references, tables and abstract), word counts for introduction + discussion in case of an original article;
3. Source(s) of support in the form of grants, equipment, drugs, or all of these;
4. Acknowledgement, if any. One or more statements should specify 1) contributions that need acknowledging but do not justify authorship, such as general support by a departmental chair; 2) acknowledgments of technical help; and 3) acknowledgments of financial and material support, which should specify the nature of the support. This should be included in the title page of the manuscript and not in the main article file.
5. If the manuscript was presented as part at a meeting, the organization, place, and exact date on which it was read. A full statement to the editor about all submissions and previous reports that might be regarded as redundant publication of the same or very similar work. Any such work should be referred to specifically, and referenced in the new paper. Copies of such material should be included with the submitted paper, to help the editor decide how to handle the matter.
6. Registration number in case of a clinical trial and where it is registered (name of the registry and its URL)
7. Conflicts of Interest of each author/ contributor. A statement of financial or other relationships that might lead to a conflict of interest, if that information is not included in the manuscript itself or in an authors' form
8. Criteria for inclusion in the authors'/ contributors' list
9. A statement that the manuscript has been read and approved by all the authors, that the requirements for authorship as stated earlier in this document have been met, and that each author believes that the manuscript represents honest work, if that information is not provided in another form (see below); and
10. The name, address, e-mail, and telephone number of the corresponding author, who is responsible for communicating with the other authors about revisions and final approval of the proofs, if that information is not included on the manuscript itself.

[2] Blinded Article file: The main text of the article, beginning from Abstract till References (including tables) should be in this file. The file must not contain any mention of the authors' names or initials or the institution at which the study was done or acknowledgements. Page headers/ running title can include the title but not the authors' names. Manuscripts not in compliance with the Journal's blinding policy will be returned to the corresponding author. Use rtf/doc files. Do not zip the files. **Limit the file size to 1 MB.** Do not incorporate images in the file. If file size is large, graphs can be submitted as images separately without incorporating them in the article file to reduce the size of the file. The pages should be numbered consecutively, beginning with the first page of the blinded article file.

[3] Images: Submit good quality color images. **Each image should be less than 2 MB in size.** Size of the image can be reduced by decreasing the actual height and width of the images (keep up to 1600 x 1200 pixels or 5-6 inches). Images can be submitted as jpeg files. Do not zip the files. Legends for the figures/images should be included at the end of the article file.

[4] The contributors' / copyright transfer form (template provided below) has to be submitted in original with the signatures of all the contributors within two weeks of submission via courier, fax or email as a scanned image. Print ready hard copies of the images (one set) or digital images should be sent to the journal office at the time of submitting revised manuscript. High resolution images (up to 5 MB each) can be sent by email.

Contributors' form / copyright transfer form can be submitted online from the authors' area on https://review.jow.medknow.com/jasi.

Preparation of Manuscripts

Manuscripts must be prepared in accordance with "Uniform requirements for Manuscripts submitted to Biomedical Journals" developed by the International Committee of Medical Journal Editors (October 2008). The uniform requirements and specific requirement of Journal of the Anatomical Society of India are summarized below. Before submitting a manuscript, contributors are requested to check for the latest instructions available. Instructions are also available from the website of the journal (www.jasi.org.in) and from the manuscript submission site https://review.jow.medknow.com/jasi.

Journal of the Anatomical Society of India accepts manuscripts written in American English.

Copies of any permission(s)

It is the responsibility of authors/ contributors to obtain permissions for reproducing any copyrighted material. A copy of the permission obtained must accompany the manuscript. Copies of any and all published articles or other manuscripts in preparation or submitted elsewhere that are related to the manuscript must also accompany the manuscript.

Types of Manuscripts

Original articles:

These include randomized controlled trials, intervention studies, studies of screening and diagnostic test, outcome studies, cost effectiveness analyses, case-control series, and surveys with high response rate. The text of original articles amounting to up to 3000 words (excluding Abstract, references and Tables) should be divided into sections with the headings Abstract, Key-words, Introduction, Material and Methods, Results, Discussion and Conclusion, References, Tables and Figure legends.

An abstract should be in a structured format under following heads: **Introduction, Material and Methods, Results,** and **Discussion and Conclusion.**

Introduction: State the purpose and summarize the rationale for the study or observation.

Material and Methods: It should include and describe the following aspects:

Ethics: When reporting studies on human beings, indicate whether the procedures followed were in accordance with the ethical standards of the responsible committee on human experimentation (institutional or regional) and with the Helsinki Declaration of 1975, as revised in 2000 (available at http://www.wma.net/e/policy/17-c_e.html). For prospective studies involving human participants, authors are expected to mention about approval of (regional/ national/ institutional or independent Ethics Committee or Review Board, obtaining informed consent from adult research participants and obtaining assent for children aged over 7 years participating in the trial. The age beyond which assent would be required could vary as per regional and/ or national guidelines. Ensure confidentiality of subjects by desisting from mentioning participants' names, initials or hospital numbers, especially in illustrative material. When reporting experiments on animals, indicate whether the institution's or a national research council's guide for, or any national law on the care and use of laboratory animals was followed. Evidence for approval by a local Ethics Committee (for both human as well as animal studies) must be supplied by the authors on demand. Animal experimental procedures should be as humane as possible and the details of anesthetics and analgesics used should be clearly stated. The ethical standards of experiments must be in accordance with the guidelines provided by the CPCSEA and World Medical Association Declaration of Helsinki on Ethical Principles for Medical Research Involving Humans for studies involving experimental animals and human beings, respectively). The journal will not consider any paper which is ethically unacceptable. A statement on ethics committee permission and ethical practices must be included in all research articles under the 'Materials and Methods' section.

Study design:

Selection and Description of Participants: Describe your selection of the observational or experimental participants (patients or laboratory animals, including controls) clearly, including eligibility and exclusion criteria and a description of the source population. *Technical information*: Identify the methods, apparatus (give the manufacturer›s name and address in parentheses), and procedures in sufficient detail to allow other workers to reproduce the results. Give references to established methods, including statistical methods (see below); provide references and brief descriptions for methods that have been published but are not well known; describe new or substantially modified methods, give reasons for using them, and evaluate their limitations. Identify precisely all drugs and chemicals used, including generic name(s), dose(s), and route(s) of administration.

Reports of randomized clinical trials should present information on all major study elements, including the protocol, assignment of interventions (methods of randomization, concealment of allocation to treatment groups), and the method of masking (blinding), based on the CONSORT Statement (http://www.consort-statement.org).

Reporting Guidelines for Specific Study Designs

Initiative	Type of Study	Source
CONSORT	Randomized controlled trials	http://www.consort-statement.org
STARD	Studies of diagnostic accuracy	http://www.consort-statement.org/stardstatement.htm
QUOROM	Systematic reviews and meta-analyses	http://www.consort- statement.org/Initiatives/MOOSE/moose.pdf statement.org/Initiatives/MOOSE/moose.pdf
STROBE	Observational studies in epidemiology	http://www.strobe-statement.org
MOOSE	Meta-analyses of observational studies in epidemiology	http://www.consort- statement.org/Initiatives/MOOSE/moose.pdf

Statistics: Whenever possible quantify findings and present them with appropriate indicators of measurement error or uncertainty (such as confidence intervals). Authors should report losses to observation (such as, dropouts from a clinical trial). When data are summarized in the Results section, specify the statistical methods used to analyze them. Avoid non-technical uses of technical terms in statistics, such as 'random' (which implies a randomizing device), 'normal', 'significant', 'correlations', and 'sample'. Define statistical terms, abbreviations, and most symbols. Specify the computer software used. Use upper italics (*P* 0.048). For all *P* values include the exact value and not less than 0.05 or 0.001. Mean differences in continuous variables, proportions in categorical variables and relative risks including odds ratios and hazard ratios should be accompanied by their confidence intervals.

Results: Present your results in a logical sequence in the text, tables, and illustrations, giving the main or most important findings first. Do not repeat in the text all the data in the tables or illustrations; emphasize or summarize only important observations. Extra- or supplementary materials and technical detail can be placed in an appendix where it will be accessible but will not interrupt the flow of the text; alternatively, it can be published only in the electronic version of the journal.

When data are summarized in the Results section, give numeric results not only as derivatives (for example, percentages) but also as the absolute numbers from which the derivatives were calculated, and specify the statistical methods used to analyze them. Restrict tables and figures to those needed to explain the argument of the paper and to assess its support. Use graphs as an alternative to tables with many entries; do not duplicate data in graphs and tables. Where scientifically appropriate, analyses of the data by variables such as age and sex should be included.

Discussion: Include summary of *key findings* (primary outcome measures, secondary outcome measures, results as they relate to a prior hypothesis); *Strengths and limitations* of the study (study question, study design, data collection, analysis and interpretation); *Interpretation and implications* in the context of the totality of evidence (is there a systematic review to refer to, if not, could one be reasonably done here and now?, what this study adds to the available evidence, effects on patient care and health policy, possible mechanisms); *Controversies* raised by this study; and *Future research directions* (for this particular research collaboration, underlying mechanisms, clinical research).

Do not repeat in detail data or other material given in the Introduction or the Results section. In particular, contributors should avoid making statements on economic benefits and costs unless their manuscript includes economic data and analyses. Avoid claiming priority and alluding to work that has not been completed. New hypotheses may be stated if needed, however they should be clearly labeled as such. About 30 references can be included. These articles generally should not have more than six authors.

Review Articles:

These are comprehensive review articles on topics related to various fields of Anatomy. The entire manuscript should not exceed 7000 words with no more than 50 references and two authors. Following types of articles can be submitted under this category:

- Newer techniques of dissection and histology
- New methodology in Medical Education
- Review of a current concept

Please note that generally review articles are by invitation only. But unsolicited review articles will be considered for publication on merit basis.

Case reports:

New, interesting and rare cases can be reported. They should be unique, describing a great diagnostic or therapeutic challenge and providing a learning point for the readers. Cases with clinical significance or implications will be given priority. These communications could be of up to 1000 words (excluding Abstract and references) and should have the following headings: Abstract (unstructured), Key-words, Introduction, Case report, Discussion and Conclusion, Reference, Tables and Legends in that order.

The manuscript could be of up to 1000 words (excluding references and abstract) and could be supported with up to 10 references. Case Reports could be authored by up to four authors.

Letter to the Editor:

These should be short and decisive observations. They should preferably be related to articles previously published in the Journal or views expressed in the journal. They should not be preliminary observations that need a later

paper for validation. The letter could have up to 500 words and 5 references. It could be generally authored by not more than four authors.

Book Review: This consists of a critical appraisal of selected books on Anatomy. Potential authors or publishers may submit books, as well as a list of suggested reviewers, to the editorial office. The author/publisher has to pay INR 10,000 per book review.

Other:

Editorial, Guest Editorial, Commentary and Opinion are solicited by the editorial board.

References

References should be *numbered* consecutively in the order in which they are first mentioned in the text (not in alphabetic order). Identify references *in text*, tables, and legends by Arabic numerals in superscript with square bracket after the punctuation *marks. References cited only* in tables or figure legends should be numbered in accordance with the sequence established by the first identification in the text of the particular table or figure. Use the style of the examples below, which are based on the formats used by the NLM *in Index Medicus*. The titles of journals *should be abbreviated* according to the style used in Index Medicus. Use complete name of the journal for non-indexed journals. Avoid using abstracts as references. Information from manuscripts submitted but not accepted should be cited in the text as "unpublished observations" with written permission from the source. Avoid citing a "personal communication" unless it provides essential information not available from a public source, in which case the name of the person and date of communication should be cited in parentheses in the text. The commonly cited types of references are shown here, for other types of references such as newspaper items please refer to ICMJE Guidelines (http://www.icmje.org or http://www.nlm.nih.gov/bsd/uniform_requirements.html).

Articles in Journals

1. Standard journal article (for up to six authors): Parija S C, Ravinder PT, Shariff M. Detection of hydatid antigen in the fluid samples from hydatid cysts by co-agglutination. Trans. R.Soc. Trop. Med. Hyg.1996; 90:255–256.
2. Standard journal article (for more than six authors): List the first six contributors followed by *et al*.

Roddy P, Goiri J, Flevaud L, Palma PP, Morote S, Lima N. *et al*., Field Evaluation of a Rapid Immunochromatographic Assay for Detection of Trypanosoma cruzi Infection by Use of Whole Blood. J. Clin. Microbiol. 2008; 46: 2022-2027.

3. Volume with supplement: Otranto D, Capelli G, Genchi C: Changing distribution patterns of canine vector borne diseases in Italy: leishmaniosis vs. dirofilariosis. Parasites & Vectors 2009; Suppl 1:S2.

Books and Other Monographs

1. Personal author(s): Parija SC. Textbook of Medical Parasitology. 3rd ed. All India Publishers and Distributors. 2008.
2. Editor(s), compiler(s) as author: Garcia LS, Filarial Nematodes In: Garcia LS (editor) Diagnostic Medical Parasitology ASM press Washington DC 2007: pp 319-356.
3. Chapter in a book: Nesheim M C. Ascariasis and human nutrition. In Ascariasis and its prevention and control, D. W. T. Crompton, M. C. Nesbemi, and Z. S. Pawlowski (eds.). Taylor and Francis,London, U.K.1989, pp. 87–100.

Electronic Sources as reference

Journal article on the Internet: Parija SC, Khairnar K. Detection of excretory *Entamoeba histolytica* DNA in the urine, and detection of *E. histolytica* DNA and lectin antigen in the liver abscess pus for the diagnosis of amoebic liver abscess. *BMC Microbiology* 2007, **7**:41. doi:10.1186/1471-2180-7-41. http://www.biomedcentral.com/1471-2180/7/41

Tables

- Tables should be self-explanatory and should not duplicate textual material.
- Tables with more than 10 columns and 25 rows are not acceptable.
- Number tables, in Arabic numerals, consecutively in the order of their first citation in the text and supply a brief title for each.
- Place explanatory matter in footnotes, not in the heading.
- Explain in footnotes all non-standard abbreviations that are used in each table.
- Obtain permission for all fully borrowed, adapted, and modified tables and provide a credit line in the footnote.
- For footnotes use the following symbols, in this sequence: *, †, ‡, §, ‖,¶ , **, ††, ‡‡
- Tables with their legends should be provided at the end of the text after the references. The tables along with their number should be cited at the relevant place in the text

Illustrations (Figures)

- Upload the images in JPEG format. The file size should be within 1024 kb in size while uploading.
- Figures should be numbered consecutively according to the order in which they have been first cited in the text.
- Labels, numbers, and symbols should be clear and of uniform size. The lettering for figures should be large enough to be legible after reduction to fit the width of a printed column.
- Symbols, arrows, or letters used in photomicrographs

should contrast with the background and should be marked neatly with transfer type or by tissue overlay and not by pen.
- Titles and detailed explanations belong in the legends for illustrations not on the illustrations themselves.
- When graphs, scatter-grams or histograms are submitted the numerical data on which they are based should also be supplied.
- The photographs and figures should be trimmed to remove all the unwanted areas.
- If photographs of individuals are used, their pictures must be accompanied by written permission to use the photograph.
- If a figure has been published elsewhere, acknowledge the original source and submit written permission from the copyright holder to reproduce the material. A credit line should appear in the legend for such figures.
- Legends for illustrations: Type or print out legends (maximum 40 words, excluding the credit line) for illustrations using double spacing, with Arabic numerals corresponding to the illustrations. When symbols, arrows, numbers, or letters are used to identify parts of the illustrations, identify and explain each one in the legend. Explain the internal scale (magnification) and identify the method of staining in photomicrographs.
- Final figures for print production: Send sharp, glossy, un-mounted, color photographic prints, with height of 4 inches and width of 6 inches at the time of submitting the revised manuscript. Print outs of digital photographs are not acceptable. If digital images are the only source of images, ensure that the image has minimum resolution of 300 dpi or 1800 x 1600 pixels in TIFF format. Send the images on a CD. Each figure should have a label pasted (avoid use of liquid gum for pasting) on its back indicating the number of the figure, the running title, top of the figure and the legends of the figure. Do not write the contributor/s' name/s. Do not write on the back of figures, scratch, or mark them by using paper clips.
- The Journal reserves the right to crop, rotate, reduce, or enlarge the photographs to an acceptable size.

Protection of Patients' Rights to Privacy

Identifying information should not be published in written descriptions, photographs, sonograms, CT scans, etc., and pedigrees unless the information is essential for scientific purposes and the patient (or parent or guardian, wherever applicable) gives informed consent for publication. Authors should remove patients' names from figures unless they have obtained informed consent from the patients. The journal abides by ICMJE guidelines:

1. Authors, not the journals nor the publisher, need to obtain the patient consent form before the publication and have the form properly archived. The consent forms are not to be uploaded with the cover letter or sent through email to editorial or publisher offices.
2. If the manuscript contains patient images that preclude anonymity, or a description that has obvious indication to the identity of the patient, a statement about obtaining informed patient consent should be indicated in the manuscript.

Sending a revised manuscript

The revised version of the manuscript should be submitted online in a manner similar to that used for submission of the manuscript for the first time. However, there is no need to submit the "First Page" or "Covering Letter" file while submitting a revised version. When submitting a revised manuscript, contributors are requested to include, the 'referees' remarks along with point to point clarification at the beginning in the revised file itself. In addition, they are expected to mark the changes as underlined or colored text in the article.

Reprints and proofs

Journal provides no free printed reprints. Authors can purchase reprints, payment for which should be done at the time of submitting the proofs.

Publication schedule

The journal publishes articles on its website immediately on acceptance and follows a 'continuous publication' schedule. Articles are compiled in issues for 'print on demand' quarterly.

Copyrights

Checklist

Covering letter

- Signed by all contributors
- Previous publication / presentations mentioned
- Source of funding mentioned
- Conflicts of interest disclosed

Authors

- Last name and given name provided along with Middle name initials (where applicable)
- Author for correspondence, with e-mail address provided
- Number of contributors restricted as per the instructions
- Identity not revealed in paper except title page (e.g. name of the institute in Methods, citing previous study as 'our study', names on figure labels, name of institute in photographs, etc.)

Presentation and format

- Double spacing
- Margins 2.5 cm from all four sides
- Page numbers included at bottom
- Title page contains all the desired information
- Running title provided (not more than 50 characters)
- Abstract page contains the full title of the manuscript
- Abstract provided (structured abstract of 250 words for original articles, unstructured abstracts of about 150 words for all other manuscripts excluding letters to the Editor)
- Key words provided (three or more)
- Introduction of 75-100 words
- Headings in title case (not ALL CAPITALS)
- The references cited in the text should be after punctuation marks, in superscript with square bracket.
- References according to the journal's instructions, punctuation marks checked
- Send the article file without 'Track Changes'

Language and grammar

- Uniformly American English
- Write the full term for each abbreviation at its first use in the title, abstract, keywords and text separately unless it is a standard unit of measure. Numerals from 1 to 10 spelt out
- Numerals at the beginning of the sentence spelt out
- Check the manuscript for spelling, grammar and punctuation errors
- If a brand name is cited, supply the manufacturer's name and address (city and state/country).
- Species names should be in italics

Tables and figures

- No repetition of data in tables and graphs and in text
- Actual numbers from which graphs drawn, provided
- Figures necessary and of good quality (colour)
- Table and figure numbers in Arabic letters (not Roman)
- Labels pasted on back of the photographs (no names written)
- Figure legends provided (not more than 40 words)
- Patients' privacy maintained (if not permission taken)
- Credit note for borrowed figures/tables provided
- Write the full term for each abbreviation used in the table as a footnote

Journal of
The Anatomical Society of India

Salient Features:

- Publishes research articles related to all aspects of Anatomy and Allied medical/surgical sciences.
- Pre-Publication Peer Review and Post-Publication Peer Review
- Online Manuscript Submission System
- Selection of articles on the basis of MRS system
- Eminent academicians across the globe as the Editorial board members
- Electronic Table of Contents alerts
- Available in both online and print form.

The journal is registered with the following abstracting partners:
Baidu Scholar, CNKI (China National Knowledge Infrastructure), EBSCO Publishing's Electronic Databases, Ex Libris – Primo Central, Google Scholar, Hinari, Infotrieve, Netherlands ISSN center, ProQuest, TdNet, Wanfang Data

The journal is indexed with, or included in, the following:
SCOPUS, Science Citation Index Expanded, IndMed, MedInd, Scimago Journal Ranking, Emerging Sources Citation Index.

Impact Factor® as reported in the 2024 Journal Citation Reports® (Clarivate Analytics, 2025): 0.2

Editorial Office:
Dr. Vishram Singh, Editor-in-Chief, JASI
B5/3 Hahnemann Enclave, Plot No. 40, Sector 6,
Dwarka Phase – 2, New Delhi - 110 075, India.
Email: editorjasi@gmail.com
(O) | Website: www.asiindia.in

The journal is owned and run by The Anatomical Society of India